FIVE-HOLE PITOT PROBE TIME-MEAN VELOCITY MEASUREMENTS IN CYCLONE CHAMBERS WITH DOWNSTREAM NOZZLE

By

GHASSAN ALI EGHNEIM

Bachelor of Science in Mechanical Engineering

Oklahoma State University

Stillwater, Oklahoma

1987

Submitted to the Faculty of the
Graduate College of the
Oklahoma State University
in partial fulfillment of
the requirements for
the Degree of
MASTER OF SCIENCE
July, 1988

FIVE-HOLE PITOT PROBE TIME-MEAN VELOCITY MEASUREMENTS IN CYCLONE CHAMBERS WITH DOWNSTREAM NOZZLE

Thesis Approved:

D. G. Reilly
Thesis Adviser

Flint O. Thomas

Ronald L. Dougherty

Norman N. Durham
Dean of the Graduate College

ACKNOWLEDGMENTS

The author wishes to express his appreciation to his major advisor, Dr. D. G. Lilley for his extensive advice, guidance, and support throughout his entire master's degree program. Dr. Lilley has been a professor, an adviser, and a friend. Appreciation is also expressed to the other committee members, Dr. F. O. Thomas and Dr. R. L. Dougherty for their critique and advice in the preparation of the final manuscript.

The author also wishes to gratefully acknowledge A. K. H. Khalil for building the experimental facility and W. D. Chai for typing the final copy. Appreciation is also extended to the authors' brothers, sisters, relatives and friends for their love and encouragement.

Special thanks go to my brothers, Atef, Yousif, and Walid, for their care, love, and support.

Special thanks go to my uncle Shafic and his wife Kamleh for the care and love they have given me during my stay in the United States.

Finally this study is dedicated to the authors'parents, Mr. and Mrs. Ali and Fatima Eghneim. Without their continued love, emotional support, understanding, and prayers, this project could not have been completed.

TABLE OF CONTENTS

LIST OF TABLES

LIST OF FIGURES

NOMENCLATURE

English Symbols

D	test section diameter
d	axial air inlet diameter
m	mass flow rate
P	time-mean pressure
Re	Reynolds number
u	axial velocity
v	radial velocity
w	tangential velocity
x, r	axial, radial

Greek Symbols

β	yaw angle of probe = $\tan^{-1}(w/u)$
δ	pitch angle probe = $\tan^{-1}[v/(u^2 + w^2)^{1/2}]$
	density
	probe rotation angle
θ	azimuthal cylindrical polar coordinates

Subscripts

a	relating to axial flow at inlet
av	average in the large test section
C	central location

N,S,E,W	north, south, east, west locations
p	probe sensing tip
t	relating to tangential flow at inlet

CHAPTER I

INTRODUCTION

1.1 The Phenomenon

Recently, concentrated effort has been expended on understanding and characterizing the combustion aerodynamics of swirl flow burning processes of gaseous, liquid, and solid fuels. Economical design and operation of practical combustion equipment can be facilitated greatly by estimates made from complementary experimental and modeling studies. Such work combines experimental and theoretical combustion aerodynamics with sophisticated computational fluid dynamics and its important and use will reduce the cost of development programs significantly. Detailed surveys of these studies are to be found in the literature (1-11).

Swirling flows result from the application of a spiraling motion, with a swirl velocity component (also known as a tangential) being imparted to the flow via the use of swirl vanes, in axial plus tangential entry swirl generator, or by direct tangential entry into the combustion chamber. Experimental studies show that swirl has large-scale effects on flowfields: jet growth, entrainment, and decay (for inert jets) and flame size, shape, stability, and combustion intensity (for reacting flows) are affected by the degree of

swirl imparted to the flow. This degree of swirl usually is characterized by either swirl number S, which is a nondimensional number representing axial flux of swirl momentum divided by axial flux of axial momentum times equivalent nozzle radius, or by the ratio of the tangential velocity to the average exit velocity (w_t/u_{av}).

1.2 The Problem

Swirl flows occur in a very wide range of engineering applications. In combustion systems, the strong favorable effects of applying swirl to injected air and fuel are extensively used as an aid to stabilization of high intensity combustion process and efficient clean combustion in a variety of practical situations. Cyclones have been used in the combustion process of low calorific value fuels, high ash content coals, or fuels requiring long residence time for complete combustion.

There are many advantages of the cyclone combustion in comparison to conventional combustion chambers. They lie mainly on a unique flow pattern produced by the dominant circumference velocity component. The strong centrifugal field, created by the tangential inlet, alters the two-dimensional radial-axial flow and aids the combustion process in several ways. The spiral fluid motion enhances the residence of solid fuel in the chamber, and provides adequate time even for the most difficult fuel to be completely burned (12-16). At certain fuel loading, the flame is stabilized in the exhaust by a large toroidal

recirculation zone analogous to that found in the conventional swirl burner.

As part of an on-going project at Oklahoma State University, studies are in progress concerned with experimental and theoretical research of a model cyclone chamber with one axial inlet and one tangential inlet, air blower, stilling chamber for tangential inlet, downstream contraction nozzle, and exhaust system. The expansion ratio D/d of the chamber in study is 4.5. The general aim is to characterize the time-mean and turbulence model advances, and implement and exhibit results of flowfield predictions. The present contribution concentrates on the time-mean flow characterization via the five-hole pitot probe technique for time-mean velocity measurements (17).

1.3 Background

1.3.1 Swirl Flows

Swirl flows are generated by three principal methods:

(a) Tangential entry (axial-plus-tangential entry swirl generator).

(b) Guided vanes (swirl vane pack or swirl).

(c) Direct rotation (rotating pipe).

Tangential entry has been used extensively for providing uniform stable jets for detailed experimental study. The quantities of air can be controlled and metered separately so that simply by adjusting the air flow rates the degree of swirl can be varied from that of zero swirl to that of a

strongly swirling jet with reverse flow. Total pressure requirements of this system are relatively high, and commercial burners have tended to adopt the guided vane system, where vanes are so positioned that they deflect the flow direction. In radial flow into a swirl generating device, radial and tangential vane angles can be altered in situ via the movable block system is efficient in that pressure drop required for producing a certain swirl level is relatively low, and high swirl strengths are obtainable. Swirl may be generated by direct rotation of the flow, whereby in one experiment a rotating cylinder at 9500 rev/min was used to induce a swirl motion solely by frictional drag of the cylinder wall upon the air stream passing through it. Because of the relatively low viscosity of air it is possible to generate only weak swirl by this method (1).

1.3.2 Furnace Flames

The cyclone principle of aerodynamic organization of combustion in a furnace is closely related to the necessity of intensifying combustion to diminish the dimensions of the furnaces of large and very large combustion aggregates. A flame organized after the cyclone principle is called a "cyclone flame", and a furnace with such a flame is called a "cyclone-furnace".

Figure 1 shows different cyclone-furnace arrangements: (a) horizontal cyclone-furnace (or slightly slanting at an angle of 5-20 degrees), (b) vertical cyclone-furnace not concentric with the furnace, and (c) vertical cyclone furnace

concentric (18).

Compared to other flames, the cyclone flame has several advantages:

(a) Increase of fuel and oxidizer mixing rate.

(b) Heat release concentrated over a reduced volume (high thermal load).

(c) High temperature level (small air excess).

(d) Burning possibility not only for gaseous and liquid fuels, but also a large range of solid fuels with a granulation from that of coal powder to that of the fine coal of sunflower seeds and of milled peat coal, etc.

1.4 Objective

The objective of the present research is to characterize the effects of several parameters on the time-mean flowfields of a cyclone chamber with two inlets: one axial and one tangential. The parameters to be studied are the inlet axial velocity and flow rate, the inlet tangential velocity and flow rate, and the axial location of a downstream nozzle.

Chapter II reviews the previous experimental studies that had been done in this area; Chapter III describes facilities used in the investigations; Chapter IV describes the measuring techniques; Chapter V presents the results and discusses the findings; and finally Chapter VI concludes and make recommendations for further study.

The general goal of this experiment is to study the effect of the axial location of the downstream nozzle on the

upstream time-mean velocity for several values of inlet axial and tangential velocities.

The research is limited by the following factors:

(a) The difficulty in investigating the exact reattachment points of the flows, because of the measurement problem in low velocity regions.

(b) The low sensitivity of the probe in low velocity regions.

CHAPTER II

REVIEW OF THE LITERATURE

2.1 Historical Development of Cyclones

The first applications employing the cyclone principles data back to 1885 when the dust cyclone came into use. During the early part of 1900's, dust collector cyclones became more or less common in industry. Based on available literature, the only uses of the cyclone during this period were as dust collectors or fly-ash collectors, operating in conjunction with coal and wood-fire furnaces.

According to Pownall (19), over a thousand references on cyclone performance and application are available. However, Pownall indicated only a few references that analytically or experimentally reveal any information on the flow pattern in the cyclone.

Shepherd and Lapple (20) studied the flow patterns in a 12 inch gas cyclone by observing streamer angles and recording pitot probe measurements. They verified the existence of the double vortex flow pattern. They found that the outer vortex descended at a rate just sufficient to prevent interference on successive revolutions and that the rate of ascent of the inner vortex was relatively high. The inner vortex diameter was approximately equal to the internal

diameter of the vortex finder. As reported by Pownall (19), Ter Linden made a rather comprehensive investigation of the flow pattern in the gas cyclone by probing the flowing stream. His results agreed with the results of Shepherd and Lapple.

Kelsall's (21) determination of the approximate nature of the flow in a three inch water field hydrocyclone by optical methods remains the most comprehensive data available. By using a microscope with a rotating objective in conjunction with a stroboscope he measured the velocities of aluminum particles suspended in water. Kelsall claims an agreement of less than 5% deviation of the vertical and horizontal components of the tracer particles from those of the fluid components. In a later study, Bouchillon (22) indicated that the above was a reasonable estimate for the accuracy of the technique.

A qualitative study of the flow in a three-inch water-field hydrocyclone using dye injection and photography was presented by Bradley and Pulling (23). Flow rates investigated ranged from 7.9 to 11.9 gallons per minute (gpm). They expanded on Kelsall's work by more accurately defining the locus of zero vertical velocity and the nature of the secondary recirculation flow.

Photographs presented in the study of Bradley and Pulling (23) indicated that the vapor core and thus the surrounding inner vortex assumed some type of standing wave pattern. The wave appeared to be identical for flow rates of 7.9 and 11.9 gpm. The vapor core is formed by the rotation

of the fluid creating a low pressure axial core. Gilbert (24) stated that correct application of back pressure on the overflow of the cyclone would eliminate the vapor core without loss of separation efficiency.

Pownall (19) compared the velocity distribution found by Ter Linden in the gas cyclone and those obtained by Kelsall in the hydrocyclone and concluded that the nature of the flows are similar in character.

Smith (25) investigated the flow in a cylindrical gas cyclone with a flat bottom by smoke injection and photography. At low velocities he observed that inner vortex formed into a rotating wave with its end attached to the wall of the gas cyclone. The behavior of the wave resembled that of a whipped shaft. When the flow rate was increased, the level of attachment moved erratically down the cylindrical wall. With further increase in flow rate, the bottom of the inner vortex would attach itself to the center of the bottom of the cylindrical section. Smith observed that once the wave was established at bottom it was very stable through a wide range of flow rates.

The vortex flow perpendicular to the axis of the hydrocyclone has been analyzed by Milne-Thompson (26), Dreissen (27), and Binder (28) from the Navier-Stokes equations. The application of each of these analyses has been hampered by the lack of knowledge of boundary conditions needed in the solution of the differential equations.

Bouchillon (22) obtained a first approximation for the pressure and the distribution of each velocity component for

the conical section of the hydrocyclone. His basic solution procedure consisted of solving the Navier-Stokes equations simplified through an order of magnitude study based upon Kelsall's experimental data. Bouchillon compared theoretical velocity profiles with the experimental profiles of Kelsall and obtained good agreement.

Gilbert (24) showed that the tangential velocity was primarily responsible for the radial pressure gradient in the hydrocyclone. Since, as indicated earlier, the tangential velocity distribution is independent of vertical position, the radial pressure gradient must be substantially constant with respect to the axial position.

The above survey is intended to provide the reader with some information and background about the early development of cyclones and the kind of research that has been done it. For more details refer to literature (29). The next section will cover the most recent experimental studies on cyclones and swirl flows which is more related to our present study.

2.2 Experimental Research on Cyclones

Several researchers (see, for example, Baluev and Troyankin (30), Syred and Dahman (31), Vatistas et al. (32), and Khalil and Lilley (35)) measured the time-mean velocity field with a five-hole pitot probe. Baluev and Tyoyankin also investigated the effects of design parameters on the flow pattern.

Ustimenko and Bukhaman (33) carried out the measurement of fluctuating velocity components by hot-wire anemometer in

a cyclone chamber with four tangential inlets positioned equidistant over the circumference. They showed that symmetry in the cyclone flowfield is obtained not only for the time-mean values but for the turbulent characteristics of the flow. Vatistas (32) found that the dimensional core size, pressure drop, and radial pressure distribution depend solely upon the geometrical parameters of cyclone chamber from the analytical model with potential flow assumption and confirmed their findings with experiment.

Styles et al (34) have done detailed experimental measurements on a multi-inlet cyclone combustion under both isothermal and combustion conditions. They visualized the flow structure within the combustor with a water model. Pressure drop and processing vortex core frequency were measured for a fuel gas/air mixture model under both conditions using a pressure transducer. Temperature measurements were also obtained in the downstream region of the exit on combustion condition by thermocouples.

Khalil and Lilley (35), characterized the exit flow of a cyclone chamber with exit nozzle, and visualized the particle distribution at the cyclone exit. They also measured the concentration of particles in a mixed air particle flow by a direct probe sampling method. The same facility was used by Chai (36) to measure the time-mean velocity in the cyclone, at several station locations for seven different swirl strengths. In the present study, a movable contraction nozzle of area ratio 4 is inserted in the cyclone test section and its location and effect on the upstream mean

velocity flowfield is studied.

2.3 Swirl Flows

Time-mean flowfield measurements were performed by Rhode (37) and Yoon and Lilley (38) with a traversing five-hole pitot probe in a confined jet with downstream blockage. These measurements were performed on a confined nonswirling flow and various swirling flows. It was determined that the downstream blockage had an increasingly significant effect on corner recirculation patterns as the blockage became positioned closer to the inlet. The data obtained from these experiments were important in evaluating the predictive capability of the k-ε turbulence model and STARPIC computer code. They also assisted in turbulence model developments.

Time-mean velocity measurements immediately downstream of the swirl pack were performed by Sander (39). These measurements were performed and documented for various blade settings, and showed the flowfield typically had a swirl flow angle which was a few degrees smaller than the blade angle. Also, the measurements revealed a larger axial flow in the outer annular portion of the dust, presumably a result of the centrifugal forces associated with the swirl as the flow passed through the swirler.

A significant effort at Oklahoma State University was made in the application of three hot-wire methods to the measurement of time-mean and turbulence properties. Later experiments were performed by Janjua and Jackson (40). It was designed to provide the information necessary for

turbulence modeling development in the confined jet facility. For more detailed information, refer to literature (41).

2.4 Nozzle Effects

Initial work by Rhode (37) utilized the five-hole pitot probe technique to measure time-mean velocities u, v, and w in the large diameter test section with D/d = 2, low swirl strength ϕ = 0 (swirl removed), 38 and 45 degrees, and no nozzles. Later, Yoon (38) extended the study to higher swirl strengths ϕ = 60 and 70 degree, and downstream nozzle effects with both weak and strong nozzles of area ratios A/a = 2 and 4 located at x/D = 1 and 2. Velocities were extensively plotted and artistic impressions of recirculation zones were presented. Findings included that the nonswirling confined jet possesses a corner recirculation zone extending to just beyond x/D = 2 with no central recirculation zone. The presence of a swirler shortens the corner recirculation zone and generates a central recirculation zone followed by a precessing vortex core. The effect of a gradual inlet expansion is to encourage the flow to remain close to the sidewall and shorten the extent of the corner recirculation zone in all cases investigated. A contraction nozzle of area ratio 2 has little effect on weak swirling and strongly swirling flows, which are dominated by forward flow and centrifugal forces, respectively. For intermediate swirl cases, the weak downstream nozzle encourages forward movement of otherwise slow-moving air and thereby shortens the central recirculation zone. A strong contraction nozzle of area

ratio 4 has a more dramatic effect on the flowfield, particularly affecting both intermediate and strong swirling flow cases. Central recirculation zones are shortened considerably, and axial velocities near the facility axis become highly positive. Core regions become narrower with very strong swirl velocity magnitudes and gradients.

More recently, Scharrer (42,43) used the same measurement technique with small diameter test-section tubes with D/d = 1.5 and 1, again with downstream nozzles and a full range of swirl strengths. Findings included that the corner recirculation zone is prominent in nonswirling expanding flows, but it decreases when swirl is introduced. The presence of swirl results in the formation of a central recirculation zone. Initially increases in inlet swirl strength result in an increase in length of this zone. However, increasing to very high swirl strengths results in a shortening and widening of this zone. Placing a downstream nozzle in the flowfield creates an adverse pressure gradient near the wall and a favorable pressure gradient near the centerline. The pressure gradient and the area reduction would increase axial and swirl velocities near the centerline and decrease velocities near the wall. They also decrease the central recirculation zone length. The degree of the effect increases as the degree of the blockage increases. Reduction of the expansion ratio results in a reduction of the central recirculation zone length. The corner recirculation zone length does not change appreciably with expansion ratio for ratios greater than 1. Gradual expansion

has minimal effect on the flow.

CHAPTER III

EXPERIMENTAL FACILITY

The test facility of this experiment has been built by Khalil (35) at the Mechanical Engineering Laboratory of Oklahoma State University. It consists of a cyclone chamber with two inlets (axial and tangential), air blower and stilling chamber for the tangential inlet and exhaust system. The facilities are reviewed here for completeness.

3.1 Test Section

The test section was constructed from different parts and materials; nine inch internal diameter plexiglas tube with 1/8" thickness was used; the convergent divergent nozzle was manufactured from a group of 3/4" thickness very hard wood (Mahogany) stuck together forming a block. The tangential inlet was made up of a box according to the required dimensions and was fixed to an opening made in the 9" tube. The test section is supported by two wooden cradles which are mounted on a table.

The design of the cyclone chamber is shown in figure 2 and the assembly of the different parts forming the cyclone is shown in figure 3.

3.2 Axial Air Arrangements

The axial air is provided from the main compressor of the Laboratory. A pressure regulator is used to control the volume flow rate which is measured by a calibrated rotameter. A pressure manometer is connected to the compressed air line to measure the static pressure. To damp any pressure fluctuation in the compressed air line, a 25 liter pressurized air tank was used.

3.3 Tangential Inlet Arrangements

A centrifugal blower directly coupled to a 1.5 horse power motor was used for the tangential air supply. To control the volume flow rate, a system of two coaxial orifices with slots was used to partially block the blower intake. The maximum output of this blower is 200 cfm.

The stilling chamber consists of a jet facing plate followed by two fine mesh screens. The area reduction section which was designed by the method of Morel (44) to produce a minimum adverse pressure gradient on the boundary layer to avoid the flow unsteadiness phenomenon associated with local separation regions. The slope angle was 5 degrees. The final reduced cross-sectional area was the same like that of the rectangular tangential inlet of the cyclone chamber. A two-hole pitot static pressure probe is embedded in the rectangular section just before the cyclone inlet, to measure the dynamic pressure from which the air velocity and its flow rate can be calculated. Figure 4 illustrate the

design of the stilling chamber which insure the supply of a uniform air velocity to the tangential air inlet of the cyclone.

3.4 Exhaust System

A 25 cm internal diameter flexible duct was fixed to the 9" (22.86 cm) plexiglas tube to exhaust the mixed air-particles flow if present after exiting from the test section.

CHAPTER IV

INSTRUMENTATION AND MEASUREMENT TECHNIQUES

4.1 Velocity Measurements

4.1.1 Introduction

The five-hole pitot probe is one of the few instruments capable of measuring both the magnitude and direction of fluid velocity simultaneously. It has been extensively used in numerous experimental studies (20, 35-38).

4.1.2 Instrumentation

The five-hole pitot probe used in this study is a model DC-125-12-CD manufactured by United Sensor and Control Corp. The sensing head is hook-shaped to allow for probe shaft rotation without altering the probe shaft location. Little information is available concerning the effects of turbulence on a pressure probe in a swirling flows. However it is asserted that the five-hole pitot probe is accurate within approximately 5 percent for most of the measurements (37). This value may increase to 10 percent as the velocity falls below approximately 2.0 m/s because of the insensitivity of probe to low dynamic pressure and the dependence of probe calibration on the probe Reynold's number. The probe is

shown schematically in figure 5 and has a 3.2 mm diameter steel sensing tip and shaft containing five tubes.

The instrumentation assembly, in addition to the five-hole pitot probe, is composed of a manual traverse mechanism, two five-way ball valves, a differential pressure transducer, a power supply, and an integrating digital voltmeter. The differential pressure transduser is model 590D from Data Metrics, Inc. It has a differential pressure range from 0 to 1.3×10^3 N/m^2. The sensing element is high precision stable capacitive potentiometer in which the variable element is a thin, highly, prestressed metal diaphragm. Power for the transducer is provided by a model 721 A Hewlet Pachard power supply. The manual traverse mechanism shown in figure 6 is made entirely of steel with a linear vernier accurately readable within ±0.25 mm. This allows the probe to traverse vertically across the chamber diameter with the capability of manually rotating the probe about its shaft axis to null the yaw angle felt by the pressure sensing tip. This yaw angle is read from the rotary vernier of the traverse unit which is accurately readable within ±0.2 degree.

The pressure transducer output is read as the d.c. signal from the TSI model 1076 integrating voltmeter. Use of an integrating voltmeter removes pressure fluctuations from the vibrating tygon tubing connecting the probe to the valves and transducer. These valves along with the pressure transducer are mounted on a small portable platform (shown in figure 7) in order to minimize the length of tygon tubing for improved dynamic response of the measurement system. Thus

the traverse unit and platform are moved together to each successive axial station.

Finally, auxiliary equipment is used, including a barometer/thermometer unit from Cenco Corp. for local temperature and pressure readings.

4.2 Method of Operation

There are three methods of operation. The first and most lengthy is to adjust the horizontal and vertical orientations of the probe until both pairs of opposing direction-sensing pressures are nulled, which means the probe is aligned perfectly with the local flow direction. With the second method, the probe is fixed and the flow direction and magnitude are determined from the calibration relationships between pressure and flow direction. The third method is simply a hybrid of the first two, where the yaw angle in the horizontal plane is nulled and the pitch angle in the vertical plane is correlated.

The first method is avoided since complicated probe orientation equipment is required. Furthermore, this equipment would probably disturb the flowfield more seriously than approximately 60 degrees and the yaw angle often exceeds this limit. This limit is caused by flow separation at the probe tip. This is why the second method is also avoided. The third method is exclusively employed in this investigation, as pitch angles are always less than 60 degrees except in a very small fraction of the measurement locations.

4.3 Measurement Procedure and Data Reduction

The measurement procedure involves a five-hole pitot probe. It is aligned with the flow yaw angle $\beta = \tan^{-1}(w/u)$ in the plane perpendicular to the radius, while the pitch angle $\delta = \tan^{-1}[v/(u^2 + w^2)^{1/2}]$ and total velocity magnitude V can then be found from the previous corresponding free jet calibrations (37).

Two kinds of calibration are employed to reduce the raw data from the direct measurements. One is the calibration of the voltmeter, which determines a relationship between the voltmeter output and velocity magnitude. The other is the calibration of the five-hole pitot probe, which consists of two calibration characteristics:

(a) Pitch angle δ versus differential pressure ratio $(p_N - p_S)/(p_C - p_W)$.

(b) Velocity coefficient $C = \rho V^2/[2(p_C - p_W)]$ versus pitch angle δ.

In measuring the flow of the test section, a series of radial traverses are taken in a vertical line with probe tip pointing horizontally. With obvious compass notation given to the five-holes, the first measurement for each location is the yaw angle β for a zero reading of $p_W - p_E$. This means that the probe tip is aligned with the local flow direction in a horizontal plane. Then the five-way switching valves are set so that $p_N - p_S$ is sensed by the pressure transducer. Finally the reading of $p_C - p_W$ is similarly measured.

The data reduction employs two calibration curves which

were obtained for a single calibration velocity. The underlying principle is that the calibration is independent of probe Reynold's number Re_p, which is based on probe tip diameter. Careful calibration experiments reveal that this condition exists for Re_p greater than 1090 or a local velocity of 5.4 m/s (37). Hence measurements of such low velocities suffer from a necessary calibration error. However, this error affects the velocity measurements typically by less than 6 percent for $Re_p \geq 400$ corresponding to a local velocity greater than 2.0 m/s. Table 1 includes the calibrated Reynolds numbers that corresponds to all exit velocities.

The differential pressure reading from the five-hole pitot probe are utilized directly to obtain the square of the vector velocity. In turbulent flow conditions, the time-mean pressures give rise to the time mean average of the square of the vector velocity $\overline{V^2}$. Since

$$\overline{V^2} = \bar{V}^2 + \overline{V'^2} \tag{4.1}$$

where V' is the fluctuating portion of the velocity magnitude and the overbar denote time-averaging; It is slightly incorrect to infer that $\overline{V^2}$ is equal to the square of the magnitude of the time-mean velocity vector $\bar{V}^2$. However, the fluctuation term $\overline{V'^2}$ is not known and very little information is available for the effect of turbulence in swirl flows on pressure probes, which is probably considerable, especially for turbulence intensities greater than about 20 percent (1). Furthermore, the procedures for

making corrections for turbulence levels are long and tedious, and even then the confidence in their applicability is unknown. Therefore, no attempt is presently made to incorporate such corrections, and the deduced velocity is taken to be the time-mean velocity magnitude V which is written without the overbar from here onward.

The data at each measurement location are reduced with a Fortran computer program listed in the Appendix, by first calculating the pitch coefficient $(p_N - p_S)/(p_C - p_W)$. From this value a cubic spline interpolation technique is used to obtain the pitch angle δ in the vertical plane from the calibration characteristic presented in figure 8. The resulting value of δ is similarly utilized to determine the velocity coefficient $\rho V^2/2[(p_C - p_W)]$ from the calibration characteristic given in figure 9. The magnitude of the velocity vector is then calculated from

$$V = \left[\frac{2}{\rho}(PC - PW)\cdot C)\right]^{\frac{1}{2}} \tag{4.2}$$

The axial, radial, and swirl velocity components u, v, and w, shown in figure 10, are easily calculated from the velocity coefficient, pitch angle δ, and yaw angle β, which is in the horizontal plane. The latter angle is given by:

$$\beta = 360° - \psi \tag{4.3}$$

where ψ is the probe rotation angle read on the rotary vernier of the traverse mechanism. The velocity components are obtainable from

$$u = V \cos\delta \cos\beta \tag{4.4}$$

$$v = V \sin\delta \tag{4.5}$$

$$w = V \cos\delta \sin\beta \tag{4.6}$$

Further calculations include mass flow rate and axial flux of angular momentum which are respectively expressed as:

$$m = 2\pi \int_0^R \rho\, ur\, dr \tag{4.7}$$

$$G_\theta = \int_0^R \rho uwr^2\, dr \tag{4.8}$$

These are evaluated from the velocity measurements in the vertical plane with the data reduction computer program. It is assumed that measurements in the vertical plane are also applicable in other Θ planes.

4.4 Calibration

Proper calibration of the five-hole pressure probe is extremely critical to the accuracy of the experimental work. Consequently, considerable care was exercised in the construction and use of the calibration equipment. The calibration equipment consists of a small air jet, a rotary table, a probe mounting bracket, and the instrumentation system previously described. The calibration jet supply line consists of a compressed air line which delivers the desired flow rate through a small pressure regulator and a Fischer and Porter model 10A1735A rotameter. The jet housing consists of an effective flow management section followed by a contoured nozzle with a 3.5 cm diameter throat. The rotary table is model BH-9 from Troyke Manufacturing Co. Its rotary

vernier is readable within ± 0.5 minutes. As shown in figure 11, the aluminum probe mounting bracket is secured to the rotary table, and it supports the probe which rests in a cylindrical steel collect.

The motion of the rotary table orients the probe at the desired pitch angle, whereas the yaw is aerodynamically nulled. The probe sensing tip remains at the centerline within the potential core of the jet and less than one throat diameter downstream of the nozzle discharge plane. The pitch angle is zeroed by very carefully aligning the probe shaft in a plane parallel to that of the nozzle throat.

The calibration procedure consists of recording the voltage output from the pressure transducer for differential pressure $p_N - p_s$ and $p_c - p_w$, where these pressures are identified in Fig.5. These data are measured at 5 degrees increments in δ over the range $-58° \leq \delta \leq 58°$. The measurement technique requires the entire calibration to be conducted at a constant jet velocity. This is permitted since the dimensional calibration coefficients are independent of Re_p for $Re_p \geq 1090$ (5.4 m/s) determined by careful calibration experiments. Measurements of much lower velocities suffer from a calibration error. However, this is rarely over 6 percent for $Re_p \geq 400$.

Figures 9 and 10 show the calibration characteristics from which δ and velocity coefficient $\rho V^2/[2(p_c - p_w)]$ are obtained, respectively. Both curves exhibit considerable symmetry, as the five pressure sensing holes are almost symmetrical about the probe tip axis.

CHAPTER V

RESULTS

The major outcome of the current study is the experimental characterization of the flow in a cyclone chamber for four basic flowfields via a five-hole pitot probe technique. It is a continuation and part of an ongoing research at Oklahoma State University. The four flowfield cases are numbered, 2, 4, 6, and 7 to correspond and match the cases studied earlier (35,36). A complete description of the facility and experimental procedure are discussed in Chapters III and IV. The parameters considered in this investigation are the ratios of the tangential air mass flow rate to the axial air mass flow rate (m_t/m_a), tangential air velocity to the mean axial velocity of the cyclone exit (w_t/u_{av}), and the axial location of the contraction nozzle. Four nozzle locations are considered with x/D = 1, 2, 4, and 6, for cases 4 and 7 and two nozzle locations with x/D = 1 and 4 for cases 2, 4, 6, and 7.

The Reynolds numbers employed in this study are high enough to ensure that the flowfields are investigated under conditions independent of Reynolds number variation. A typical percent error is estimated to be 5 percent throughout this study. A summary of operating conditions are listed in

Table 1. It should be noted here that the voltmeter settings are approximate since the tangential velocity depends on the density of the flow which is very much dominated by the atmospheric pressure and temperature of the room. A short computer program was written and used to adjust the exact voltmeter reading that gave the correct tangential velocity for different atmospheric pressure and temperature conditions. Results are tabulated in Table 2. Flow characteristics are tabulated in terms of normalized u, v, and w components, yaw angle β and pitch angle δ in Tables 3 through 14. Axial and swirl velocity profiles for all flowfields studied are shown in Figs. 12 through 23. Note here that the radial velocities are small compared to axial and swirl velocities and therefore not presented in the figures; their values are given, however, in the tables.

5.1 First Nozzle Location (L/D = 1)

5.1.1 Case 2 ($m_t/m_a = 2$ and $w_t/u_{av} = 5.64$)

Figure 12 shows axial and tangential velocity profiles for two station locations, x/D = 0.25 and 0.75. The contraction nozzle with area ratio A/a of 4 is located one diameter downstream of the inlet expansion plane. In this region, the flow is not uniform because it is very much dominated by the inlets. The axial velocity peaks near the centerline with no backflow occuring near the tube wall. Chai (36) investigated Case 2 without the nozzle, and his results show a corner recirculation zone near the upper and

lower half of the cross-section. Again the axial velocity at both stations peaks near the centerline with just only slight differences compared to the results obtained in this study. This indicates that the nozzle has negligible effect on the axial velocity and confirms the nonuniformity of the flow in this region.

On the other hand, the nozzle shows a more considerable influence on swirl velocity. The maximum swirl velocity occurs near the centerline, because having a downstream nozzle would create an adverse pressure gradient near the wall and a favorable pressure gradient near the centerline. This, along with the area reduction results in increased axial and swirl velocities near the centerline and decreased velocities near the wall. Chai (36) showed a maximum swirl velocity at the wall attributed to the incoming tangential inlet flow and the strong centrifugal forces present in this region.

Other experimenters investigated the effect of the nozzle on the upstream flowfield. Yoon and Lilley (38) studied the effect of a nozzle of area ratio 4 in a sudden expansion axisymmetric test section with expansion ratio D/d = 2, equipped with a vane swirler. Yoon and Lilley (38) concluded that a strong contraction nozzle generates a high positive axial velocity near the axis, and decelerates the axial velocity close to the top wall. This is due to the favorable pressure gradient created at the centerline. Scharrer and Lilley (42) also studied the effect of a nozzle of area ratio 4 in a sudden expansion axisymmetric test

section with expansion ratio 1 and 1.5. Swirl was provided by a vane swirler. Their results show accelerated axial and swirl velocities at the centerline and decelerated velocities at the wall.

Both Yoon and Lilley (38) and Scharrer (42) had based their investigations on studying the effect of the downstream nozzle on the central recirculation zones and vortex cores. The central recirculation zone is defined as the wide reverse flow region encountered near the inlet. The precessing vortex core is defined as the region of high swirl low axial velocity flow along the axis, which has a relatively constant diameter. No central recirculation zones or vortex cores could be obtained for the type of geometry considered in this investigation. Therefore, only the nozzle influence on the location and magnitude of the maximum axial and tangential velocities are discussed and compared to the present contribution.

5.1.2 Case 4 ($m_t/m_a = 4$ and $w_t/u_{av} = 6.78$)

This is a stronger swirl case with $w_t/u_{av} = 6.78$ compared to 5.64 as in Case 2. The maximum normalized axial velocities in figure 13(a) occur at the centerline and they are less in magnitude compared to axial velocities in Case 2, because of the smaller axial mass flow rate. Again no corner recirculation zone present at the tube wall. Chai's results (36) show a corner recirculation zone with a maximum axial velocity occuring at the centerline. The maximum axial velocities obtained by Chai (36) are somewhat less than those

presented in our present study. This indicates the nozzle role in creating favorable pressure gradient at the centerline that would sharpen and increase the axial velocities.

The swirl velocities in figure 13(b) on the other hand behaves in the same manner as Case 2. The maximum normalized swirl velocities occur near the centerline and have a magnitude greater than those presented in Case 2 as expected. Chai's results (36) show a maximum swirl velocity of about 10, occuring at the tube wall. This swirl velocity is a bit less than the maximum swirl velocity presented here which is about 13. Again this brings up the fact of having a favorable pressure gradient at the centerline of the test section.

In discusing their results, Scharrer and Lilley (42) and Yoon and Lilley (38) concluded that the nozzle would accelerate the axial and swirl velocities at the centerline and decelerate the velocities at the tube wall in the downstream stations close to the nozzle. This again is in good agreement with the present study.

5.1.3 Case 6 ($m_t/m_a = 8$ and $w_t/u_{av} = 7.51$)

This is the strongest inlet swirl velocity considered in this investigation. Figure 14(a) shows the axial velocity profiles occuring at the centerline with a considerable backflow in the lower half of the tube at station 1 (x/D = 0.25). This corner recirculation zone is caused by first, the sudden enlargement of the cross-sectional area, and

second, the dominant inlet swirl velocity. Figure 14(a) shows disturbance and nonhomogenity of the axial velocities caused by the strong inlet swirl velocity. The maximum axial velocity occuring at the centerline is much greater than those obtained in Case 2 even though the axial mass flow rate is smaller.

Swirl velocities on the other hand, figure 14(b), have its maximum near the centerline as expected. Its values are much greater than those obtained in Case 2 (40 to 15). Chai (36) experimented the same case without the nozzle, ended up having much smaller axial and swirl velocities. This again could be explained by the relatively strong favorable pressure gradient created at the centerline due to the nozzle presence. This is in good agreement with Yoon's (38), Scharrer's (42), and Jackson's (44) results. Jackson investigated swirling and nonswirling flows in a sudden expansion axisymmetric test section using a single hot wire technique. Yoon (38), Scharrer (42), and Jackson (44) concluded that increasing the swirl velocity would increase the favorable pressure gradient at the centerline and the adverse pressure gradient at the wall. This raises the possibility of having this adverse pressure gradient to overcome the axial momentum at the wall and therefore a corner recirculation zone to occur.

It should be noted here that no trusted conclusions could be made at this point, because for this geometry and this nozzle location, the flow is very much dominated by the

inlets. Therefore conclusions could be misleading.

5.1.4 Case 7 ($m_t/m_a = 0$ and $w_t/u_{av} = 0$)

In this case there is no swirl present. Figure 15 shows the normalized axial velocity at stations x/D = 0.25 and 0.75. The maximum axial velocity at both stations is about 30, with a backflow occuring at the first station. Chai (36) experimented the same case without the nozzle, his results showed a maximum axial velocity of about 30, very much consistent with our results. This indicates that the nozzle has negligible effect when there is no swirl present.

Yoon (38) studied the effect of a nozzle of area ratio 4 in a sudden expansion axisymmetric test section with expansion ratio D/d = 2 and no swirl present. His results show that the flowfield with a strong contraction nozzle (area ratio 4) changes very little as compared to the corresponding flowfield with a weak contraction nozzle, or the corresponding flowfield without a contraction nozzle. This is in good agreement with our present study. Scharrer (42) experimented the same case with an expansion ratio of 1.5. He concluded that the nozzle shortens somewhat the corner recirculation zone with reattachment point x/D = 1.2. Jackson (44) concluded that results would vary very little from that of the corresponding flowfield without a contraction nozzle. The major difference appears to be a slight reduction in the length of the corner recirculation zone.

5.2 Second Nozzle Location (L/D = 2)

5.2.1 Case 4 (m_t/m_a = 4 and w_t/u_{av} = 6.78)

This is a strong swirl case with w_t/u_{av} = 6.78. The nozzle is located 2 diameters down the stream (L/D = 2). Figure 16 shows the normalized axial and swirl velocities at two station locations (x/D = 0.75 and x/D = 1.75). The maximum axial velocities take place at the centerline. It is about 7 at the first station and 5 at the second station. The maximum axial velocity at the first station is about 4 when the nozzle was placed one diameter downstream. This indicates that the flow at this station is dominated by the inlets. The axial and swirl velocities at the wall are greater than those presented at nozzle location (L/D = 1), because we have much less adverse pressure gradient as we move the nozzle downstream. Chai's results (36) show that the maximum axial velocity at the second station right before the nozzle is about 3. It occurs at the wall rather than the centerline as in our case. This is explained by the expected favorable pressure gradient created at the centerline due to the nozzle presence. This pressure gradient would accelerate the axial and swirl velocity at the centerline and decelerate the velocities at the wall.

Yoon and Lilley (38), Scharrer and Lilley (42), and Jackson (44) agreed that the nozzle would create favorable pressure gradient at the centerline and adverse pressure gradient at the wall. They also concluded that its influence on the upstream velocity profiles would decrease as we move

it down the stream.

5.2.2 Case 7 ($m_t/m_a = 0$ and $w_t/u_{av} = 0$)

In this case there is no swirl present. Figure 17 shows the normalized axial velocities at stations (x/D = 0.75 and 1.75). The nozzle is placed two diameters down the stream. The maximum axial velocities is about 30 at the first station and 20 at the second station, very much consistent with the results obtained, when the nozzle was placed one diameter down the stream. Chai (36) experimented the same case without the nozzle, his results show a maximum axial velocities of about 30 and 20 very much similar to our results. This indicates the negligible effect of the nozzle when there is no swirl present.

As discussed before, Yoon's (38), Scharrer's (42), and Jackson's (44) results show that the flowfield with a strong contraction nozzle (area ratio 4) changes very little as compared to the corresponding flowfield without a contraction nozzle. The only difference appeared to be a slight reduction in the length of the corner recirculation zone. These conclusions are in good agreement with our present study. It should be noted that the flowfield is more axisymmetric and homogeneous compared to the previous cases.

5.3 Third Nozzle Location (L/D = 4)

5.3.1 Case 2 ($m_t/m_a = 2$ and $w_t/u_{av} = 5.64$)

Figure 18 shows the normalized axial and swirl velocities at station locations x/D = 0.25, 0.75, 1.25, 1.75, 2.25, 2.75, and 3.75. The nozzle is placed 4 diameters down stream. The maximum axial velocities occur at the centerline at all station. Its value is about 7 at station (x/D = 3.75), right before the nozzle. Results obtained by Chai (36) show that the axial velocity at this station is about 2, 3.5 times less. This is due to the favorable pressure gradient created at the centerline due to the nozzle's presence. This pressure gradient would accelerate the axial and swirl velocities at the centerline and the adverse pressure gradient will decelerate the velocities at the wall. As we go up the stream the axial velocity at the centerline decreases until we get to station 2, (x/D = 0.75) then it will increase again. The decrease in axial velocity is due to the decrease in the favorable pressure gradient as we go up the stream. The increase in axial velocity at station one (x/D = 0.25) is due to the domination of the inlets.

The axial velocities at the first two stations (x/D = 0.25 and 0.75) match very much with the profiles obtained by Chai (36). This indicates that the axial velocities in this region are dominated by the inlets and therefore the nozzle has negligible effect on it. Moving further downstream, the axial velocities increase because they fall under the influence of the favorable pressure gradient created by the

nozzle located at (L/D = 4).

The swirl velocity in Fig.18(b) fall under the influence of the favorable pressure gradient as well. The maximum swirl velocity occurs near the centerline. As we go up the stream the swirl velocity starts decreasing near the centerline and increasing at the wall. This is due to the decrease in favorable pressure gradient at the centerline and adverse pressure gradient at the wall. At the first two station, the flowfield is dominated by the inlets and the adverse pressure gradient is not large enough to overcome the centrifugal forces. This is why swirl velocity at these stations occurs at the wall rather than the centerline. Again as we go downstream, the flow tends to be more axisymmetric due to the presence of the nozzle.

Note that Yoon and Lilley (38), Scharrer (42), and Jackson (44) agreed that the nozzle influence on the upstream flowfields gradually decrease as what happened.

5.3.2 Case 4 ($m_t/m_a = 2$ and $w_t/u_{av} = 6.78$)

This is a stronger swirl velocity compared to Case 2. Figure 19 shows the normalized axial and swirl velocities at stations x/D = 0.25, 0.75, 1.25, 1.75, 2.25, 2.75, and 3.75. The nozzle is placed four diameters downstream. The flowfield behaves in the same manner as Case 2. The maximum axial velocities occur at the centerline at all stations. The axial velocity at the station right before the nozzle is about 8, 4 times greater than that without the nozzle. This indicates a stronger nozzle influence compared to Case 2.

Again this is due to the favorable pressure gradient created at the centerline. Going further upstream, the axial velocity decreases at the centerline and increases at the wall. Back flow occurs at the first three stations around a dimensionless radius of 0.25. The expansion of the tangential flow in the cross section, the increase in axial velocity at the wall due to a minimum adverse pressure gradient, and decrease in axial velocity at the centerline due to a minimum favorable pressure gradient, all contributed to cause this back flow between the wall and the centerline.

The swirl velocity again occurs near the centerline. Its maximum value is about w/u_{av} = 10 at station 7, (x/D = 3.75) compared to 5 for the same case without the nozzle, and 8 for Case 2. This again indicates a stronger nozzle effect compared to Case 2. Going further upstream, the maximum swirl velocity starts decreasing near the centerline and increasing at the wall, due to the decrease in the favorable pressure gradient at the centerline and the adverse pressure gradient at the wall created by the nozzle. At station 2 (x/D = 0.75), the maximum swirl velocity starts to occur at the wall rather than the centerline. This indicates the domination of the centrifugal forces in this region, eventhough the favorable pressure gradient near the centerline is still noticeable. It should be noted that the flow tends to be more axisymmetric as we go downstream because of the nozzle role in providing homogenity to the flow.

5.3.3 Case 6 ($m_t/m_a = 8$ and $w_t/u_{av} = 7.51$)

This is the strongest swirl velocity considered in this investigation. Figure 20 shows the normalized axial and swirl velocity profiles at stations, x/D = 0.25, 0.75, 1.25, 1.75, 2.25, 2.75, and 3.75. The maximum axial velocity occurs at the centerline, it is about four times larger than that without the nozzle. Going further upstream, the axial velocity decreases at the centerline and increases at the wall due to the decrease in the favorable pressure gradient at the centerline and adverse pressure gradient at the wall. Considerable back flow occurs around a dimensionless radius of 0.25 at all upstream stations. This is due to the expansion of the strong tangential inflow and the decrease in the favorable and adverse pressure gradients. Results obtained by Chai (36) show a maximum axial velocity occuring at the wall because the centrifugal forces developed by the tangential inflow dominate the flow and disturb the axial velocity. Figure 20(a) shows a nonuniform axial velocity at the centerline which indicates the disturbance of the flow by the strong centrifugal forces. It seems like the flow at the centerline does not have enough momentum to carry on. Again the back flow in this case is more considerable compared to Cases 4 and 2 due to a stronger tangential inlet.

The maximum swirl velocity occurs near the centerline with a maximum velocity of about 40, five times greater than that without the nozzle. This again indicates a stronger nozzle effect compared to Cases 2 and 4. Going further

upstream, the maximum swirl velocity starts decreasing near the centerline and increasing at the wall due to the decrease in the favorable pressure gradient at the centerline and adverse pressure gradient at the wall created by the nozzle. Figure 20(b) shows that the favorable pressure gradient at all stations is large enough to overcome the centrifugal forces created by the tangential inlet flow. At the first two stations (x/D = 0.25 and 0.75), the maximum swirl velocity occurs near the centerline and then at the wall because this region is under the effect of the strong centrifugal forces that will damp out as we go down the stream.

Again, it must be noted here that Yoon and Lilley (38), Scharrer (42), and Jackson (44) concluded that the nozzle influence on the upstream flowfields would gradually decrease at measuring stations progressively further upstream from the nozzle

5.3.4 Case 7 ($m_t/m_a = 0$ and $w_t/u_{av} = 0$)

There is no swirl present in this case. Figure 21 shows the normalized axial velocity at stations, x/D = 0.25, 0.75, 1.25, 1.75, 2.25, 2.75, and 3.75. The maximum normalized axial velocity occurs at the centerline, it is about 4 at the last station (x/D = 3.75) compared to almost zero for the case without the nozzle. This indicates the nozzle influence in accelerating the flow at the centerline due to the created favorable pressure gradient. At the measuring stations close to the inlets, the flowfield is less influenced by the

nozzle. It tends to be very similar to the flowfields obtained by Chai (36) at station 4 (x/D = 1.75). This indicates that the nozzle has no effect what so ever on the flowfield of the first 4 stations (up to x/D = 1.75). Measurements were taken at five stations only (x/D = 1.25, 1.75, 2.25, 2.75, and 3.75). Experimental data at the first two stations were borrowed from Chai's results (36) after the flowfield's independency of the nozzle was proved.

Yoon and Lilley (38), Scharrer and Lilley (42), and Jackson (44) who had done similar experiments on different geometries, concluded that results would vary very little from that of the corresponding flowfield without a contraction nozzle. This is in good agreement with the present study.

5.4 Fourth Nozzle Location (L/D = 6)

5.4.1 Case 4 ($m_t/m_a = 2$ and $w_t/u_{av} = 6.78$)

Figure 22 shows the normalized axial and swirl velocities at stations (x/D = 0.75, 1.75, 2.25, 3.75, 4.75, and 5.75). The nozzle is placed six diameters down the stream. The maximum normalized axial velocity occurs at the centerline. It peaks at the centerline due to the favorable pressure gradient created by the nozzle. At the measuring stations, close to the inlets, the maximum axial velocity starts decreasing due to the decrease in the favorable pressure gradient. At station three (x/D = 2.25) the flowfield would tend to be similar to the flowfield obtained

by Chai (36) without the nozzle. This is an indication that the upstream nozzle influence on the normalized axial velocity ends at station 3 (x/D = 2.25). The normalized axial velocity at the first two stations (x/D = 0.75 and 1.75) match exactly with the profiles obtained by Chai (36). Figure 22(a) shows a nonuniform normalized axial velocity at the centerline. The flowfield at the centerline is affected by the axial inlet, the strong centrifugal forces, the favorable pressure gradient at the centerline, and the adverse pressure near the wall. All this caused this nonhomogenity in the flowfield, add to it the insensitivity of the probe in providing non exact readings.

Swirl velocity on the other hand occurs near the centerline, it is about w/u_{av} = 8 at the last station (x/D = 5.75) compared to 5 for the case without the nozzle. The favorable pressure gradient created by the nozzle, would accelerate the flow near the centerline. Further upstream, the normalized swirl velocity starts decreasing at the centerline and increasing at the wall, due to the decrease in adverse pressure gradient created by the nozzle. At station 2 (x/D = 1.75) the maximum starts to occur at the wall rather than near the centerline, this is an indication of having negligible adverse pressure gradient and dominant centrifugal forces. The domination of centrifugal forces at the first two stations (x/D = 0.75 and 1.75) causes the normalized swirl velocity to occur at the wall, even though the favorable pressure gradient is still noticeable.

5.4.2 Case 7 ($m_t/m_a = 0$ and $w_t/u_{av} = 0$)

In this case there is no swirl present. Figure 23 shows the normalized axial velocity at stations (x/D = 0.75, 1.75, 2.25, 3.75, and 5.75). The nozzle is placed six diameters downstream. Figure 23 shows that the nozzle has no effect what so ever on the flowfield down the stream since it is a weak region and the velocity is almost zero. Further upstream we start getting into a much stronger region, the normalized axial velocity peaks at the centerline because it falls under the influence of the inlet. The flowfields obtained at almost all stations are very similar to the flowfields obtained by Chai (36). This indicates that the nozzle has very negligible effect on the upstream flowfield.

5.5 Nozzle Effects

The nozzle effects on the upstream flowfield can best be seen by plotting the maximum axial and swirl velocity magnitudes for both situations, with and without the nozzle. Experimental data for the cases without the nozzle are adapted from Chai (36).

Figures 24, 26, 28, and 30 show the variations in the magnitude of the downstream axial velocity at the centerline for all cases, with and without the nozzle. Figures 25, 27, and 29 show the variations in the magnitude of the downstream maximum swirl velocities for all cases, with and without the nozzle. In Case 2, the weak swirl case, a nozzle has no effects on the flowfield close to the inlets. Further

downstream, the flow without a nozzle would encounter a weak region and damp out consequently, whereas the flow with a nozzle would slow down first then pick up speed due to the favorable pressure gradient created by the nozzle. For the moderate and strong swirl cases, the effect of a nozzle on the upstream flowfield would still be considerable up to the inlets. The centrifugal forces created by the tangential inlet are not high enough to overcome the favorable pressure gradient created by the downstream nozzle. Therefore the effects of the nozzle dominates the flow throughout. For the no swirl case, Figure 30 shows that the nozzle has no remarkable effects on the upstream flowfield.

5.6 Recirculation Zones

General observations of recirculation zones in the test section for all nozzle locations are given in Figs. 31 through 34. Figure 31 shows recirculation zones for Cases 2, 4, 6, and 7 when the nozzle is placed one diameter downstream. For all the cases, recirculation zones are more prominent in the lower half of the test section. They also get wide and wide (in r-direction) as swirl increases. For the case with no swirl, corner recirculation zones appear due to the sudden enlargement of the axial inlet. Figure 32 shows recirculation zones for Cases 4 and 7 when the nozzle is two diameters downstream. The figure shows two long but narrow downstream recirculation zones in Case 4, the moderate swirl case and no recirculation zones in Case 7, the case with no swirl. Figure 33 shows recirculation zones for all

the cases and four diameters downstream nozzle location. Results show that moving the nozzle downstream would create longer recirculation zones and increasing the swirl would widen it.

Figure 34 shows recirculation zones for Cases 4 and 7 when the nozzle is placed six diameters downstream. Two narrow recirculation zones are observed in Case 4, the moderate swirl case and nothing observed in Case 7, the case with no swirl.

5.7 Spreading Rate of Jets

Spreading rate of jets, Figure 35 was sketched for the vertical plane of the measurements when the nozzle was placed four diameters downstream. Results did not show any jet spreading for the weak, moderate, and strong swirl cases. However, the jet spreaded significantly when there was no swirl present. The spreading half angle of the jet was measured to be 6.5 degrees compared to 4.8 degrees for turbulent axisymmetric free jets (1).

The free jets were sketched for the vertical plane of the measurements in an attempt to draw useful conclusions on the effect of swirl and a downstream nozzle on the spreading rate of the jet. It turned out that such conclusions could be misleading since the flow is fully three-dimensional. It should also be noted that there are two inlets (axial and tangential) and that the vertical plane measurements are insufficient to draw useful conclusions about the jet spread.

CHAPTER VI

6.1 CONCLUSION

The ability to predict the influence of design parameters on the aerodynamics of cyclone chambers flows is of prime concern in furnace engineering and a number of high temperature processes. The advantages and main characteristics of cyclone processes are primarily due to the particular pattern of the flowfields produced, which depends on a number of design parameters, including diameter and length of the chamber, size of outlet, size and location of inlets, and the velocity and supply rates through the inlets.

A major outcome of the current study is the experimental characterization of the flow in a cyclone chamber for four basic flowfields. Parameter variations investigated are the ratio of the tangential air mass flow rate to the axial air mass flow rate (m_t/m_a), the ratio of the tangential air velocity to the average axial velocity at the cyclone exit (w_t/u_{av}), and the contraction nozzle location. Measurements of time-mean velocity components to characterize the air flow patterns were done via a five-hole pitot probe. Velocities are extensively plotted and artistic impressions of recirculation zones are presented.

Results showed that having a nozzle downstream would

create favorable pressure gradient at the centerline and adverse pressure gradient at the wall, this would accelerate axial and swirl velocities near the centerline and decelerate the velocities near the wall. Four nozzle locations were considered with L/d = 1, 2, 4, and 6.

Placing the nozzle one diameter downstream would have no effect on the upstream flowfield when there is no swirl present. However, it would have considerable effect if swirl is introduced. Case 2, the weak swirl case would give 1.16 times greater axial velocity compared to the same case without the nozzle. Case 4, the moderate swirl case gives 1.6 times greater axial velocity. Case 6, the strong swirl case would give a dramatic increase in axial velocity. It is about six times greater than the case without the nozzle. This indicates that the nozzle effects are more considerable as swirl velocities increase. Again increasing the swirl would generate a back flow in the lower half of the test section due to the expansion of the tangential inflow.

Moving the nozzle further downstream would reduce the nozzle influence on the upstream flowfield since we start getting into a much weaker region. When the nozzle is placed four diameters downstream, the upstream nozzle effects would still be noticeable at all station for Cases 4 and 6, the high swirl cases, up to the second station location (x/D = 0.75) for Case 2, the low swirl case, and no remarkable influence for the case with no swirl. At six diameters downstream, the upstream nozzle influence would still be noticeable to about 2.5 diameters downstream (x/D = 0.25).

We should note here that the nozzle provided axisymmetric flowfields throughout the test section, except at the first two stations (x/D =0.25 and 0.75) where the flow is dominated by the inlets.

6.2 Recommendations

The five-hole pitot probe technique is a useful cost-effective tool to investigate turbulent swirling recirculating flows. It enables time-mean axial, radial and swirl velocities to be deduced at any location in the flowfield. It has, however, some disadvantages

1. Weak sensitivity to small velocities.
2. Turbulence effects cannot be accounted for.
3. We can not measure normal and shear turbulent stresses.

It should also be noted here that finding the mass from the experimental values of the velocities does not prove conservation of mass since measurements were taken for the vertical plane while the flow is three-dimensional and not axisymmetric. This research could be extended in several areas. The nozzle angles and size can be studied to obtain a more complete fundamental understanding of the nozzle effect on the upstream flowfield.

To have much more reliable and accurate results in regions of small velocities, the use of hot-wire and laser doppler anemometer are highly recommended.

REFERENCES

(1) Gupta, A. K., Lilley, D. G.,and Syred, N. Swirl Flows. Abacus Press, Turnbrige Wells, England, 1984.

(2) Gupta, A. K. and Lilley, D. G., Flowfield Modeling and Diagnostics. Abacus Press, Turnbrige Wells, England, 1985 .

(3) Lilley, D G., "Swirl Flows in Combustion: A Review." AIAA Journal, Vol. 15, No. 8, Aug. 1977, pp 1063-1078

(4) Beer, J. M. and Chigier, N. A., Combustion Aerodynamics. Halsted-wiley, New York, 1972

(5) Syred, N. and Beer, J. M., "Combustion in Swirling Flows: A Review", Combustion and Flame, Vol.23, 1974, pp 143-201

(6) Chigier, N. A., "Gasdynamics of Swirling Flow in Combustion System", Astronautica Acta, Vol.17, 1972, pp 387-395

(7) Putnam, A. A., "Swirl Burning", American Flame Research Committee, Jan 18, 1967.

(8) Beer, J. M., "Recent Advances in the Technology of Furnace Flames" Journal of Institute of Fuel, Vol.45, July 1972, pp 370-382

(9) Bradshan, P., "Effects of Streamline Curvature on Turbulent Flow." AGARD-AG0169, Aug, 1973.

(10) Murthy, S. N. B., "Survey of Some Aspects of Swirling Flows." Aeronautical Research Lab., Cornell, ARL-71-0244, and National Technical Information Service, NTIS-AD737381.

(11) Lewellen, W. S., "A Review of Confined Vortex Flows." NASA CR-1772, 1971.

(12) Rietema, K. and Verver, C. G. Cyclones in Industry. Elsevier Pub. Co., New York, 1961.

(13) Priestly, G. and Stephens, H. S. "Hydrocyclones."

International Conference on Hydrocyclones, Cambridge, England, October 1-3, 1980.

(14) Bradley, D. The Hydrocyclone. Technomic Pub. Co., New York, 1984.

(15) Svarovsky, L. Hydrocyclone. Pergamon Press, New York, 1965.

(16) Poole, J. B. and Doyle, D. Solid-liquid Separation Chemical Pub. Co., New York, 1968.

(17) Bryer, D. W. and Pankhurst, R. C. Pressure-Probe Methods for Determining Wind Speed and Flow Direction. Her Magesty's Stationary Office, London, 1971.

(18) Stambuleanu, A. Flame Combustion Processes in Industry. Abacus Press, 1980.

(19) Pownall, J. H., "Cyclones in the Chemical and Process Industry." Chemical and Industry, pp 1888-1896, November, 1961.

(20) Shepherd, C. B. and Lapple, C. E., "Flow Pattern and Pressure Drop in Cyclone Dust Collectors." Industrial and Engineering Chemistry, 31, pp 972, 1939.

(21) Kelsall, D. F., "A Study of the Motion of Solid Particles in a Hydraulic Cyclone." Trans. Inst. Chem. Engr., 30, pp 87-103.

(22) Bouchillon, C. W., "Particle Trajectories in a Hydrocyclone." Ph.D Thesis, Georgia Institute of Technology, 1963.

(23) Bradley, D. and Pulling, D. J., "Flow Patterns in the Hydroulic Cyclone and their Interpretation in Terms of Performance." Trans, Inst. Chem. Engr. 37, pp 34-44, 1959.

(24) Gilbert, S. G., "An Evaluation of a Small Hydrocyclone Using Electrical Analog Techniques." Master Thesis, University of Oklahoma, 1958

(25) Smith, J. L. "An Experimental Study of the Vortex in the Cyclone Separator." ASME, Paper No 61-WA-188.

(26) Milne-Thompson, L. M., Theoretical Hydrodynamics, The Macmillan Co., New York, pp 352-355, 1968.

(27) Drissen, M. G., "Theory of Flow in a Cyclone." Rev. Industr. Min, p.449, 1950.

(28) Binder, R. C., Fluid Mechanics. Prentiss-Hall Inc., Englewood Cliffs, pp 168-171, 1955

(29) Smith, D. R., "An Investigation of the Flow In a Hydrocyclone By Axial Probing." Thesis, Mississippi State University, 1970.

(30) Baluev, E. D., and Troyankin, Y. V., "Study of the Aerodynamic Structure of Gas Flow in a Cyclone Chamber." Thermal Engineering, Vol. 14, No. 1, pp 84-87, 1967

(31) Syred, N., and Dahman, K. R., "The Combustion of Low Calorific Value Waste Gas." Proc. 2nd European Symposium on Combustion, Orleans, France, pp 414-419, 1975

(32) Vatistas, G. H., Lin, S., and Kwok, C. K. "Theoretical and Experimental Studies on Vortex Chamber Flows." AIAA Journal, Vol. 24, No. 4, April 1986, pp.635-642.

(33) Ustimenko, B. P. and Bukhman, M. A. "Turbulent Flow Structure in a Cyclone Chamber." Thermal Engineering, Vol. 15, No. 2, 1968, pp.90-

(34) Styles, A. C., Syred, N., and Najim, S. E., "A Study of Modulatable Cyclone Combustors Using Gaseous Fuel." Paper presented at Spring Meeting of Central Section, The Combustion Institute, NASA Lewis Research Center, OH, March 1977.

(35) Khalil, A. H. and Lilley, D. G. "Experimental Study of Exit Velocity and Relative Particle Concen-tration Distributions from Two-Phase Flow in a Cyclone Mixer." Report, 1987, Oklahoma State University.

(36) Chai, W. D., "Time-Mean Velocity Measurements in Sudden Expansion Confined Flow with Tangential Injection." M.S. Thesis, Oklahoma State University, Stillwater, Ok, May, 1988.

(37) Rhode, D. L. "Predictions and Measurements of Isothermal Flowfields in Axisymmetric Combustion Geometries." Ph.D. Thesis (December, 1981), Oklahoma State University.

(38) Yoon, H. K. and Lilley, D. G. "Five-Hole Pitot Probe Time-Mean Velocity Measurements in Confined Swirling Flows." Paper AIAA-83-0, Reno, Nevada, Jan 10-13, 1983, Also AIAA Journal, Vol. 22, No. 4, pp 514-515, April 1984.

(39) Sander, G. F., and Lilley, D. G., "The Performance of an Annular Vane Swirler." Paper AIAA 83-1326, Seattle, Washington, June 27-29, 1983.

(40) Janjua, S. I., Mclaughlin, D. K., Jackson, T. W. and Lilley, D. G., "Turbulence Measurements in a Confined Jet Using A Six-Orientation Hot-Wire Probe Technique." Paper AIAA-82-1262, Cleveland, Ohio, June 21-23, 1982, Also AIAA Journal, Vol. 21, No. 12, pp 1609-1610, 1983.

(41) Lilley, D. G. "Investigations of Flowfields Found in Typical Combustor Geometries." NASA Contractor Report 3869, February, 1985.

(42) Scharrer, G. L. "Swirl Expansion Ratio and Blockage Effects on Confined Turbulent Flow." M.S. Thesis , Oklahoma State University, Stillwater, OK, May 1984.

(43) Scharrer, G. L. and Lilley, D. G. "Five-Hole Pitot Probe Measurements of Swirl Confinement and Nozzle Effects on Confined Turbulent Flow." Paper AIAA-84-1605, Snowmass, Colorado, June 25-27, 1984.

(44) Morel, T. "Comprehensive Design of Axisymmetric Wind Tunnel Constructions" ASME paper 75-FE-17, Minneapolis ,Minn, May 5-7, 1975.

(45) Jackson, T. W. "Turbulence Characteristics of Swirling Flowfields" Ph.D. Thesis (December, 1983), Oklahoma State University.

APPENDIX A

TABLES

TABLE I

SUMMARY OF OPERATING CONDITIONS

Case No	m_t (CFM)	m_a (CFM)	m_t/m_a	w_t/u_{av}	Voltmeter Reading	u_{av} (m/s)	Re_D
2	70	35	2	2.83	0.052	1.207	18302
4	80	20	4	6.78	0.068	1.14	17431
6	128	16	8	7.5	0.172	1.655	25100
7	0	38.5	0	0	0	0.44	6688

TABLE II

VOLTMETER CALIBRATION CHARTS

(a) CASE 2

Atmospheric Pressure	Temperature	Density (kg/m^3)	Voltmeter Reading
740	12	1.206162	5.257856E-02
740	14	1.197762	5.221241E-02
740	16	1.189479	5.185133E-02
740	18	1.18131	5.149521E-02
740	20	1.173251	5.114395E-02
740	22	1.165303	5.079744E-02
740	24	1.157461	.0504556
740	26	1.149724	5.011833E-02
743	12	1.211052	5.279172E-02
743	14	1.202618	5.242408E-02
743	16	1.194301	5.206154E-02
743	18	1.186099	5.170397E-02
743	20	1.178008	5.135129E-02
743	22	1.170027	5.100338E-02
743	24	1.162153	5.066015E-02
743	26	1.154385	5.032152E-02
746	12	1.215941	5.300487E-02
746	14	1.207474	5.263576E-02
746	16	1.199123	5.227175E-02
746	18	1.190888	5.191274E-02
746	20	1.182764	5.155863E-02
746	22	1.174751	5.120931E-02
746	24	1.166846	5.086471E-02
746	26	1.159046	.0505247
749	12	1.220831	5.321803E-02
749	14	1.21233	5.284743E-02
749	16	1.203946	5.248195E-02
749	18	1.195677	.0521215
749	20	1.187521	5.176597E-02
749	22	1.179475	5.141525E-02
749	24	1.171538	5.106925E-02
749	26	1.163707	5.072788E-02
752	12	1.225721	5.343119E-02
752	14	1.217185	.0530591

TABLE II (Continued)

CASE 2 (Continued)

752	16	1.208768	5.269216E-02
752	18	1.200466	5.233027E-02
752	20	1.192277	5.197331E-02
752	22	1.184199	5.162118E-02
752	24	1.17623	.0512738
752	26	1.168368	5.093106E-02
755	12	1.230611	5.364434E-02
755	14	1.222041	5.327077E-02
755	16	1.21359	5.290237E-02
755	18	1.205255	5.253904E-02
755	20	1.197034	5.218065E-02
755	22	1.188924	5.182712E-02
755	24	1.180923	5.147835E-02
755	26	1.173029	5.113424E-02
758	12	1.235501	.0538575
758	14	1.226897	5.348245E-02
758	16	1.218412	5.311258E-02
758	18	1.210044	.0527478
758	20	1.20179	5.238799E-02
758	22	1.193648	5.203306E-02
758	24	1.185615	.0516829
758	26	1.17769	5.133742E-02
761	12	1.240391	5.407065E-02
761	14	1.231753	5.369411E-02
761	16	1.223234	5.332279E-02
761	18	1.214833	5.295656E-02
761	20	1.206546	5.259533E-02
761	22	1.198372	.052239
761	24	1.190308	5.188745E-02
761	26	1.182351	5.154061E-02
764	12	1.245281	5.428381E-02
764	14	1.236609	5.390579E-02
764	16	1.228057	.053533
764	18	1.219622	5.316533E-02
764	20	1.211303	5.280267E-02
764	22	1.203096	5.244493E-02
764	24	1.195	.052092
764	26	1.187012	5.174379E-02

TABLE II (continued)

(b) CASE 4

Atmospheric Pressure	Temperature	Density (kg/m^3)	Voltmeter Reading
740	12	1.206162	6.867404E-02
740	14	1.197762	.0681958
740	16	1.189479	6.772418E-02
740	18	1.18131	6.725905E-02
740	20	1.173251	6.680025E-02
740	22	1.165303	6.634768E-02
740	24	1.157461	6.590119E-02
740	26	1.149724	6.546068E-02
743	12	1.211052	6.895245E-02
743	14	1.202618	6.847227E-02
743	16	1.194301	6.799874E-02
743	18	1.186099	6.753172E-02
743	20	1.178008	6.707106E-02
743	22	1.170027	6.661666E-02
743	24	1.162153	6.616836E-02
743	26	1.154385	6.572606E-02
746	12	1.215941	6.923086E-02
746	14	1.207474	6.874875E-02
746	16	1.199123	.0682733
746	18	1.190888	.0678044
746	20	1.182764	6.734188E-02
746	22	1.174751	6.688564E-02
746	24	1.166846	6.643553E-02
746	26	1.159046	6.599143E-02
749	12	1.220831	6.950926E-02
749	14	1.21233	6.902521E-02
749	16	1.203946	6.854785E-02
749	18	1.195677	6.807706E-02
749	20	1.187521	.0676127
749	22	1.179475	6.715461E-02
749	24	1.171538	6.670269E-02
749	26	1.163707	6.625681E-02
752	12	1.225721	6.978767E-02
752	14	1.217185	6.930168E-02

TABLE II (Continued)

CASE 4 (Continued)

752	16	1.208768	6.882241E-02
752	18	1.200466	6.834973E-02
752	20	1.192277	.0678835
752	22	1.184199	6.742358E-02
752	24	1.17623	6.696986E-02
752	26	1.168368	.0665222
755	12	1.230611	7.006608E-02
755	14	1.222041	6.957816E-02
755	16	1.21359	6.909698E-02
755	18	1.205255	6.862241E-02
755	20	1.197034	6.815432E-02
755	22	1.188924	6.769256E-02
755	24	1.180923	6.723703E-02
755	26	1.173029	6.678758E-02
758	12	1.235501	7.034449E-02
758	14	1.226897	6.985462E-02
758	16	1.218412	6.937153E-02
758	18	1.210044	6.889509E-02
758	20	1.20179	6.842513E-02
758	22	1.193648	6.796155E-02
758	24	1.185615	.0675042
758	26	1.17769	6.705296E-02
761	12	1.240391	.0706229
761	14	1.231753	7.013109E-02
761	16	1.223234	6.964609E-02
761	18	1.214833	6.916775E-02
761	20	1.206546	6.869594E-02
761	22	1.198372	6.823053E-02
761	24	1.190308	6.777136E-02
761	26	1.182351	6.731834E-02
764	12	1.245281	7.090131E-02
764	14	1.236609	7.040756E-02
764	16	1.228057	6.992065E-02
764	18	1.219622	6.944042E-02
764	20	1.211303	6.896676E-02
764	22	1.203096	6.849949E-02
764	24	1.195	6.803853E-02
764	26	1.187012	6.758373E-02

TABLE II (continued)

(c) CASE 6

Atmospheric Pressure	Temperature	Density (kg/m^3)	Voltmeter Reading
740	12	1.206162	.1758055
740	14	1.197762	.1745813
740	16	1.189479	.1733739
740	18	1.18131	.1721832
740	20	1.173251	.1710086
740	22	1.165303	.16985
740	24	1.157461	.168707
740	26	1.149724	.1675793
743	12	1.211052	.1765183
743	14	1.202618	.175289
743	16	1.194301	.1740768
743	18	1.186099	.1728812
743	20	1.178008	.1717019
743	22	1.170027	.1705386
743	24	1.162153	.169391
743	26	1.154385	.1682587
746	12	1.215941	.177231
746	14	1.207474	.1759968
746	16	1.199123	.1747796
746	18	1.190888	.1735792
746	20	1.182764	.1723952
746	22	1.174751	.1712272
746	24	1.166846	.170075
746	26	1.159046	.1689381
749	12	1.220831	.1779437
749	14	1.21233	.1767045
749	16	1.203946	.1754825
749	18	1.195677	.1742773
749	20	1.187521	.1730885
749	22	1.179475	.1719158
749	24	1.171538	.1707589
749	26	1.163707	.1696174
752	12	1.225721	.1786564
752	14	1.217185	.1774123
752	16	1.208768	.1761854
752	18	1.200466	.1749753
752	20	1.192277	.1737818

TABLE II (Continued)

CASE 6 (Continued)

752	22	1.184199	.1726044
752	24	1.17623	.1714428
752	26	1.168368	.1702968
755	12	1.230611	.1793692
755	14	1.222041	.1781201
755	16	1.21359	.1768882
755	18	1.205255	.1756734
755	20	1.197034	.1744751
755	22	1.188924	.173293
755	24	1.180923	.1721268
755	26	1.173029	.1709762
758	12	1.235501	.1800819
758	14	1.226897	.1788278
758	16	1.218412	.1775911
758	18	1.210044	.1763714
758	20	1.20179	.1751683
758	22	1.193648	.1739816
758	24	1.185615	.1728108
758	26	1.17769	.1716556
761	12	1.240391	.1807946
761	14	1.231753	.1795356
761	16	1.223234	.178294
761	18	1.214833	.1770694
761	20	1.206546	.1758616
761	22	1.198372	.1746701
761	24	1.190308	.1734947
761	26	1.182351	.1723349
764	12	1.245281	.1815073
764	14	1.236609	.1802433
764	16	1.228057	.1789969
764	18	1.219622	.1777675
764	20	1.211303	.1765549
764	22	1.203096	.1753587
764	24	1.195	.1741786
764	26	1.187012	.1730143
767	12	1.25017	.1822201
767	14	1.241464	.1809511

TABLE III

VELOCITY DATA, CASE 2 (L/D = 1), WEAK SWIRL

O	I =	1	2
	X =	0.0063	0.0190
O J	Y		
27	0.0991	0.274E+03	0.280E+03
26	0.0914	0.275E+03	0.278E+03
25	0.0838	0.275E+03	0.277E+03
24	0.0762	0.276E+03	0.276E+03
23	0.0686	0.281E+03	0.276E+03
22	0.0610	0.291E+03	0.278E+03
21	0.0533	0.313E+03	0.280E+03
20	0.0457	0.333E+03	0.283E+03
19	0.0381	0.343E+03	0.289E+03
18	0.0305	0.347E+03	0.296E+03
17	0.0229	0.350E+03	0.307E+03
16	0.0152	0.353E+03	0.324E+03
15	0.0076	0.350E+03	0.346E+03
14	0.0000	0.355E+03	0.700E+01
13	-0.0076	0.900E+01	0.200E+02
12	-0.0152	0.530E+02	0.305E+02
11	-0.0229	0.860E+02	0.420E+02
10	-0.0305	0.920E+02	0.565E+02
9	-0.0381	0.930E+02	0.770E+02
8	-0.0457	0.910E+02	0.840E+02
7	-0.0533	0.900E+02	0.880E+02
6	-0.0610	0.900E+02	0.905E+02
5	-0.0686	0.910E+02	0.930E+02
4	-0.0762	0.910E+02	0.930E+02
3	-0.0838	0.940E+02	0.915E+02
2	-0.0914	0.960E+02	0.900E+02
1	-0.0991	0.930E+02	0.895E+02

(a) Yaw Angle

TABLE III (Continued)

	I =	1	2
	X =	0.0063	0.0190
O J	Y		
27	0.0991	0.293E+01	0.271E+01
26	0.0914	0.400E+01	0.667E+00
25	0.0838	0.589E+01	0.102E+01
24	0.0762	0.808E+01	0.143E+01
23	0.0686	0.111E+02	0.194E+01
22	0.0610	0.134E+02	0.157E+01
21	0.0533	0.186E+02	0.220E+01
20	0.0457	0.132E+02	-0.638E+01
19	0.0381	0.927E+01	0.372E+01
18	0.0305	0.698E+01	0.337E+01
17	0.0229	0.550E+01	0.186E+01
16	0.0152	0.571E+01	-0.101E+01
15	0.0076	0.406E+01	-0.638E+01
14	0.0000	0.368E+01	-0.794E+01
13	-0.0076	0.628E+01	-0.739E+01
12	-0.0152	0.302E+02	-0.496E+01
11	-0.0229	0.185E+02	-0.886E+00
10	-0.0305	0.130E+02	0.375E+01
9	-0.0381	0.111E+02	0.571E+01
8	-0.0457	0.943E+01	0.641E+01
7	-0.0533	0.903E+01	0.646E+01
6	-0.0610	0.912E+01	0.684E+01
5	-0.0686	0.798E+01	0.634E+01
4	-0.0762	0.820E+01	0.564E+01
3	-0.0838	0.581E+01	0.502E+01
2	-0.0914	0.403E+01	0.449E+01
1	-0.0991	0.359E+01	0.396E+01

(b) Pitch Angle

TABLE III (Continued)

	I =	1	2
	X =	0.0278	0.0833
O J	Y		
27	0.4333	0.489E+00	0.112E+01
26	0.4000	0.656E+00	0.979E+00
25	0.3667	0.696E+00	0.890E+00
24	0.3333	0.855E+00	0.809E+00
23	0.3000	0.148E+01	0.863E+00
22	0.2667	0.233E+01	0.116E+01
21	0.2333	0.332E+01	0.155E+01
20	0.2000	0.471E+01	0.135E+01
19	0.1667	0.651E+01	0.310E+01
18	0.1333	0.773E+01	0.407E+01
17	0.1000	0.788E+01	0.502E+01
16	0.0667	0.721E+01	0.576E+01
15	0.0333	0.743E+01	0.604E+01
14	0.0000	0.681E+01	0.631E+01
13	-0.0333	0.480E+01	0.675E+01
12	-0.0667	0.185E+01	0.639E+01
11	-0.1000	0.508E+00	0.567E+01
10	-0.1333	-0.342E+00	0.454E+01
9	-0.1667	-0.522E+00	0.215E+01
8	-0.2000	-0.165E+00	0.105E+01
7	-0.2333	0.277E-04	0.349E+00
6	-0.2667	0.264E-04	-0.820E-01
5	-0.3000	-0.134E+00	-0.468E+00
4	-0.3333	-0.134E+00	-0.437E+00
3	-0.3667	-0.511E+00	-0.207E+00
2	-0.4000	-0.720E+00	0.249E-04
1	-0.4333	-0.341E+00	0.697E-01

(c) u/u_{av}

TABLE III (Continued)

	I =	1	2
	X =	0.0278	0.0833
O J	Y		
27	0.4333	0.359E+00	0.321E+00
26	0.4000	0.526E+00	0.819E-01
25	0.3667	0.825E+00	0.130E+00
24	0.3333	0.116E+01	0.193E+00
23	0.3000	0.152E+01	0.279E+00
22	0.2667	0.155E+01	0.242E+00
21	0.2333	0.164E+01	0.361E+00
20	0.2000	0.124E+01	-0.696E+00
19	0.1667	0.111E+01	0.636E+00
18	0.1333	0.971E+00	0.557E+00
17	0.1000	0.770E+00	0.274E+00
16	0.0667	0.727E+00	-0.126E+00
15	0.0333	0.536E+00	-0.696E+00
14	0.0000	0.440E+00	-0.887E+00
13	-0.0333	0.535E+00	-0.931E+00
12	-0.0667	0.179E+01	-0.643E+00
11	-0.1000	0.244E+01	-0.118E+00
10	-0.1333	0.226E+01	0.539E+00
9	-0.1667	0.196E+01	0.955E+00
8	-0.2000	0.157E+01	0.113E+01
7	-0.2333	0.138E+01	0.113E+01
6	-0.2667	0.134E+01	0.113E+01
5	-0.3000	0.108E+01	0.992E+00
4	-0.3333	0.110E+01	0.823E+00
3	-0.3667	0.745E+00	0.694E+00
2	-0.4000	0.485E+00	0.615E+00
1	-0.4333	0.409E+00	0.553E+00

(d) v/u_{av}

TABLE III (Continued)

	I =	1	2
	X =	0.0278	0.0833
O J	Y		
27	0.4333	-0.699E+01	-0.668E+01
26	0.4000	-0.750E+01	-0.697E+01
25	0.3667	-0.796E+01	-0.725E+01
24	0.3333	-0.814E+01	-0.770E+01
23	0.3000	-0.762E+01	-0.821E+01
22	0.2667	-0.606E+01	-0.878E+01
21	0.2333	-0.356E+01	-0.927E+01
20	0.2000	-0.240E+01	-0.607E+01
19	0.1667	-0.199E+01	-0.926E+01
18	0.1333	-0.179E+01	-0.854E+01
17	0.1000	-0.139E+01	-0.678E+01
16	0.0667	-0.886E+00	-0.427E+01
15	0.0333	-0.131E+01	-0.151E+01
14	0.0000	-0.596E+00	0.775E+00
13	-0.0333	0.761E+00	0.246E+01
12	-0.0667	0.245E+01	0.376E+01
11	-0.1000	0.726E+01	0.511E+01
10	-0.1333	0.980E+01	0.685E+01
9	-0.1667	0.997E+01	0.931E+01
8	-0.2000	0.946E+01	0.998E+01
7	-0.2333	0.871E+01	0.999E+01
6	-0.2667	0.832E+01	0.940E+01
5	-0.3000	0.769E+01	0.892E+01
4	-0.3333	0.766E+01	0.833E+01
3	-0.3667	0.731E+01	0.790E+01
2	-0.4000	0.685E+01	0.784E+01
1	-0.4333	0.651E+01	0.798E+01

(e) w/u_{av}

TABLE IV

VELOCITY DATA, CASE 4 (L/D = 1), MODERATE SWIRL

	I =	1	2
	X =	0.0063	0.0190
O J	Y		
27	0.0991	0.270E+03	0.278E+03
26	0.0914	0.270E+03	0.277E+03
25	0.0838	0.272E+03	0.276E+03
24	0.0762	0.275E+03	0.275E+03
23	0.0686	0.275E+03	0.275E+03
22	0.0610	0.274E+03	0.275E+03
21	0.0533	0.276E+03	0.276E+03
20	0.0457	0.278E+03	0.278E+03
19	0.0381	0.286E+03	0.281E+03
18	0.0305	0.303E+03	0.286E+03
17	0.0229	0.327E+03	0.297E+03
16	0.0152	0.347E+03	0.313E+03
15	0.0076	0.357E+03	0.334E+03
14	0.0000	0.120E+02	0.357E+03
13	-0.0076	0.410E+02	0.230E+02
12	-0.0152	0.690E+02	0.470E+02
11	-0.0229	0.820E+02	0.660E+02
10	-0.0305	0.900E+02	0.770E+02
9	-0.0381	0.920E+02	0.835E+02
8	-0.0457	0.920E+02	0.885E+02
7	-0.0533	0.900E+02	0.890E+02
6	-0.0610	0.900E+02	0.900E+02
5	-0.0686	0.910E+02	0.910E+02
4	-0.0762	0.940E+02	0.910E+02
3	-0.0838	0.965E+02	0.900E+02
2	-0.0914	0.965E+02	0.880E+02
1	-0.0991	0.920E+02	0.890E+02

(a) Yaw Angle

TABLE IV (Continued)

	I =	1	2
	X =	0.0063	0.0190
O J	Y		
27	0.0991	0.867E+01	0.309E+01
26	0.0914	0.185E+01	0.399E+00
25	0.0838	0.217E+01	0.370E+00
24	0.0762	0.247E+01	0.773E+00
23	0.0686	0.338E+01	0.129E+01
22	0.0610	0.558E+01	0.155E+01
21	0.0533	0.640E+01	0.234E+01
20	0.0457	0.811E+01	0.263E+01
19	0.0381	0.957E+01	0.264E+01
18	0.0305	0.140E+02	0.269E+01
17	0.0229	0.161E+02	0.406E+01
16	0.0152	0.103E+02	0.795E+01
15	0.0076	0.785E+01	0.678E+01
14	0.0000	0.120E+02	0.186E+02
13	-0.0076	0.310E+02	0.158E+02
12	-0.0152	0.315E+02	0.245E+02
11	-0.0229	0.246E+02	0.166E+02
10	-0.0305	0.173E+02	0.130E+02
9	-0.0381	0.000E+00	0.102E+02
8	-0.0457	0.112E+02	0.926E+01
7	-0.0533	0.111E+02	0.995E+01
6	-0.0610	0.101E+02	0.103E+02
5	-0.0686	0.855E+01	0.917E+01
4	-0.0762	0.543E+01	0.761E+01
3	-0.0838	0.356E+01	0.601E+01
2	-0.0914	0.354E+01	0.535E+01
1	-0.0991	0.310E+01	0.226E+01

(b) Pitch Angle

TABLE IV (Continued)

	I =	1	2
	X =	0.0278	0.0833
O J	Y		
27	0.4333	-0.401E-04	0.118E+01
26	0.4000	-0.413E-04	0.107E+01
25	0.3667	0.322E+00	0.951E+00
24	0.3333	0.859E+00	0.844E+00
23	0.3000	0.939E+00	0.915E+00
22	0.2667	0.822E+00	0.991E+00
21	0.2333	0.110E+01	0.127E+01
20	0.2000	0.148E+01	0.165E+01
19	0.1667	0.250E+01	0.214E+01
18	0.1333	0.350E+01	0.261E+01
17	0.1000	0.365E+01	0.350E+01
16	0.0667	0.439E+01	0.366E+01
15	0.0333	0.491E+01	0.427E+01
14	0.0000	0.473E+01	0.425E+01
13	-0.0333	0.323E+01	0.422E+01
12	-0.0667	0.214E+01	0.361E+01
11	-0.1000	0.126E+01	0.311E+01
10	-0.1333	0.357E-04	0.217E+01
9	-0.1667	-0.432E+00	0.125E+01
8	-0.2000	-0.424E+00	0.331E+00
7	-0.2333	0.363E-04	0.222E+00
6	-0.2667	0.338E-04	0.376E-04
5	-0.3000	-0.173E+00	-0.192E+00
4	-0.3333	-0.652E+00	-0.181E+00
3	-0.3667	-0.100E+01	0.312E-04
2	-0.4000	-0.975E+00	0.333E+00
1	-0.4333	-0.317E+00	0.170E+00

(c) u/u_{av}

TABLE IV (Continued)

	I =	1	2
	X =	0.0278	0.0833
O J	Y		
27	0.4333	0.129E+01	0.456E+00
26	0.4000	0.281E+00	0.610E-01
25	0.3667	0.350E+00	0.588E-01
24	0.3333	0.426E+00	0.131E+00
23	0.3000	0.637E+00	0.237E+00
22	0.2667	0.115E+01	0.307E+00
21	0.2333	0.128E+01	0.497E+00
20	0.2000	0.152E+01	0.546E+00
19	0.1667	0.153E+01	0.516E+00
18	0.1333	0.160E+01	0.459E+00
17	0.1000	0.125E+01	0.557E+00
16	**0.0667**	**0.819E+00**	**0.718E+00**
15	0.0333	0.678E+00	0.564E+00
14	0.0000	0.103E+01	0.143E+01
13	-0.0333	0.257E+01	0.129E+01
12	-0.0667	0.365E+01	0.241E+01
11	-0.1000	0.414E+01	0.228E+01
10	-0.1333	0.350E+01	0.224E+01
9	-0.1667	0.000E+00	0.199E+01
8	-0.2000	0.241E+01	0.206E+01
7	-0.2333	0.224E+01	0.223E+01
6	-0.2667	0.190E+01	0.215E+01
5	-0.3000	0.149E+01	0.178E+01
4	-0.3333	0.889E+00	0.139E+01
3	-0.3667	0.551E+00	0.103E+01
2	-0.4000	0.533E+00	0.894E+00
1	-0.4333	0.491E+00	0.383E+00

(d) v/u_{av}

TABLE IV (Continued)

	I =	1	2
	X =	0.0278	0.0833
O J	Y		
27	0.4333	-0.843E+01	-0.836E+01
26	0.4000	-0.869E+01	-0.869E+01
25	0.3667	-0.921E+01	-0.905E+01
24	0.3333	-0.982E+01	-0.964E+01
23	0.3000	-0.107E+02	-0.105E+02
22	0.2667	-0.118E+02	-0.113E+02
21	0.2333	-0.114E+02	-0.121E+02
20	0.2000	-0.106E+02	-0.118E+02
19	0.1667	-0.870E+01	-0.110E+02
18	0.1333	-0.538E+01	-0.942E+01
17	0.1000	-0.237E+01	-0.702E+01
16	0.0667	-0.101E+01	-0.392E+01
15	0.0333	-0.300E+00	-0.208E+01
14	0.0000	0.101E+01	-0.223E+00
13	-0.0333	0.281E+01	0.179E+01
12	-0.0667	0.556E+01	0.387E+01
11	-0.1000	0.898E+01	0.700E+01
10	-0.1333	0.112E+02	0.941E+01
9	-0.1667	0.124E+02	0.110E+02
8	-0.2000	0.121E+02	0.126E+02
7	-0.2333	0.114E+02	0.127E+02
6	-0.2667	0.107E+02	0.118E+02
5	-0.3000	0.991E+01	0.110E+02
4	-0.3333	0.933E+01	0.104E+02
3	-0.3667	0.881E+01	0.982E+01
2	-0.4000	0.856E+01	0.953E+01
1	-0.4333	0.907E+01	0.972E+01

(e) w/u_{av}

TABLE V

VELOCITY DATA, CASE 6 (L/D = 1), STRONG SWIRL

	I =	1	2
	X =	0.0063	0.0190
O J	Y		
27	0.0991	0.269E+03	0.278E+03
26	0.0914	0.271E+03	0.276E+03
25	0.0838	0.275E+03	0.276E+03
24	0.0762	0.277E+03	0.276E+03
23	0.0686	0.276E+03	0.276E+03
22	0.0610	0.276E+03	0.276E+03
21	0.0533	0.276E+03	0.277E+03
20	0.0457	0.276E+03	0.277E+03
19	0.0381	0.277E+03	0.278E+03
18	0.0305	0.284E+03	0.280E+03
17	0.0229	0.299E+03	0.284E+03
16	0.0152	0.326E+03	0.295E+03
15	0.0076	0.101E+03	0.313E+03
14	0.0000	0.270E+02	0.348E+03
13	-0.0076	0.540E+02	0.315E+02
12	-0.0152	0.765E+02	0.585E+02
11	-0.0229	0.870E+02	0.750E+02
10	-0.0305	0.905E+02	0.840E+02
9	-0.0381	0.910E+02	0.895E+02
8	-0.0457	0.910E+02	0.900E+02
7	-0.0533	0.895E+02	0.885E+02
6	-0.0610	0.890E+02	0.885E+02
5	-0.0686	0.920E+02	0.900E+02
4	-0.0762	0.955E+02	0.900E+02
3	-0.0838	0.975E+02	0.890E+02
2	-0.0914	0.975E+02	0.890E+02
1	-0.0991	0.940E+02	0.895E+02

(a) Yaw Angle

TABLE V (Continued)

	I =	1	2
	X =	0.0063	0.0190
O J	Y		
27	0.0991	0.766E+01	0.362E+02
26	0.0914	0.353E+01	0.147E+01
25	0.0838	0.412E+01	0.113E+01
24	0.0762	0.425E+01	0.175E+01
23	0.0686	0.521E+01	0.127E+01
22	0.0610	0.709E+01	0.190E+01
21	0.0533	0.101E+02	0.329E+01
20	0.0457	0.134E+02	0.442E+01
19	0.0381	0.174E+02	0.501E+01
18	0.0305	0.248E+02	0.571E+01
17	0.0229	0.314E+02	0.590E+01
16	0.0152	0.486E+02	0.817E+01
15	0.0076	0.472E+02	0.190E+02
14	0.0000	0.463E+02	0.406E+02
13	-0.0076	0.440E+02	0.383E+02
12	-0.0152	0.361E+02	0.307E+02
11	-0.0229	0.289E+02	0.231E+02
10	-0.0305	0.210E+02	0.151E+02
9	-0.0381	0.156E+02	0.112E+02
8	-0.0457	0.134E+02	0.100E+02
7	-0.0533	0.127E+02	0.112E+02
6	-0.0610	0.119E+02	0.117E+02
5	-0.0686	0.923E+01	0.104E+02
4	-0.0762	0.622E+01	0.869E+01
3	-0.0838	0.467E+01	0.750E+01
2	-0.0914	0.397E+01	0.635E+01
1	-0.0991	0.329E+01	0.428E+01

(b) Pitch Angle

TABLE V (Continued)

	I =	1	2
	X =	0.0278	0.0833
O J	Y		
27	0.4333	-0.547E+00	0.379E+01
26	0.4000	0.571E+00	0.336E+01
25	0.3667	0.273E+01	0.350E+01
24	0.3333	0.422E+01	0.373E+01
23	0.3000	0.423E+01	0.401E+01
22	0.2667	0.420E+01	0.437E+01
21	0.2333	0.467E+01	0.554E+01
20	0.2000	0.446E+01	0.553E+01
19	0.1667	0.464E+01	0.544E+01
18	0.1333	0.700E+01	0.634E+01
17	0.1000	0.971E+01	0.747E+01
16	0.0667	0.848E+01	0.100E+02
15	0.0333	-0.207E+01	0.103E+02
14	0.0000	0.108E+02	0.102E+02
13	-0.0333	0.905E+01	0.120E+02
12	-0.0667	0.565E+01	0.107E+02
11	-0.1000	0.183E+01	0.773E+01
10	-0.1333	-0.385E+00	0.392E+01
9	-0.1667	-0.803E+00	0.392E+00
8	-0.2000	-0.776E+00	0.157E-03
7	-0.2333	0.369E+00	0.125E+01
6	-0.2667	0.689E+00	0.116E+01
5	-0.3000	-0.130E+01	0.130E-03
4	-0.3333	-0.341E+01	0.124E-03
3	-0.3667	-0.437E+01	0.636E+00
2	-0.4000	-0.422E+01	0.619E+00
1	-0.4333	-0.236E+01	0.316E+00

(c) u/u_{av}

TABLE V (Continued)

	I =	1	2
	X =	0.0278	0.0833
O J	Y		
27	0.4333	0.421E+01	0.212E+02
26	0.4000	0.202E+01	0.826E+00
25	0.3667	0.250E+01	0.657E+00
24	0.3333	0.277E+01	0.109E+01
23	0.3000	0.369E+01	0.848E+00
22	0.2667	0.545E+01	0.139E+01
21	0.2333	0.798E+01	0.261E+01
20	0.2000	0.101E+02	0.351E+01
19	0.1667	0.119E+02	0.366E+01
18	0.1333	0.138E+02	0.365E+01
17	0.1000	0.122E+02	0.319E+01
16	0.0667	0.116E+02	0.347E+01
15	0.0333	0.117E+02	0.527E+01
14	0.0000	0.127E+02	0.896E+01
13	-0.0333	0.149E+02	0.111E+02
12	-0.0667	0.176E+02	0.121E+02
11	-0.1000	0.193E+02	0.127E+02
10	-0.1333	0.170E+02	0.101E+02
9	-0.1667	0.128E+02	0.887E+01
8	-0.2000	0.106E+02	0.877E+01
7	-0.2333	0.951E+01	0.945E+01
6	-0.2667	0.832E+01	0.913E+01
5	-0.3000	0.604E+01	0.749E+01
4	-0.3333	0.388E+01	0.595E+01
3	-0.3667	0.274E+01	0.480E+01
2	-0.4000	0.225E+01	0.395E+01
1	-0.4333	0.194E+01	0.271E+01

(d) v/u_{av}

TABLE V (Continued)

	I =	1	2
	X =	0.0278	0.0833
O J	Y		
27	0.4333	-0.313E+02	-0.288E+02
26	0.4000	-0.327E+02	-0.320E+02
25	0.3667	-0.347E+02	-0.333E+02
24	0.3333	-0.371E+02	-0.355E+02
23	0.3000	-0.403E+02	-0.382E+02
22	0.2667	-0.436E+02	-0.416E+02
21	0.2333	-0.444E+02	-0.451E+02
20	0.2000	-0.424E+02	-0.450E+02
19	0.1667	-0.378E+02	-0.413E+02
18	0.1333	-0.291E+02	-0.360E+02
17	0.1000	-0.175E+02	-0.300E+02
16	0.0667	-0.572E+01	-0.220E+02
15	0.0333	0.107E+02	-0.113E+02
14	0.0000	0.548E+01	-0.218E+01
13	-0.0333	0.125E+02	0.738E+01
12	-0.0667	0.235E+02	0.175E+02
11	-0.1000	0.349E+02	0.288E+02
10	-0.1333	0.441E+02	0.373E+02
9	-0.1667	0.460E+02	0.449E+02
8	-0.2000	0.445E+02	0.495E+02
7	-0.2333	0.422E+02	0.479E+02
6	-0.2667	0.395E+02	0.442E+02
5	-0.3000	0.371E+02	0.410E+02
4	-0.3333	0.354E+02	0.389E+02
3	-0.3667	0.332E+02	0.364E+02
2	-0.4000	0.321E+02	0.355E+02
1	-0.4333	0.338E+02	0.362E+02

(e) w/u_{av}

TABLE VI

VELOCITY DATA, CASE 7 (L/D = 1), NO SWIRL

	I =	1	2
	X =	0.0063	0.0190
O J	Y		
27	0.0991	0.129E+03	0.440E+02
26	0.0914	0.129E+03	0.102E+03
25	0.0838	0.129E+03	0.102E+03
24	0.0762	0.129E+03	0.102E+03
23	0.0686	0.129E+03	0.102E+03
22	0.0610	0.129E+03	0.102E+03
21	0.0533	0.129E+03	0.102E+03
20	0.0457	0.129E+03	0.102E+03
19	0.0381	0.129E+03	0.102E+03
18	0.0305	0.180E+02	0.360E+03
17	0.0229	0.101E+03	0.360E+03
16	0.0152	0.360E+03	0.359E+03
15	0.0076	0.360E+03	0.359E+03
14	0.0000	0.360E+03	0.359E+03
13	-0.0076	0.360E+03	0.359E+03
12	-0.0152	0.360E+03	0.359E+03
11	-0.0229	0.500E+00	0.359E+03
10	-0.0305	0.155E+02	0.359E+03
9	-0.0381	0.140E+03	0.359E+03
8	-0.0457	0.140E+03	0.359E+03
7	-0.0533	0.140E+03	0.359E+03
6	-0.0610	0.140E+03	0.359E+03
5	-0.0686	0.140E+03	0.359E+03
4	-0.0762	0.140E+03	0.359E+03
3	-0.0838	0.140E+03	0.359E+03
2	-0.0914	0.140E+03	0.359E+03
1	-0.0991	0.140E+03	0.359E+03

(a) Yaw Angle

TABLE VI (Continued)

	I =	1	2
	X =	0.0063	0.0190
O J	Y		
27	0.0991	0.000E+00	0.000E+00
26	0.0914	0.000E+00	-0.433E+02
25	0.0838	-0.393E+02	-0.433E+02
24	0.0762	-0.465E+02	0.000E+00
23	0.0686	-0.315E+02	-0.433E+02
22	0.0610	-0.315E+02	-0.393E+02
21	0.0533	-0.393E+02	-0.197E+02
20	0.0457	-0.393E+02	-0.248E+01
19	0.0381	-0.465E+02	0.000E+00
18	0.0305	0.000E+00	0.000E+00
17	0.0229	0.321E+01	0.366E+00
16	0.0152	0.119E+01	-0.816E+00
15	0.0076	-0.884E-01	-0.301E+01
14	0.0000	-0.847E+00	-0.401E+01
13	-0.0076	-0.157E+01	-0.503E+01
12	-0.0152	-0.240E+01	-0.669E+01
11	-0.0229	-0.592E+01	-0.874E+01
10	-0.0305	-0.101E+02	-0.108E+02
9	-0.0381	-0.218E+02	-0.121E+02
8	-0.0457	-0.393E+02	-0.853E+01
7	-0.0533	-0.110E+02	-0.218E+02
6	-0.0610	-0.853E+01	-0.433E+02
5	-0.0686	-0.393E+02	-0.853E+01
4	-0.0762	-0.110E+02	-0.315E+02
3	-0.0838	-0.315E+02	-0.315E+02
2	-0.0914	-0.510E+02	-0.315E+02
1	-0.0991	-0.433E+02	-0.433E+02

(b) Pitch Angle

TABLE VI (Continued)

	I =	1	2
	X =	0.0278	0.0833
O J	Y		
27	0.4333	-0.117E+01	0.111E+01
26	0.4000	-0.959E+00	-0.236E+00
25	0.3667	-0.945E+00	-0.236E+00
24	0.3333	-0.891E+00	-0.217E+00
23	0.3000	-0.997E+00	-0.236E+00
22	0.2667	-0.814E+00	-0.302E+00
21	0.2333	-0.945E+00	-0.443E+00
20	0.2000	-0.945E+00	-0.867E+00
19	0.1667	-0.891E+00	-0.134E+01
18	0.1333	0.463E+01	0.877E+01
17	0.1000	-0.294E+01	0.150E+02
16	0.0667	0.209E+02	0.191E+02
15	0.0333	0.218E+02	0.224E+02
14	0.0000	0.224E+02	0.222E+02
13	-0.0333	0.222E+02	0.214E+02
12	-0.0667	0.212E+02	0.188E+02
11	-0.1000	0.156E+02	0.138E+02
10	-0.1333	0.479E+01	0.922E+01
9	-0.1667	-0.131E+01	0.561E+01
8	-0.2000	-0.116E+01	0.363E+01
7	-0.2333	-0.137E+01	0.241E+01
6	-0.2667	-0.161E+01	0.119E+01
5	-0.3000	-0.116E+01	0.209E+01
4	-0.3333	-0.137E+01	0.160E+01
3	-0.3667	-0.100E+01	0.131E+01
2	-0.4000	-0.631E+00	0.185E+01
1	-0.4333	-0.897E+00	0.119E+01

(c) u/u_{av}

TABLE VI (Continued)

	I =	1	2
	X =	0.0278	0.0833
O J	Y		
27	0.4333	0.000E+00	0.000E+00
26	0.4000	0.000E+00	-0.143E+01
25	0.3667	-0.160E+01	-0.143E+01
24	0.3333	-0.194E+01	0.000E+00
23	0.3000	-0.126E+01	-0.143E+01
22	0.2667	-0.103E+01	-0.159E+01
21	0.2333	-0.160E+01	-0.102E+01
20	0.2000	-0.160E+01	-0.232E+00
19	0.1667	-0.194E+01	0.000E+00
18	0.1333	0.000E+00	0.000E+00
17	0.1000	0.111E+01	0.123E+00
16	0.0667	0.558E+00	-0.348E+00
15	0.0333	-0.431E-01	-0.151E+01
14	0.0000	-0.425E+00	-0.199E+01
13	-0.0333	-0.781E+00	-0.242E+01
12	-0.0667	-0.114E+01	-0.283E+01
11	-0.1000	-0.208E+01	-0.273E+01
10	-0.1333	-0.114E+01	-0.225E+01
9	-0.1667	-0.877E+00	-0.154E+01
8	-0.2000	-0.160E+01	-0.698E+00
7	-0.2333	-0.446E+00	-0.124E+01
6	-0.2667	-0.404E+00	-0.143E+01
5	-0.3000	-0.160E+01	-0.403E+00
4	-0.3333	-0.446E+00	-0.126E+01
3	-0.3667	-0.103E+01	-0.103E+01
2	-0.4000	-0.130E+01	-0.145E+01
1	-0.4333	-0.142E+01	-0.143E+01

(d) v/u_{∞}

TABLE VI (Continued)

	I =	1	2
	X =	0.0278	0.0833
O J	Y		
27	0.4333	0.148E+01	0.107E+01
26	0.4000	0.121E+01	0.116E+01
25	0.3667	0.119E+01	0.116E+01
24	0.3333	0.112E+01	0.107E+01
23	0.3000	0.125E+01	0.116E+01
22	0.2667	0.102E+01	0.149E+01
21	0.2333	0.119E+01	0.218E+01
20	0.2000	0.119E+01	0.408E+01
19	0.1667	0.112E+01	0.629E+01
18	0.1333	0.151E+01	-0.528E-04
17	0.1000	0.151E+02	-0.902E-04
16	0.0667	-0.183E+00	-0.333E+00
15	0.0333	-0.190E+00	-0.391E+00
14	0.0000	-0.135E-03	-0.387E+00
13	-0.0333	-0.134E-03	-0.374E+00
12	-0.0667	-0.185E+00	-0.328E+00
11	-0.1000	0.136E+00	-0.241E+00
10	-0.1333	0.133E+01	-0.161E+00
9	-0.1667	0.110E+01	-0.979E-01
8	-0.2000	0.976E+00	-0.633E-01
7	-0.2333	0.115E+01	-0.422E-01
6	-0.2667	0.135E+01	-0.207E-01
5	-0.3000	0.976E+00	-0.366E-01
4	-0.3333	0.115E+01	-0.279E-01
3	-0.3667	0.841E+00	-0.228E-01
2	-0.4000	0.530E+00	-0.322E-01
1	-0.4333	0.753E+00	-0.207E-01

(e) w/u_{av}

TABLE VII

VELOCITY DATA, CASE 4 (L/D = 2), MODERATE SWIRL

	I =	1	2
	X =	0.0190	0.0444
O J	Y		
27	0.0991	0.278E+03	0.281E+03
26	0.0914	0.278E+03	0.278E+03
25	0.0838	0.276E+03	0.274E+03
24	0.0762	0.272E+03	0.271E+03
23	0.0686	0.269E+03	0.269E+03
22	0.0610	0.268E+03	0.269E+03
21	0.0533	0.268E+03	0.271E+03
20	0.0457	0.271E+03	0.275E+03
19	0.0381	0.275E+03	0.281E+03
18	0.0305	0.281E+03	0.288E+03
17	0.0229	0.292E+03	0.295E+03
16	0.0152	0.312E+03	0.306E+03
15	0.0076	0.336E+03	0.323E+03
14	0.0000	0.354E+03	0.355E+03
13	-0.0076	0.120E+02	0.320E+02
12	-0.0152	0.390E+02	0.540E+02
11	-0.0229	0.620E+02	0.670E+02
10	-0.0305	0.755E+02	0.750E+02
9	-0.0381	0.830E+02	0.820E+02
8	-0.0457	0.875E+02	0.880E+02
7	-0.0533	0.900E+02	0.912E+02
6	-0.0610	0.905E+02	0.935E+02
5	-0.0686	0.890E+02	0.920E+02
4	-0.0762	0.860E+02	0.895E+02
3	-0.0838	0.830E+02	0.865E+02
2	-0.0914	0.830E+02	0.840E+02
1	-0.0991	0.845E+02	0.800E+02

(a) Yaw Angle

TABLE VII (Continued)

	I =	1	2
	X =	0.0190	0.0444
O J	Y		
27	0.0991	0.290E+01	-0.233E+01
26	0.0914	0.763E+00	-0.620E+01
25	0.0838	0.232E+00	-0.655E+01
24	0.0762	0.850E+00	-0.710E+01
23	0.0686	0.986E+00	-0.683E+01
22	0.0610	0.932E+00	-0.666E+01
21	0.0533	0.824E+00	-0.650E+01
20	0.0457	0.103E+00	-0.683E+01
19	0.0381	-0.114E+00	-0.728E+01
18	0.0305	0.000E+00	-0.863E+01
17	0.0229	0.154E+01	-0.104E+02
16	0.0152	0.509E+01	-0.102E+02
15	0.0076	0.801E+01	-0.101E+02
14	0.0000	0.985E+01	0.189E+02
13	-0.0076	0.142E+02	0.229E+02
12	-0.0152	0.191E+02	0.129E+02
11	-0.0229	0.183E+02	0.862E+01
10	-0.0305	0.124E+02	0.574E+01
9	-0.0381	0.896E+01	0.435E+01
8	-0.0457	0.744E+01	0.345E+01
7	-0.0533	0.683E+01	0.347E+01
6	-0.0610	0.588E+01	0.328E+01
5	-0.0686	0.495E+01	0.170E+01
4	-0.0762	0.354E+01	0.716E+00
3	-0.0838	0.258E+01	-0.459E+00
2	-0.0914	0.289E+01	-0.305E+00
1	-0.0991	0.264E+01	-0.114E+01

(b) Pitch Angle

TABLE VII (Continued)

	I =	1	2
	X =	0.0833	0.1944
O J	Y		
27	0.4333	0.122E+01	0.137E+01
26	0.4000	0.121E+01	0.961E+00
25	0.3667	0.835E+00	0.474E+00
24	0.3333	0.314E+00	0.709E-01
23	0.3000	-0.163E+00	-0.154E+00
22	0.2667	-0.346E+00	-0.201E+00
21	0.2333	-0.368E+00	0.875E-01
20	0.2000	0.186E+00	0.870E+00
19	0.1667	0.888E+00	0.190E+01
18	0.1333	0.182E+01	0.250E+01
17	0.1000	0.303E+01	0.310E+01
16	0.0667	0.428E+01	0.362E+01
15	0.0333	0.517E+01	0.374E+01
14	0.0000	0.595E+01	0.365E+01
13	-0.0333	0.546E+01	0.377E+01
12	-0.0667	0.474E+01	0.388E+01
11	-0.1000	0.360E+01	0.323E+01
10	-0.1333	0.234E+01	0.245E+01
9	-0.1667	0.130E+01	0.142E+01
8	-0.2000	0.485E+00	0.381E+00
7	-0.2333	0.342E-04	-0.222E+00
6	-0.2667	-0.898E-01	-0.600E+00
5	-0.3000	0.170E+00	-0.314E+00
4	-0.3333	0.663E+00	0.737E-01
3	-0.3667	0.115E+01	0.489E+00
2	-0.4000	0.116E+01	0.794E+00
1	-0.4333	0.956E+00	0.125E+01

(c) u/u_{av}

TABLE VII (Continued)

	I =	1	2
	X =	0.0833	0.1944
O J	Y		
27	0.4333	0.443E+00	-0.293E+00
26	0.4000	0.116E+00	-0.800E+00
25	0.3667	0.352E-01	-0.891E+00
24	0.3333	0.133E+00	-0.101E+01
23	0.3000	0.160E+00	-0.106E+01
22	0.2667	0.161E+00	-0.112E+01
21	0.2333	0.152E+00	-0.114E+01
20	0.2000	0.193E-01	-0.120E+01
19	0.1667	-0.203E-01	-0.121E+01
18	0.1333	0.000E+00	-0.126E+01
17	0.1000	0.218E+00	-0.137E+01
16	0.0667	0.570E+00	-0.113E+01
15	0.0333	0.800E+00	-0.841E+00
14	0.0000	0.104E+01	0.125E+01
13	-0.0333	0.141E+01	0.187E+01
12	-0.0667	0.212E+01	0.151E+01
11	-0.1000	0.254E+01	0.125E+01
10	-0.1333	0.205E+01	0.951E+00
9	-0.1667	0.169E+01	0.775E+00
8	-0.2000	0.145E+01	0.658E+00
7	-0.2333	0.129E+01	0.643E+00
6	-0.2667	0.106E+01	0.564E+00
5	-0.3000	0.843E+00	0.267E+00
4	-0.3333	0.588E+00	0.106E+00
3	-0.3667	0.424E+00	-0.642E-01
2	-0.4000	0.478E+00	-0.405E-01
1	-0.4333	0.460E+00	-0.144E+00

(d) v/u_{av}

TABLE VII (Continued)

	I =	1	2
	X =	0.0833	0.1944
O J	Y		
27	0.4333	-0.866E+01	-0.706E+01
26	0.4000	-0.859E+01	-0.730E+01
25	0.3667	-0.867E+01	-0.775E+01
24	0.3333	-0.898E+01	-0.813E+01
23	0.3000	-0.931E+01	-0.881E+01
22	0.2667	-0.990E+01	-0.958E+01
21	0.2333	-0.105E+02	-0.100E+02
20	0.2000	-0.107E+02	-0.995E+01
19	0.1667	-0.102E+02	-0.926E+01
18	0.1333	-0.934E+01	-0.792E+01
17	0.1000	-0.749E+01	-0.681E+01
16	0.0667	-0.476E+01	-0.508E+01
15	0.0333	-0.236E+01	-0.287E+01
14	0.0000	-0.626E+00	-0.319E+00
13	-0.0333	0.116E+01	0.235E+01
12	-0.0667	0.384E+01	0.533E+01
11	-0.1000	0.677E+01	0.761E+01
10	-0.1333	0.906E+01	0.913E+01
9	-0.1667	0.106E+02	0.101E+02
8	-0.2000	0.111E+02	0.109E+02
7	-0.2333	0.108E+02	0.106E+02
6	-0.2667	0.103E+02	0.981E+01
5	-0.3000	0.973E+01	0.899E+01
4	-0.3333	0.948E+01	0.844E+01
3	-0.3667	0.935E+01	0.799E+01
2	-0.4000	0.941E+01	0.755E+01
1	-0.4333	0.993E+01	0.711E+01

(e) w/u_{av}

TABLE VIII

VELOCITY DATA, CASE 7 (L/D = 2), NO SWIRL

	I =	1	2
	X =	0.0190	0.0444
O J	Y		
27	0.0991	0.000E+00	0.000E+00
26	0.0914	0.000E+00	0.000E+00
25	0.0838	0.000E+00	0.359E+03
24	0.0762	0.000E+00	0.359E+03
23	0.0686	0.000E+00	0.359E+03
22	0.0610	0.359E+03	0.359E+03
21	0.0533	0.359E+03	0.359E+03
20	0.0457	0.359E+03	0.359E+03
19	0.0381	0.359E+03	0.359E+03
18	0.0305	0.359E+03	0.359E+03
17	0.0229	0.359E+03	0.359E+03
16	0.0152	0.359E+03	0.359E+03
15	0.0076	0.359E+03	0.359E+03
14	0.0000	0.359E+03	0.359E+03
13	-0.0076	0.359E+03	0.359E+03
12	-0.0152	0.359E+03	0.359E+03
11	-0.0229	0.359E+03	0.359E+03
10	-0.0305	0.359E+03	0.359E+03
9	-0.0381	0.359E+03	0.359E+03
8	-0.0457	0.359E+03	0.359E+03
7	-0.0533	0.359E+03	0.359E+03
6	-0.0610	0.359E+03	0.359E+03
5	-0.0686	0.000E+00	0.359E+03
4	-0.0762	0.000E+00	0.359E+03
3	-0.0838	0.000E+00	0.359E+03
2	-0.0914	0.000E+00	0.000E+00
1	-0.0991	0.000E+00	0.000E+00

(a) Yaw Angle

TABLE VIII (Continued)

	I =	1	2
	X =	0.0190	0.0444
O J	Y		
27	0.0991	0.000E+00	0.000E+00
26	0.0914	0.000E+00	0.000E+00
25	0.0838	0.000E+00	0.000E+00
24	0.0762	0.000E+00	-0.315E+02
23	0.0686	0.000E+00	-0.197E+02
22	0.0610	0.000E+00	-0.147E+02
21	0.0533	-0.433E+02	-0.116E+02
20	0.0457	-0.100E+02	-0.103E+02
19	0.0381	-0.152E+02	-0.766E+01
18	0.0305	-0.109E+02	-0.833E+01
17	0.0229	-0.891E+01	-0.707E+01
16	0.0152	-0.652E+01	-0.533E+01
15	0.0076	-0.521E+01	-0.362E+01
14	0.0000	-0.387E+01	-0.225E+01
13	-0.0076	-0.521E+01	-0.362E+01
12	-0.0152	-0.652E+01	-0.533E+01
11	-0.0229	-0.891E+01	-0.707E+01
10	-0.0305	-0.109E+02	-0.558E+02
9	-0.0381	-0.152E+02	-0.766E+01
8	-0.0457	-0.100E+02	-0.103E+02
7	-0.0533	-0.433E+02	-0.116E+02
6	-0.0610	0.000E+00	-0.147E+02
5	-0.0686	0.000E+00	-0.197E+02
4	-0.0762	0.000E+00	-0.315E+02
3	-0.0838	0.000E+00	0.000E+00
2	-0.0914	0.000E+00	0.000E+00
1	-0.0991	0.000E+00	0.000E+00

(b) Pitch Angle

TABLE VIII (Continued)

	I =	1	2
	X =	0.0833	0.1944
O J	Y		
27	0.4333	0.000E+00	0.000E+00
26	0.4000	0.000E+00	0.000E+00
25	0.3667	0.000E+00	0.000E+00
24	0.3333	0.000E+00	0.128E+01
23	0.3000	0.000E+00	0.218E+01
22	0.2667	0.000E+00	0.299E+01
21	0.2333	0.117E+01	0.451E+01
20	0.2000	0.322E+01	0.547E+01
19	0.1667	0.507E+01	0.733E+01
18	0.1333	0.847E+01	0.863E+01
17	0.1000	0.141E+02	0.104E+02
16	0.0667	0.189E+02	0.126E+02
15	0.0333	0.216E+02	0.131E+02
14	0.0000	0.220E+02	0.136E+02
13	-0.0333	0.216E+02	0.131E+02
12	-0.0667	0.189E+02	0.126E+02
11	-0.1000	0.141E+02	0.104E+02
10	-0.1333	0.847E+01	0.205E+01
9	-0.1667	0.507E+01	0.733E+01
8	-0.2000	0.322E+01	0.547E+01
7	-0.2333	0.117E+01	0.451E+01
6	-0.2667	0.000E+00	0.299E+01
5	-0.3000	0.000E+00	0.218E+01
4	-0.3333	0.000E+00	0.128E+01
3	-0.3667	0.000E+00	0.000E+00
2	-0.4000	0.000E+00	0.000E+00
1	-0.4333	0.000E+00	0.000E+00

(c) u/u_{av}

TABLE VIII (Continued)

	I =	1	2
	X =	0.0833	0.1944
O J	Y		
27	0.4333	0.000E+00	0.000E+00
26	0.4000	0.000E+00	0.000E+00
25	0.3667	0.000E+00	0.000E+00
24	0.3333	0.000E+00	-0.101E+01
23	0.3000	0.000E+00	-0.100E+01
22	0.2667	0.000E+00	-0.100E+01
21	0.2333	-0.141E+01	-0.118E+01
20	0.2000	-0.729E+00	-0.128E+01
19	0.1667	-0.177E+01	-0.127E+01
18	0.1333	-0.209E+01	-0.162E+01
17	0.1000	-0.285E+01	-0.166E+01
16	0.0667	-0.278E+01	-0.151E+01
15	0.0333	-0.252E+01	-0.107E+01
14	0.0000	-0.191E+01	-0.686E+00
13	-0.0333	-0.252E+01	-0.107E+01
12	-0.0667	-0.278E+01	-0.151E+01
11	-0.1000	-0.285E+01	-0.166E+01
10	-0.1333	-0.209E+01	-0.389E+01
9	-0.1667	-0.177E+01	-0.127E+01
8	-0.2000	-0.729E+00	-0.128E+01
7	-0.2333	-0.141E+01	-0.118E+01
6	-0.2667	0.000E+00	-0.100E+01
5	-0.3000	0.000E+00	-0.100E+01
4	-0.3333	0.000E+00	-0.101E+01
3	-0.3667	0.000E+00	0.000E+00
2	-0.4000	0.000E+00	0.000E+00
1	-0.4333	0.000E+00	0.000E+00

(d) v/u_{av}

TABLE VIII (Continued)

	I =	1	2
	X =	0.0833	0.1944
O J	Y		
27	0.4333	0.000E+00	0.000E+00
26	0.4000	0.000E+00	0.000E+00
25	0.3667	0.000E+00	0.000E+00
24	0.3333	0.000E+00	-0.224E-01
23	0.3000	0.000E+00	-0.381E-01
22	0.2667	0.000E+00	-0.522E-01
21	0.2333	-0.203E-01	-0.788E-01
20	0.2000	-0.562E-01	-0.956E-01
19	0.1667	-0.886E-01	-0.128E+00
18	0.1333	-0.148E+00	-0.151E+00
17	0.1000	-0.247E+00	-0.182E+00
16	0.0667	-0.331E+00	-0.220E+00
15	0.0333	-0.376E+00	-0.229E+00
14	0.0000	-0.384E+00	-0.237E+00
13	-0.0333	-0.376E+00	-0.229E+00
12	-0.0667	-0.331E+00	-0.220E+00
11	-0.1000	-0.247E+00	-0.182E+00
10	-0.1333	-0.148E+00	-0.359E-01
9	-0.1667	-0.886E-01	-0.128E+00
8	-0.2000	-0.562E-01	-0.956E-01
7	-0.2333	-0.203E-01	-0.788E-01
6	-0.2667	0.000E+00	-0.522E-01
5	-0.3000	0.000E+00	-0.381E-01
4	-0.3333	0.000E+00	-0.224E-01
3	-0.3667	0.000E+00	0.000E+00
2	-0.4000	0.000E+00	0.000E+00
1	-0.4333	0.000E+00	0.000E+00

(e) w/u_{av}

TABLE IX

VELOCITY DATA, CASE 2 (L/D = 4), WEAK SWIRL

	I =	1	2	3	4	5	6	7
	X =	0.0063	0.0190	0.0318	0.0444	0.0572	0.0698	0.0952
O J	Y							
27	0.0991	0.271E+03	0.281E+03	0.280E+03	0.279E+03	0.775E+02	0.275E+03	0.280E+03
26	0.0914	0.275E+03	0.280E+03	0.274E+03	0.276E+03	0.820E+02	0.273E+03	0.278E+03
25	0.0838	0.274E+03	0.278E+03	0.270E+03	0.274E+03	0.860E+02	0.268E+03	0.274E+03
24	0.0762	0.272E+03	0.276E+03	0.267E+03	0.272E+03	0.890E+02	0.266E+03	0.272E+03
23	0.0686	0.270E+03	0.274E+03	0.266E+03	0.272E+03	0.900E+02	0.266E+03	0.270E+03
22	0.0610	0.270E+03	0.273E+03	0.266E+03	0.275E+03	0.890E+02	0.268E+03	0.272E+03
21	0.0533	0.274E+03	0.279E+03	0.271E+03	0.281E+03	0.850E+02	0.274E+03	0.272E+03
20	0.0457	0.289E+03	0.288E+03	0.277E+03	0.288E+03	0.800E+02	0.281E+03	0.279E+03
19	0.0381	0.326E+03	0.299E+03	0.286E+03	0.292E+03	0.720E+02	0.290E+03	0.286E+03
18	0.0305	0.346E+03	0.317E+03	0.301E+03	0.303E+03	0.640E+02	0.299E+03	0.296E+03
17	0.0229	0.353E+03	0.334E+03	0.318E+03	0.314E+03	0.560E+02	0.310E+03	0.317E+03
16	0.0152	0.351E+03	0.348E+03	0.334E+03	0.324E+03	0.460E+02	0.328E+03	0.324E+03
15	0.0076	0.352E+03	0.359E+03	0.350E+03	0.337E+03	0.335E+02	0.348E+03	0.342E+03
14	0.0000	0.351E+03	0.700E+01	0.360E+03	0.360E+03	0.200E+02	0.110E+02	0.600E+01
13	-0.0076	0.350E+03	0.130E+02	0.150E+02	0.185E+02	0.335E+02	0.310E+02	0.290E+02
12	-0.0152	0.349E+03	0.200E+02	0.325E+02	0.410E+02	0.460E+02	0.455E+02	0.450E+02
11	-0.0229	0.360E+03	0.340E+02	0.470E+02	0.540E+02	0.560E+02	0.560E+02	0.590E+02
10	-0.0305	0.630E+02	0.500E+02	0.600E+02	0.645E+02	0.640E+02	0.670E+02	0.700E+02
9	-0.0381	0.910E+02	0.680E+02	0.690E+02	0.750E+02	0.720E+02	0.760E+02	0.780E+02
8	-0.0457	0.960E+02	0.830E+02	0.775E+02	0.815E+02	0.800E+02	0.830E+02	0.850E+02
7	-0.0533	0.950E+02	0.900E+02	0.820E+02	0.870E+02	0.850E+02	0.880E+02	0.880E+02
6	-0.0610	0.940E+02	0.930E+02	0.860E+02	0.900E+02	0.890E+02	0.900E+02	0.900E+02
5	-0.0686	0.930E+02	0.930E+02	0.885E+02	0.900E+02	0.900E+02	0.890E+02	0.885E+02
4	-0.0762	0.920E+02	0.900E+02	0.885E+02	0.860E+02	0.890E+02	0.840E+02	0.860E+02
3	-0.0838	0.930E+02	0.870E+02	0.875E+02	0.820E+02	0.860E+02	0.795E+02	0.820E+02
2	-0.0914	0.960E+02	0.870E+02	0.840E+02	0.765E+02	0.820E+02	0.750E+02	0.790E+02
1	-0.0991	0.960E+02	0.850E+02	0.800E+02	0.710E+02	0.780E+02	0.700E+02	0.775E+02

(a) Yaw Angle

TABLE IX (Continued)

	I =	1	2	3	4	5	6	7
	X =	0.0063	0.0190	0.0318	0.0444	0.0572	0.0698	0.0952
O J	Y							
27	0.0991	0.415E+01	0.205E+01	-0.351E+01	-0.338E+01	-0.147E+01	0.382E+00	0.105E+01
26	0.0914	0.113E+00	0.513E+00	-0.752E+01	-0.451E+01	0.000E+00	-0.362E+00	0.000E+00
25	0.0838	0.000E+00	0.000E+00	-0.757E+01	-0.458E+01	0.509E+00	-0.346E+00	-0.152E+01
24	0.0762	-0.122E+00	-0.156E+00	-0.714E+01	-0.470E+01	0.967E+00	0.000E+00	-0.133E+01
23	0.0686	0.259E+00	-0.834E+00	-0.696E+01	-0.479E+01	0.157E+01	0.137E+00	-0.314E+00
22	0.0610	0.202E+01	-0.690E+01	-0.696E+01	-0.536E+01	0.188E+01	0.808E+00	-0.257E+00
21	0.0533	0.821E+01	-0.109E+02	-0.617E+01	-0.527E+01	0.255E+01	0.931E+00	0.609E+00
20	0.0457	0.294E+02	-0.218E+02	-0.670E+01	-0.592E+01	0.318E+01	0.230E+01	0.208E+01
19	0.0381	0.405E+02	-0.328E+02	-0.421E+01	-0.541E+01	0.360E+01	0.382E+01	0.346E+01
18	0.0305	0.296E+02	-0.448E+02	0.877E+00	-0.476E+01	0.347E+01	0.578E+01	0.643E+01
17	0.0229	0.183E+02	-0.433E+02	0.391E+01	-0.354E+01	0.410E+01	0.675E+01	0.107E+02
16	0.0152	0.135E+02	-0.373E+02	0.867E+01	-0.427E+01	0.426E+01	0.127E+02	0.179E+02
15	0.0076	0.112E+02	-0.337E+02	0.155E+02	-0.241E+01	0.409E+01	0.204E+02	0.237E+02
14	0.0000	0.827E+01	-0.273E+02	0.146E+02	0.267E+01	0.391E+01	0.259E+02	0.273E+02
13	-0.0076	0.569E+01	-0.257E+02	0.161E+02	0.363E+01	0.409E+01	0.236E+02	0.262E+02
12	-0.0152	0.535E+01	-0.227E+02	0.137E+02	0.539E+01	0.426E+01	0.188E+02	0.217E+02
11	-0.0229	0.135E+02	-0.141E+02	0.113E+02	0.591E+01	0.410E+01	0.149E+02	0.175E+02
10	-0.0305	0.000E+00	-0.170E+01	0.805E+01	0.553E+01	0.347E+01	0.120E+02	0.150E+02
9	-0.0381	0.343E+02	0.105E+02	0.570E+01	0.433E+01	0.360E+01	0.987E+01	0.127E+02
8	-0.0457	0.157E+02	0.144E+02	0.376E+01	0.253E+01	0.318E+01	0.710E+01	0.115E+02
7	-0.0533	0.102E+02	0.132E+02	0.186E+01	0.141E+01	0.255E+01	0.501E+01	0.975E+01
6	-0.0610	0.699E+01	0.121E+02	0.855E+00	0.165E+00	0.188E+01	0.324E+01	0.810E+01
5	-0.0686	0.550E+01	0.115E+02	0.000E+00	-0.178E+00	0.157E+01	0.197E+01	0.545E+01
4	-0.0762	0.479E+01	0.884E+01	0.000E+00	-0.217E+01	0.967E+00	0.345E+00	0.367E+01
3	-0.0838	0.464E+01	0.730E+01	0.000E+00	-0.262E+01	0.509E+00	0.000E+00	0.245E+01
2	-0.0914	0.566E+01	0.599E+01	0.000E+00	-0.200E+01	0.000E+00	0.000E+00	0.166E+01
1	-0.0991	0.476E+01	0.476E+01	0.132E+00	-0.935E+00	-0.147E+01	0.000E+00	0.135E+01

(b) Pitch Angle

TABLE IX (Continued)

	I =	1	2	3	4	5	6	7
	X =	0.0278	0.0833	0.1389	0.1944	0.2500	0.3056	0.4167
O J	Y							
27	0.4333	0.122E+00	0.127E+01	0.113E+01	0.869E+00	0.959E+00	0.422E+00	0.747E+00
26	0.4000	0.600E+00	0.111E+01	0.392E+00	0.564E+00	0.636E+00	0.244E+00	0.632E+00
25	0.3667	0.473E+00	0.857E+00	-0.559E-01	0.374E+00	0.324E+00	-0.200E+00	0.359E+00
24	0.3333	0.232E+00	0.614E+00	-0.333E+00	0.188E+00	0.826E-01	-0.417E+00	0.192E+00
23	0.3000	-0.305E-04	0.399E+00	-0.498E+00	0.190E+00	0.155E-04	-0.446E+00	-0.285E-04
22	0.2667	-0.290E-04	0.263E+00	-0.438E+00	0.488E+00	0.876E-01	-0.240E+00	0.174E+00
21	0.2333	0.365E+00	0.726E+00	0.555E-01	0.103E+01	0.448E+00	0.505E+00	0.257E+00
20	0.2000	0.122E+01	0.112E+01	0.730E+00	0.177E+01	0.907E+00	0.144E+01	0.127E+01
19	0.1667	0.290E+01	0.136E+01	0.150E+01	0.209E+01	0.164E+01	0.263E+01	0.238E+01
18	0.1333	0.561E+01	0.161E+01	0.285E+01	0.297E+01	0.237E+01	0.388E+01	0.396E+01
17	0.1000	0.759E+01	0.209E+01	0.375E+01	0.377E+01	0.309E+01	0.518E+01	0.667E+01
16	0.0667	0.782E+01	0.281E+01	0.423E+01	0.420E+01	0.376E+01	0.641E+01	0.731E+01
15	0.0333	0.832E+01	0.322E+01	0.465E+01	0.474E+01	0.443E+01	0.668E+01	0.845E+01
14	0.0000	0.724E+01	0.345E+01	0.511E+01	0.482E+01	0.477E+01	0.660E+01	0.806E+01
13	-0.0333	0.589E+01	0.322E+01	0.479E+01	0.434E+01	0.443E+01	0.616E+01	0.737E+01
12	-0.0667	0.423E+01	0.294E+01	0.444E+01	0.396E+01	0.376E+01	0.532E+01	0.634E+01
11	-0.1000	0.250E+01	0.253E+01	0.386E+01	0.318E+01	0.309E+01	0.431E+01	0.452E+01
10	-0.1333	0.000E+00	0.200E+01	0.298E+01	0.248E+01	0.237E+01	0.301E+01	0.292E+01
9	-0.1667	-0.452E-01	0.129E+01	0.220E+01	0.152E+01	0.164E+01	0.181E+01	0.171E+01
8	-0.2000	-0.492E+00	0.531E+00	0.136E+01	0.873E+00	0.907E+00	0.914E+00	0.877E+00
7	-0.2333	-0.519E+00	0.164E-04	0.871E+00	0.306E+00	0.448E+00	0.245E+00	0.246E+00
6	-0.2667	-0.469E+00	-0.307E+00	0.428E+00	0.184E-04	0.876E-01	0.207E-04	0.205E-04
5	-0.3000	-0.376E+00	-0.333E+00	0.159E+00	0.179E-04	0.155E-04	0.107E+00	0.152E+00
4	-0.3333	-0.255E+00	0.219E-04	0.155E+00	0.378E+00	0.826E-01	0.593E+00	0.375E+00
3	-0.3667	-0.390E+00	0.381E+00	0.261E+00	0.748E+00	0.324E+00	0.101E+01	0.702E+00
2	-0.4000	-0.788E+00	0.397E+00	0.640E+00	0.126E+01	0.636E+00	0.142E+01	0.901E+00
1	-0.4333	-0.861E+00	0.701E+00	0.112E+01	0.180E+01	0.921E+00	0.186E+01	0.965E+00

(c) u/u_{av}

TABLE IX (Continued)

	I =	1	2	3	4	5	6	7
	X =	0.0278	0.0833	0.1389	0.1944	0.2500	0.3056	0.4167
O J	Y							
27	0.4333	0.505E+00	0.237E+00	-0.400E+00	-0.329E+00	-0.113E+00	0.359E-01	0.833E-01
26	0.4000	0.136E-01	0.573E-01	-0.848E+00	-0.426E+00	0.000E+00	-0.354E-01	0.000E+00
25	0.3667	0.000E+00	0.000E+00	-0.850E+00	-0.429E+00	0.413E-01	-0.346E-01	-0.137E+00
24	0.3333	-0.142E-01	-0.160E-01	-0.797E+00	-0.443E+00	0.799E-01	0.000E+00	-0.128E+00
23	0.3000	0.290E-01	-0.832E-01	-0.775E+00	-0.456E+00	0.133E+00	0.152E-01	-0.329E-01
22	0.2667	0.215E+00	-0.608E+00	-0.767E+00	-0.526E+00	0.165E+00	0.969E-01	-0.297E-01
21	0.2333	0.756E+00	-0.894E+00	-0.688E+00	-0.522E+00	0.229E+00	0.118E+00	0.782E-01
20	0.2000	0.210E+01	-0.145E+01	-0.703E+00	-0.594E+00	0.290E+00	0.302E+00	0.294E+00
19	0.1667	0.299E+01	-0.184E+01	-0.401E+00	-0.528E+00	0.334E+00	0.526E+00	0.523E+00
18	0.1333	0.329E+01	-0.219E+01	0.847E-01	-0.455E+00	0.328E+00	0.810E+00	0.102E+01
17	0.1000	0.253E+01	-0.219E+01	0.345E+00	-0.336E+00	0.396E+00	0.955E+00	0.172E+01
16	0.0667	0.190E+01	-0.219E+01	0.720E+00	-0.387E+00	0.404E+00	0.170E+01	0.291E+01
15	0.0333	0.166E+01	-0.215E+01	0.131E+01	-0.216E+00	0.380E+00	0.254E+01	0.390E+01
14	0.0000	0.107E+01	-0.179E+01	0.133E+01	0.225E+00	0.347E+00	0.327E+01	0.419E+01
13	-0.0333	0.596E+00	-0.159E+01	0.143E+01	0.290E+00	0.380E+00	0.315E+01	0.415E+01
12	-0.0667	0.403E+00	-0.131E+01	0.128E+01	0.495E+00	0.404E+00	0.259E+01	0.357E+01
11	-0.1000	0.602E+00	-0.767E+00	0.113E+01	0.560E+00	0.396E+00	0.205E+01	0.277E+01
10	-0.1333	0.000E+00	-0.926E-01	0.843E+00	0.557E+00	0.328E+00	0.163E+01	0.230E+01
9	-0.1667	0.177E+01	0.640E+00	0.613E+00	0.445E+00	0.334E+00	0.130E+01	0.184E+01
8	-0.2000	0.132E+01	0.112E+01	0.415E+00	0.260E+00	0.290E+00	0.934E+00	0.158E+01
7	-0.2333	0.107E+01	0.121E+01	0.203E+00	0.143E+00	0.229E+00	0.616E+00	0.121E+01
6	-0.2667	0.825E+00	0.126E+01	0.917E-01	0.168E-01	0.165E+00	0.369E+00	0.921E+00
5	-0.3000	0.691E+00	0.130E+01	0.000E+00	-0.175E-01	0.133E+00	0.210E+00	0.553E+00
4	-0.3333	0.613E+00	0.107E+01	0.000E+00	-0.205E+00	0.799E-01	0.341E-01	0.345E+00
3	-0.3667	0.604E+00	0.931E+00	0.000E+00	-0.246E+00	0.413E-01	0.000E+00	0.216E+00
2	-0.4000	0.747E+00	0.796E+00	0.000E+00	-0.188E+00	0.000E+00	0.000E+00	0.137E+00
1	-0.4333	0.686E+00	0.670E+00	0.149E-01	-0.902E-01	-0.113E+00	0.000E+00	0.105E+00

(d) v/u_{av}

TABLE IX (Continued)

	I =	1	2	3	4	5	6	7
	X =	0.0278	0.0833	0.1389	0.1944	0.2500	0.3056	0.4167
O J	Y							
27	0.4333	-0.697E+01	-0.651E+01	-0.642E+01	-0.549E+01	0.432E+01	-0.536E+01	-0.447E+01
26	0.4000	-0.686E+01	-0.631E+01	-0.642E+01	-0.537E+01	0.453E+01	-0.558E+01	-0.480E+01
25	0.3667	-0.677E+01	-0.610E+01	-0.640E+01	-0.534E+01	0.464E+01	-0.571E+01	-0.514E+01
24	0.3333	-0.664E+01	-0.584E+01	-0.635E+01	-0.539E+01	0.473E+01	-0.596E+01	-0.550E+01
23	0.3000	-0.641E+01	-0.570E+01	-0.632E+01	-0.544E+01	0.487E+01	-0.638E+01	-0.600E+01
22	0.2667	-0.610E+01	-0.502E+01	-0.627E+01	-0.558E+01	0.502E+01	-0.687E+01	-0.663E+01
21	0.2333	-0.523E+01	-0.459E+01	-0.637E+01	-0.556E+01	0.512E+01	-0.723E+01	-0.735E+01
20	0.2000	-0.353E+01	-0.345E+01	-0.595E+01	-0.544E+01	0.514E+01	-0.739E+01	-0.799E+01
19	0.1667	-0.196E+01	-0.251E+01	-0.524E+01	-0.517E+01	0.505E+01	-0.742E+01	-0.831E+01
18	0.1333	-0.140E+01	-0.150E+01	-0.474E+01	-0.458E+01	0.486E+01	-0.701E+01	-0.811E+01
17	0.1000	-0.100E+01	-0.102E+01	-0.338E+01	-0.390E+01	0.459E+01	-0.618E+01	-0.622E+01
16	0.0667	-0.124E+01	-0.597E+00	-0.211E+01	-0.305E+01	0.390E+01	-0.401E+01	-0.531E+01
15	0.0333	-0.117E+01	-0.562E-01	-0.820E+00	-0.201E+01	0.293E+01	-0.148E+01	-0.275E+01
14	0.0000	-0.121E+01	0.423E+00	-0.308E-04	-0.290E-04	0.174E+01	0.128E+01	0.847E+00
13	-0.0333	-0.104E+01	0.742E+00	0.128E+01	0.145E+01	0.293E+01	0.370E+01	0.408E+01
12	-0.0667	-0.823E+00	0.107E+01	0.283E+01	0.344E+01	0.390E+01	0.541E+01	0.634E+01
11	-0.1000	-0.151E-04	0.170E+01	0.413E+01	0.438E+01	0.459E+01	0.639E+01	0.752E+01
10	-0.1333	0.000E+00	0.239E+01	0.517E+01	0.519E+01	0.486E+01	0.709E+01	0.803E+01
9	-0.1667	0.259E+01	0.321E+01	0.573E+01	0.569E+01	0.505E+01	0.727E+01	0.802E+01
8	-0.2000	0.468E+01	0.433E+01	0.616E+01	0.584E+01	0.514E+01	0.744E+01	0.774E+01
7	-0.2333	0.593E+01	0.516E+01	0.620E+01	0.584E+01	0.512E+01	0.702E+01	0.706E+01
6	-0.2667	0.671E+01	0.585E+01	0.612E+01	0.581E+01	0.502E+01	0.652E+01	0.647E+01
5	-0.3000	0.718E+01	0.635E+01	0.607E+01	0.562E+01	0.487E+01	0.611E+01	0.579E+01
4	-0.3333	0.731E+01	0.690E+01	0.591E+01	0.541E+01	0.473E+01	0.564E+01	0.537E+01
3	-0.3667	0.743E+01	0.726E+01	0.599E+01	0.532E+01	0.464E+01	0.543E+01	0.499E+01
2	-0.4000	0.750E+01	0.757E+01	0.609E+01	0.523E+01	0.453E+01	0.530E+01	0.463E+01
1	-0.4333	0.820E+01	0.801E+01	0.636E+01	0.523E+01	0.433E+01	0.512E+01	0.435E+01

(e) w/u_{av}

TABLE X

VELOCITY DATA, CASE 4 (L/D = 4), MODERATE SWIRL

	I =	1	2	3	4	5	6	7
	X =	0.0063	0.0190	0.0318	0.0444	0.0572	0.0698	0.0952
J	Y							
27	0.0991	0.273E+03	0.283E+03	0.282E+03	0.281E+03	0.770E+02	0.281E+03	0.281E+03
26	0.0914	0.276E+03	0.283E+03	0.277E+03	0.278E+03	0.795E+02	0.276E+03	0.278E+03
25	0.0838	0.277E+03	0.280E+03	0.274E+03	0.273E+03	0.840E+02	0.273E+03	0.274E+03
24	0.0762	0.277E+03	0.274E+03	0.270E+03	0.270E+03	0.870E+02	0.268E+03	0.273E+03
23	0.0686	0.275E+03	0.268E+03	0.266E+03	0.266E+03	0.900E+02	0.265E+03	0.272E+03
22	0.0610	0.274E+03	0.266E+03	0.264E+03	0.264E+03	0.930E+02	0.264E+03	0.270E+03
21	0.0533	0.274E+03	0.266E+03	0.265E+03	0.266E+03	0.930E+02	0.265E+03	0.270E+03
20	0.0457	0.276E+03	0.270E+03	0.270E+03	0.272E+03	0.910E+02	0.270E+03	0.274E+03
19	0.0381	0.281E+03	0.275E+03	0.275E+03	0.279E+03	0.840E+02	0.278E+03	0.280E+03
18	0.0305	0.290E+03	0.282E+03	0.282E+03	0.286E+03	0.755E+02	0.286E+03	0.285E+03
17	0.0229	0.305E+03	0.292E+03	0.292E+03	0.297E+03	0.650E+02	0.297E+03	0.296E+03
16	0.0152	0.325E+03	0.310E+03	0.307E+03	0.310E+03	0.540E+02	0.310E+03	0.320E+03
15	0.0076	0.346E+03	0.342E+03	0.332E+03	0.332E+03	0.415E+02	0.331E+03	0.329E+03
14	0.0000	0.800E+01	0.351E+03	0.400E+01	0.300E+01	0.235E+02	0.175E+02	0.110E+02
13	-0.0076	0.290E+02	0.130E+02	0.305E+02	0.330E+02	0.415E+02	0.410E+02	0.370E+02
12	-0.0152	0.500E+02	0.395E+02	0.490E+02	0.520E+02	0.540E+02	0.545E+02	0.515E+02
11	-0.0229	0.760E+02	0.650E+02	0.640E+02	0.635E+02	0.650E+02	0.675E+02	0.640E+02
10	-0.0305	0.910E+02	0.770E+02	0.750E+02	0.750E+02	0.755E+02	0.760E+02	0.765E+02
9	-0.0381	0.970E+02	0.840E+02	0.835E+02	0.835E+02	0.840E+02	0.860E+02	0.860E+02
8	-0.0457	0.100E+03	0.880E+02	0.900E+02	0.910E+02	0.910E+02	0.905E+02	0.880E+02
7	-0.0533	0.100E+03	0.920E+02	0.940E+02	0.940E+02	0.930E+02	0.920E+02	0.900E+02
6	-0.0610	0.960E+02	0.925E+02	0.945E+02	0.950E+02	0.930E+02	0.910E+02	0.885E+02
5	-0.0686	0.920E+02	0.920E+02	0.945E+02	0.930E+02	0.900E+02	0.875E+02	0.870E+02
4	-0.0762	0.880E+02	0.890E+02	0.905E+02	0.890E+02	0.870E+02	0.840E+02	0.850E+02
3	-0.0838	0.900E+02	0.850E+02	0.870E+02	0.850E+02	0.840E+02	0.800E+02	0.820E+02
2	-0.0914	0.935E+02	0.840E+02	0.820E+02	0.800E+02	0.795E+02	0.750E+02	0.800E+02
1	-0.0991	0.935E+02	0.855E+02	0.765E+02	0.740E+02	0.770E+02	0.700E+02	0.770E+02

(a) Yaw Angle

TABLE X (Continued)

	I =	1	2	3	4	5	6	7
	X =	0.0063	0.0190	0.0318	0.0444	0.0572	0.0698	0.0952
O J	Y							
27	0.0991	0.439E+01	0.339E+01	-0.321E+00	-0.253E+01	-0.199E+01	-0.123E+00	0.956E+00
26	0.0914	-0.601E+00	0.151E+01	-0.416E+01	-0.390E+01	-0.195E+01	-0.178E+01	-0.168E+01
25	0.0838	-0.207E+01	0.131E+01	-0.462E+01	-0.428E+01	-0.136E+01	-0.193E+01	-0.211E+01
24	0.0762	-0.131E+01	0.962E+00	-0.469E+01	-0.417E+01	-0.116E+01	-0.206E+01	-0.145E+01
23	0.0686	-0.111E+00	0.337E+00	-0.521E+01	-0.416E+01	-0.461E+00	-0.216E+01	-0.709E+00
22	0.0610	0.175E+01	0.000E+00	-0.527E+01	-0.456E+01	0.000E+00	-0.175E+01	0.327E+00
21	0.0533	0.390E+01	-0.498E+00	-0.560E+01	-0.481E+01	0.121E+00	-0.164E+01	0.124E+01
20	0.0457	0.639E+01	-0.125E+01	-0.612E+01	-0.645E+01	0.184E+01	-0.232E+01	0.247E+01
19	0.0381	0.851E+01	-0.939E+00	-0.702E+01	-0.765E+01	0.367E+01	-0.181E+01	0.368E+01
18	0.0305	0.113E+02	-0.231E+01	-0.767E+01	-0.895E+01	0.566E+01	-0.146E+01	0.513E+01
17	0.0229	0.157E+02	-0.281E+00	-0.774E+01	-0.939E+01	0.767E+01	0.147E+01	0.732E+01
16	0.0152	0.264E+02	0.263E+01	-0.667E+01	-0.107E+02	0.102E+02	0.181E+01	0.122E+02
15	0.0076	0.225E+02	0.836E+01	0.335E+01	-0.869E+01	0.131E+02	0.942E+01	0.212E+02
14	0.0000	0.338E+02	0.119E+02	0.125E+02	-0.383E+01	0.171E+02	0.265E+02	0.360E+02
13	-0.0076	0.389E+02	0.149E+02	0.127E+02	0.296E+01	0.131E+02	0.179E+02	0.290E+02
12	-0.0152	0.406E+02	0.162E+02	0.119E+02	0.440E+01	0.102E+02	0.135E+02	0.216E+02
11	-0.0229	0.365E+02	0.140E+02	0.908E+01	0.401E+01	0.767E+01	0.997E+01	0.188E+02
10	-0.0305	0.286E+02	0.106E+02	0.644E+01	0.310E+01	0.566E+01	0.792E+01	0.148E+02
9	-0.0381	0.192E+02	0.820E+01	0.452E+01	0.183E+01	0.367E+01	0.601E+01	0.112E+02
8	-0.0457	0.134E+02	0.693E+01	0.272E+01	0.820E+00	0.184E+01	0.441E+01	0.944E+01
7	-0.0533	0.924E+01	0.616E+01	0.144E+01	-0.215E+00	0.000E+00	0.378E+01	0.836E+01
6	-0.0610	0.716E+01	0.549E+01	0.501E+00	-0.847E+00	0.000E+00	0.359E+01	0.729E+01
5	-0.0686	0.466E+01	0.526E+01	0.419E+00	-0.774E+00	-0.461E+00	0.287E+01	0.528E+01
4	-0.0762	0.376E+01	0.487E+01	0.000E+00	-0.948E+00	-0.116E+01	0.194E+01	0.351E+01
3	-0.0838	0.340E+01	0.415E+01	0.000E+00	-0.125E+01	-0.136E+01	0.108E+01	0.222E+01
2	-0.0914	0.381E+01	0.389E+01	0.000E+00	-0.170E+01	-0.195E+01	0.513E+00	0.903E+00
1	-0.0991	0.425E+01	0.371E+01	0.000E+00	-0.165E+01	-0.199E+01	0.269E+00	0.171E+00

(b) Pitch Angle

TABLE X (Continued)

	I =	1	2	3	4	5	6	7
	X =	0.0278	0.0833	0.1389	0.1944	0.2500	0.3056	0.4167
O J	Y							
27	0.4333	0.348E+00	0.190E+01	0.157E+01	0.128E+01	0.133E+01	0.128E+01	0.111E+01
26	0.4000	0.742E+00	0.184E+01	0.907E+00	0.916E+00	0.108E+01	0.733E+00	0.834E+00
25	0.3667	0.935E+00	0.135E+01	0.516E+00	0.334E+00	0.632E+00	0.314E+00	0.465E+00
24	0.3333	0.908E+00	0.510E+00	-0.345E-04	-0.308E-04	0.320E+00	-0.258E+00	0.376E+00
23	0.3000	0.638E+00	-0.252E+00	-0.511E+00	-0.467E+00	0.201E-04	-0.680E+00	0.204E+00
22	0.2667	0.514E+00	-0.519E+00	-0.794E+00	-0.730E+00	-0.354E+00	-0.956E+00	-0.408E-04
21	0.2333	0.534E+00	-0.540E+00	-0.702E+00	-0.511E+00	-0.370E+00	-0.778E+00	-0.437E-04
20	0.2000	0.833E+00	-0.717E-01	-0.741E-01	0.261E+00	-0.134E+00	-0.428E-04	0.596E+00
19	0.1667	0.152E+01	0.659E+00	0.813E+00	0.119E+01	0.856E+00	0.127E+01	0.171E+01
18	0.1333	0.250E+01	0.168E+01	0.186E+01	0.220E+01	0.212E+01	0.255E+01	0.248E+01
17	0.1000	0.332E+01	0.299E+01	0.332E+01	0.367E+01	0.361E+01	0.414E+01	0.406E+01
16	0.0667	0.384E+01	0.453E+01	0.472E+01	0.487E+01	0.493E+01	0.560E+01	0.687E+01
15	0.0333	0.558E+01	0.619E+01	0.599E+01	0.584E+01	0.584E+01	0.592E+01	0.668E+01
14	0.0000	0.435E+01	0.616E+01	0.649E+01	0.570E+01	0.625E+01	0.586E+01	0.575E+01
13	-0.0333	0.386E+01	0.597E+01	0.634E+01	0.551E+01	0.584E+01	0.618E+01	0.618E+01
12	-0.0667	0.308E+01	0.492E+01	0.533E+01	0.478E+01	0.493E+01	0.546E+01	0.596E+01
11	-0.1000	0.144E+01	0.325E+01	0.389E+01	0.367E+01	0.361E+01	0.388E+01	0.435E+01
10	-0.1333	-0.136E+00	0.197E+01	0.238E+01	0.219E+01	0.212E+01	0.214E+01	0.237E+01
9	-0.1667	-0.107E+01	0.946E+00	0.103E+01	0.939E+00	0.856E+00	0.718E+00	0.735E+00
8	-0.2000	-0.149E+01	0.307E+00	0.280E-04	-0.140E+00	-0.134E+00	-0.830E-01	0.350E+00
7	-0.2333	-0.148E+01	-0.292E+00	-0.575E+00	-0.525E+00	-0.370E+00	-0.305E+00	0.292E-04
6	-0.2667	-0.882E+00	-0.350E+00	-0.605E+00	-0.623E+00	-0.354E+00	-0.143E+00	0.217E+00
5	-0.3000	-0.299E+00	-0.278E+00	-0.593E+00	-0.362E+00	0.201E-04	0.332E+00	0.398E+00
4	-0.3333	0.305E+00	0.141E+00	-0.641E-01	0.118E+00	0.320E+00	0.759E+00	0.617E+00
3	-0.3667	0.276E-04	0.755E+00	0.386E+00	0.584E+00	0.632E+00	0.121E+01	0.914E+00
2	-0.4000	-0.535E+00	0.945E+00	0.107E+01	0.115E+01	0.108E+01	0.176E+01	0.109E+01
1	-0.4333	-0.585E+00	0.757E+00	0.187E+01	0.186E+01	0.133E+01	0.229E+01	0.134E+01

(c) u/u_{av}

TABLE X (Continued)

	I =	1	2	3	4	5	6	7
	X =	0.0278	0.0833	0.1389	0.1944	0.2500	0.3056	0.4167
J	Y							
27	0.4333	0.612E+00	0.499E+00	-0.424E-01	-0.295E+00	-0.204E+00	-0.151E-01	0.101E+00
26	0.4000	-0.811E-01	0.215E+00	-0.541E+00	-0.448E+00	-0.202E+00	-0.218E+00	-0.188E+00
25	0.3667	-0.278E+00	0.178E+00	-0.598E+00	-0.477E+00	-0.144E+00	-0.243E+00	-0.246E+00
24	0.3333	-0.170E+00	0.123E+00	-0.595E+00	-0.471E+00	-0.124E+00	-0.266E+00	-0.182E+00
23	0.3000	-0.142E-01	0.424E-01	-0.668E+00	-0.488E+00	-0.508E-01	-0.295E+00	-0.965E-01
22	0.2667	0.225E+00	0.000E+00	-0.700E+00	-0.557E+00	0.000E+00	-0.258E+00	0.489E-01
21	0.2333	0.521E+00	-0.673E-01	-0.789E+00	-0.616E+00	0.149E-01	-0.256E+00	0.199E+00
20	0.2000	0.893E+00	-0.180E+00	-0.910E+00	-0.844E+00	0.246E+00	-0.365E+00	0.421E+00
19	0.1667	0.120E+01	-0.138E+00	-0.109E+01	-0.103E+01	0.526E+00	-0.288E+00	0.632E+00
18	0.1333	0.146E+01	-0.341E+00	-0.121E+01	-0.126E+01	0.840E+00	-0.236E+00	0.861E+00
17	0.1000	0.163E+01	-0.391E-01	-0.120E+01	-0.134E+01	0.115E+01	0.239E+00	0.121E+01
16	0.0667	0.234E+01	0.323E+00	-0.917E+00	-0.143E+01	0.150E+01	0.275E+00	0.195E+01
15	0.0333	0.238E+01	0.960E+00	0.397E+00	-0.101E+01	0.181E+01	0.112E+01	0.302E+01
14	0.0000	0.295E+01	0.132E+01	0.144E+01	-0.383E+00	0.209E+01	0.307E+01	0.426E+01
13	-0.0333	0.356E+01	0.163E+01	0.166E+01	0.339E+00	0.181E+01	0.265E+01	0.429E+01
12	-0.0667	0.411E+01	0.185E+01	0.171E+01	0.597E+00	0.150E+01	0.226E+01	0.378E+01
11	-0.1000	0.441E+01	0.192E+01	0.142E+01	0.577E+00	0.115E+01	0.178E+01	0.337E+01
10	-0.1333	0.424E+01	0.163E+01	0.104E+01	0.458E+00	0.840E+00	0.143E+01	0.269E+01
9	-0.1667	0.306E+01	0.130E+01	0.723E+00	0.264E+00	0.526E+00	0.108E+01	0.208E+01
8	-0.2000	0.204E+01	0.107E+01	0.419E+00	0.115E+00	0.246E+00	0.735E+00	0.167E+01
7	-0.2333	0.138E+01	0.903E+00	0.208E+00	-0.283E-01	0.000E+00	0.578E+00	0.135E+01
6	-0.2667	0.106E+01	0.772E+00	0.674E-01	-0.106E+00	0.000E+00	0.514E+00	0.106E+01
5	-0.3000	0.697E+00	0.733E+00	0.552E-01	-0.934E-01	-0.508E-01	0.382E+00	0.702E+00
4	-0.3333	0.575E+00	0.689E+00	0.000E+00	-0.112E+00	-0.124E+00	0.246E+00	0.434E+00
3	-0.3667	0.517E+00	0.629E+00	0.000E+00	-0.146E+00	-0.144E+00	0.132E+00	0.255E+00
2	-0.4000	0.584E+00	0.615E+00	0.000E+00	-0.197E+00	-0.202E+00	0.610E-01	0.985E-01
1	-0.4333	0.713E+00	0.626E+00	0.000E+00	-0.194E+00	-0.204E+00	0.314E-01	0.177E-01

(d) v/u_{av}

TABLE X (Continued)

	I =	1	2	3	4	5	6	7
	X =	0.0278	0.0833	0.1389	0.1944	0.2500	0.3056	0.4167
J	Y							
27	0.4333	-0.797E+01	-0.821E+01	-0.740E+01	-0.657E+01	0.574E+01	-0.692E+01	-0.597E+01
26	0.4000	-0.770E+01	-0.797E+01	-0.739E+01	-0.652E+01	0.585E+01	-0.697E+01	-0.634E+01
25	0.3667	-0.762E+01	-0.765E+01	-0.738E+01	-0.637E+01	0.601E+01	-0.719E+01	-0.665E+01
24	0.3333	-0.740E+01	-0.729E+01	-0.725E+01	-0.647E+01	0.611E+01	-0.740E+01	-0.718E+01
23	0.3000	-0.729E+01	-0.720E+01	-0.731E+01	-0.668E+01	0.632E+01	-0.777E+01	-0.780E+01
22	0.2667	-0.735E+01	-0.742E+01	-0.756E+01	-0.695E+01	0.676E+01	-0.839E+01	-0.857E+01
21	0.2333	-0.764E+01	-0.773E+01	-0.802E+01	-0.730E+01	0.706E+01	-0.890E+01	-0.918E+01
20	0.2000	-0.793E+01	-0.822E+01	-0.849E+01	-0.746E+01	0.768E+01	-0.901E+01	-0.975E+01
19	0.1667	-0.784E+01	-0.837E+01	-0.885E+01	-0.754E+01	0.814E+01	-0.902E+01	-0.968E+01
18	0.1333	-0.686E+01	-0.828E+01	-0.876E+01	-0.767E+01	0.820E+01	-0.888E+01	-0.925E+01
17	0.1000	-0.474E+01	-0.739E+01	-0.821E+01	-0.721E+01	0.774E+01	-0.830E+01	-0.851E+01
16	0.0667	-0.274E+01	-0.540E+01	-0.626E+01	-0.580E+01	0.679E+01	-0.667E+01	-0.586E+01
15	0.0333	-0.139E+01	-0.207E+01	-0.319E+01	-0.310E+01	0.517E+01	-0.328E+01	-0.402E+01
14	0.0000	0.612E+00	-0.976E+00	0.454E+00	0.299E+00	0.272E+01	0.185E+01	0.112E+01
13	-0.0333	0.214E+01	0.138E+01	0.374E+01	0.358E+01	0.517E+01	0.537E+01	0.466E+01
12	-0.0667	0.367E+01	0.406E+01	0.613E+01	0.611E+01	0.679E+01	0.766E+01	0.749E+01
11	-0.1000	0.578E+01	0.698E+01	0.797E+01	0.737E+01	0.774E+01	0.936E+01	0.892E+01
10	-0.1333	0.778E+01	0.853E+01	0.888E+01	0.816E+01	0.820E+01	0.100E+02	0.985E+01
9	-0.1667	0.872E+01	0.900E+01	0.908E+01	0.824E+01	0.814E+01	0.103E+02	0.105E+02
8	-0.2000	0.844E+01	0.878E+01	0.883E+01	0.804E+01	0.768E+01	0.952E+01	0.100E+02
7	-0.2333	0.838E+01	0.837E+01	0.823E+01	0.751E+01	0.706E+01	0.875E+01	0.919E+01
6	-0.2667	0.839E+01	0.802E+01	0.769E+01	0.712E+01	0.676E+01	0.819E+01	0.829E+01
5	-0.3000	0.855E+01	0.795E+01	0.754E+01	0.691E+01	0.632E+01	0.761E+01	0.759E+01
4	-0.3333	0.873E+01	0.809E+01	0.735E+01	0.676E+01	0.611E+01	0.722E+01	0.705E+01
3	-0.3667	0.869E+01	0.863E+01	0.736E+01	0.668E+01	0.601E+01	0.686E+01	0.651E+01
2	-0.4000	0.874E+01	0.899E+01	0.761E+01	0.654E+01	0.585E+01	0.658E+01	0.615E+01
1	-0.4333	0.957E+01	0.962E+01	0.779E+01	0.648E+01	0.574E+01	0.629E+01	0.579E+01

(e) w/u_{av}

TABLE XI

VELOCITY DATA, CASE 6 (L/D = 4), STRONG SWIRL

	I =	1	2	3	4	5	6	7
	X =	0.0063	0.0190	0.0318	0.0444	0.0572	0.0698	0.0952
J	Y							
27	0.0991	0.272E+03	0.280E+03	0.283E+03	0.282E+03	0.755E+02	0.279E+03	0.278E+03
26	0.0914	0.275E+03	0.281E+03	0.278E+03	0.278E+03	0.785E+02	0.276E+03	0.275E+03
25	0.0838	0.277E+03	0.279E+03	0.273E+03	0.273E+03	0.820E+02	0.272E+03	0.273E+03
24	0.0762	0.276E+03	0.273E+03	0.269E+03	0.270E+03	0.855E+02	0.268E+03	0.271E+03
23	0.0686	0.274E+03	0.269E+03	0.266E+03	0.266E+03	0.895E+02	0.265E+03	0.270E+03
22	0.0610	0.273E+03	0.267E+03	0.265E+03	0.264E+03	0.920E+02	0.263E+03	0.269E+03
21	0.0533	0.272E+03	0.268E+03	0.264E+03	0.265E+03	0.925E+02	0.264E+03	0.268E+03
20	0.0457	0.274E+03	0.269E+03	0.268E+03	0.268E+03	0.905E+02	0.269E+03	0.271E+03
19	0.0381	0.276E+03	0.273E+03	0.274E+03	0.274E+03	0.850E+02	0.277E+03	0.279E+03
18	0.0305	0.281E+03	0.279E+03	0.280E+03	0.280E+03	0.785E+02	0.284E+03	0.288E+03
17	0.0229	0.291E+03	0.286E+03	0.287E+03	0.286E+03	0.695E+02	0.290E+03	0.294E+03
16	0.0152	0.314E+03	0.295E+03	0.294E+03	0.294E+03	0.595E+02	0.296E+03	0.298E+03
15	0.0076	0.340E+03	0.310E+03	0.307E+03	0.303E+03	0.460E+02	0.304E+03	0.315E+03
14	0.0000	0.500E+01	0.342E+03	0.348E+03	0.340E+03	0.200E+02	0.200E+02	0.330E+02
13	-0.0076	0.380E+02	0.131E+03	0.380E+02	0.405E+02	0.460E+02	0.530E+02	0.535E+02
12	-0.0152	0.660E+02	0.570E+02	0.590E+02	0.580E+02	0.595E+02	0.640E+02	0.620E+02
11	-0.0229	0.880E+02	0.720E+02	0.705E+02	0.695E+02	0.695E+02	0.725E+02	0.715E+02
10	-0.0305	0.935E+02	0.820E+02	0.795E+02	0.785E+02	0.785E+02	0.810E+02	0.810E+02
9	-0.0381	0.960E+02	0.870E+02	0.855E+02	0.855E+02	0.850E+02	0.870E+02	0.865E+02
8	-0.0457	0.975E+02	0.910E+02	0.905E+02	0.905E+02	0.905E+02	0.910E+02	0.895E+02
7	-0.0533	0.980E+02	0.935E+02	0.935E+02	0.945E+02	0.925E+02	0.930E+02	0.900E+02
6	-0.0610	0.965E+02	0.930E+02	0.935E+02	0.945E+02	0.920E+02	0.910E+02	0.885E+02
5	-0.0686	0.920E+02	0.910E+02	0.925E+02	0.925E+02	0.895E+02	0.880E+02	0.860E+02
4	-0.0762	0.895E+02	0.875E+02	0.900E+02	0.895E+02	0.855E+02	0.840E+02	0.835E+02
3	-0.0838	0.905E+02	0.835E+02	0.870E+02	0.845E+02	0.820E+02	0.800E+02	0.800E+02
2	-0.0914	0.940E+02	0.830E+02	0.820E+02	0.795E+02	0.785E+02	0.750E+02	0.770E+02
1	-0.0991	0.945E+02	0.860E+02	0.780E+02	0.735E+02	0.755E+02	0.710E+02	0.745E+02

(a) Yaw Angle

TABLE XI (Continued)

	I =	1	2	3	4	5	6	7
	X =	0.0063	0.0190	0.0318	0.0444	0.0572	0.0698	0.0952
J	Y							
27	0.0991	0.335E+01	0.354E+01	0.282E+00	-0.168E+01	-0.447E+00	0.395E+02	0.576E+00
26	0.0914	-0.366E+01	0.196E+01	-0.312E+01	-0.331E+01	-0.320E+00	-0.276E+01	-0.542E+00
25	0.0838	-0.585E+01	0.150E+01	-0.392E+01	-0.345E+01	-0.308E+00	-0.320E+01	-0.587E+00
24	0.0762	-0.586E+01	0.186E+01	-0.373E+01	-0.298E+01	0.962E-01	-0.303E+01	-0.698E+00
23	0.0686	-0.520E+01	0.185E+01	-0.383E+01	-0.318E+01	0.814E+00	-0.317E+01	0.383E-01
22	0.0610	-0.386E+01	0.201E+01	-0.347E+01	-0.323E+01	0.144E+01	-0.339E+01	0.150E+01
21	0.0533	-0.117E+01	0.211E+01	-0.382E+01	-0.360E+01	0.169E+01	-0.314E+01	0.251E+01
20	0.0457	0.123E+01	0.256E+01	-0.326E+01	-0.354E+01	0.203E+01	-0.425E+01	0.315E+01
19	0.0381	0.187E+01	-0.130E+01	-0.454E+01	-0.585E+01	0.319E+01	-0.670E+01	0.355E+01
18	0.0305	0.377E+01	-0.302E+01	-0.576E+01	-0.735E+01	0.407E+01	-0.915E+01	0.475E+01
17	0.0229	0.537E+01	-0.555E+01	-0.675E+01	-0.887E+01	0.589E+01	-0.132E+02	0.550E+01
16	0.0152	0.102E+02	-0.748E+01	-0.674E+01	-0.110E+02	0.807E+01	-0.204E+02	0.918E+01
15	0.0076	0.172E+02	-0.659E+01	-0.476E+01	-0.158E+02	0.118E+02	-0.369E+02	0.331E+02
14	0.0000	0.378E+02	0.113E+02	0.309E+02	-0.150E+01	0.149E+02	0.176E+02	0.474E+02
13	-0.0076	0.395E+02	0.246E+02	0.296E+02	0.183E+02	0.118E+02	0.111E+02	0.301E+02
12	-0.0152	0.372E+02	0.179E+02	0.191E+02	0.107E+02	0.807E+01	0.682E+01	0.200E+02
11	-0.0229	0.285E+02	0.133E+02	0.125E+02	0.753E+01	0.589E+01	0.485E+01	0.157E+02
10	-0.0305	0.200E+02	0.101E+02	0.828E+01	0.501E+01	0.407E+01	0.395E+01	0.131E+02
9	-0.0381	0.149E+02	0.824E+01	0.558E+01	0.324E+01	0.319E+01	0.360E+01	0.118E+02
8	-0.0457	0.117E+02	0.790E+01	0.436E+01	0.226E+01	0.203E+01	0.307E+01	0.111E+02
7	-0.0533	0.825E+01	0.680E+01	0.321E+01	0.142E+01	0.169E+01	0.278E+01	0.961E+01
6	-0.0610	0.520E+01	0.608E+01	0.226E+01	0.101E+01	0.144E+01	0.224E+01	0.780E+01
5	-0.0686	0.324E+01	0.579E+01	0.149E+01	0.875E+00	0.814E+00	0.159E+01	0.652E+01
4	-0.0762	0.326E+01	0.526E+01	0.656E+00	0.257E+00	0.962E-01	0.550E+00	0.461E+01
3	-0.0838	0.346E+01	0.454E+01	0.429E-01	-0.896E-01	-0.308E+00	0.507E-01	0.264E+01
2	-0.0914	0.418E+01	0.414E+01	0.000E+00	-0.552E+00	-0.320E+00	0.000E+00	0.162E+01
1	-0.0991	0.529E+01	0.392E+01	0.000E+00	-0.768E+00	-0.447E+00	0.000E+00	0.924E+00

(b) Pitch Angle

TABLE XI (Continued)

J	Y	I = 1 X = 0.0278	2 0.0833	3 0.1389	4 0.1944	5 0.2500	6 0.3056	7 0.4167
27	0.4333	0.104E+01	0.538E+01	0.594E+01	0.497E+01	0.588E+01	0.337E+01	0.302E+01
26	0.4000	0.251E+01	0.565E+01	0.379E+01	0.324E+01	0.479E+01	0.231E+01	0.198E+01
25	0.3667	0.349E+01	0.412E+01	0.139E+01	0.129E+01	0.341E+01	0.653E+00	0.126E+01
24	0.3333	0.284E+01	0.140E+01	-0.461E+00	-0.119E-03	0.197E+01	-0.909E+00	0.452E+00
23	0.3000	0.188E+01	-0.471E+00	-0.188E+01	-0.181E+01	0.230E+00	-0.242E+01	-0.135E-03
22	0.2667	0.124E+01	-0.150E+01	-0.275E+01	-0.288E+01	-0.976E+00	-0.371E+01	-0.545E+00
21	0.2333	0.108E+01	-0.137E+01	-0.327E+01	-0.285E+01	-0.131E+01	-0.351E+01	-0.120E+01
20	0.2000	0.209E+01	-0.579E+00	-0.147E+01	-0.139E+01	-0.283E+00	-0.613E+00	0.324E+00
19	0.1667	0.377E+01	0.178E+01	0.209E+01	0.196E+01	0.304E+01	0.416E+01	0.587E+01
18	0.1333	0.622E+01	0.476E+01	0.561E+01	0.543E+01	0.677E+01	0.725E+01	0.105E+02
17	0.1000	0.102E+02	0.794E+01	0.849E+01	0.785E+01	0.109E+02	0.865E+01	0.108E+02
16	0.0667	0.135E+02	0.103E+02	0.999E+01	0.952E+01	0.137E+02	0.801E+01	0.896E+01
15	0.0333	0.141E+02	0.122E+02	0.109E+02	0.903E+01	0.132E+02	0.531E+01	0.755E+01
14	0.0000	0.141E+02	0.126E+02	0.108E+02	0.863E+01	0.939E+01	0.683E+01	0.825E+01
13	-0.0333	0.117E+02	-0.103E+02	0.133E+02	0.116E+02	0.132E+02	0.121E+02	0.115E+02
12	-0.0667	0.732E+01	0.125E+02	0.129E+02	0.124E+02	0.137E+02	0.127E+02	0.135E+02
11	-0.1000	0.974E+00	0.890E+01	0.101E+02	0.103E+02	0.109E+02	0.102E+02	0.109E+02
10	-0.1333	-0.216E+01	0.481E+01	0.634E+01	0.655E+01	0.677E+01	0.594E+01	0.614E+01
9	-0.1667	-0.372E+01	0.194E+01	0.289E+01	0.278E+01	0.304E+01	0.198E+01	0.240E+01
8	-0.2000	-0.436E+01	-0.610E+00	-0.297E+00	-0.291E+00	-0.283E+00	-0.603E+00	0.311E+00
7	-0.2333	-0.445E+01	-0.201E+01	-0.192E+01	-0.242E+01	-0.131E+01	-0.166E+01	0.102E-03
6	-0.2667	-0.346E+01	-0.161E+01	-0.180E+01	-0.225E+01	-0.976E+00	-0.508E+00	0.770E+00
5	-0.3000	-0.107E+01	-0.523E+00	-0.122E+01	-0.119E+01	0.230E+00	0.948E+00	0.183E+01
4	-0.3333	0.278E+00	0.132E+01	0.858E-04	0.233E+00	0.197E+01	0.269E+01	0.280E+01
3	-0.3667	-0.281E+00	0.365E+01	0.140E+01	0.252E+01	0.341E+01	0.429E+01	0.398E+01
2	-0.4000	-0.225E+01	0.407E+01	0.379E+01	0.474E+01	0.479E+01	0.624E+01	0.486E+01
1	-0.4333	-0.273E+01	0.248E+01	0.594E+01	0.747E+01	0.588E+01	0.776E+01	0.547E+01

(c) u/u_{av}

TABLE XI (Continued)

	I =	1	2	3	4	5	6	7
	X =	0.0278	0.0833	0.1389	0.1944	0.2500	0.3056	0.4167
J	Y							
27	0.4333	0.175E+01	0.192E+01	0.135E+00	-0.731E+00	-0.183E+00	0.178E+02	0.218E+00
26	0.4000	-0.184E+01	0.101E+01	-0.149E+01	-0.144E+01	-0.134E+00	-0.116E+01	-0.215E+00
25	0.3667	-0.294E+01	0.727E+00	-0.182E+01	-0.149E+01	-0.131E+00	-0.139E+01	-0.248E+00
24	0.3333	-0.279E+01	0.864E+00	-0.172E+01	-0.131E+01	0.422E-01	-0.138E+01	-0.316E+00
23	0.3000	-0.245E+01	0.873E+00	-0.180E+01	-0.144E+01	0.374E+00	-0.154E+01	0.190E-01
22	0.2667	-0.192E+01	0.101E+01	-0.174E+01	-0.156E+01	0.706E+00	-0.180E+01	0.817E+00
21	0.2333	-0.634E+00	0.116E+01	-0.209E+01	-0.187E+01	0.888E+00	-0.184E+01	0.151E+01
20	0.2000	0.732E+00	0.148E+01	-0.191E+01	-0.197E+01	0.115E+01	-0.261E+01	0.204E+01
19	0.1667	0.118E+01	-0.770E+00	-0.272E+01	-0.330E+01	0.195E+01	-0.401E+01	0.233E+01
18	0.1333	0.225E+01	-0.170E+01	-0.326E+01	-0.403E+01	0.242E+01	-0.500E+01	0.282E+01
17	0.1000	0.266E+01	-0.280E+01	-0.344E+01	-0.444E+01	0.321E+01	-0.591E+01	0.257E+01
16	0.0667	0.349E+01	-0.320E+01	-0.290E+01	-0.456E+01	0.383E+01	-0.693E+01	0.309E+01
15	0.0333	0.464E+01	-0.219E+01	-0.150E+01	-0.469E+01	0.397E+01	-0.714E+01	0.702E+01
14	0.0000	0.110E+02	0.266E+01	0.661E+01	-0.240E+00	0.265E+01	0.230E+01	0.107E+02
13	-0.0333	0.122E+02	0.725E+01	0.963E+01	0.503E+01	0.397E+01	0.392E+01	0.112E+02
12	-0.0667	0.137E+02	0.742E+01	0.866E+01	0.444E+01	0.383E+01	0.346E+01	0.105E+02
11	-0.1000	0.152E+02	0.679E+01	0.673E+01	0.387E+01	0.321E+01	0.289E+01	0.970E+01
10	-0.1333	0.128E+02	0.613E+01	0.506E+01	0.288E+01	0.242E+01	0.262E+01	0.913E+01
9	-0.1667	0.946E+01	0.536E+01	0.360E+01	0.201E+01	0.195E+01	0.238E+01	0.820E+01
8	-0.2000	0.693E+01	0.485E+01	0.260E+01	0.132E+01	0.115E+01	0.186E+01	0.696E+01
7	-0.2333	0.464E+01	0.393E+01	0.176E+01	0.763E+00	0.888E+00	0.154E+01	0.546E+01
6	-0.2667	0.278E+01	0.329E+01	0.116E+01	0.505E+00	0.706E+00	0.114E+01	0.403E+01
5	-0.3000	0.174E+01	0.304E+01	0.727E+00	0.418E+00	0.374E+00	0.754E+00	0.300E+01
4	-0.3333	0.181E+01	0.279E+01	0.309E+00	0.120E+00	0.422E-01	0.247E+00	0.199E+01
3	-0.3667	0.195E+01	0.256E+01	0.200E-01	-0.411E-01	-0.131E+00	0.219E-01	0.106E+01
2	-0.4000	0.236E+01	0.242E+01	0.000E+00	-0.251E+00	-0.134E+00	0.000E+00	0.611E+00
1	-0.4333	0.322E+01	0.244E+01	0.000E+00	-0.353E+00	-0.183E+00	0.000E+00	0.330E+00

(d) v/u_{av}

TABLE XI (Continued)

	I =	1	2	3	4	5	6	7
	X =	0.0278	0.0833	0.1389	0.1944	0.2500	0.3056	0.4167
J	Y							
27	0.4333	-0.299E+02	-0.305E+02	-0.268E+02	-0.245E+02	0.227E+02	-0.213E+02	-0.215E+02
26	0.4000	-0.286E+02	-0.291E+02	-0.270E+02	-0.246E+02	0.235E+02	-0.240E+02	-0.227E+02
25	0.3667	-0.284E+02	-0.275E+02	-0.266E+02	-0.246E+02	0.243E+02	-0.249E+02	-0.241E+02
24	0.3333	-0.270E+02	-0.266E+02	-0.264E+02	-0.251E+02	0.251E+02	-0.260E+02	-0.259E+02
23	0.3000	-0.269E+02	-0.270E+02	-0.269E+02	-0.259E+02	0.263E+02	-0.276E+02	-0.283E+02
22	0.2667	-0.284E+02	-0.287E+02	-0.285E+02	-0.274E+02	0.280E+02	-0.302E+02	-0.312E+02
21	0.2333	-0.310E+02	-0.313E+02	-0.311E+02	-0.296E+02	0.300E+02	-0.334E+02	-0.344E+02
20	0.2000	-0.341E+02	-0.332E+02	-0.336E+02	-0.318E+02	0.325E+02	-0.351E+02	-0.371E+02
19	0.1667	-0.359E+02	-0.340E+02	-0.341E+02	-0.321E+02	0.348E+02	-0.339E+02	-0.371E+02
18	0.1333	-0.336E+02	-0.319E+02	-0.318E+02	-0.308E+02	0.333E+02	-0.302E+02	-0.322E+02
17	0.1000	-0.265E+02	-0.277E+02	-0.278E+02	-0.274E+02	0.291E+02	-0.238E+02	-0.243E+02
16	0.0667	-0.139E+02	-0.221E+02	-0.224E+02	-0.214E+02	0.232E+02	-0.168E+02	-0.169E+02
15	0.0333	-0.513E+01	-0.145E+02	-0.144E+02	-0.139E+02	0.136E+02	-0.787E+01	-0.768E+01
14	0.0000	0.124E+01	-0.410E+01	-0.239E+01	-0.314E+01	0.342E+01	0.248E+01	0.536E+01
13	-0.0333	0.913E+01	0.120E+02	0.104E+02	0.987E+01	0.136E+02	0.160E+02	0.155E+02
12	-0.0667	0.165E+02	0.193E+02	0.214E+02	0.198E+02	0.232E+02	0.260E+02	0.254E+02
11	-0.1000	0.279E+02	0.274E+02	0.286E+02	0.274E+02	0.291E+02	0.325E+02	0.327E+02
10	-0.1333	0.352E+02	0.343E+02	0.342E+02	0.322E+02	0.333E+02	0.375E+02	0.388E+02
9	-0.1667	0.353E+02	0.370E+02	0.367E+02	0.354E+02	0.348E+02	0.379E+02	0.393E+02
8	-0.2000	0.331E+02	0.349E+02	0.340E+02	0.333E+02	0.325E+02	0.346E+02	0.356E+02
7	-0.2333	0.317E+02	0.329E+02	0.314E+02	0.307E+02	0.300E+02	0.316E+02	0.323E+02
6	-0.2667	0.304E+02	0.308E+02	0.295E+02	0.286E+02	0.280E+02	0.291E+02	0.294E+02
5	-0.3000	0.307E+02	0.300E+02	0.280E+02	0.274E+02	0.263E+02	0.272E+02	0.262E+02
4	-0.3333	0.318E+02	0.302E+02	0.270E+02	0.267E+02	0.251E+02	0.256E+02	0.245E+02
3	-0.3667	0.322E+02	0.321E+02	0.267E+02	0.261E+02	0.243E+02	0.243E+02	0.226E+02
2	-0.4000	0.322E+02	0.331E+02	0.269E+02	0.256E+02	0.235E+02	0.233E+02	0.211E+02
1	-0.4333	0.347E+02	0.355E+02	0.280E+02	0.252E+02	0.227E+02	0.225E+02	0.197E+02

(e) w/u_{av}

TABLE XII

VELOCITY DATA, CASE 7 (L/D = 4), NO SWIRL

	I =	1	2	3	4	5	6	7
	X =	0.0063	0.0190	0.0318	0.0444	0.0572	0.0698	0.0952
O J	Y							
27	0.0991	0.161E+03	0.000E+00	0.895E+02	0.360E+03	0.360E+03	0.000E+00	0.690E+02
26	0.0914	0.250E+03	0.000E+00	0.895E+02	0.360E+03	0.360E+03	0.357E+03	0.440E+02
25	0.0838	0.234E+03	0.000E+00	0.895E+02	0.360E+03	0.360E+03	0.000E+00	0.440E+02
24	0.0762	0.234E+03	0.000E+00	0.895E+02	0.360E+03	0.360E+03	0.000E+00	0.420E+02
23	0.0686	0.229E+03	0.000E+00	0.395E+02	0.360E+03	0.360E+03	0.000E+00	0.350E+02
22	0.0610	0.210E+03	0.000E+00	0.400E+01	0.360E+03	0.360E+03	0.357E+03	0.350E+02
21	0.0533	0.204E+03	0.000E+00	0.400E+01	0.360E+03	0.360E+03	0.357E+03	0.110E+02
20	0.0457	0.100E+02	0.000E+00	0.100E+01	0.360E+03	0.360E+03	0.357E+03	0.110E+02
19	0.0381	0.400E+01	0.360E+03	0.100E+01	0.360E+03	0.360E+03	0.357E+03	0.110E+02
18	0.0305	0.400E+01	0.360E+03	0.100E+01	0.360E+03	0.360E+03	0.357E+03	0.110E+02
17	0.0229	0.200E+01	0.360E+03	0.100E+01	0.360E+03	0.360E+03	0.357E+03	0.110E+02
16	0.0152	0.360E+03	0.360E+03	0.360E+03	0.360E+03	0.360E+03	0.357E+03	0.110E+02
15	0.0076	0.360E+03	0.360E+03	0.360E+03	0.360E+03	0.360E+03	0.357E+03	0.110E+02
14	0.0000	0.360E+03	0.360E+03	0.360E+03	0.360E+03	0.360E+03	0.353E+03	0.357E+03
13	-0.0076	0.360E+03	0.360E+03	0.360E+03	0.360E+03	0.360E+03	0.353E+03	0.360E+03
12	-0.0152	0.360E+03	0.360E+03	0.360E+03	0.360E+03	0.360E+03	0.357E+03	0.360E+03
11	-0.0229	0.360E+03	0.360E+03	0.360E+03	0.360E+03	0.360E+03	0.357E+03	0.300E+01
10	-0.0305	0.100E+01	0.360E+03	0.360E+03	0.360E+03	0.360E+03	0.357E+03	0.300E+01
9	-0.0381	0.200E+01	0.360E+03	0.360E+03	0.360E+03	0.360E+03	0.357E+03	0.300E+01
8	-0.0457	0.000E+00	0.360E+03	0.360E+03	0.360E+03	0.360E+03	0.357E+03	0.250E+01
7	-0.0533	0.152E+03	0.102E+03	0.100E+01	0.360E+03	0.360E+03	0.357E+03	0.250E+01
6	-0.0610	0.161E+03	0.000E+00	0.100E+01	0.360E+03	0.360E+03	0.357E+03	0.250E+01
5	-0.0686	0.161E+03	0.100E+03	0.100E+01	0.360E+03	0.360E+03	0.357E+03	0.200E+01
4	-0.0762	0.161E+03	0.138E+03	0.100E+01	0.360E+03	0.360E+03	0.357E+03	0.200E+01
3	-0.0838	0.161E+03	0.138E+03	0.100E+01	0.360E+03	0.360E+03	0.357E+03	0.360E+03
2	-0.0914	0.161E+03	0.138E+03	0.200E+01	0.360E+03	0.360E+03	0.000E+00	0.300E+01
1	-0.0991	0.161E+03	0.138E+03	0.110E+02	0.360E+03	0.360E+03	0.000E+00	0.140E+02

(a) Yaw Angle

TABLE XII (Continued)

	I =	1	2	3	4	5	6	7
	X =	0.0063	0.0190	0.0318	0.0444	0.0572	0.0698	0.0952
O J	Y							
27	0.0991	0.000E+00	0.000E+00	-0.510E+02	-0.433E+02	0.000E+00	0.000E+00	-0.510E+02
26	0.0914	0.000E+00	0.000E+00	-0.433E+02	-0.393E+02	-0.510E+02	0.000E+00	-0.315E+02
25	0.0838	-0.510E+02	0.000E+00	-0.510E+02	-0.315E+02	-0.510E+02	0.000E+00	-0.510E+02
24	0.0762	-0.510E+02	0.000E+00	0.000E+00	-0.373E+02	-0.244E+02	0.000E+00	-0.315E+02
23	0.0686	-0.510E+02	0.000E+00	-0.707E+01	-0.277E+02	-0.315E+02	0.000E+00	-0.165E+02
22	0.0610	-0.510E+02	0.000E+00	-0.287E+01	-0.197E+02	-0.259E+02	0.000E+00	0.000E+00
21	0.0533	-0.315E+02	0.000E+00	0.108E+02	-0.119E+02	-0.154E+02	0.000E+00	0.000E+00
20	0.0457	0.000E+00	0.000E+00	0.463E+01	-0.124E+02	-0.119E+02	0.000E+00	-0.853E+01
19	0.0381	0.000E+00	0.607E+01	0.125E+02	-0.114E+02	-0.110E+02	0.607E+01	-0.707E+01
18	0.0305	0.867E+01	0.607E+01	0.341E+01	-0.817E+01	-0.761E+01	0.351E+01	0.000E+00
17	0.0229	0.339E+01	0.318E+01	0.235E+01	-0.788E+01	-0.512E+01	0.351E+01	0.000E+00
16	0.0152	0.512E+00	0.820E+00	0.207E+01	-0.655E+01	-0.402E+01	0.000E+00	-0.707E+01
15	0.0076	-0.860E+00	-0.853E+00	0.512E+00	-0.352E+01	-0.212E+01	0.000E+00	-0.527E+01
14	0.0000	-0.204E+01	-0.403E+01	-0.768E+00	-0.204E+01	0.000E+00	0.269E+01	0.000E+00
13	-0.0076	-0.299E+01	-0.289E+01	-0.304E+01	-0.352E+01	-0.212E+01	0.218E+01	0.000E+00
12	-0.0152	-0.357E+01	-0.567E+01	-0.588E+01	-0.655E+01	-0.402E+01	0.000E+00	-0.218E+02
11	-0.0229	-0.581E+01	-0.758E+01	-0.805E+01	-0.788E+01	-0.512E+01	0.000E+00	-0.707E+01
10	-0.0305	-0.125E+02	-0.107E+02	-0.113E+02	-0.817E+01	-0.761E+01	-0.311E+01	-0.165E+02
9	-0.0381	0.000E+00	-0.807E+01	-0.100E+02	-0.114E+02	-0.110E+02	-0.311E+01	-0.165E+02
8	-0.0457	0.000E+00	-0.152E+02	-0.165E+02	-0.124E+02	-0.119E+02	-0.110E+02	-0.165E+02
7	-0.0533	0.000E+00	-0.315E+02	-0.315E+02	-0.119E+02	-0.154E+02	-0.110E+02	-0.110E+02
6	-0.0610	0.000E+00	0.000E+00	-0.315E+02	-0.197E+02	-0.259E+02	-0.773E+01	-0.853E+01
5	-0.0686	0.000E+00	0.000E+00	-0.510E+02	-0.277E+02	-0.315E+02	-0.707E+01	-0.315E+02
4	-0.0762	0.000E+00	0.000E+00	-0.315E+02	-0.373E+02	-0.244E+02	-0.165E+02	-0.165E+02
3	-0.0838	-0.315E+02	0.000E+00	0.000E+00	-0.315E+02	-0.510E+02	0.000E+00	-0.165E+02
2	-0.0914	0.000E+00	0.000E+00	-0.315E+02	-0.393E+02	-0.510E+02	0.000E+00	-0.315E+02
1	-0.0991	0.000E+00	0.000E+00	-0.315E+02	-0.433E+02	0.000E+00	0.000E+00	-0.165E+02

(b) Pitch Angle

TABLE XII (Continued)

	I =	1	2	3	4	5	6	7
	X =	0.0278	0.0833	0.1389	0.1944	0.2500	0.3056	0.4167
O J	Y							
27	0.4333	0.000E+00	0.000E+00	0.713E-02	0.118E+01	0.000E+00	0.000E+00	0.290E+00
26	0.4000	0.000E+00	0.000E+00	0.103E-01	0.150E+01	0.816E+00	0.109E+01	0.653E+00
25	0.3667	-0.473E+00	0.000E+00	0.101E-01	0.159E+01	0.816E+00	0.000E+00	0.581E+00
24	0.3333	-0.473E+00	0.000E+00	0.942E-02	0.178E+01	0.192E+01	0.000E+00	0.674E+00
23	0.3000	-0.528E+00	0.000E+00	0.181E+01	0.249E+01	0.205E+01	0.000E+00	0.115E+01
22	0.2667	-0.698E+00	0.000E+00	0.384E+01	0.312E+01	0.301E+01	0.109E+01	0.124E+01
21	0.2333	-0.826E+00	0.000E+00	0.480E+01	0.509E+01	0.389E+01	0.153E+01	0.182E+01
20	0.2000	0.000E+00	0.000E+00	0.687E+01	0.642E+01	0.509E+01	0.153E+01	0.202E+01
19	0.1667	0.000E+00	0.244E+01	0.535E+01	0.756E+01	0.560E+01	0.245E+01	0.228E+01
18	0.1333	0.283E+01	0.488E+01	0.124E+02	0.932E+01	0.776E+01	0.327E+01	0.182E+01
17	0.1000	0.126E+02	0.906E+01	0.145E+02	0.110E+02	0.851E+01	0.327E+01	0.210E+01
16	0.0667	0.196E+02	0.139E+02	0.149E+02	0.113E+02	0.856E+01	0.376E+01	0.228E+01
15	0.0333	0.206E+02	0.185E+02	0.154E+02	0.139E+02	0.894E+01	0.420E+01	0.271E+01
14	0.0000	0.215E+02	0.212E+02	0.165E+02	0.129E+02	0.903E+01	0.374E+01	0.185E+01
13	-0.0333	0.210E+02	0.207E+02	0.135E+02	0.139E+02	0.894E+01	0.418E+01	0.185E+01
12	-0.0667	0.207E+02	0.195E+02	0.102E+02	0.113E+02	0.856E+01	0.420E+01	0.168E+01
11	-0.1000	0.171E+02	0.160E+02	0.808E+01	0.110E+02	0.851E+01	0.420E+01	0.232E+01
10	-0.1333	0.708E+01	0.987E+01	0.603E+01	0.932E+01	0.776E+01	0.371E+01	0.140E+01
9	-0.1667	0.000E+00	0.715E+01	0.460E+01	0.756E+01	0.560E+01	0.371E+01	0.140E+01
8	-0.2000	0.000E+00	0.362E+01	0.316E+01	0.642E+01	0.509E+01	0.308E+01	0.140E+01
7	-0.2333	-0.940E+00	-0.258E+00	0.159E+01	0.509E+01	0.389E+01	0.308E+01	0.175E+01
6	-0.2667	-0.101E+01	0.000E+00	0.130E+01	0.312E+01	0.301E+01	0.315E+01	0.206E+01
5	-0.3000	-0.101E+01	0.000E+00	0.816E+00	0.249E+01	0.205E+01	0.236E+01	0.907E+00
4	-0.3333	-0.101E+01	0.000E+00	0.916E+00	0.178E+01	0.192E+01	0.142E+01	0.140E+01
3	-0.3667	-0.855E+00	0.000E+00	0.000E+00	0.159E+01	0.816E+00	0.109E+01	0.140E+01
2	-0.4000	0.000E+00	0.000E+00	0.916E+00	0.150E+01	0.816E+00	0.000E+00	0.906E+00
1	-0.4333	0.000E+00	0.000E+00	0.900E+00	0.118E+01	0.000E+00	0.000E+00	0.136E+01

(c) u/u_{av}

TABLE XII (Continued)

	I =	1	2	3	4	5	6	7
	X =	0.0278	0.0833	0.1389	0.1944	0.2500	0.3056	0.4167
J	Y							
27	0.4333	0.000E+00	0.000E+00	-0.129E+01	-0.142E+01	0.000E+00	0.000E+00	-0.128E+01
26	0.4000	0.000E+00	0.000E+00	-0.142E+01	-0.158E+01	-0.129E+01	0.000E+00	-0.714E+00
25	0.3667	-0.128E+01	0.000E+00	-0.183E+01	-0.125E+01	-0.129E+01	0.000E+00	-0.128E+01
24	0.3333	-0.128E+01	0.000E+00	0.000E+00	-0.174E+01	-0.112E+01	0.000E+00	-0.714E+00
23	0.3000	-0.128E+01	0.000E+00	-0.374E+00	-0.167E+01	-0.161E+01	0.000E+00	-0.531E+00
22	0.2667	-0.128E+01	0.000E+00	-0.248E+00	-0.143E+01	-0.188E+01	0.000E+00	0.000E+00
21	0.2333	-0.711E+00	0.000E+00	0.117E+01	-0.137E+01	-0.137E+01	0.000E+00	0.000E+00
20	0.2000	0.000E+00	0.000E+00	0.713E+00	-0.181E+01	-0.137E+01	0.000E+00	-0.396E+00
19	0.1667	0.000E+00	0.333E+00	0.152E+01	-0.196E+01	-0.140E+01	0.335E+00	-0.370E+00
18	0.1333	0.555E+00	0.666E+00	0.944E+00	-0.172E+01	-0.133E+01	0.257E+00	0.000E+00
17	0.1000	0.962E+00	0.646E+00	0.764E+00	-0.194E+01	-0.978E+00	0.257E+00	0.000E+00
16	0.0667	0.224E+00	0.256E+00	0.692E+00	-0.166E+01	-0.773E+00	0.000E+00	-0.370E+00
15	0.0333	-0.397E+00	-0.354E+00	0.176E+00	-0.110E+01	-0.424E+00	0.000E+00	-0.327E+00
14	0.0000	-0.986E+00	-0.192E+01	-0.283E+00	-0.589E+00	0.000E+00	0.227E+00	0.000E+00
13	-0.0333	-0.141E+01	-0.134E+01	-0.918E+00	-0.110E+01	-0.424E+00	0.206E+00	0.000E+00
12	-0.0667	-0.165E+01	-0.249E+01	-0.134E+01	-0.166E+01	-0.773E+00	0.000E+00	-0.860E+00
11	-0.1000	-0.223E+01	-0.274E+01	-0.147E+01	-0.194E+01	-0.978E+00	0.000E+00	-0.370E+00
10	-0.1333	-0.202E+01	-0.239E+01	-0.155E+01	-0.172E+01	-0.133E+01	-0.260E+00	-0.531E+00
9	-0.1667	0.000E+00	-0.130E+01	-0.104E+01	-0.196E+01	-0.140E+01	-0.260E+00	-0.531E+00
8	-0.2000	0.000E+00	-0.126E+01	-0.120E+01	-0.181E+01	-0.137E+01	-0.772E+00	-0.531E+00
7	-0.2333	0.000E+00	-0.102E+01	-0.125E+01	-0.137E+01	-0.137E+01	-0.772E+00	-0.438E+00
6	-0.2667	0.000E+00	0.000E+00	-0.102E+01	-0.143E+01	-0.188E+01	-0.550E+00	-0.396E+00
5	-0.3000	0.000E+00	0.000E+00	-0.129E+01	-0.167E+01	-0.161E+01	-0.376E+00	-0.714E+00
4	-0.3333	0.000E+00	0.000E+00	-0.721E+00	-0.174E+01	-0.112E+01	-0.540E+00	-0.531E+00
3	-0.3667	-0.711E+00	0.000E+00	0.000E+00	-0.125E+01	-0.129E+01	0.000E+00	-0.531E+00
2	-0.4000	0.000E+00	0.000E+00	-0.721E+00	-0.158E+01	-0.129E+01	0.000E+00	-0.714E+00
1	-0.4333	0.000E+00	0.000E+00	-0.721E+00	-0.142E+01	0.000E+00	0.000E+00	-0.531E+00

(d) v/u_{av}

TABLE XII (Continued)

	I =	1	2	3	4	5	6	7
	X =	0.0278	0.0833	0.1389	0.1944	0.2500	0.3056	0.4167
O J	Y							
27	0.4333	0.000E+00	0.000E+00	0.816E+00	-0.709E-05	0.000E+00	0.000E+00	0.755E+00
26	0.4000	0.000E+00	0.000E+00	0.118E+01	-0.906E-05	-0.492E-05	-0.569E-01	0.630E+00
25	0.3667	-0.652E+00	0.000E+00	0.115E+01	-0.956E-05	-0.492E-05	0.000E+00	0.561E+00
24	0.3333	-0.652E+00	0.000E+00	0.108E+01	-0.107E-04	-0.116E-04	0.000E+00	0.607E+00
23	0.3000	-0.608E+00	0.000E+00	0.149E+01	-0.150E-04	-0.123E-04	0.000E+00	0.803E+00
22	0.2667	-0.403E+00	0.000E+00	0.268E+00	-0.188E-04	-0.181E-04	-0.569E-01	0.867E+00
21	0.2333	-0.368E+00	0.000E+00	0.336E+00	-0.306E-04	-0.234E-04	-0.804E-01	0.353E+00
20	0.2000	0.000E+00	0.000E+00	0.120E+00	-0.387E-04	-0.306E-04	-0.804E-01	0.393E+00
19	0.1667	0.000E+00	-0.147E-04	0.934E-01	-0.455E-04	-0.337E-04	-0.128E+00	0.443E+00
18	0.1333	0.198E+00	-0.294E-04	0.216E+00	-0.561E-04	-0.467E-04	-0.171E+00	0.353E+00
17	0.1000	0.441E+00	-0.546E-04	0.253E+00	-0.660E-04	-0.513E-04	-0.171E+00	0.408E+00
16	0.0667	-0.118E-03	-0.839E-04	-0.897E-04	-0.680E-04	-0.516E-04	-0.197E+00	0.443E+00
15	0.0333	-0.124E-03	-0.111E-03	-0.925E-04	-0.836E-04	-0.539E-04	-0.220E+00	0.527E+00
14	0.0000	-0.130E-03	-0.128E-03	-0.992E-04	-0.776E-04	-0.544E-04	-0.460E+00	-0.969E-01
13	-0.0333	-0.127E-03	-0.124E-03	-0.813E-04	-0.836E-04	-0.539E-04	-0.513E+00	-0.111E-04
12	-0.0667	-0.125E-03	-0.118E-03	-0.613E-04	-0.680E-04	-0.516E-04	-0.220E+00	-0.101E-04
11	-0.1000	-0.103E-03	-0.966E-04	-0.487E-04	-0.660E-04	-0.513E-04	-0.220E+00	0.122E+00
10	-0.1333	0.124E+00	-0.595E-04	-0.364E-04	-0.561E-04	-0.467E-04	-0.195E+00	0.733E-01
9	-0.1667	0.000E+00	-0.431E-04	-0.277E-04	-0.455E-04	-0.337E-04	-0.195E+00	0.733E-01
8	-0.2000	0.000E+00	-0.218E-04	-0.190E-04	-0.387E-04	-0.306E-04	-0.161E+00	0.611E-01
7	-0.2333	0.500E+00	0.127E+01	0.277E-01	-0.306E-04	-0.234E-04	-0.161E+00	0.764E-01
6	-0.2667	0.347E+00	0.000E+00	0.226E-01	-0.188E-04	-0.181E-04	-0.165E+00	0.897E-01
5	-0.3000	0.347E+00	0.000E+00	0.142E-01	-0.150E-04	-0.123E-04	-0.124E+00	0.317E-01
4	-0.3333	0.347E+00	0.000E+00	0.160E-01	-0.107E-04	-0.116E-04	-0.745E-01	0.489E-01
3	-0.3667	0.294E+00	0.000E+00	0.000E+00	-0.956E-05	-0.492E-05	-0.569E-01	-0.843E-05
2	-0.4000	0.000E+00	0.000E+00	0.320E-01	-0.906E-05	-0.492E-05	0.000E+00	0.475E-01
1	-0.4333	0.000E+00	0.000E+00	0.175E+00	-0.709E-05	0.000E+00	0.000E+00	0.339E+00

(e) w/u_{av}

TABLE XIII

VELOCITY DATA, CASE 4 (L/D = 6), MODERATE SWIRL

	I =	1	2	3	4	5	6
	X =	0.0190	0.0444	0.0572	0.0952	0.1206	0.1460
J	Y						
27	0.0991	0.280E+03	0.280E+03	0.281E+03	0.287E+03	0.710E+02	0.720E+02
26	0.0914	0.278E+03	0.277E+03	0.277E+03	0.282E+03	0.760E+02	0.750E+02
25	0.0838	0.275E+03	0.273E+03	0.272E+03	0.277E+03	0.820E+02	0.780E+02
24	0.0762	0.272E+03	0.270E+03	0.268E+03	0.272E+03	0.850E+02	0.818E+02
23	0.0686	0.272E+03	0.267E+03	0.265E+03	0.270E+03	0.880E+02	0.845E+02
22	0.0610	0.272E+03	0.266E+03	0.264E+03	0.267E+03	0.925E+02	0.845E+02
21	0.0533	0.275E+03	0.267E+03	0.266E+03	0.266E+03	0.925E+02	0.845E+02
20	0.0457	0.279E+03	0.273E+03	0.272E+03	0.270E+03	0.900E+02	0.860E+02
19	0.0381	0.287E+03	0.279E+03	0.278E+03	0.278E+03	0.838E+02	0.850E+02
18	0.0305	0.294E+03	0.285E+03	0.284E+03	0.285E+03	0.740E+02	0.785E+02
17	0.0229	0.298E+03	0.290E+03	0.290E+03	0.292E+03	0.655E+02	0.685E+02
16	0.0152	0.309E+03	0.295E+03	0.294E+03	0.298E+03	0.570E+02	0.598E+02
15	0.0076	0.316E+03	0.304E+03	0.300E+03	0.298E+03	0.670E+02	0.530E+02
14	0.0000	0.330E+03	0.334E+03	0.460E+02	0.200E+02	0.358E+03	0.600E+02
13	-0.0076	0.356E+03	0.560E+02	0.520E+02	0.570E+02	0.670E+02	0.600E+02
12	-0.0152	0.530E+02	0.590E+02	0.580E+02	0.600E+02	0.570E+02	0.598E+02
11	-0.0229	0.650E+02	0.680E+02	0.680E+02	0.680E+02	0.655E+02	0.685E+02
10	-0.0305	0.740E+02	0.760E+02	0.740E+02	0.750E+02	0.740E+02	0.790E+02
9	-0.0381	0.800E+02	0.830E+02	0.830E+02	0.820E+02	0.838E+02	0.850E+02
8	-0.0457	0.835E+02	0.895E+02	0.890E+02	0.900E+02	0.900E+02	0.860E+02
7	-0.0533	0.880E+02	0.940E+02	0.920E+02	0.920E+02	0.925E+02	0.845E+02
6	-0.0610	0.880E+02	0.940E+02	0.920E+02	0.920E+02	0.925E+02	0.845E+02
5	-0.0686	0.880E+02	0.915E+02	0.900E+02	0.880E+02	0.880E+02	0.845E+02
4	-0.0762	0.855E+02	0.880E+02	0.860E+02	0.840E+02	0.850E+02	0.818E+02
3	-0.0838	0.820E+02	0.830E+02	0.800E+02	0.800E+02	0.820E+02	0.780E+02
2	-0.0914	0.810E+02	0.800E+02	0.760E+02	0.755E+02	0.760E+02	0.750E+02
1	-0.0991	0.840E+02	0.745E+02	0.710E+02	0.730E+02	0.710E+02	0.720E+02

(a) Yaw Angle

TABLE XIII (Continued)

	I =	1	2	3	4	5	6
	X =	0.0190	0.0444	0.0572	0.0952	0.1206	0.1460
J	Y						
27	0.0991	0.190E+01	-0.139E+01	-0.542E+00	0.000E+00	-0.237E+00	-0.631E+00
26	0.0914	-0.109E+00	-0.588E+01	-0.215E+01	-0.139E+01	0.000E+00	-0.285E+00
25	0.0838	-0.132E+00	-0.614E+01	-0.265E+01	-0.181E+01	0.421E+00	0.000E+00
24	0.0762	-0.626E+00	-0.658E+01	-0.239E+01	-0.278E+01	0.947E+00	0.702E+00
23	0.0686	-0.845E+00	-0.727E+01	-0.340E+01	-0.215E+01	0.137E+01	0.100E+01
22	0.0610	-0.141E+01	-0.791E+01	-0.357E+01	-0.951E+00	0.261E+01	0.231E+01
21	0.0533	-0.176E+01	-0.879E+01	-0.393E+01	-0.977E+00	0.441E+01	0.286E+01
20	0.0457	-0.313E+01	-0.903E+01	-0.514E+01	-0.155E+01	0.546E+01	0.409E+01
19	0.0381	-0.317E+01	-0.977E+01	-0.596E+01	-0.104E+01	0.592E+01	0.494E+01
18	0.0305	-0.185E+01	-0.106E+02	-0.767E+01	-0.471E+00	0.665E+01	0.675E+01
17	0.0229	-0.220E+01	-0.124E+02	-0.924E+01	-0.399E+00	0.846E+01	0.943E+01
16	0.0152	0.000E+00	-0.154E+02	-0.121E+02	0.244E+01	0.140E+02	0.127E+02
15	0.0076	0.000E+00	-0.224E+02	-0.121E+02	0.153E+02	0.303E+02	0.224E+02
14	0.0000	0.000E+00	-0.534E+02	0.294E+02	0.000E+00	0.000E+00	0.437E+02
13	-0.0076	-0.878E+01	0.265E+02	0.129E+02	0.298E+02	0.303E+02	0.437E+02
12	-0.0152	0.491E+01	0.122E+02	0.766E+01	0.169E+02	0.140E+02	0.127E+02
11	-0.0229	0.152E+01	0.753E+01	0.511E+01	0.122E+02	0.846E+01	0.943E+01
10	-0.0305	0.499E+01	0.503E+01	0.370E+01	0.936E+01	0.665E+01	0.675E+01
9	-0.0381	0.545E+01	0.356E+01	0.262E+01	0.846E+01	0.592E+01	0.494E+01
8	-0.0457	0.502E+01	0.186E+01	0.142E+01	0.637E+01	0.546E+01	0.409E+01
7	-0.0533	0.517E+01	0.000E+00	0.415E+00	0.457E+01	0.441E+01	0.286E+01
6	-0.0610	0.487E+01	-0.906E+00	0.613E+00	0.394E+01	0.261E+01	0.231E+01
5	-0.0686	0.433E+01	-0.137E+01	0.766E+00	0.317E+01	0.137E+01	0.100E+01
4	-0.0762	0.399E+01	-0.133E+01	0.121E+01	0.235E+01	0.947E+00	0.702E+00
3	-0.0838	0.317E+01	-0.115E+01	0.993E+00	0.176E+01	0.421E+00	0.000E+00
2	-0.0914	0.278E+01	-0.803E+00	0.688E+00	0.835E+00	0.000E+00	-0.285E+00
1	-0.0991	0.270E+01	-0.625E+00	-0.145E+00	0.229E+00	-0.237E+00	-0.631E+00

(b) Pitch Angle

TABLE XIII (Continued)

	I =	1	2	3	4	5	6
	X =	0.0833	0.1944	0.2500	0.4167	0.5278	0.6389
J	Y						
27	0.4333	0.142E+01	0.120E+01	0.126E+01	0.164E+01	0.163E+01	0.135E+01
26	0.4000	0.103E+01	0.729E+00	0.765E+00	0.115E+01	0.124E+01	0.118E+01
25	0.3667	0.583E+00	0.317E+00	0.211E+00	0.671E+00	0.733E+00	0.980E+00
24	0.3333	0.259E+00	-0.283E-04	-0.260E+00	0.194E+00	0.479E+00	0.709E+00
23	0.3000	0.187E+00	-0.300E+00	-0.508E+00	-0.511E-01	0.200E+00	0.512E+00
22	0.2667	0.204E+00	-0.450E+00	-0.624E+00	-0.377E+00	-0.268E+00	0.554E+00
21	0.2333	0.461E+00	-0.308E+00	-0.433E+00	-0.516E+00	-0.294E+00	0.606E+00
20	0.2000	0.926E+00	0.269E+00	0.224E+00	-0.326E-04	0.239E-04	0.489E+00
19	0.1667	0.172E+01	0.103E+01	0.960E+00	0.101E+01	0.861E+00	0.671E+00
18	0.1333	0.233E+01	0.176E+01	0.181E+01	0.206E+01	0.232E+01	0.163E+01
17	0.1000	0.221E+01	0.261E+01	0.275E+01	0.324E+01	0.383E+01	0.329E+01
16	0.0667	0.230E+01	0.339E+01	0.337E+01	0.409E+01	0.509E+01	0.488E+01
15	0.0333	0.184E+01	0.408E+01	0.333E+01	0.295E+01	0.264E+01	0.521E+01
14	0.0000	0.501E+00	0.192E+01	0.379E+01	0.172E+01	0.000E+00	0.221E+01
13	-0.0333	0.298E+01	0.362E+01	0.491E+01	0.413E+01	0.264E+01	0.221E+01
12	-0.0667	0.175E+01	0.423E+01	0.464E+01	0.464E+01	0.509E+01	0.488E+01
11	-0.1000	0.181E+01	0.315E+01	0.304E+01	0.320E+01	0.383E+01	0.329E+01
10	-0.1333	0.166E+01	0.189E+01	0.203E+01	0.202E+01	0.232E+01	0.156E+01
9	-0.1667	0.120E+01	0.894E+00	0.875E+00	0.104E+01	0.861E+00	0.671E+00
8	-0.2000	0.781E+00	0.601E-01	0.120E+00	0.228E-04	0.239E-04	0.489E+00
7	-0.2333	0.245E+00	-0.469E+00	-0.225E+00	-0.228E+00	-0.294E+00	0.606E+00
6	-0.2667	0.245E+00	-0.439E+00	-0.213E+00	-0.211E+00	-0.268E+00	0.554E+00
5	-0.3000	0.255E+00	-0.165E+00	0.194E-04	0.199E+00	0.200E+00	0.512E+00
4	-0.3333	0.612E+00	0.223E+00	0.426E+00	0.576E+00	0.479E+00	0.709E+00
3	-0.3667	0.116E+01	0.788E+00	0.110E+01	0.929E+00	0.733E+00	0.980E+00
2	-0.4000	0.138E+01	0.116E+01	0.156E+01	0.131E+01	0.124E+01	0.118E+01
1	-0.4333	0.986E+00	0.185E+01	0.208E+01	0.148E+01	0.163E+01	0.135E+01

(c) u/u_{av}

TABLE XIII (Continued)

	I =	1	2	3	4	5	6
	X =	0.0833	0.1944	0.2500	0.4167	0.5278	0.6389
J	Y						
27	0.4333	0.271E+00	-0.168E+00	-0.626E-01	0.000E+00	-0.208E-01	-0.481E-01
26	0.4000	-0.140E-01	-0.664E+00	-0.236E+00	-0.134E+00	0.000E+00	-0.228E-01
25	0.3667	-0.154E-01	-0.651E+00	-0.280E+00	-0.174E+00	0.387E-01	0.000E+00
24	0.3333	-0.674E-01	-0.687E+00	-0.249E+00	-0.270E+00	0.909E-01	0.609E-01
23	0.3000	-0.878E-01	-0.731E+00	-0.346E+00	-0.219E+00	0.137E+00	0.934E-01
22	0.2667	-0.144E+00	-0.797E+00	-0.373E+00	-0.102E+00	0.280E+00	0.233E+00
21	0.2333	-0.180E+00	-0.909E+00	-0.426E+00	-0.112E+00	0.520E+00	0.315E+00
20	0.2000	-0.324E+00	-0.980E+00	-0.577E+00	-0.186E+00	0.718E+00	0.502E+00
19	0.1667	-0.326E+00	-0.113E+01	-0.720E+00	-0.131E+00	0.826E+00	0.666E+00
18	0.1333	-0.185E+00	-0.132E+01	-0.101E+01	-0.656E-01	0.979E+00	0.970E+00
17	0.1000	-0.181E+00	-0.169E+01	-0.131E+01	-0.603E-01	0.137E+01	0.149E+01
16	0.0667	0.000E+00	-0.221E+01	-0.177E+01	0.378E+00	0.233E+01	0.219E+01
15	0.0333	0.000E+00	-0.305E+01	-0.143E+01	0.172E+01	0.394E+01	0.357E+01
14	0.0000	0.000E+00	-0.288E+01	0.307E+01	0.000E+00	0.000E+00	0.422E+01
13	-0.0333	-0.462E+00	0.323E+01	0.182E+01	0.434E+01	0.394E+01	0.422E+01
12	-0.0667	0.250E+00	0.177E+01	0.118E+01	0.282E+01	0.233E+01	0.219E+01
11	-0.1000	0.114E+00	0.111E+01	0.725E+00	0.184E+01	0.137E+01	0.149E+01
10	-0.1333	0.527E+00	0.687E+00	0.476E+00	0.129E+01	0.979E+00	0.970E+00
9	-0.1667	0.658E+00	0.456E+00	0.329E+00	0.111E+01	0.826E+00	0.666E+00
8	-0.2000	0.606E+00	0.224E+00	0.170E+00	0.802E+00	0.718E+00	0.502E+00
7	-0.2333	0.635E+00	0.000E+00	0.468E-01	0.522E+00	0.520E+00	0.315E+00
6	-0.2667	0.597E+00	-0.996E-01	0.655E-01	0.416E+00	0.280E+00	0.233E+00
5	-0.3000	0.553E+00	-0.151E+00	0.816E-01	0.315E+00	0.137E+00	0.934E-01
4	-0.3333	0.544E+00	-0.148E+00	0.129E+00	0.226E+00	0.909E-01	0.609E-01
3	-0.3667	0.461E+00	-0.130E+00	0.109E+00	0.164E+00	0.387E-01	0.000E+00
2	-0.4000	0.428E+00	-0.937E-01	0.774E-01	0.765E-01	0.000E+00	-0.228E-01
1	-0.4333	0.444E+00	-0.753E-01	-0.161E-01	0.202E-01	-0.208E-01	-0.481E-01

(d) v/u_{av}

TABLE XIII (Continued)

	I =	1	2	3	4	5	6
	X =	0.0833	0.1944	0.2500	0.4167	0.5278	0.6389
J	Y						
27	0.4333	-0.804E+01	-0.681E+01	-0.650E+01	-0.535E+01	0.474E+01	0.415E+01
26	0.4000	-0.729E+01	-0.640E+01	-0.623E+01	-0.540E+01	0.497E+01	0.442E+01
25	0.3667	-0.666E+01	-0.605E+01	-0.605E+01	-0.546E+01	0.521E+01	0.461E+01
24	0.3333	-0.617E+01	-0.595E+01	-0.596E+01	-0.556E+01	0.548E+01	0.492E+01
23	0.3000	-0.595E+01	-0.572E+01	-0.580E+01	-0.585E+01	0.574E+01	0.532E+01
22	0.2667	-0.585E+01	-0.571E+01	-0.594E+01	-0.616E+01	0.613E+01	0.575E+01
21	0.2333	-0.586E+01	-0.587E+01	-0.619E+01	-0.656E+01	0.674E+01	0.629E+01
20	0.2000	-0.585E+01	-0.616E+01	-0.642E+01	-0.686E+01	0.752E+01	0.700E+01
19	0.1667	-0.562E+01	-0.649E+01	-0.683E+01	-0.718E+01	0.792E+01	0.767E+01
18	0.1333	-0.524E+01	-0.679E+01	-0.727E+01	-0.770E+01	0.808E+01	0.803E+01
17	0.1000	-0.415E+01	-0.718E+01	-0.755E+01	-0.803E+01	0.840E+01	0.836E+01
16	0.0667	-0.284E+01	-0.727E+01	-0.757E+01	-0.786E+01	0.784E+01	0.839E+01
15	0.0333	-0.181E+01	-0.616E+01	-0.577E+01	-0.555E+01	0.621E+01	0.691E+01
14	0.0000	-0.289E+00	-0.937E+00	0.392E+01	0.628E+00	0.000E+00	0.382E+01
13	-0.0333	-0.235E+00	0.536E+01	0.629E+01	0.636E+01	0.621E+01	0.382E+01
12	-0.0667	0.232E+01	0.704E+01	0.742E+01	0.804E+01	0.784E+01	0.839E+01
11	-0.1000	0.388E+01	0.780E+01	0.752E+01	0.792E+01	0.840E+01	0.836E+01
10	-0.1333	0.580E+01	0.757E+01	0.708E+01	0.755E+01	0.808E+01	0.804E+01
9	-0.1667	0.679E+01	0.728E+01	0.712E+01	0.739E+01	0.792E+01	0.767E+01
8	-0.2000	0.685E+01	0.689E+01	0.686E+01	0.718E+01	0.752E+01	0.700E+01
7	-0.2333	0.701E+01	0.670E+01	0.646E+01	0.652E+01	0.674E+01	0.629E+01
6	-0.2667	0.700E+01	0.629E+01	0.611E+01	0.603E+01	0.613E+01	0.575E+01
5	-0.3000	0.730E+01	0.629E+01	0.610E+01	0.569E+01	0.574E+01	0.532E+01
4	-0.3333	0.778E+01	0.639E+01	0.609E+01	0.548E+01	0.548E+01	0.492E+01
3	-0.3667	0.824E+01	0.641E+01	0.622E+01	0.527E+01	0.521E+01	0.461E+01
2	-0.4000	0.870E+01	0.658E+01	0.625E+01	0.508E+01	0.497E+01	0.442E+01
1	-0.4333	0.938E+01	0.666E+01	0.603E+01	0.485E+01	0.474E+01	0.415E+01

(e) w/u_{av}

TABLE XIV

VELOCITY DATA, CASE 7 (L/D = 6), NO SWIRL

	I =	1	2	3	4	5
	X =	0.0190	0.0444	0.0572	0.0952	0.1460
O J	Y					
27	0.0991	0.000E+00	0.000E+00	0.358E+03	0.000E+00	0.000E+00
26	0.0914	0.000E+00	0.000E+00	0.358E+03	0.000E+00	0.000E+00
25	0.0838	0.000E+00	0.000E+00	0.358E+03	0.000E+00	0.000E+00
24	0.0762	0.000E+00	0.357E+03	0.358E+03	0.000E+00	0.000E+00
23	0.0686	0.000E+00	0.358E+03	0.358E+03	0.000E+00	0.000E+00
22	0.0610	0.000E+00	0.358E+03	0.358E+03	0.000E+00	0.000E+00
21	0.0533	0.359E+03	0.358E+03	0.358E+03	0.000E+00	0.000E+00
20	0.0457	0.359E+03	0.358E+03	0.358E+03	0.000E+00	0.000E+00
19	0.0381	0.359E+03	0.358E+03	0.358E+03	0.353E+03	0.000E+00
18	0.0305	0.359E+03	0.358E+03	0.358E+03	0.353E+03	0.000E+00
17	0.0229	0.359E+03	0.358E+03	0.358E+03	0.355E+03	0.000E+00
16	0.0152	0.359E+03	0.358E+03	0.358E+03	0.355E+03	0.000E+00
15	0.0076	0.359E+03	0.358E+03	0.360E+03	0.355E+03	0.360E+03
14	0.0000	0.359E+03	0.358E+03	0.360E+03	0.356E+03	0.000E+00
13	-0.0076	0.359E+03	0.358E+03	0.360E+03	0.355E+03	0.360E+03
12	-0.0152	0.359E+03	0.358E+03	0.358E+03	0.355E+03	0.000E+00
11	-0.0229	0.359E+03	0.358E+03	0.358E+03	0.355E+03	0.000E+00
10	-0.0305	0.359E+03	0.358E+03	0.358E+03	0.353E+03	0.330E+03
9	-0.0381	0.359E+03	0.358E+03	0.358E+03	0.353E+03	0.000E+00
8	-0.0457	0.359E+03	0.358E+03	0.358E+03	0.000E+00	0.000E+00
7	-0.0533	0.359E+03	0.358E+03	0.358E+03	0.000E+00	0.330E+03
6	-0.0610	0.000E+00	0.358E+03	0.358E+03	0.000E+00	0.000E+00
5	-0.0686	0.000E+00	0.358E+03	0.358E+03	0.000E+00	0.000E+00
4	-0.0762	0.000E+00	0.357E+03	0.358E+03	0.000E+00	0.000E+00
3	-0.0838	0.000E+00	0.000E+00	0.358E+03	0.000E+00	0.000E+00
2	-0.0914	0.000E+00	0.000E+00	0.358E+03	0.000E+00	0.000E+00
1	-0.0991	0.000E+00	0.000E+00	0.358E+03	0.000E+00	0.000E+00

(a) Yaw Angle

TABLE XIV (Continued)

	I =	1	2	3	4	5
	X =	0.0190	0.0444	0.0572	0.0952	0.1460
O J	Y					
27	0.0991	0.000E+00	0.000E+00	-0.165E+02	0.000E+00	0.000E+00
26	0.0914	0.000E+00	0.000E+00	0.000E+00	0.000E+00	0.000E+00
25	0.0838	0.000E+00	0.000E+00	-0.218E+02	0.000E+00	0.000E+00
24	0.0762	0.000E+00	-0.315E+02	-0.510E+02	0.000E+00	0.000E+00
23	0.0686	0.000E+00	-0.315E+02	-0.315E+02	0.000E+00	0.000E+00
22	0.0610	0.000E+00	-0.233E+02	-0.373E+02	0.000E+00	0.000E+00
21	0.0533	0.000E+00	-0.192E+02	-0.798E+01	0.000E+00	0.000E+00
20	0.0457	-0.393E+02	-0.902E+01	-0.119E+02	0.000E+00	0.000E+00
19	0.0381	-0.132E+02	-0.108E+02	-0.104E+02	0.000E+00	0.000E+00
18	0.0305	-0.117E+02	-0.814E+01	-0.104E+02	0.000E+00	0.000E+00
17	0.0229	-0.821E+01	-0.707E+01	-0.104E+02	0.000E+00	0.000E+00
16	0.0152	-0.677E+01	-0.557E+01	-0.478E+01	0.000E+00	0.000E+00
15	0.0076	-0.518E+01	-0.309E+01	-0.404E+01	0.000E+00	0.000E+00
14	0.0000	-0.408E+01	-0.158E+01	-0.266E+01	0.000E+00	0.000E+00
13	-0.0076	-0.518E+01	-0.309E+01	-0.404E+01	0.000E+00	0.000E+00
12	-0.0152	-0.677E+01	-0.557E+01	-0.478E+01	0.000E+00	0.000E+00
11	-0.0229	-0.821E+01	-0.707E+01	-0.113E+02	0.000E+00	0.000E+00
10	-0.0305	-0.117E+02	-0.814E+01	-0.837E+01	0.000E+00	0.000E+00
9	-0.0381	-0.132E+02	-0.108E+02	-0.104E+02	0.000E+00	0.000E+00
8	-0.0457	-0.393E+02	-0.902E+01	-0.119E+02	0.000E+00	0.000E+00
7	-0.0533	0.000E+00	-0.192E+02	-0.798E+01	0.000E+00	0.000E+00
6	-0.0610	0.000E+00	-0.233E+02	-0.373E+02	0.000E+00	0.000E+00
5	-0.0686	0.000E+00	-0.315E+02	-0.315E+02	0.000E+00	0.000E+00
4	-0.0762	0.000E+00	-0.315E+02	-0.510E+02	0.000E+00	0.000E+00
3	-0.0838	0.000E+00	0.000E+00	-0.218E+02	0.000E+00	0.000E+00
2	-0.0914	0.000E+00	0.000E+00	0.000E+00	0.000E+00	0.000E+00
1	-0.0991	0.000E+00	0.000E+00	-0.165E+02	0.000E+00	0.000E+00

(b) Pitch Angle

TABLE XIV (Continued)

	I =	1	2	3	4	5
	X =	0.0833	0.1944	0.2500	0.4167	0.6389
O J	Y					
27	0.4333	0.000E+00	0.000E+00	0.140E+01	0.000E+00	0.000E+00
26	0.4000	0.000E+00	0.000E+00	0.000E+00	0.000E+00	0.000E+00
25	0.3667	0.000E+00	0.000E+00	0.168E+01	0.000E+00	0.000E+00
24	0.3333	0.000E+00	0.905E+00	0.114E+01	0.000E+00	0.000E+00
23	0.3000	0.000E+00	0.157E+01	0.203E+01	0.000E+00	0.000E+00
22	0.2667	0.000E+00	0.254E+01	0.176E+01	0.000E+00	0.000E+00
21	0.2333	0.107E+01	0.338E+01	0.372E+01	0.000E+00	0.000E+00
20	0.2000	0.149E+01	0.561E+01	0.503E+01	0.000E+00	0.000E+00
19	0.1667	0.388E+01	0.640E+01	0.599E+01	0.106E+01	0.000E+00
18	0.1333	0.812E+01	0.764E+01	0.599E+01	0.106E+01	0.000E+00
17	0.1000	0.138E+02	0.101E+02	0.599E+01	0.106E+01	0.000E+00
16	0.0667	0.179E+02	0.117E+02	0.874E+01	0.106E+01	0.000E+00
15	0.0333	0.203E+02	0.127E+02	0.904E+01	0.106E+01	0.000E+00
14	0.0000	0.206E+02	0.125E+02	0.883E+01	0.184E+01	0.000E+00
13	-0.0333	0.203E+02	0.127E+02	0.904E+01	0.106E+01	0.000E+00
12	-0.0667	0.179E+02	0.117E+02	0.874E+01	0.106E+01	0.000E+00
11	-0.1000	0.138E+02	0.101E+02	0.597E+01	0.106E+01	0.000E+00
10	-0.1333	0.812E+01	0.764E+01	0.690E+01	0.106E+01	0.925E+00
9	-0.1667	0.388E+01	0.640E+01	0.599E+01	0.106E+01	0.000E+00
8	-0.2000	0.149E+01	0.561E+01	0.503E+01	0.000E+00	0.000E+00
7	-0.2333	0.107E+01	0.338E+01	0.372E+01	0.000E+00	0.920E+00
6	-0.2667	0.000E+00	0.254E+01	0.176E+01	0.000E+00	0.000E+00
5	-0.3000	0.000E+00	0.157E+01	0.203E+01	0.000E+00	0.000E+00
4	-0.3333	0.000E+00	0.905E+00	0.114E+01	0.000E+00	0.000E+00
3	-0.3667	0.000E+00	0.000E+00	0.168E+01	0.000E+00	0.000E+00
2	-0.4000	0.000E+00	0.000E+00	0.000E+00	0.000E+00	0.000E+00
1	-0.4333	0.000E+00	0.000E+00	0.140E+01	0.000E+00	0.000E+00

(c) u/u_{av}

TABLE XIV (Continued)

	I =	1	2	3	4	5
	X =	0.0833	0.1944	0.2500	0.4167	0.6389
J	Y					
27	0.4333	0.000E+00	0.000E+00	-0.530E+00	0.000E+00	0.000E+00
26	0.4000	0.000E+00	0.000E+00	0.000E+00	0.000E+00	0.000E+00
25	0.3667	0.000E+00	0.000E+00	-0.859E+00	0.000E+00	0.000E+00
24	0.3333	0.000E+00	-0.713E+00	-0.181E+01	0.000E+00	0.000E+00
23	0.3000	0.000E+00	-0.124E+01	-0.160E+01	0.000E+00	0.000E+00
22	0.2667	0.000E+00	-0.140E+01	-0.172E+01	0.000E+00	0.000E+00
21	0.2333	0.000E+00	-0.151E+01	-0.669E+00	0.000E+00	0.000E+00
20	0.2000	-0.157E+01	-0.114E+01	-0.136E+01	0.000E+00	0.000E+00
19	0.1667	-0.117E+01	-0.156E+01	-0.142E+01	0.000E+00	0.000E+00
18	0.1333	-0.215E+01	-0.140E+01	-0.142E+01	0.000E+00	0.000E+00
17	0.1000	-0.256E+01	-0.161E+01	-0.142E+01	0.000E+00	0.000E+00
16	0.0667	-0.272E+01	-0.146E+01	-0.938E+00	0.000E+00	0.000E+00
15	0.0333	-0.236E+01	-0.880E+00	-0.819E+00	0.000E+00	0.000E+00
14	0.0000	-0.188E+01	-0.442E+00	-0.527E+00	0.000E+00	0.000E+00
13	-0.0333	-0.236E+01	-0.880E+00	-0.819E+00	0.000E+00	0.000E+00
12	-0.0667	-0.272E+01	-0.146E+01	-0.938E+00	0.000E+00	0.000E+00
11	-0.1000	-0.256E+01	-0.161E+01	-0.153E+01	0.000E+00	0.000E+00
10	-0.1333	-0.215E+01	-0.140E+01	-0.130E+01	0.000E+00	0.000E+00
9	-0.1667	-0.117E+01	-0.156E+01	-0.142E+01	0.000E+00	0.000E+00
8	-0.2000	-0.157E+01	-0.114E+01	-0.136E+01	0.000E+00	0.000E+00
7	-0.2333	0.000E+00	-0.151E+01	-0.669E+00	0.000E+00	0.000E+00
6	-0.2667	0.000E+00	-0.140E+01	-0.172E+01	0.000E+00	0.000E+00
5	-0.3000	0.000E+00	-0.124E+01	-0.160E+01	0.000E+00	0.000E+00
4	-0.3333	0.000E+00	-0.713E+00	-0.181E+01	0.000E+00	0.000E+00
3	-0.3667	0.000E+00	0.000E+00	-0.859E+00	0.000E+00	0.000E+00
2	-0.4000	0.000E+00	0.000E+00	0.000E+00	0.000E+00	0.000E+00
1	-0.4333	0.000E+00	0.000E+00	-0.530E+00	0.000E+00	0.000E+00

(d) v/u_{av}

TABLE XIV (Continued)

	I =	1	2	3	4	5
	X =	0.0833	0.1944	0.2500	0.4167	0.6389
O J	Y					
27	0.4333	0.000E+00	0.000E+00	-0.488E-01	0.000E+00	0.000E+00
26	0.4000	0.000E+00	0.000E+00	0.000E+00	0.000E+00	0.000E+00
25	0.3667	0.000E+00	0.000E+00	-0.585E-01	0.000E+00	0.000E+00
24	0.3333	0.000E+00	-0.474E-01	-0.399E-01	0.000E+00	0.000E+00
23	0.3000	0.000E+00	-0.548E-01	-0.707E-01	0.000E+00	0.000E+00
22	0.2667	0.000E+00	-0.887E-01	-0.614E-01	0.000E+00	0.000E+00
21	0.2333	-0.186E-01	-0.118E+00	-0.130E+00	0.000E+00	0.000E+00
20	0.2000	-0.260E-01	-0.196E+00	-0.176E+00	0.000E+00	0.000E+00
19	0.1667	-0.677E-01	-0.223E+00	-0.209E+00	-0.139E+00	0.000E+00
18	0.1333	-0.142E+00	-0.267E+00	-0.209E+00	-0.139E+00	0.000E+00
17	0.1000	-0.241E+00	-0.353E+00	-0.209E+00	-0.931E-01	0.000E+00
16	0.0667	-0.312E+00	-0.407E+00	-0.305E+00	-0.931E-01	0.000E+00
15	0.0333	-0.354E+00	-0.443E+00	-0.544E-04	-0.931E-01	0.000E+00
14	0.0000	-0.360E+00	-0.437E+00	-0.532E-04	-0.129E+00	0.000E+00
13	-0.0333	-0.354E+00	-0.443E+00	-0.544E-04	-0.931E-01	0.000E+00
12	-0.0667	-0.312E+00	-0.407E+00	-0.305E+00	-0.931E-01	0.000E+00
11	-0.1000	-0.241E+00	-0.353E+00	-0.208E+00	-0.931E-01	0.000E+00
10	-0.1333	-0.142E+00	-0.267E+00	-0.241E+00	-0.139E+00	-0.534E+00
9	-0.1667	-0.677E-01	-0.223E+00	-0.209E+00	-0.139E+00	0.000E+00
8	-0.2000	-0.260E-01	-0.196E+00	-0.176E+00	0.000E+00	0.000E+00
7	-0.2333	-0.186E-01	-0.118E+00	-0.130E+00	0.000E+00	-0.542E+00
6	-0.2667	0.000E+00	-0.887E-01	-0.614E-01	0.000E+00	0.000E+00
5	-0.3000	0.000E+00	-0.548E-01	-0.707E-01	0.000E+00	0.000E+00
4	-0.3333	0.000E+00	-0.474E-01	-0.399E-01	0.000E+00	0.000E+00
3	-0.3667	0.000E+00	0.000E+00	-0.585E-01	0.000E+00	0.000E+00
2	-0.4000	0.000E+00	0.000E+00	0.000E+00	0.000E+00	0.000E+00
1	-0.4333	0.000E+00	0.000E+00	-0.488E-01	0.000E+00	0.000E+00

(e) w/u_{av}

APPENDIX B

FIGURES

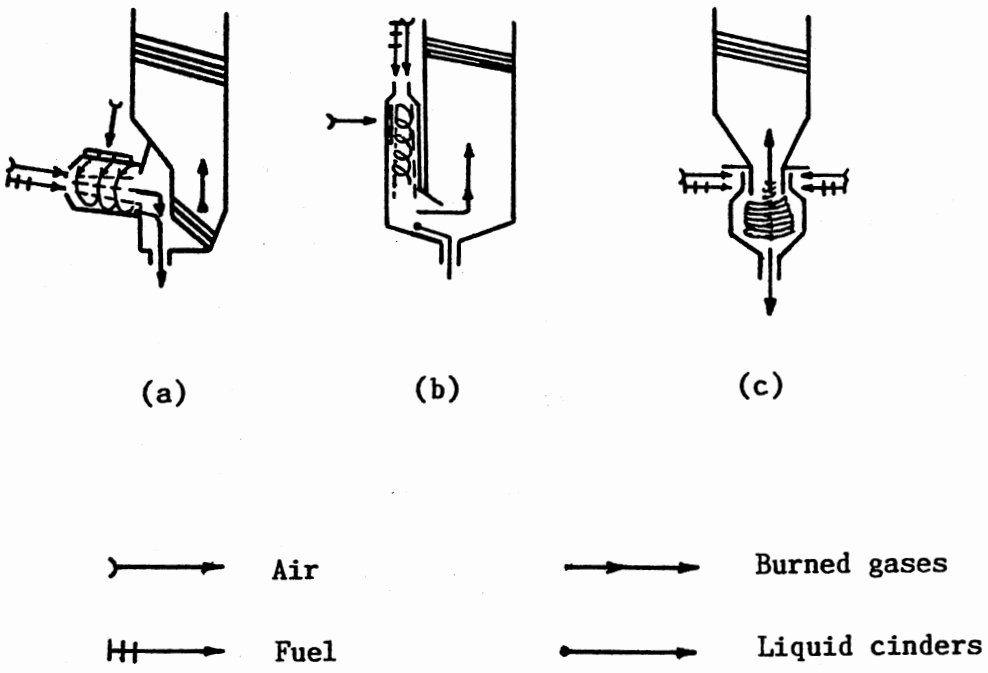

FIG. 1 The Cyclone Furnace (from Stambuleanu)

(a) Horizontal (or slightly inclined by 5-20°)

(b) Vertical VTJ (USSR)

(c) Vertical KSG (USSR)

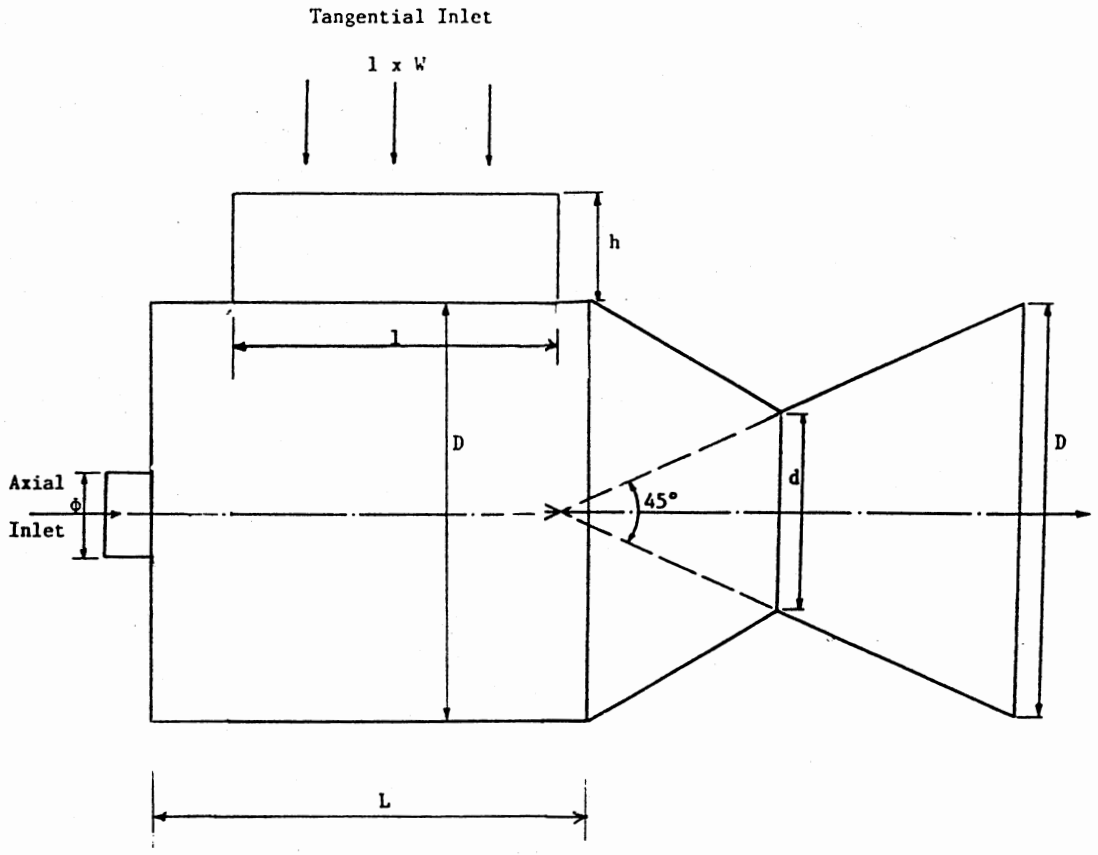

D : Internal diameter = 9" (229 mm)

L = 1.00 D
Φ = 0.20 D
l = 0.75 D
d = 0.45 D
h = 0.25 D
W = 0.25 D

FIG. 2 Cyclone Mixer Design

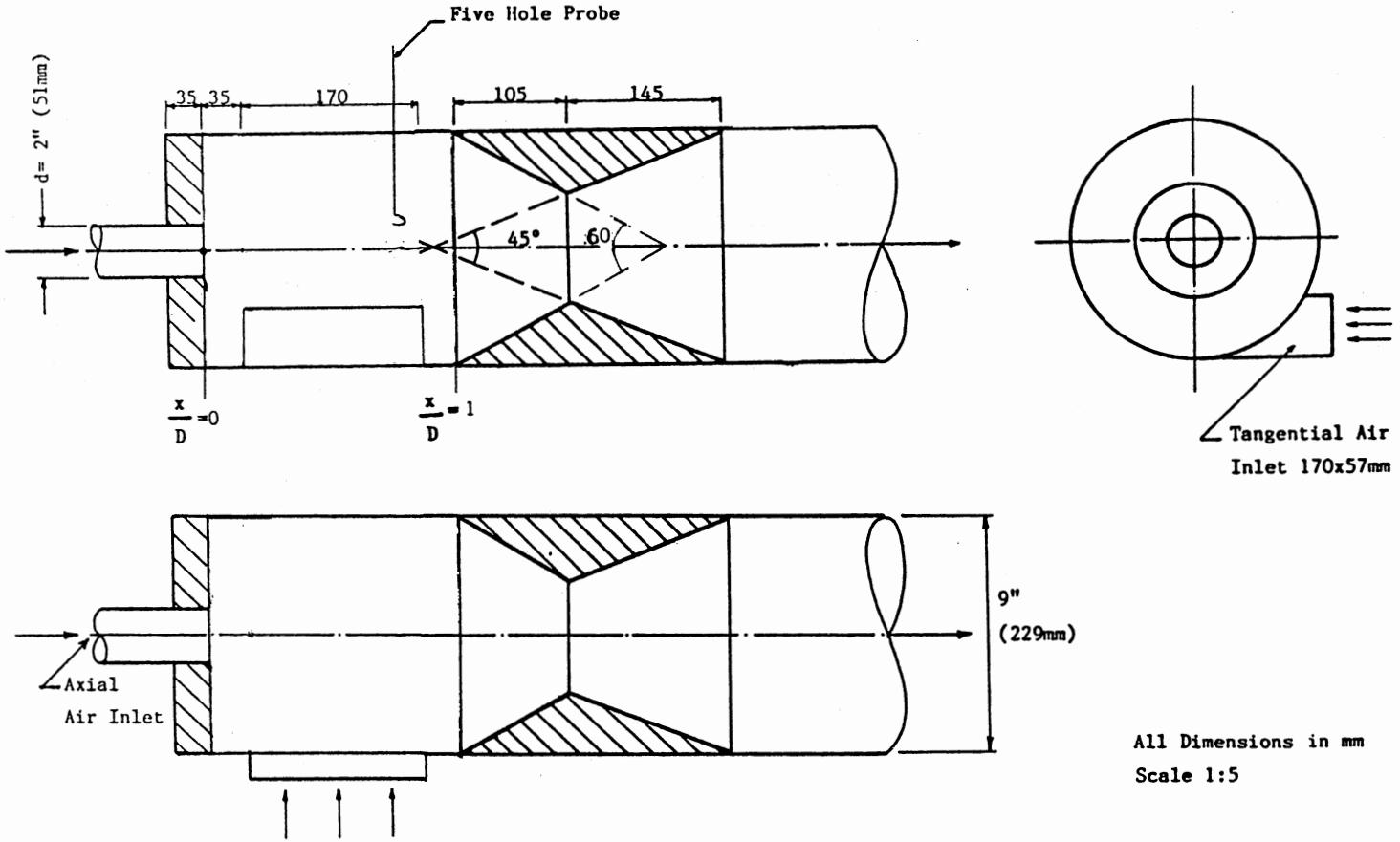

FIG. 3 Cyclone Mixer

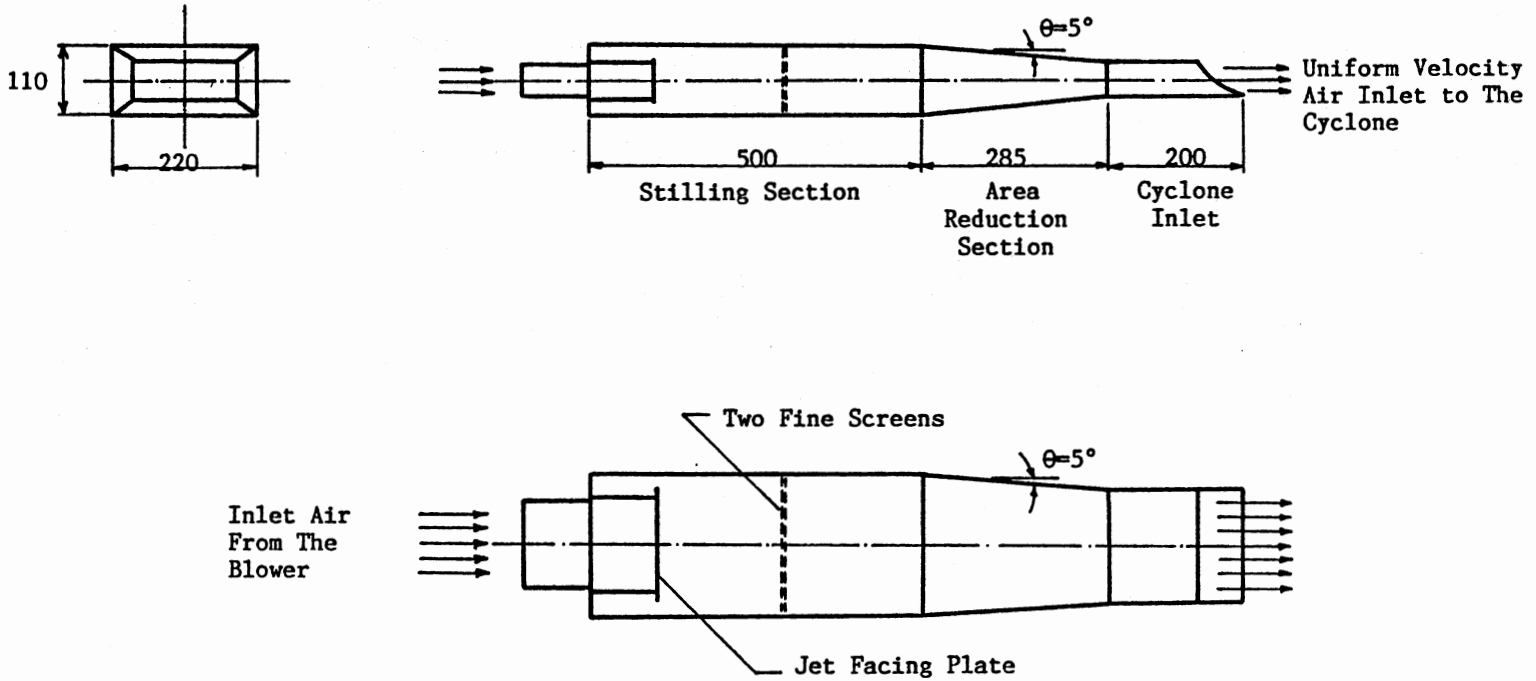

All Dimensions in mm

Scale 1 : 10

FIG. 4 Tangential Inlet Stilling Chamber

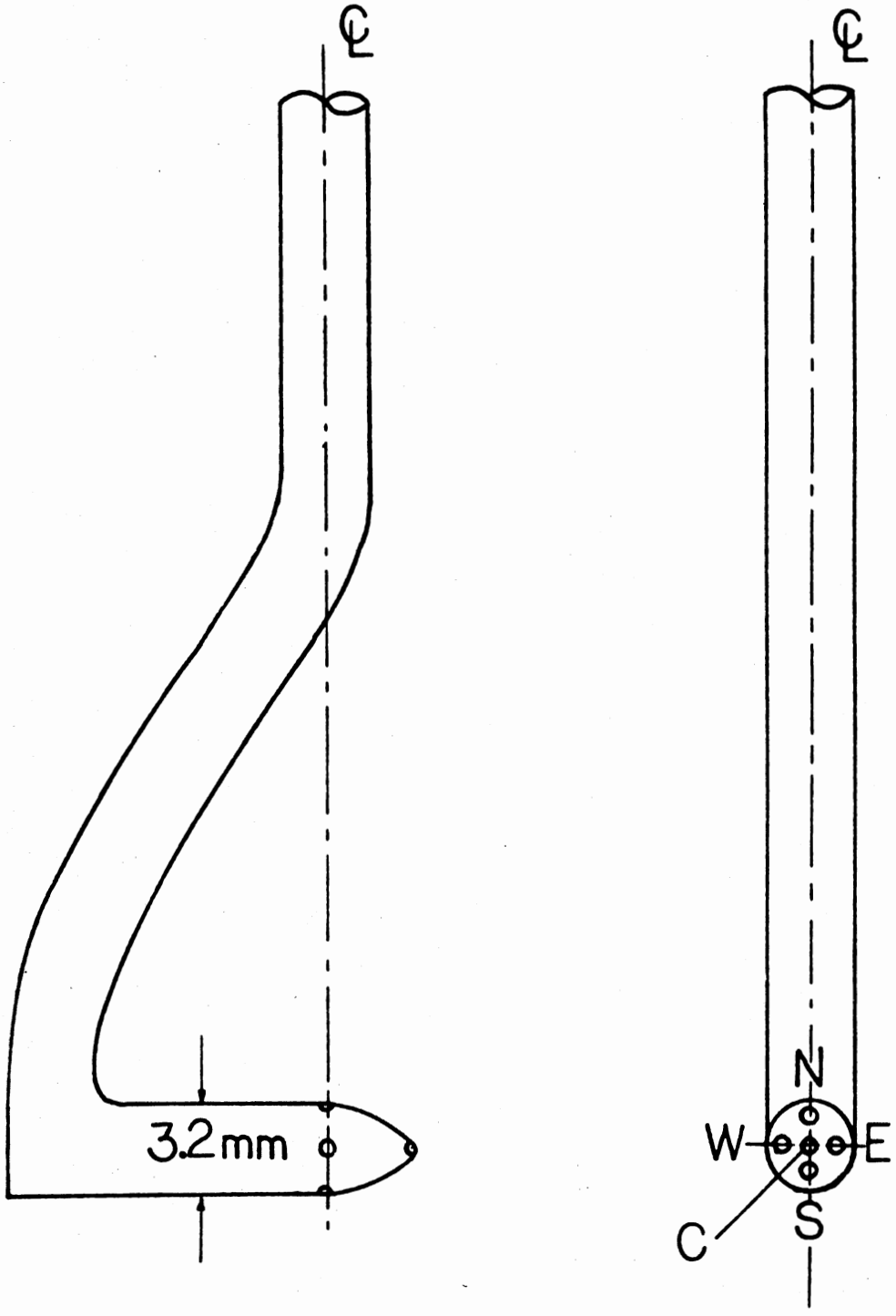

FIG. 5 Five-Hole Pitot Probe

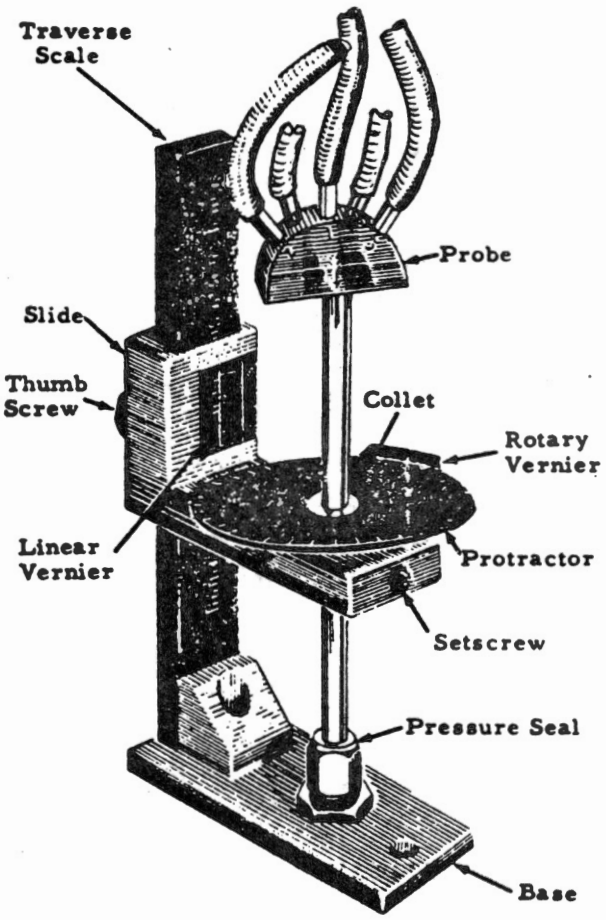

Figure 6 Manual Traverse Mechanism Used for Five-Hole Pitot Probe Measurements

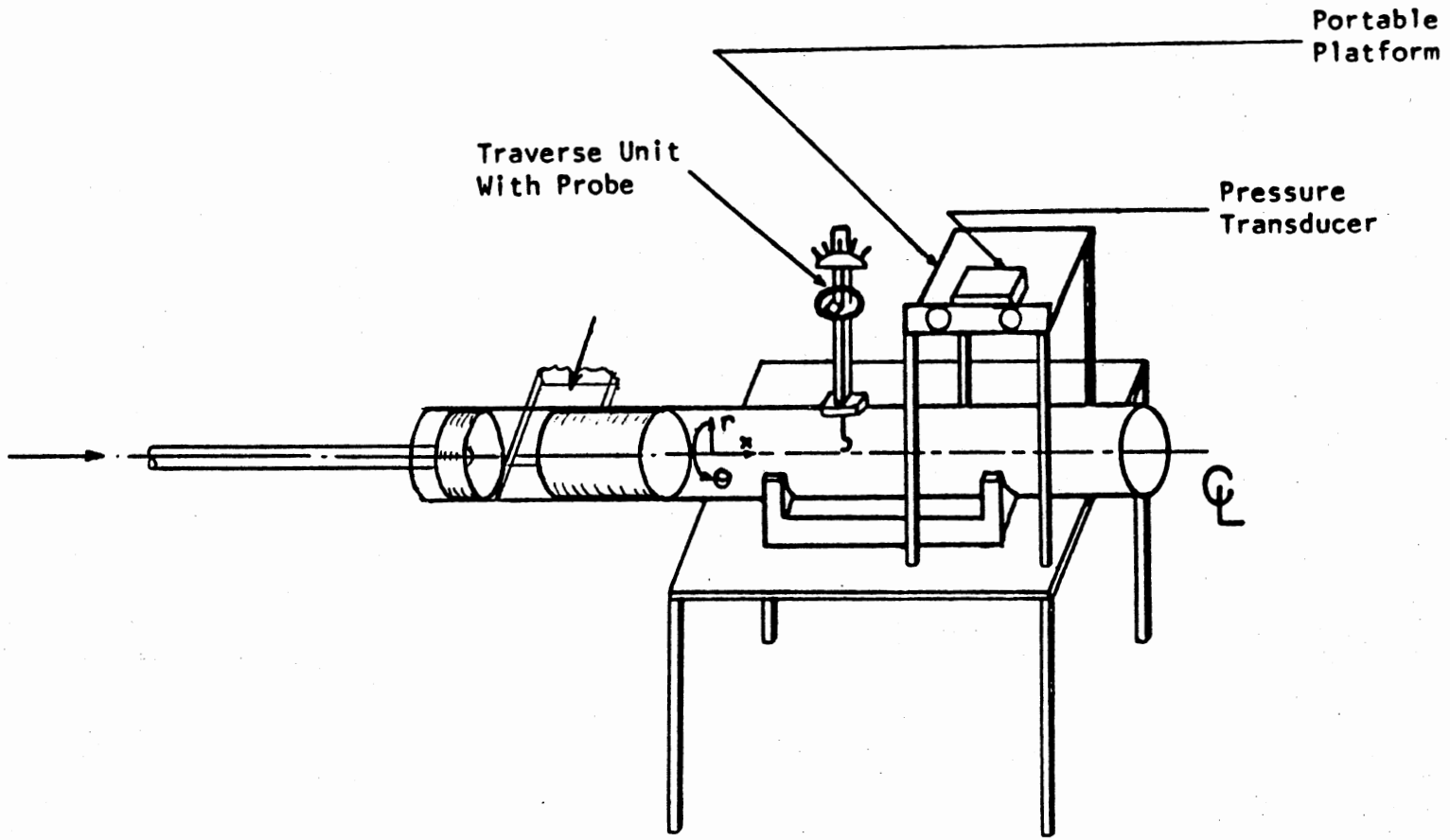

Figure 7 Apparatus for Time-Mean Velocity Measurements
Using a Five-Hole Pitot Probe

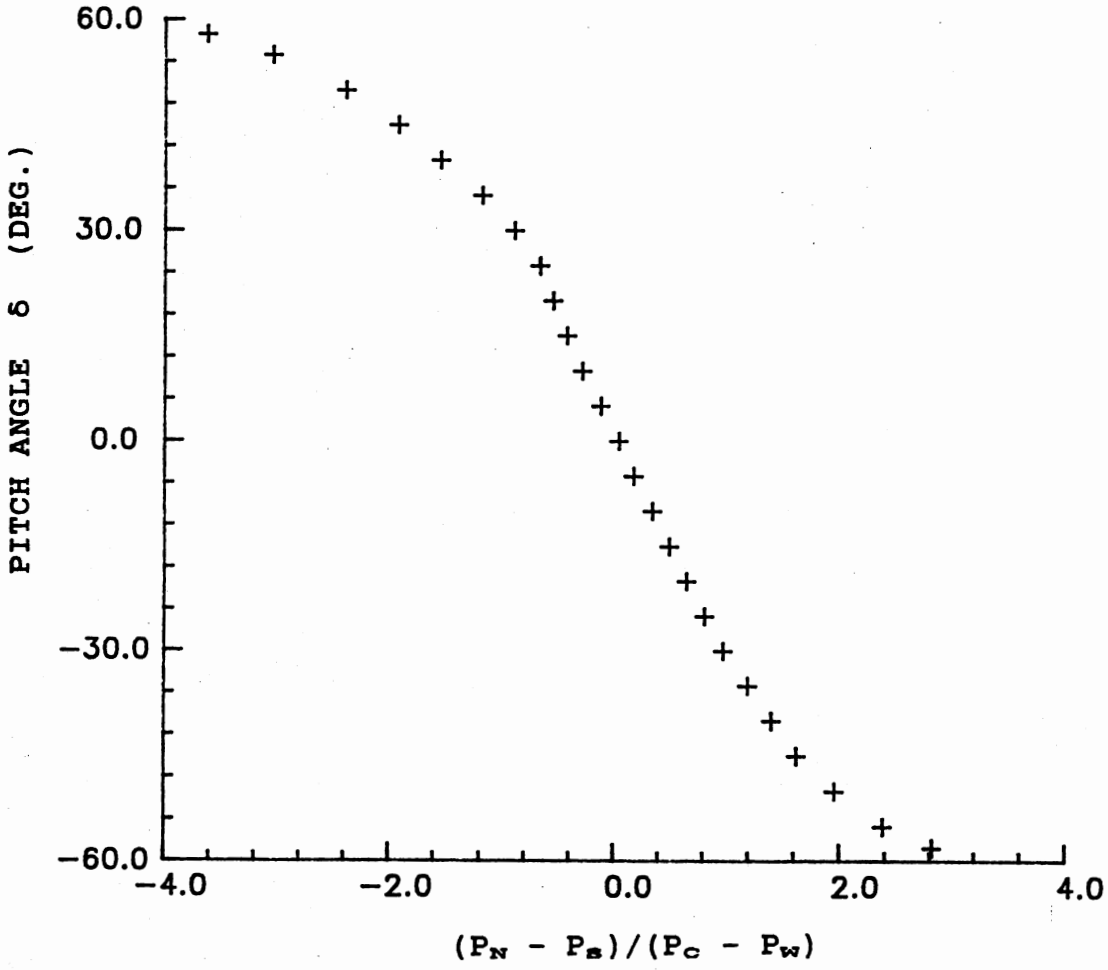

Figure 8. Pitch Angle Calibration Characteristic for Five-Hole Pitot Probe

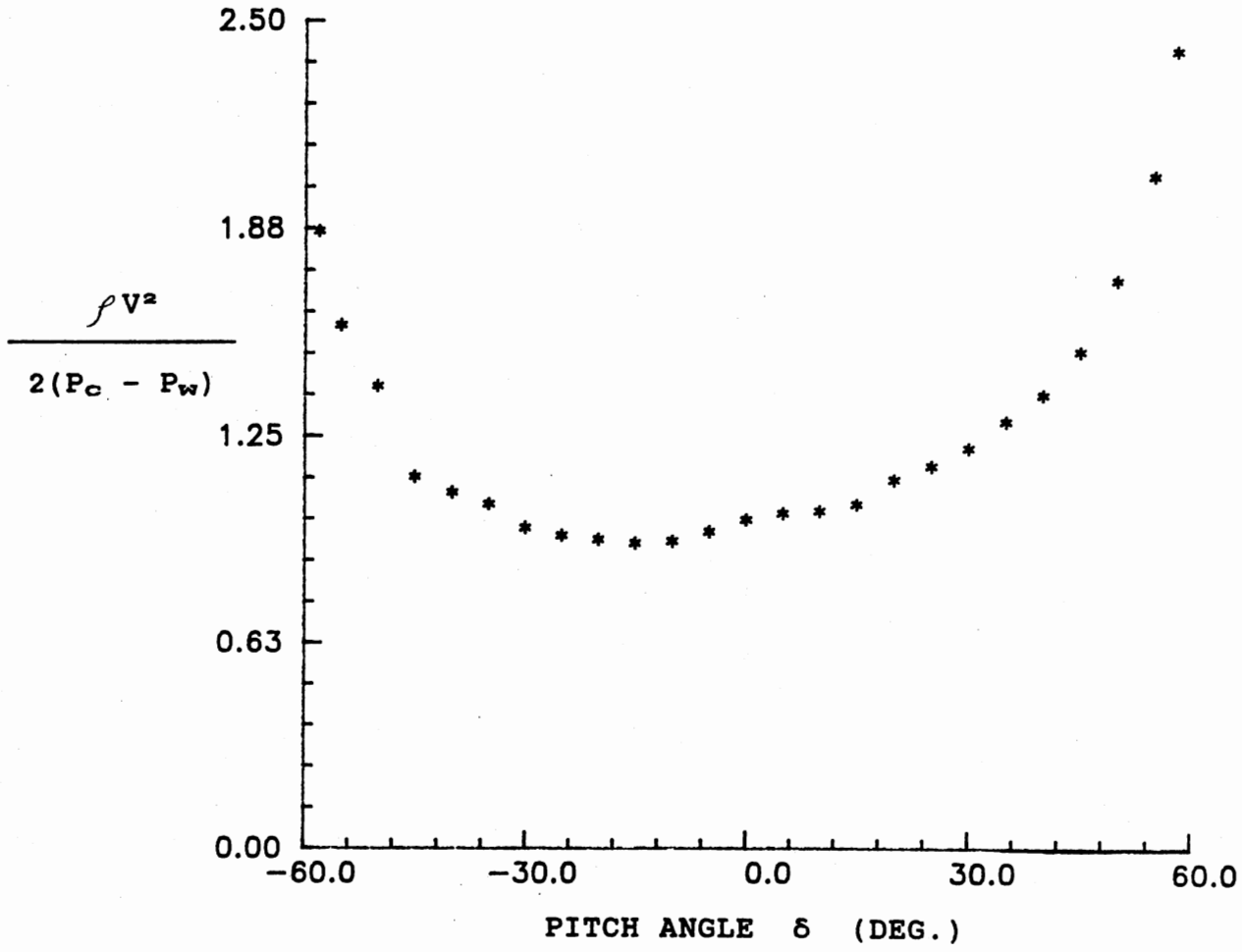

Figure 9. Velocity Coefficient Calibration Characteristic for Five-Hole Pitot Probe

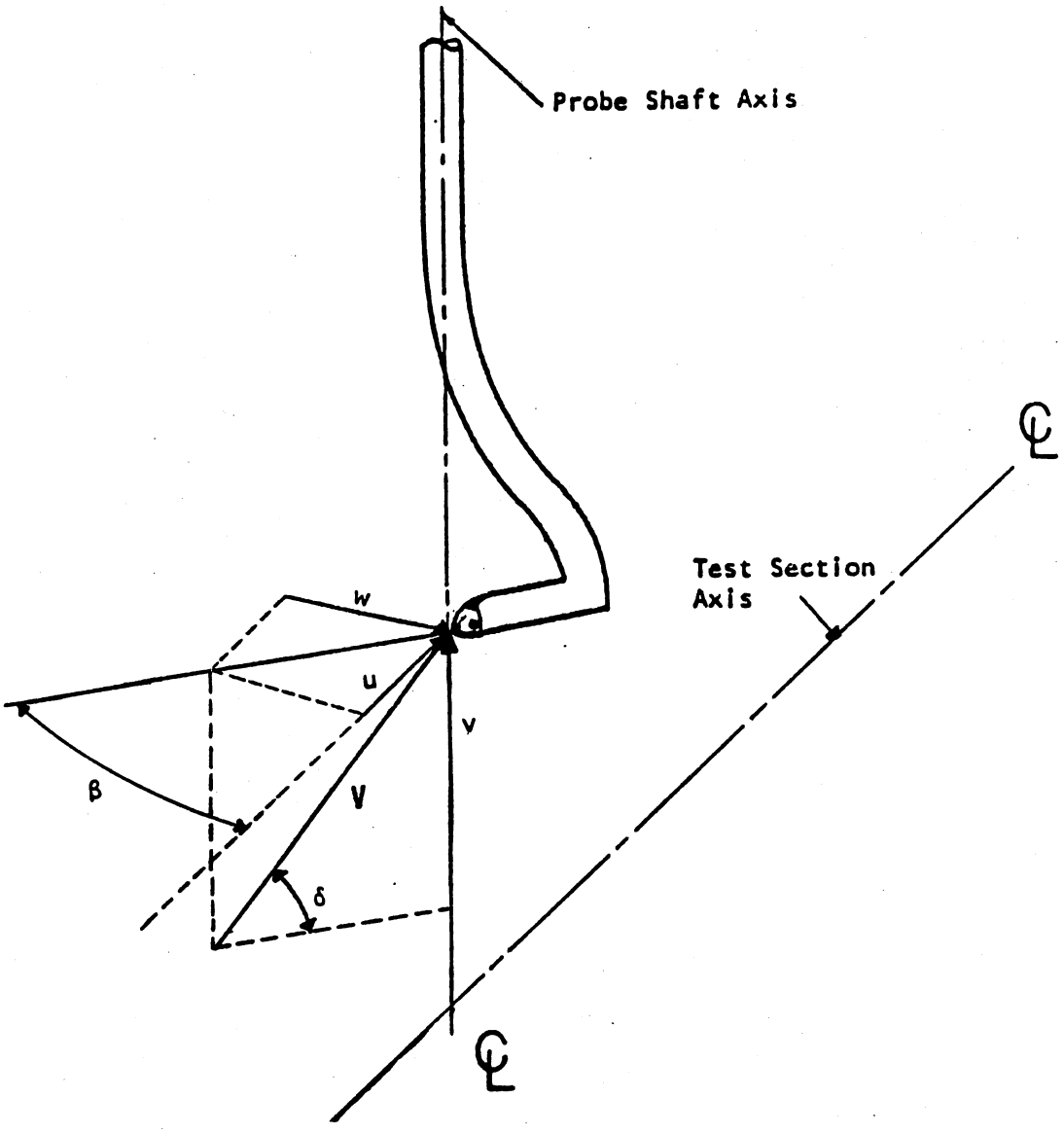

Figure 10 Velocity Components and Flow Direction Angles Associated with Five-Hole Pitot Probe

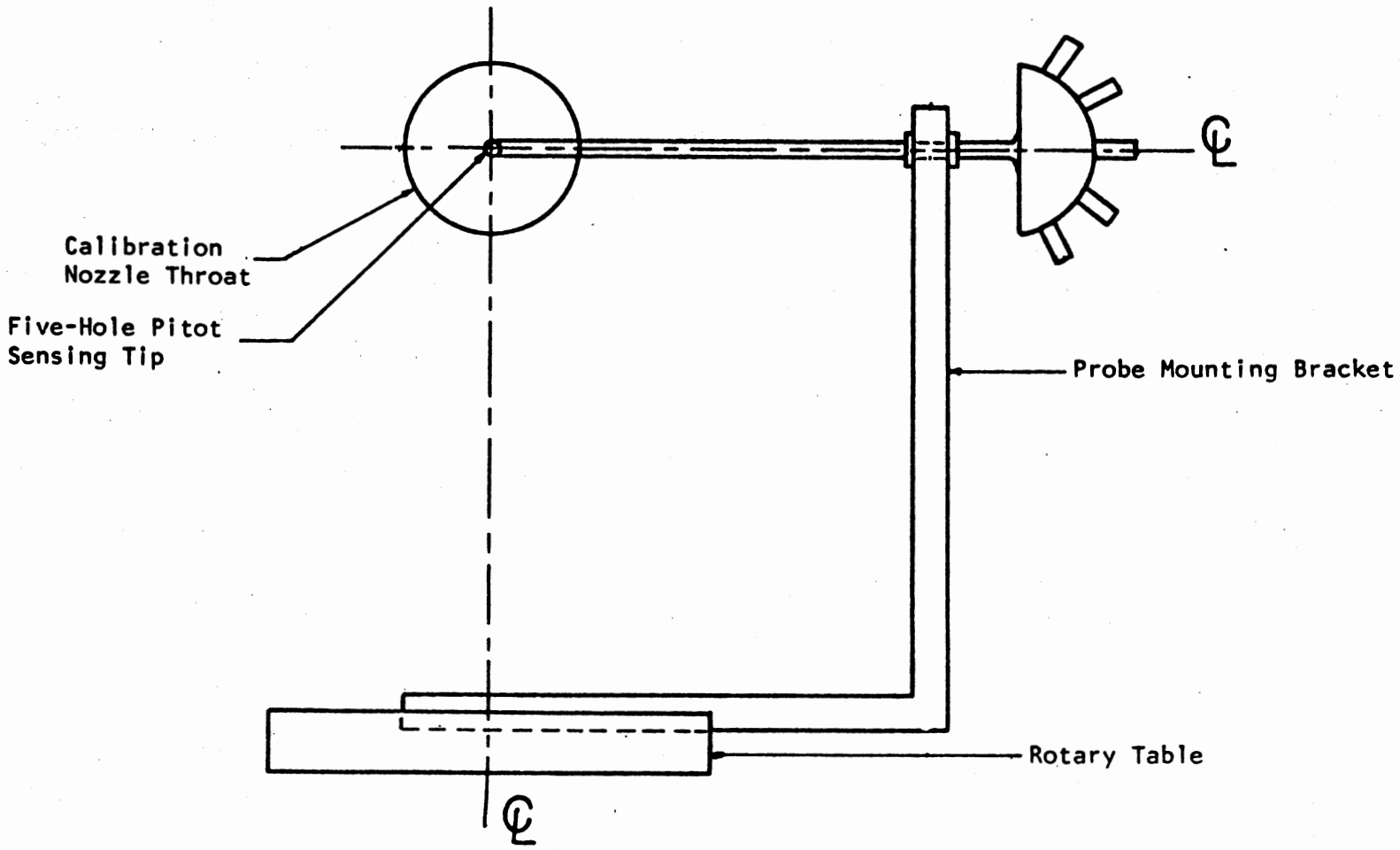

FIG. 11 Calibration Apparatus With Five-Hole Pitot Probe

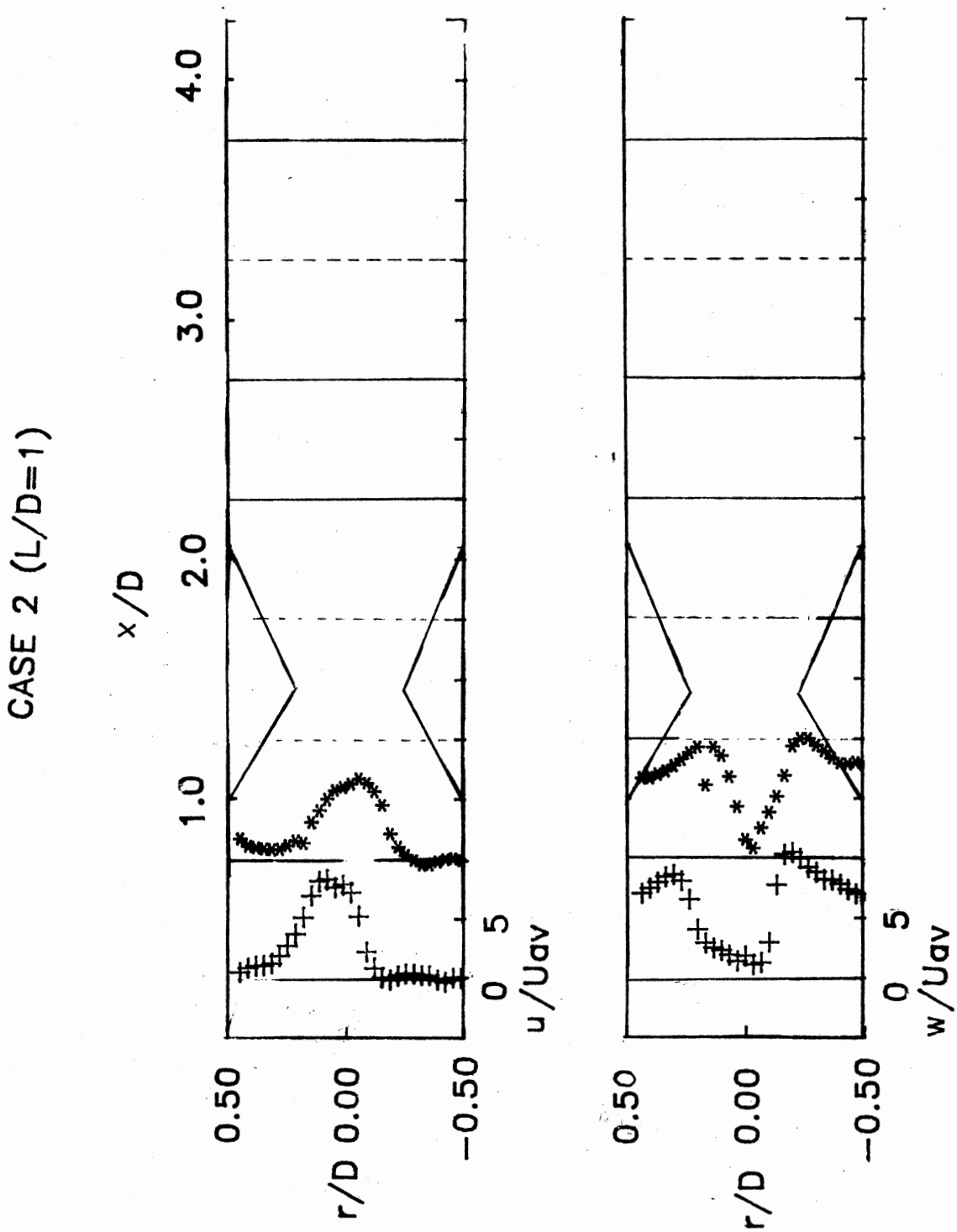

Figure 12 Weak Swirl

CASE 4 (L/D=1)

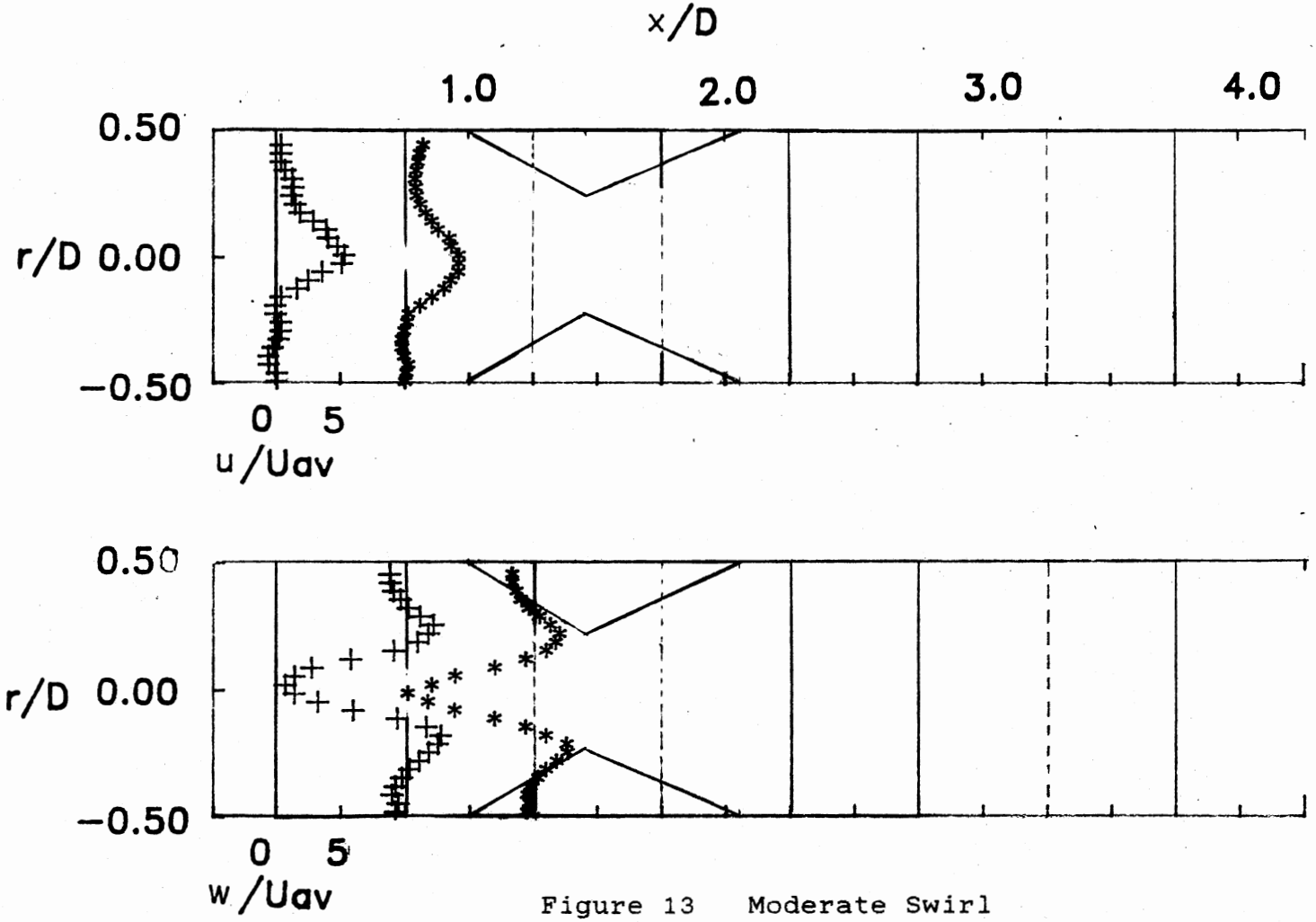

Figure 13 Moderate Swirl

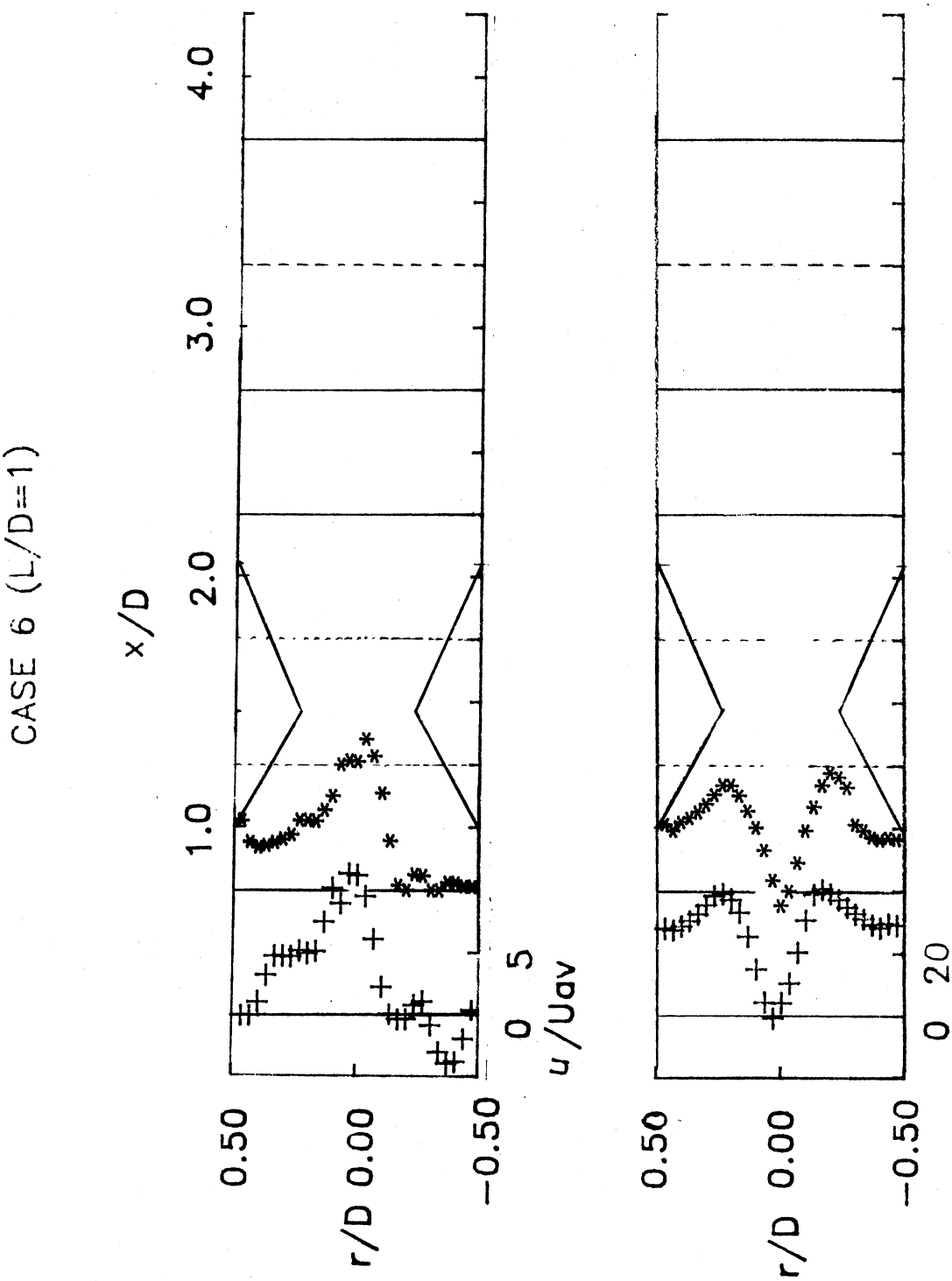

Figure 14 Strong Swirl

CASE 7 (L/D=1)

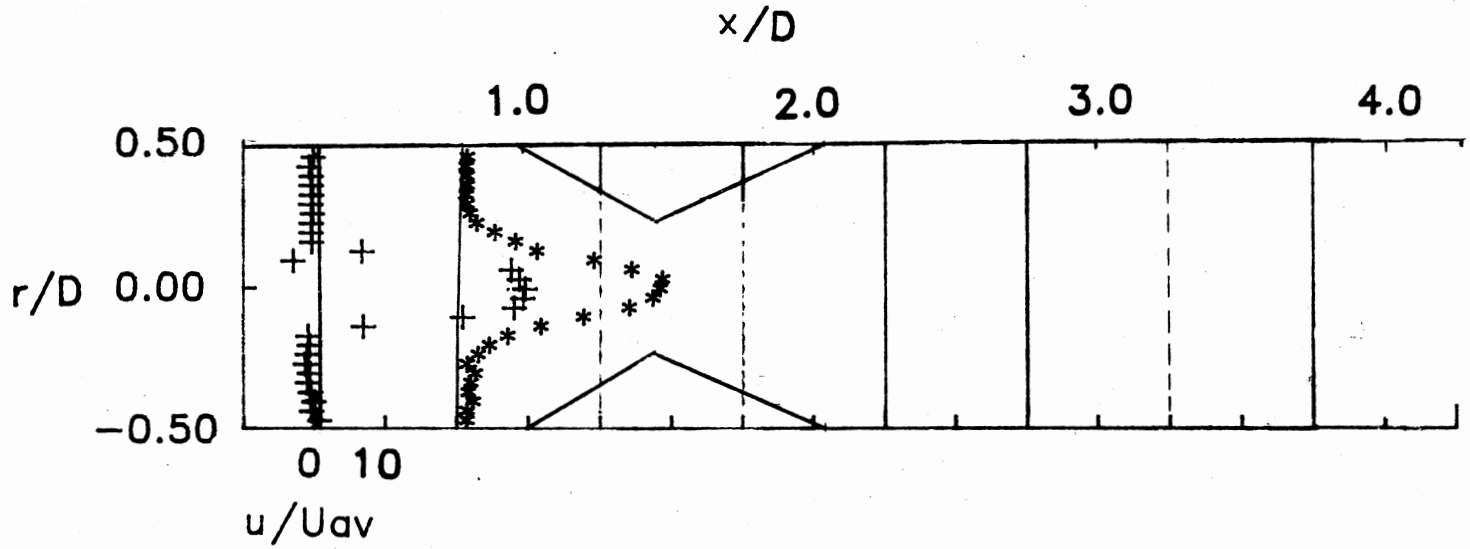

Figure 15 No Swirl

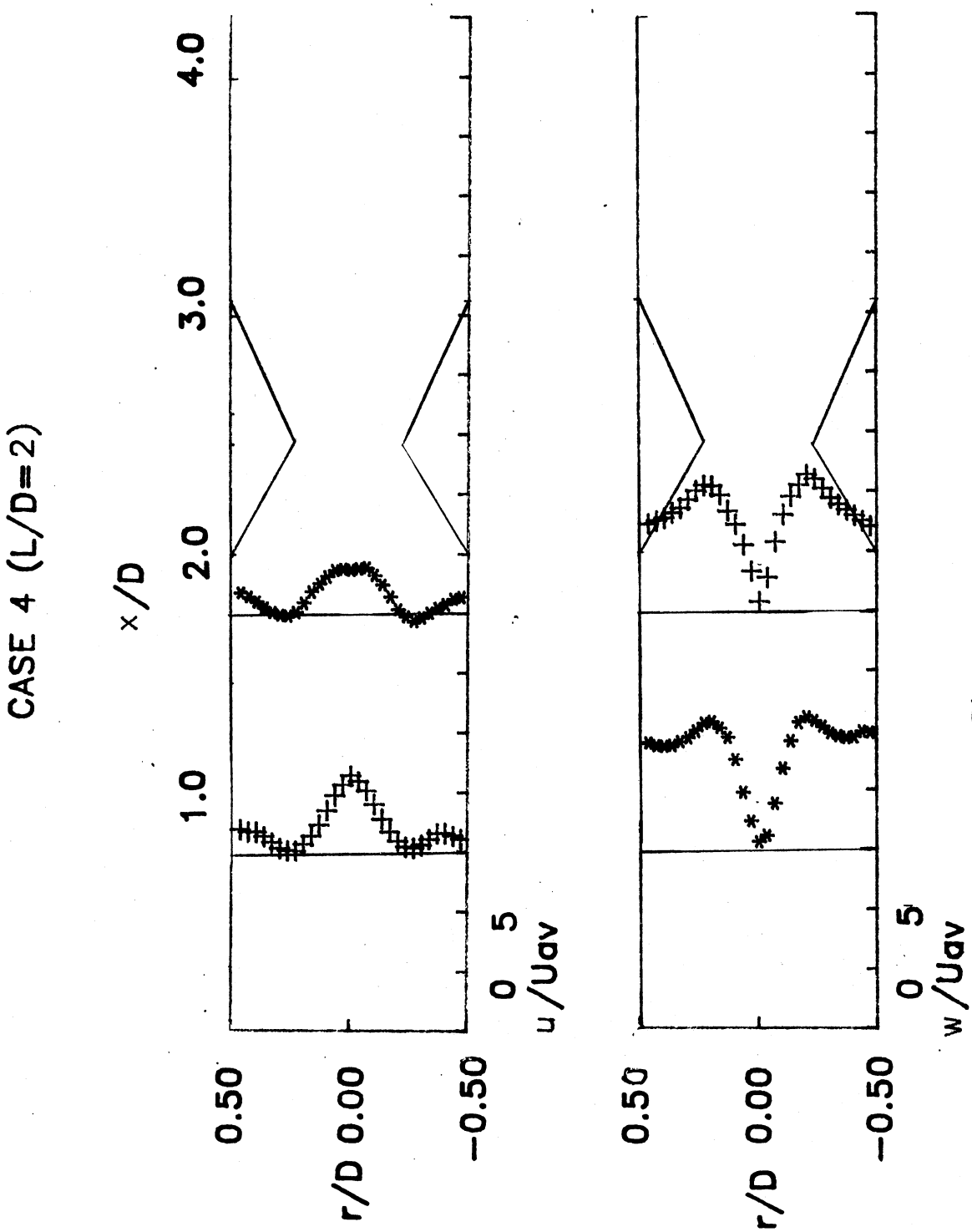

Figure 16 Moderate Swirl

CASE 7 (L/D=2)

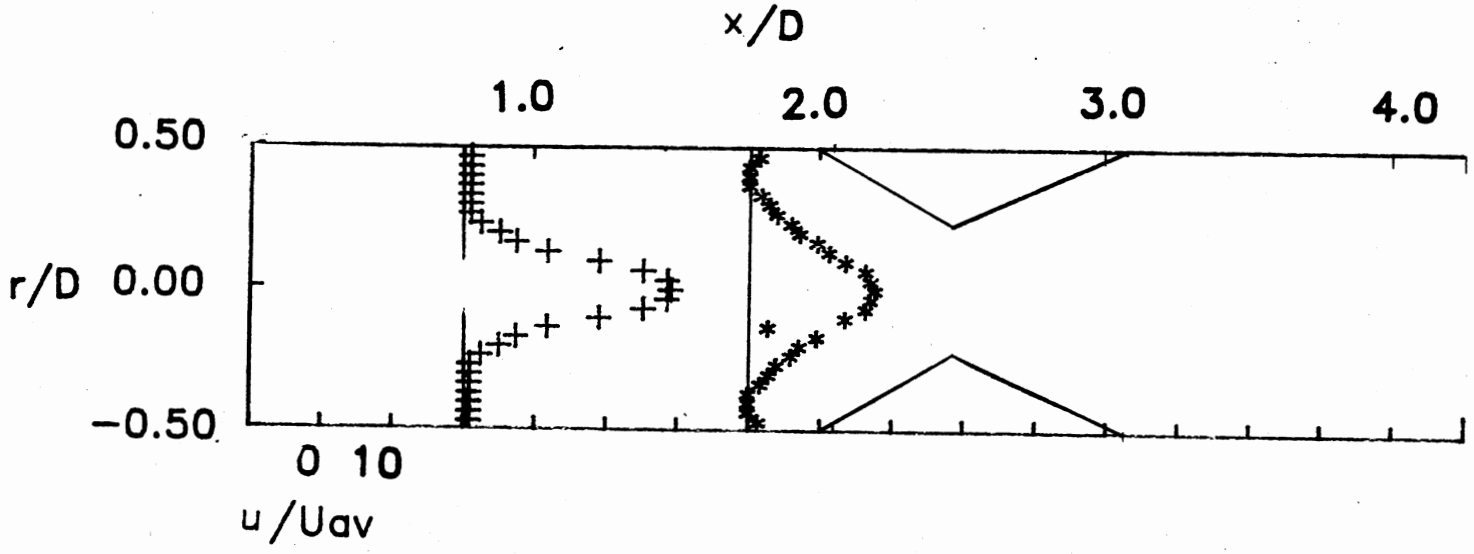

Figure 17 No Swirl

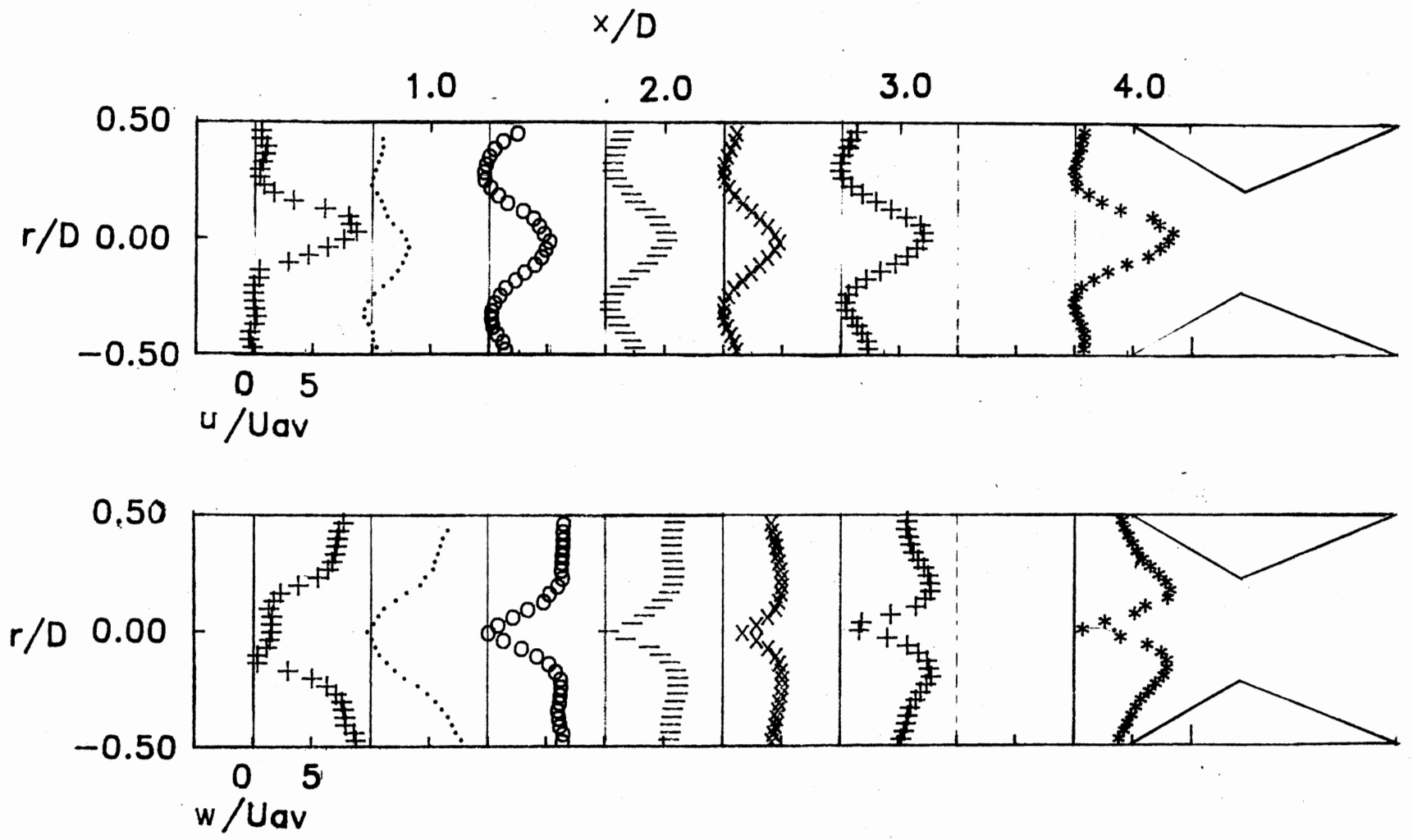

Figure 18 Weak Swirl

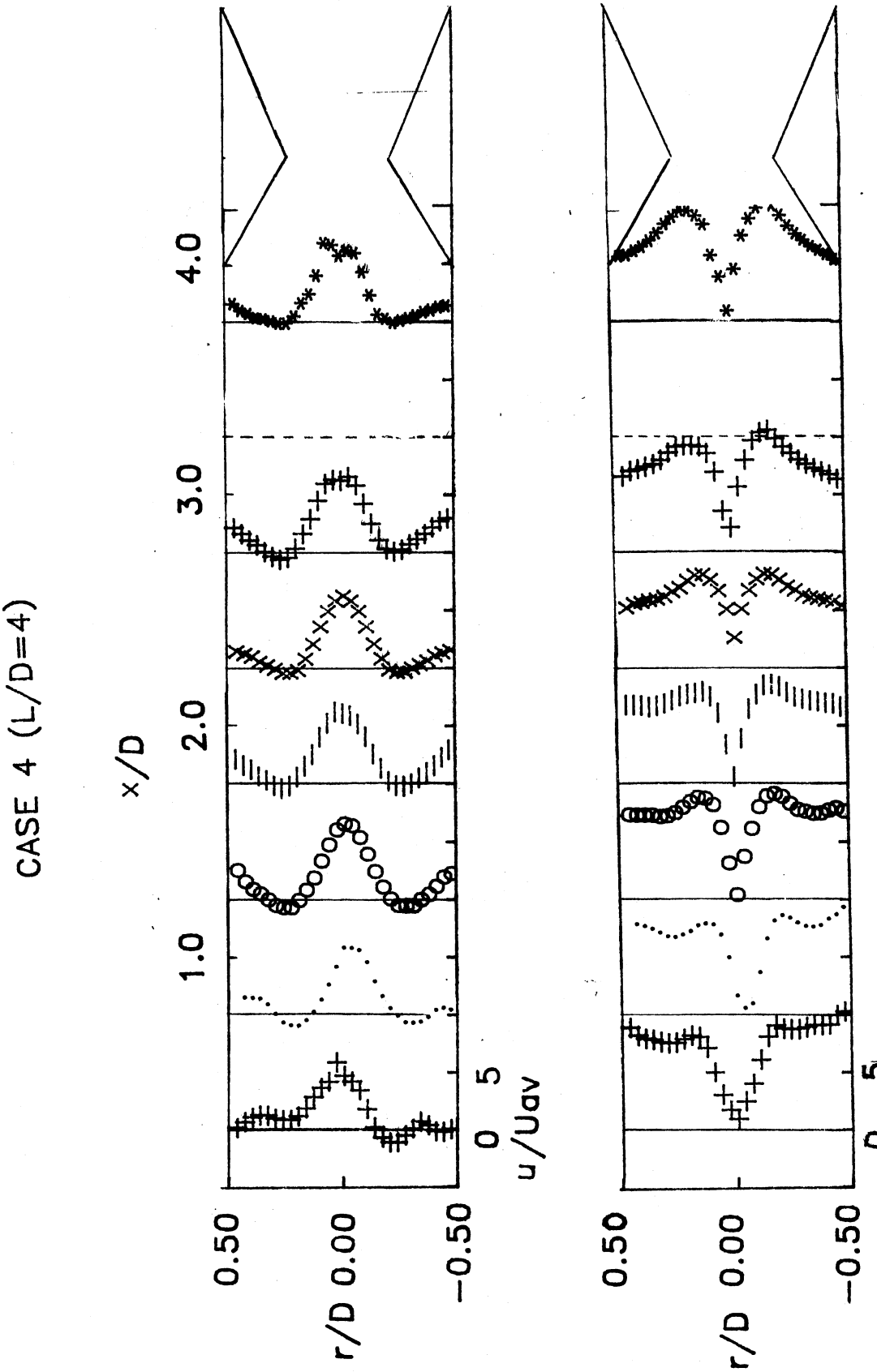

Figure 19 Moderate Swirl

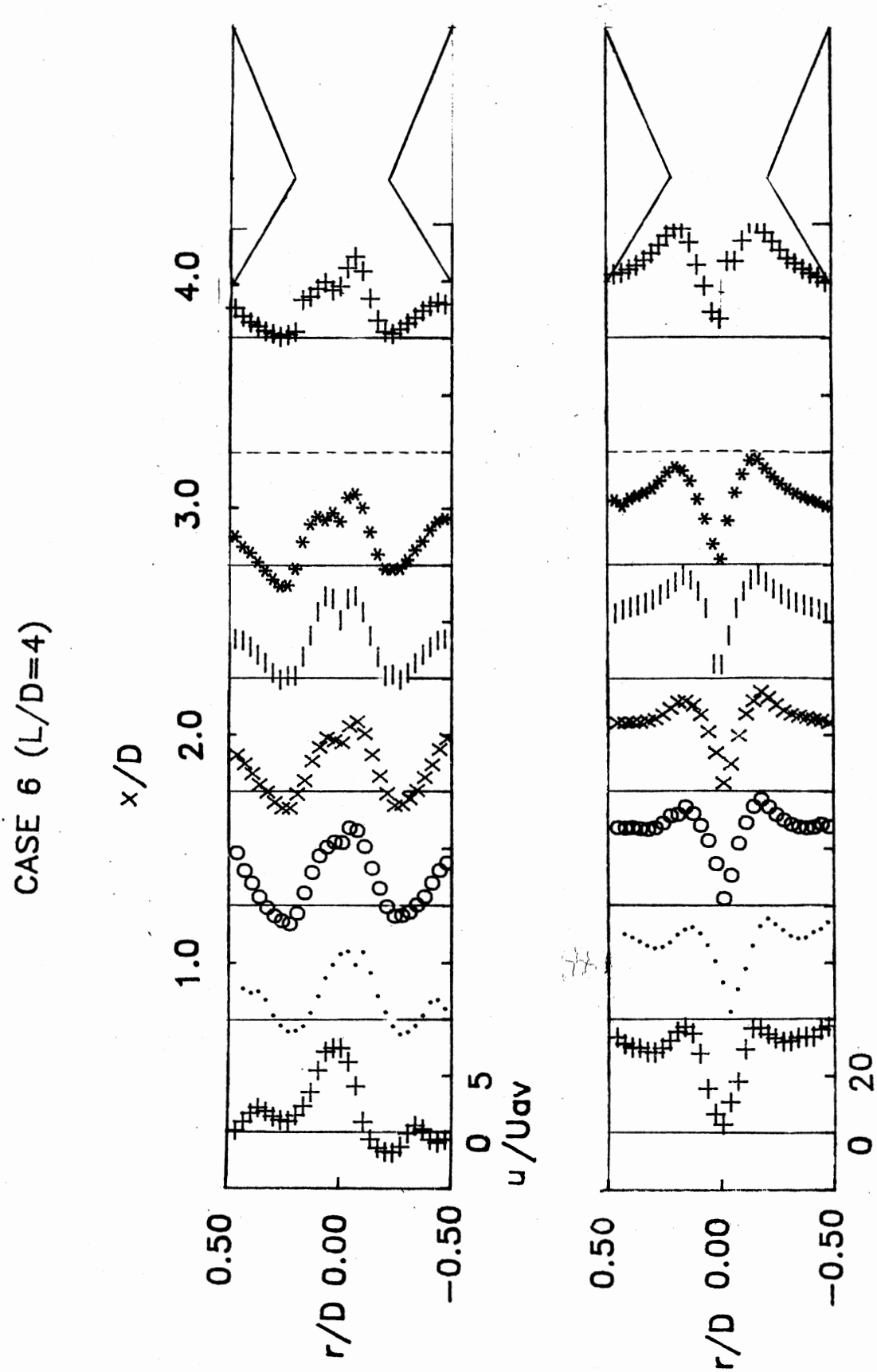

Figure 20 Strong Swirl

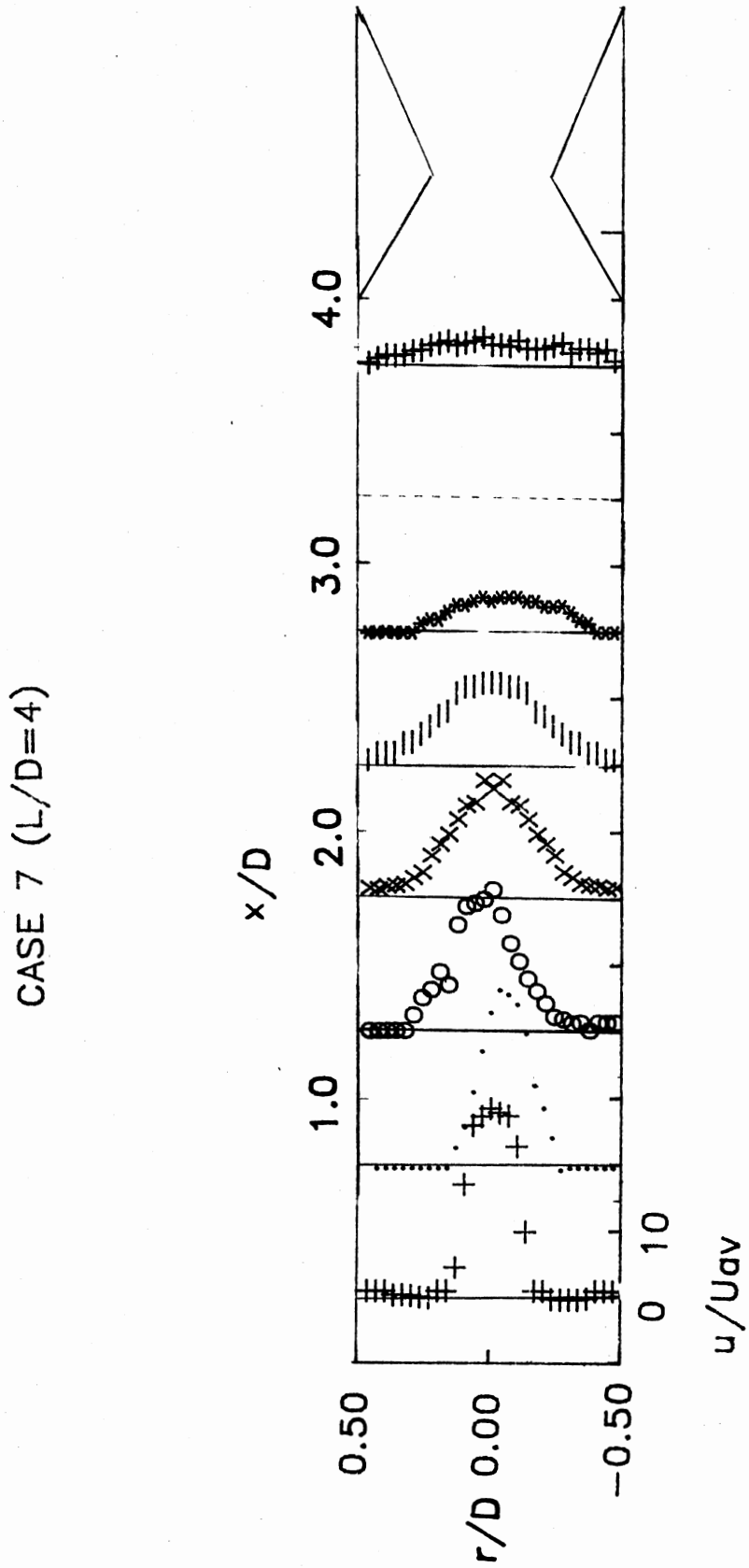

Figure 21 No Swirl

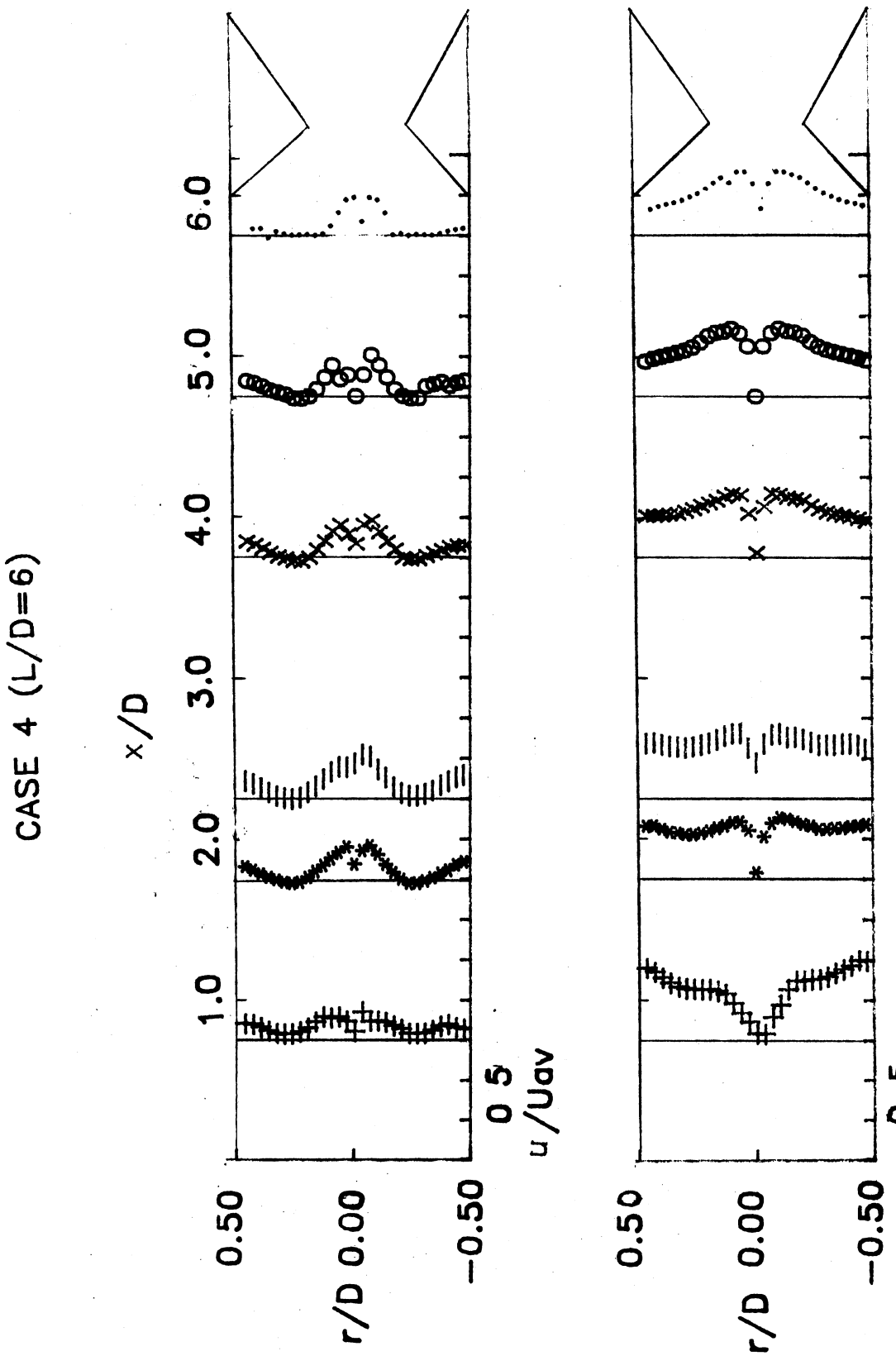

Figure 22 Moderate Swirl

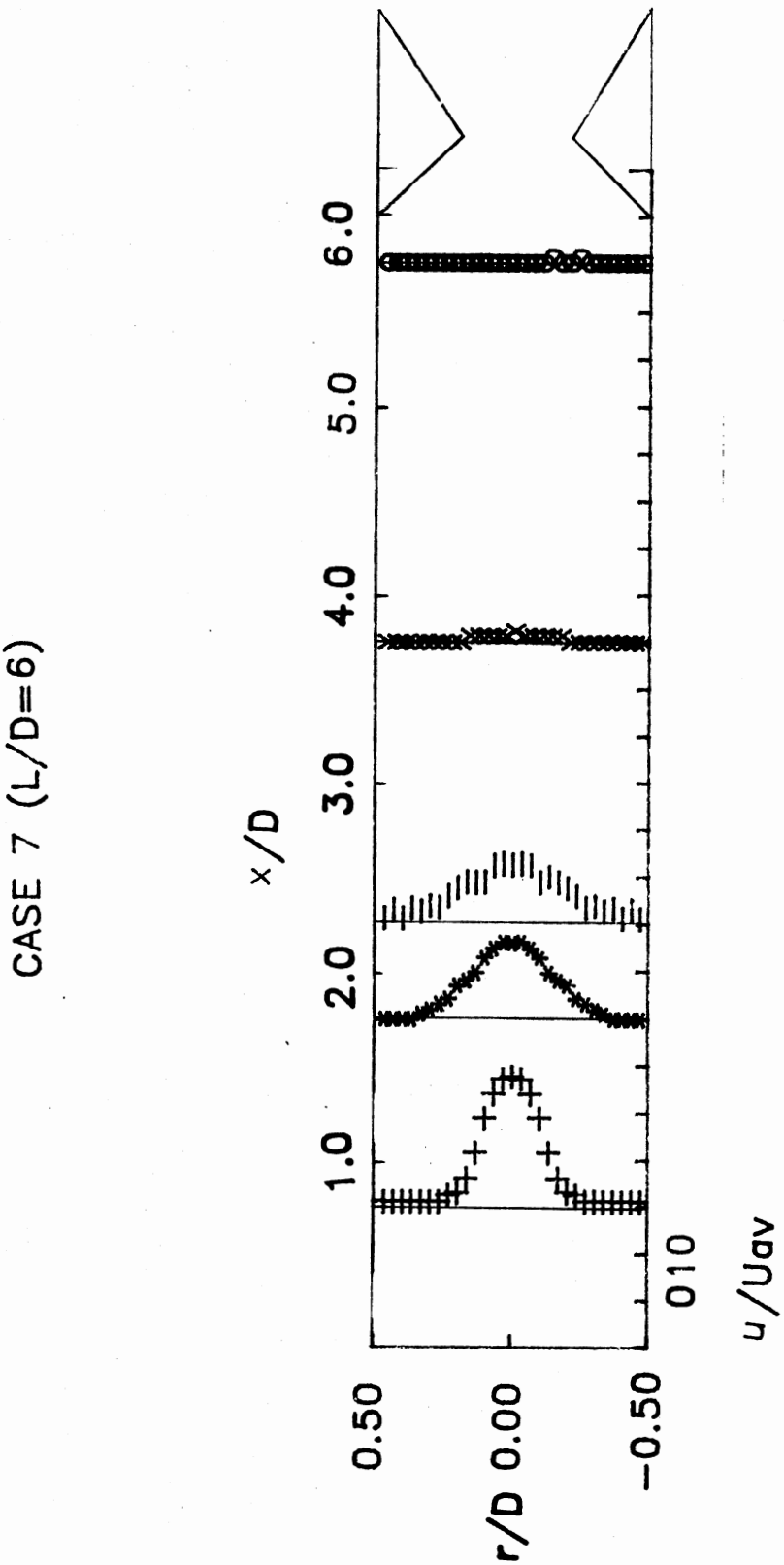

Figure 23 No Swirl

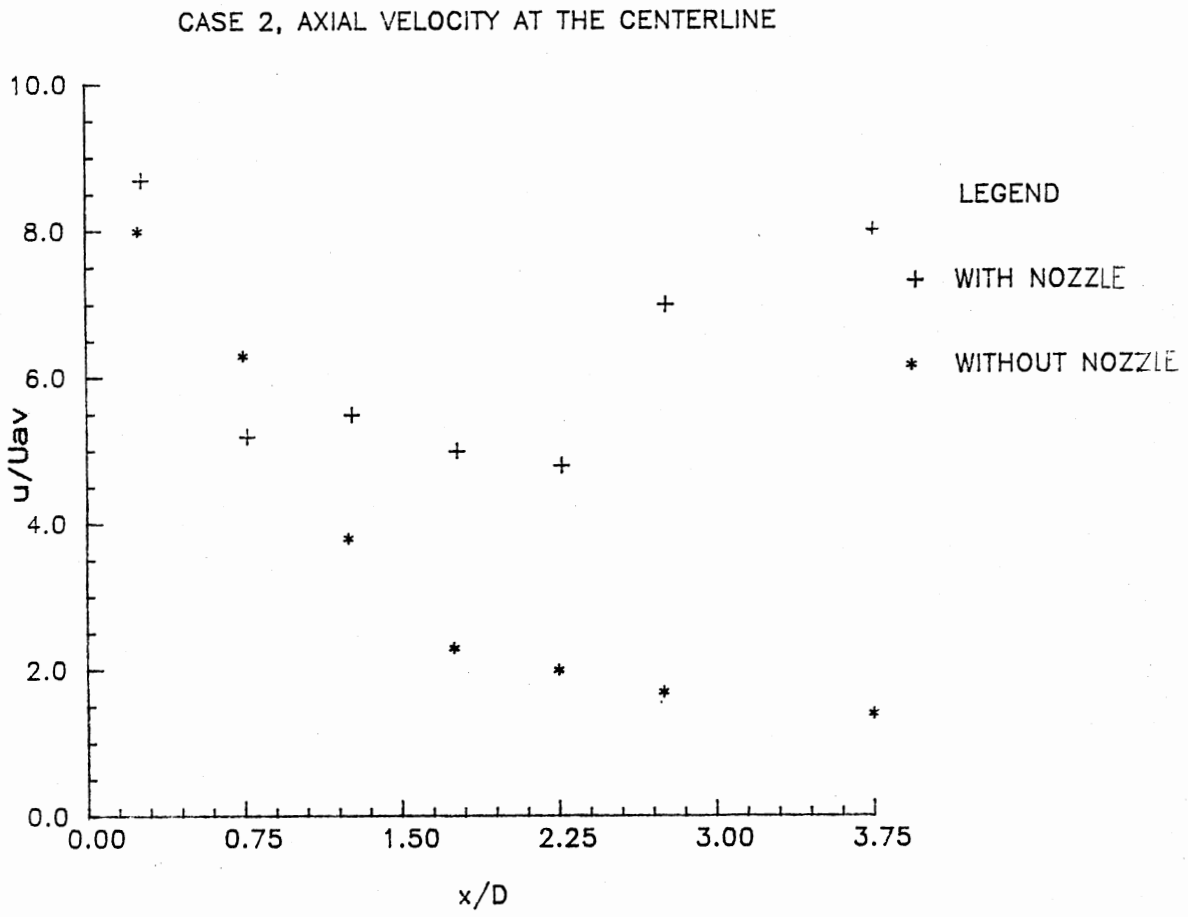

Figure 24. Case 2, Axial Velocity at the Centerline (* - Refer to Chai(36))

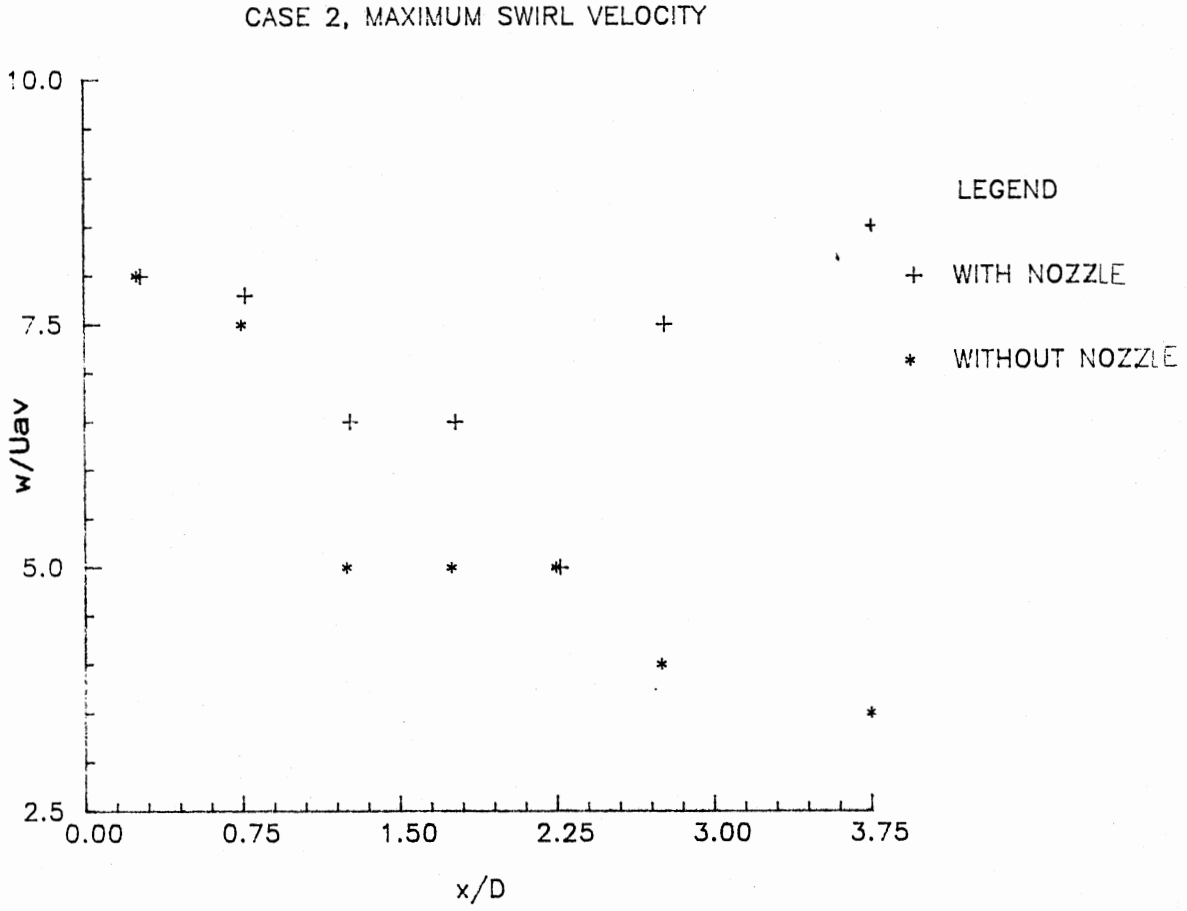

Figure 25. Case 2, Maximum Swirl Velocity
(* - Refer to Chai(36))

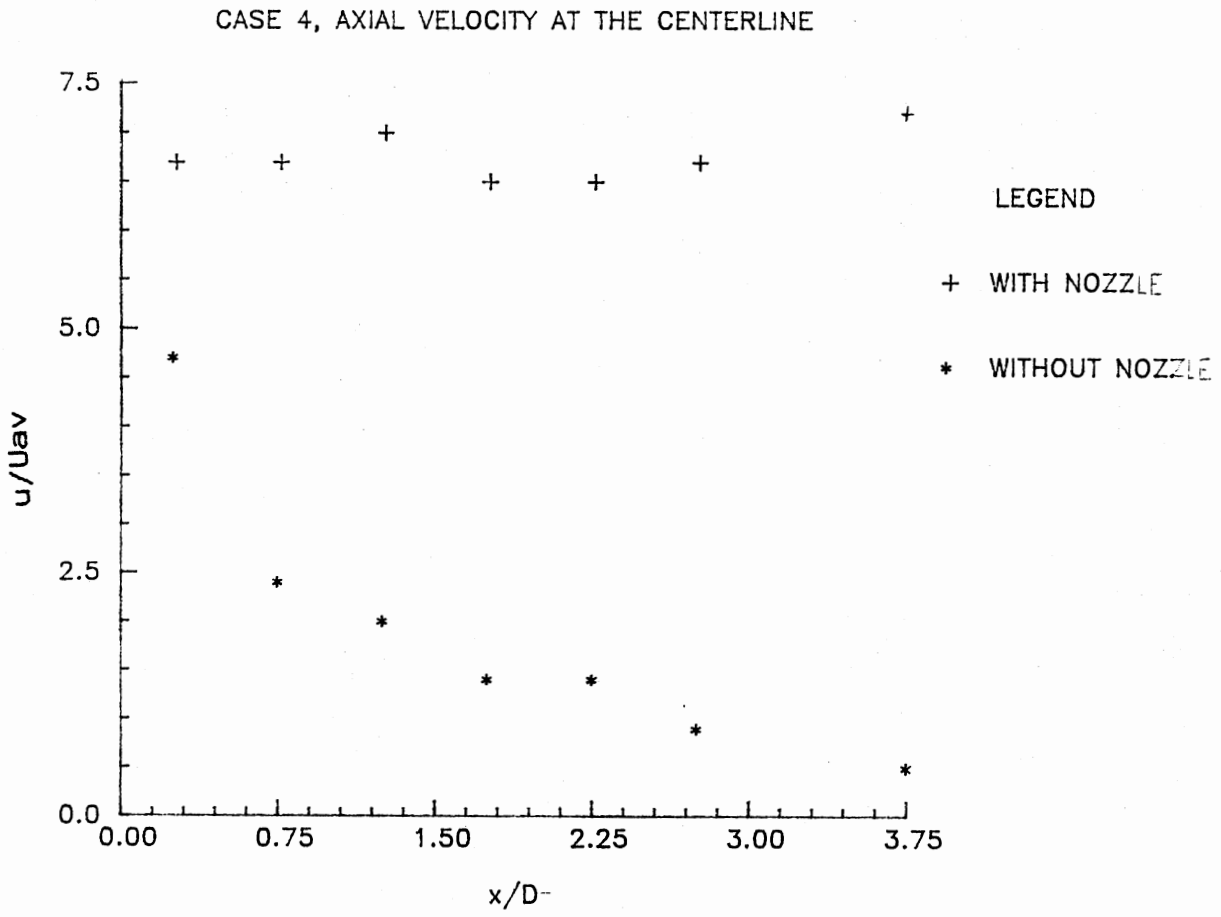

Figure 26. Case 4, Axial Velocity at the Centerline (* -Refer to Chai(36))

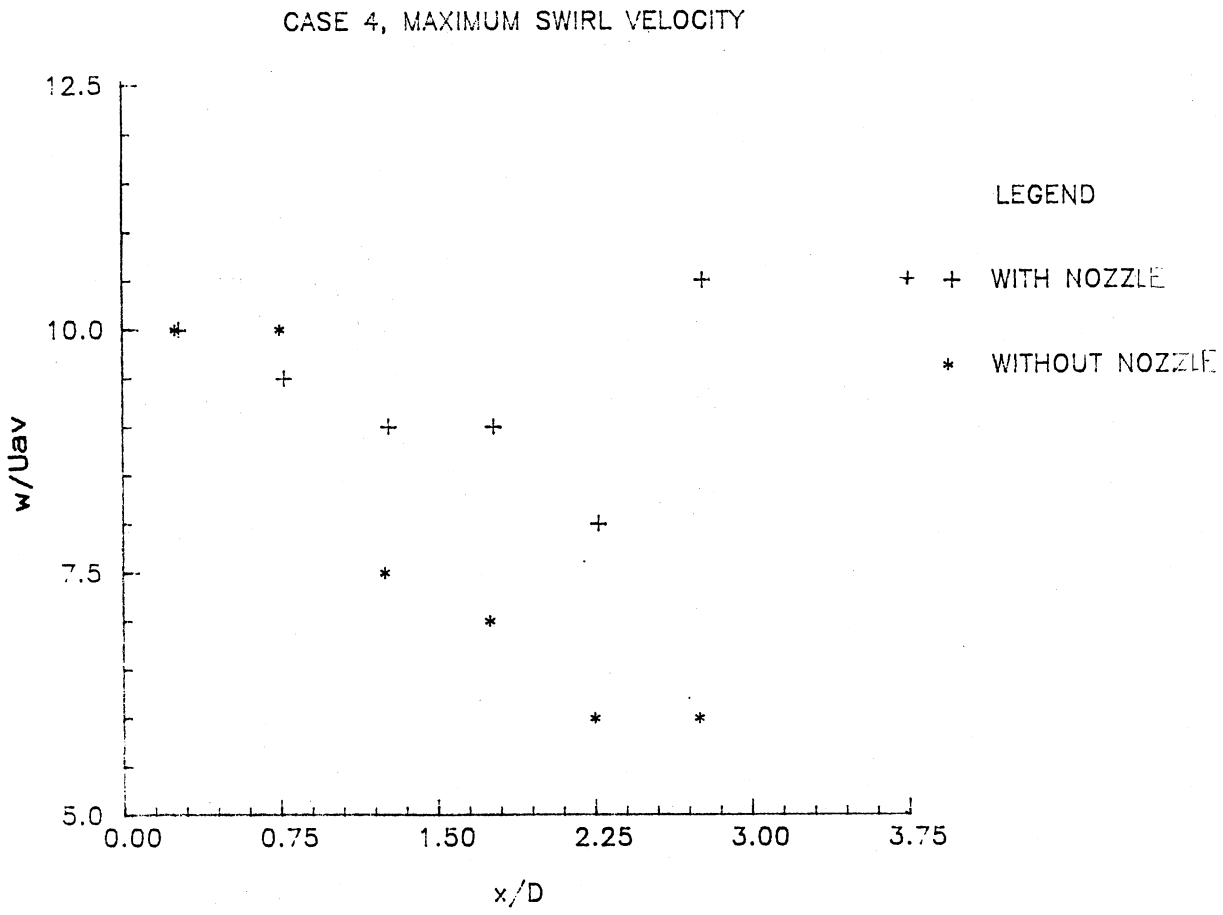

Figure 27. Case 4, Maximum Swirl Velocity (* - Refer to Chai(36))

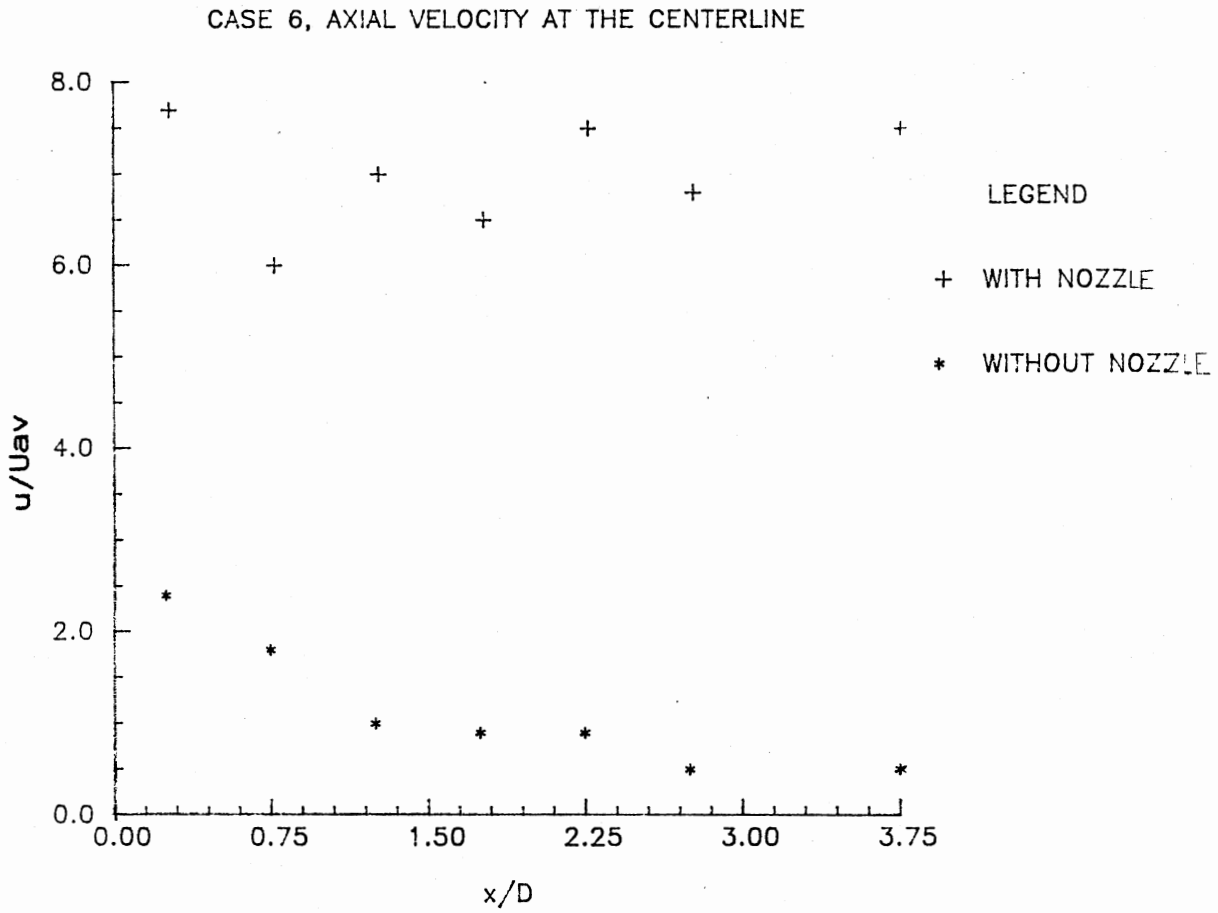

Figure 28. Case 6, Axial Velocity at the Centerline (* -Refer to Chai(36))

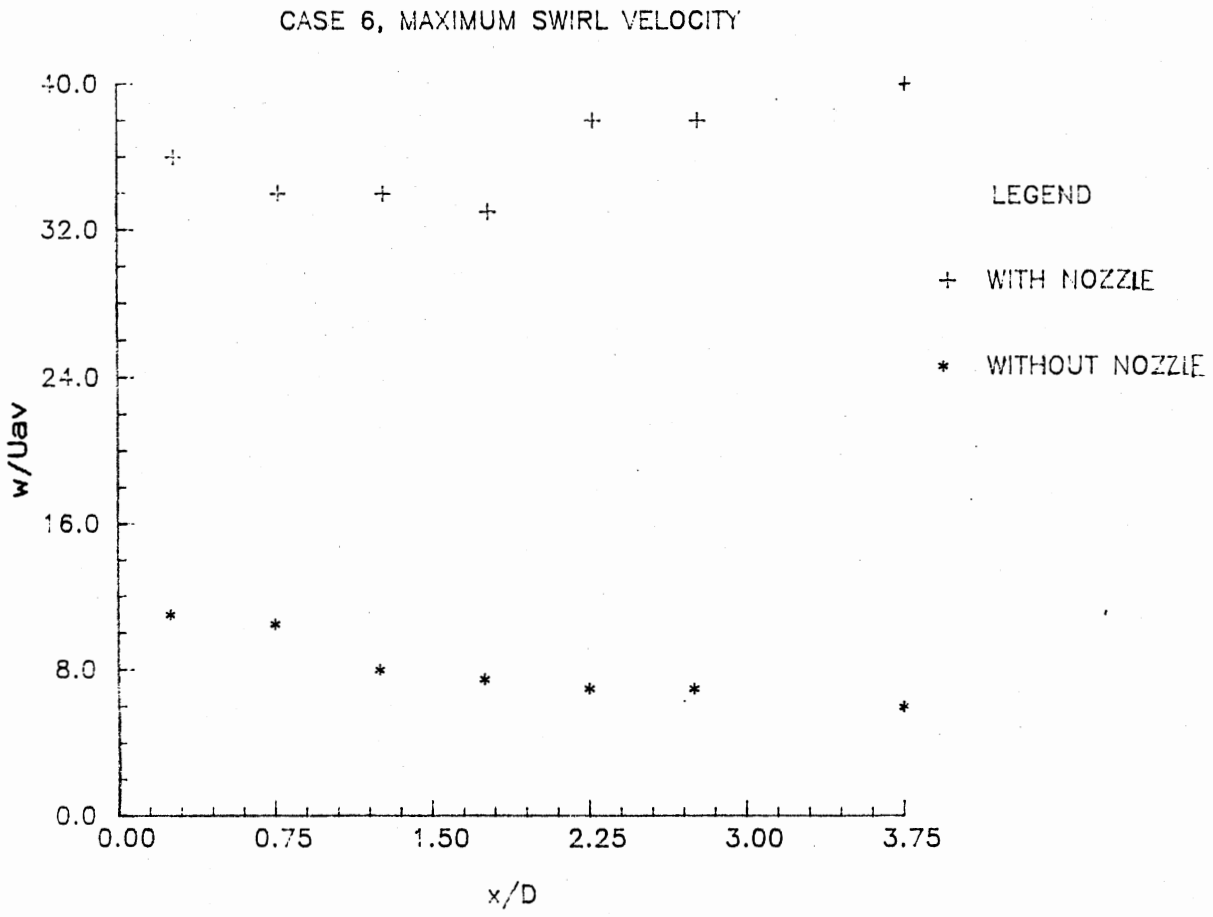

Figure 29. Case 6, Maximum Swirl Velocity
(* - Refer to Chai(36))

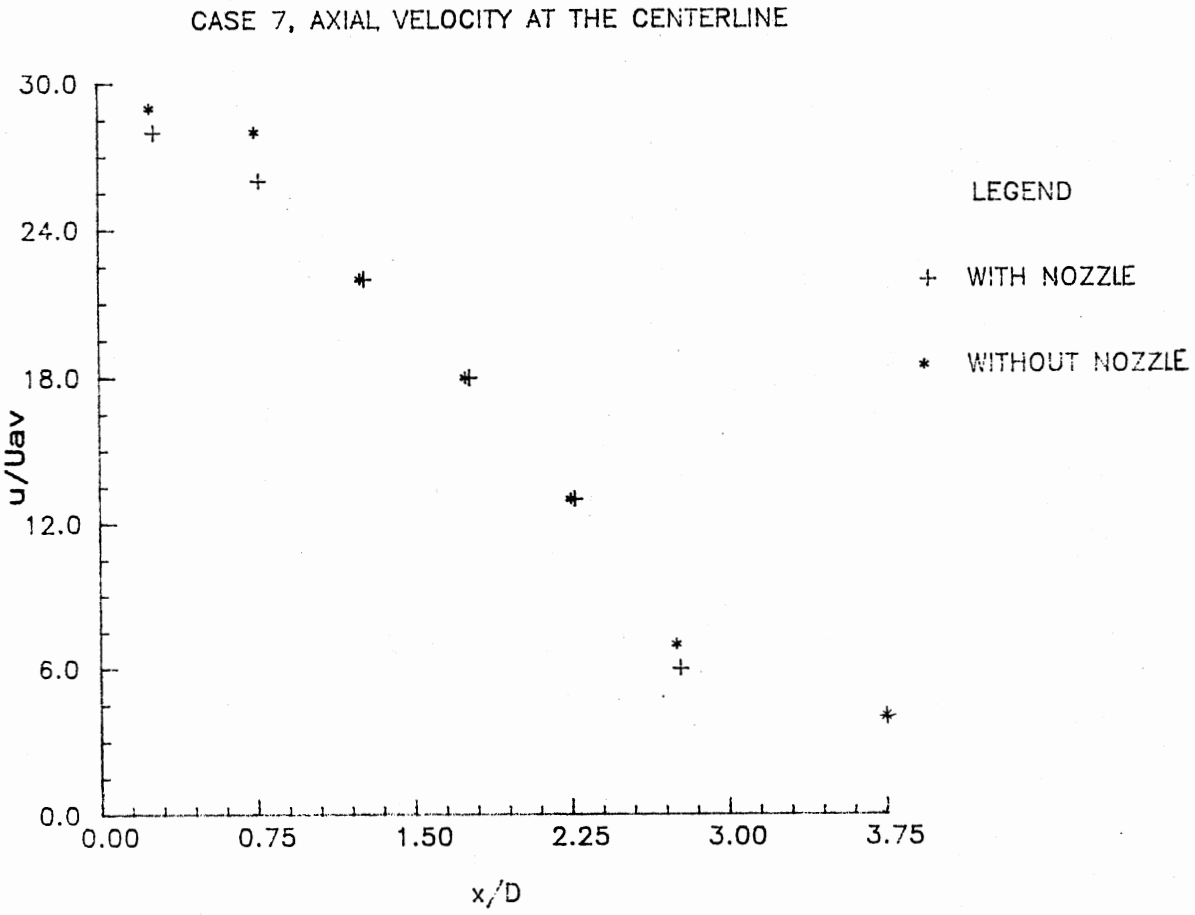

Figure 30. Case 7, Axial Velocity at the Centerline (* -Refer to Chai(36))

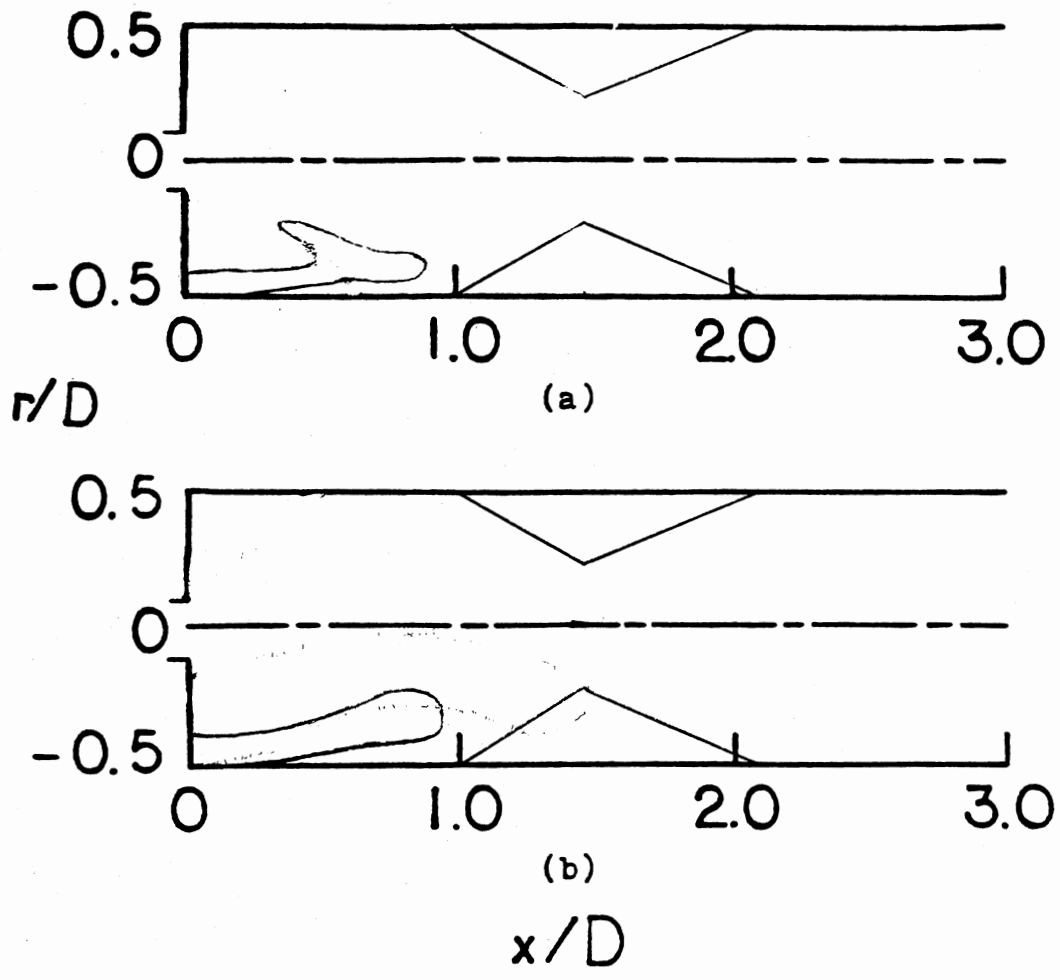

Figure 31. Sketch of Recirculation Zones: L/D =1
(a) Case 2 (b) Case 4

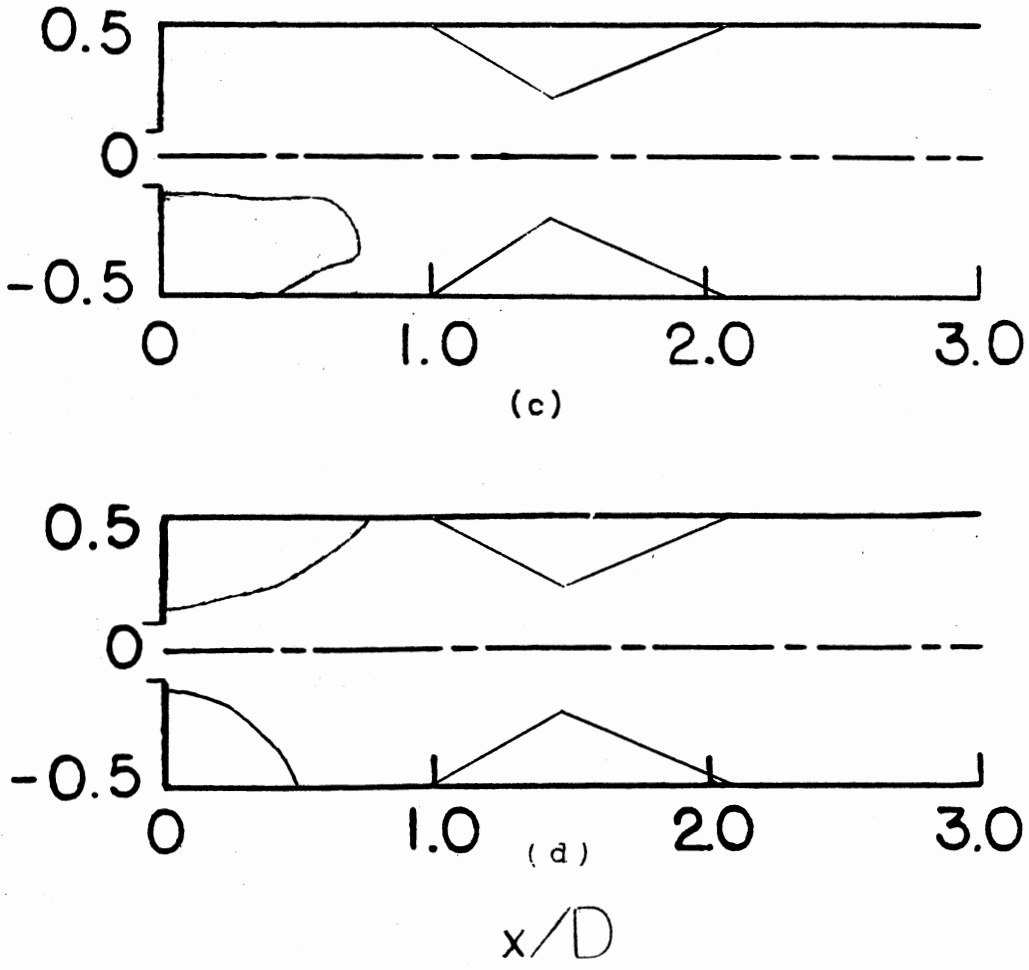

Figure 31. Continued
(c) Case 6 (d) Case 7

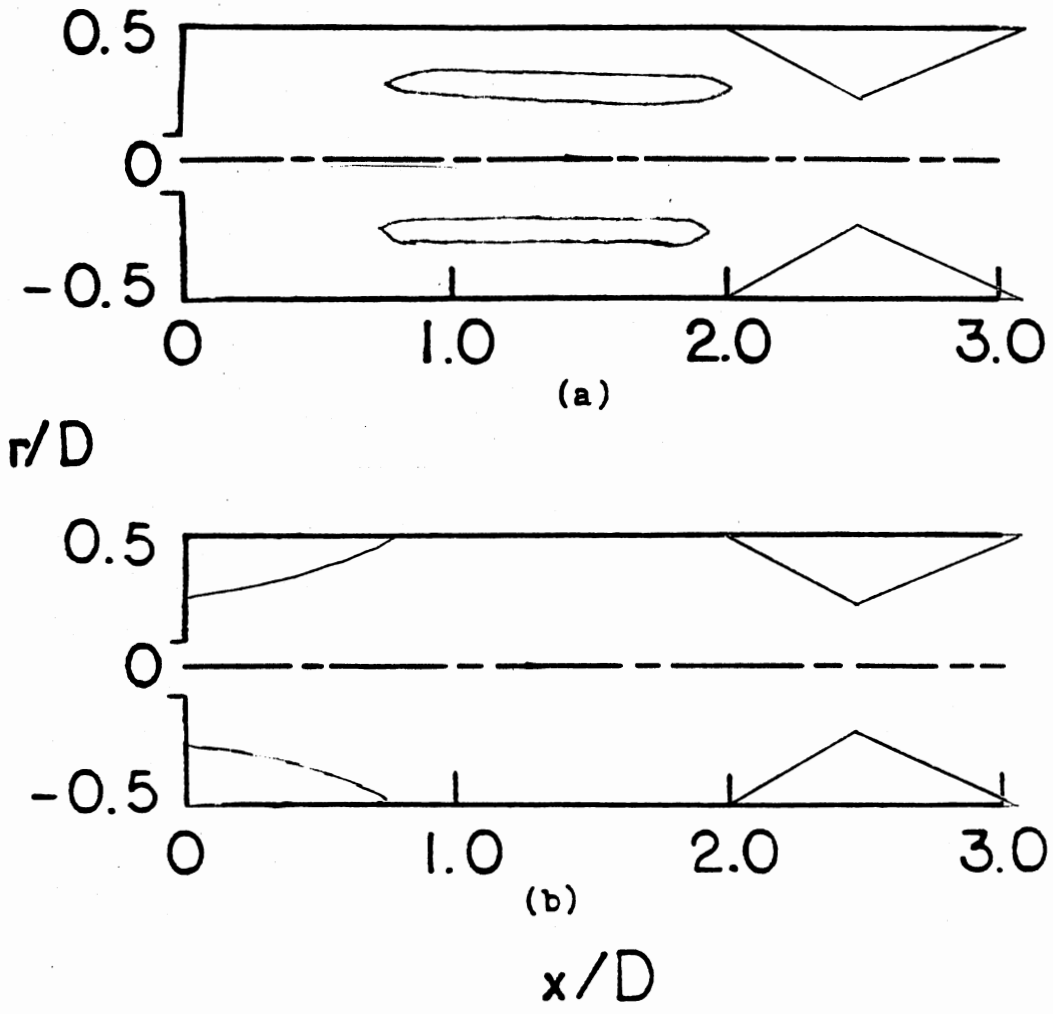

Figure 32. Sketch of Recirculation Zones: L/D =2
(a) Case 4 (b) Case 7

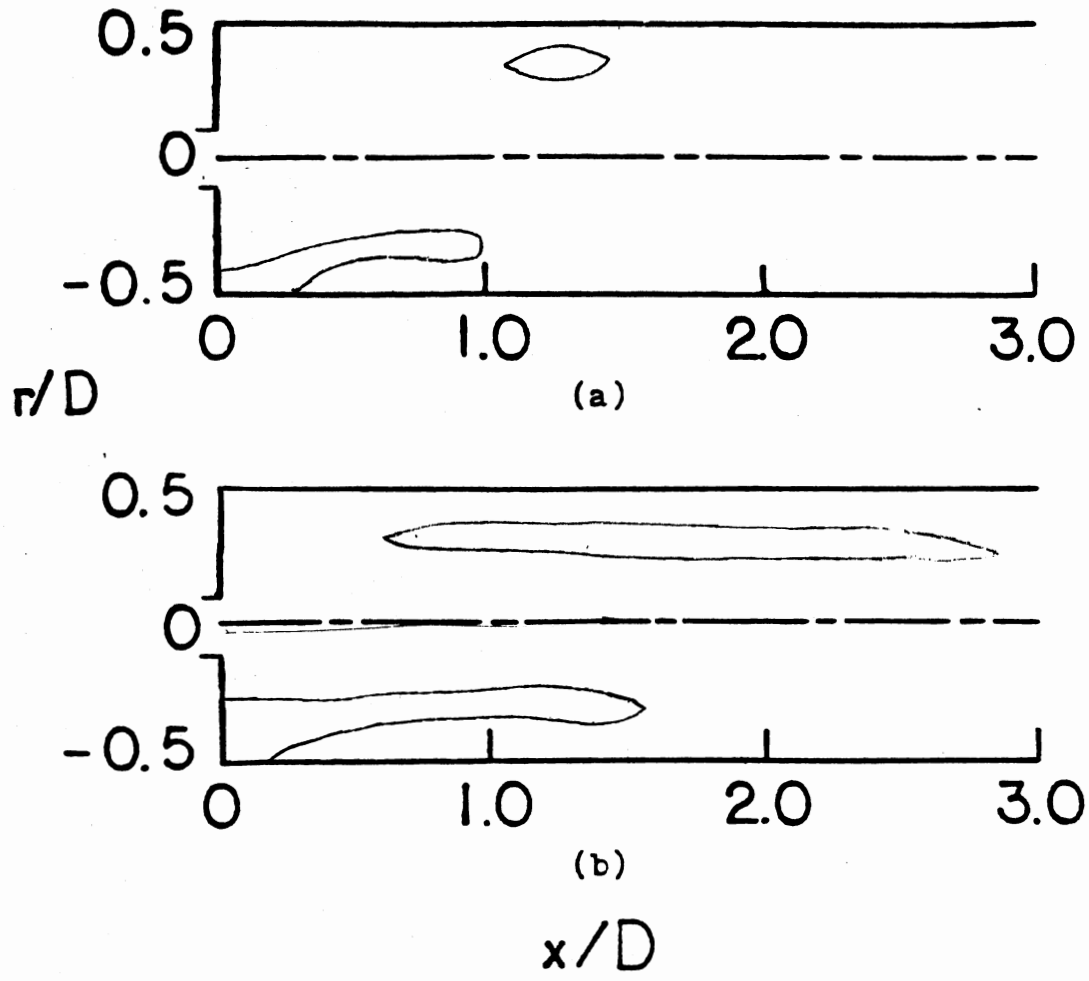

Figure 33 Sketch of Recirculation Zones: L/D =4
(a) Case 2 (b) Case 4

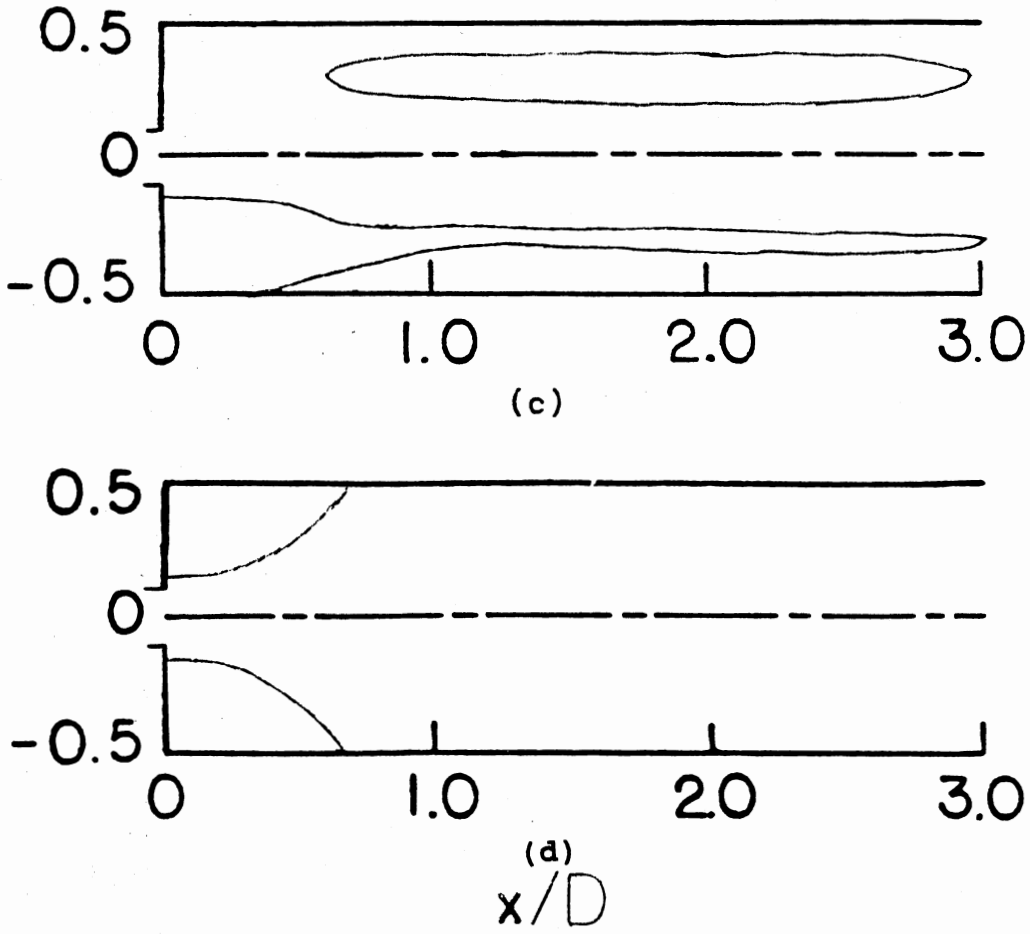

Figure 33. Continued
(c) Case 6 (d) Case 7

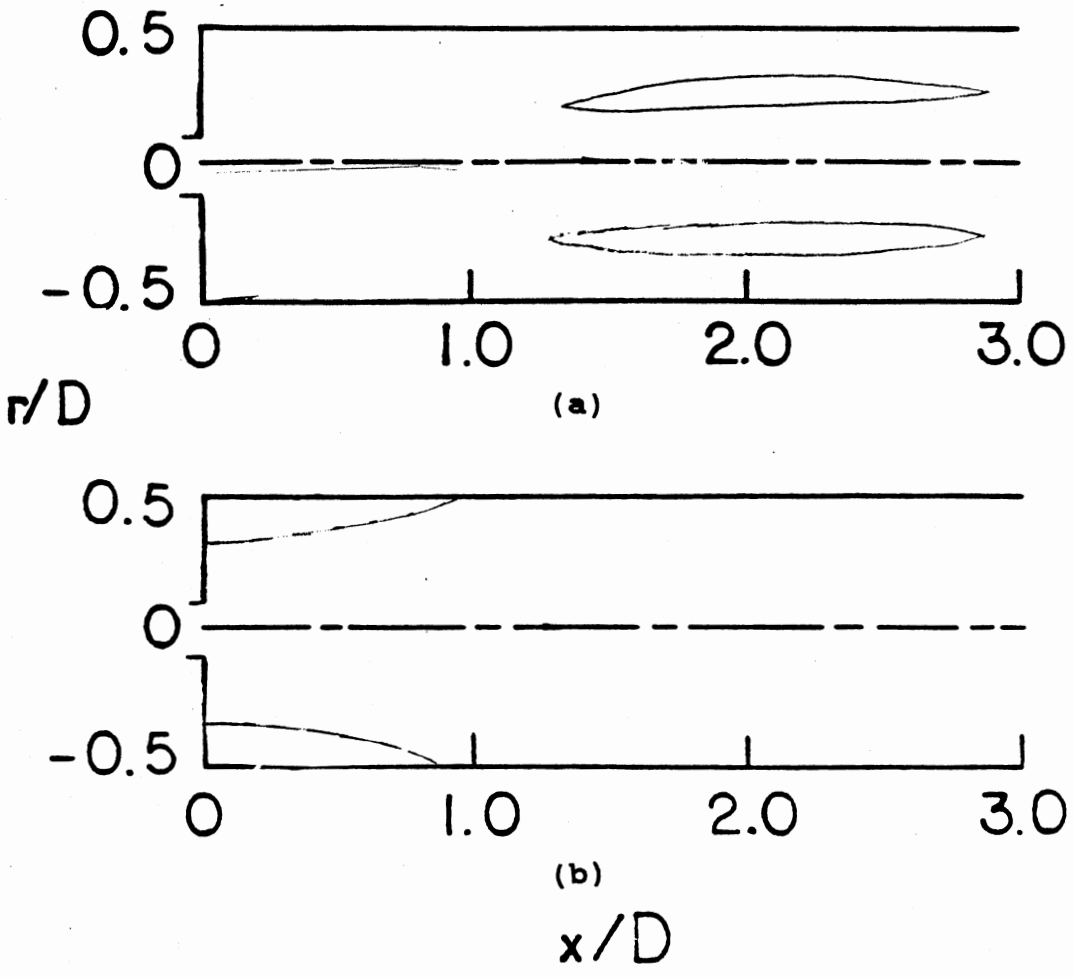

Figure 34. Sketch of Recirculation Zones: L/D =6
(a) Case 4 (b) Case 7

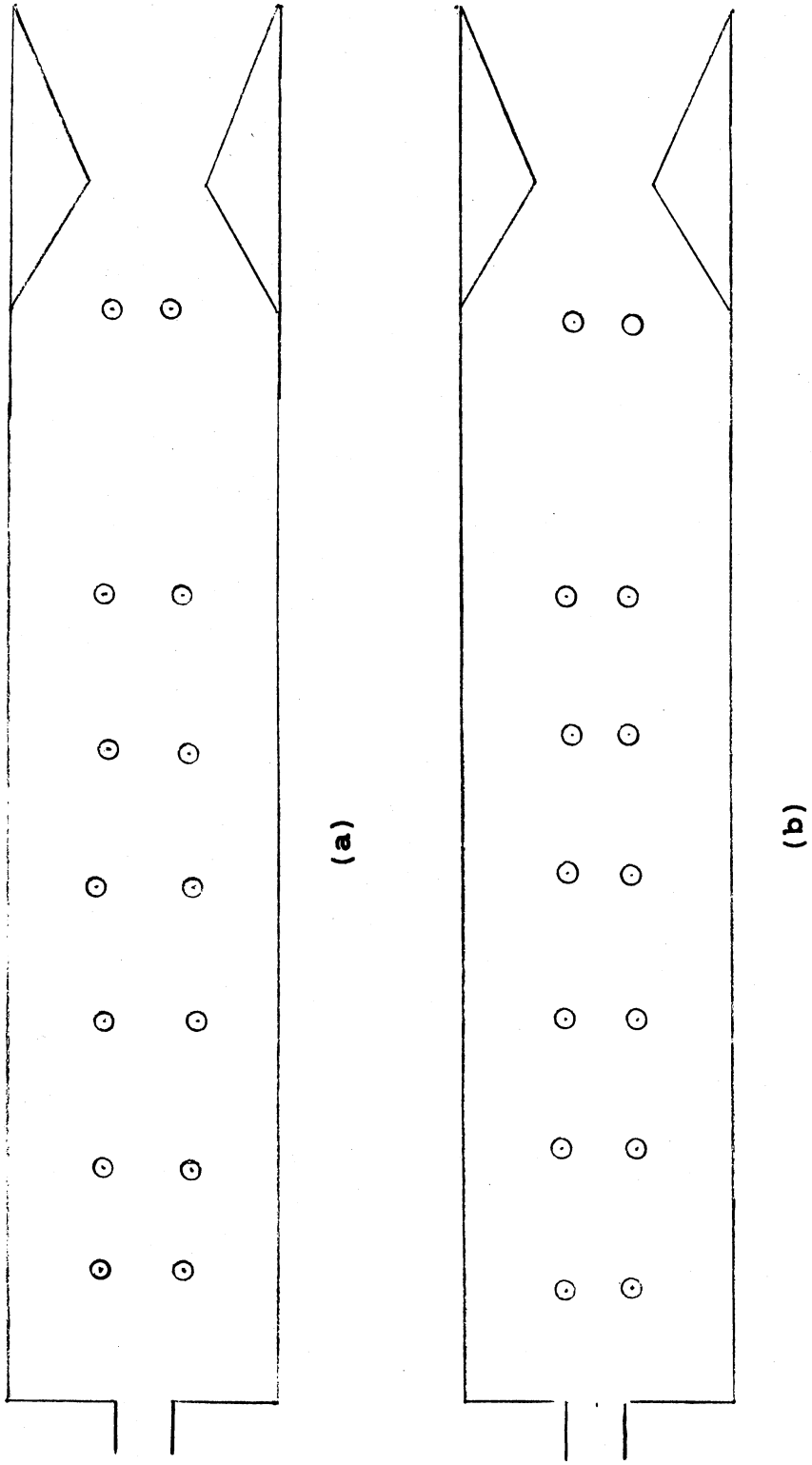

Figure 35. Spreading Free Jet: L/D = 4
(a) Case 2 (b) Case 4

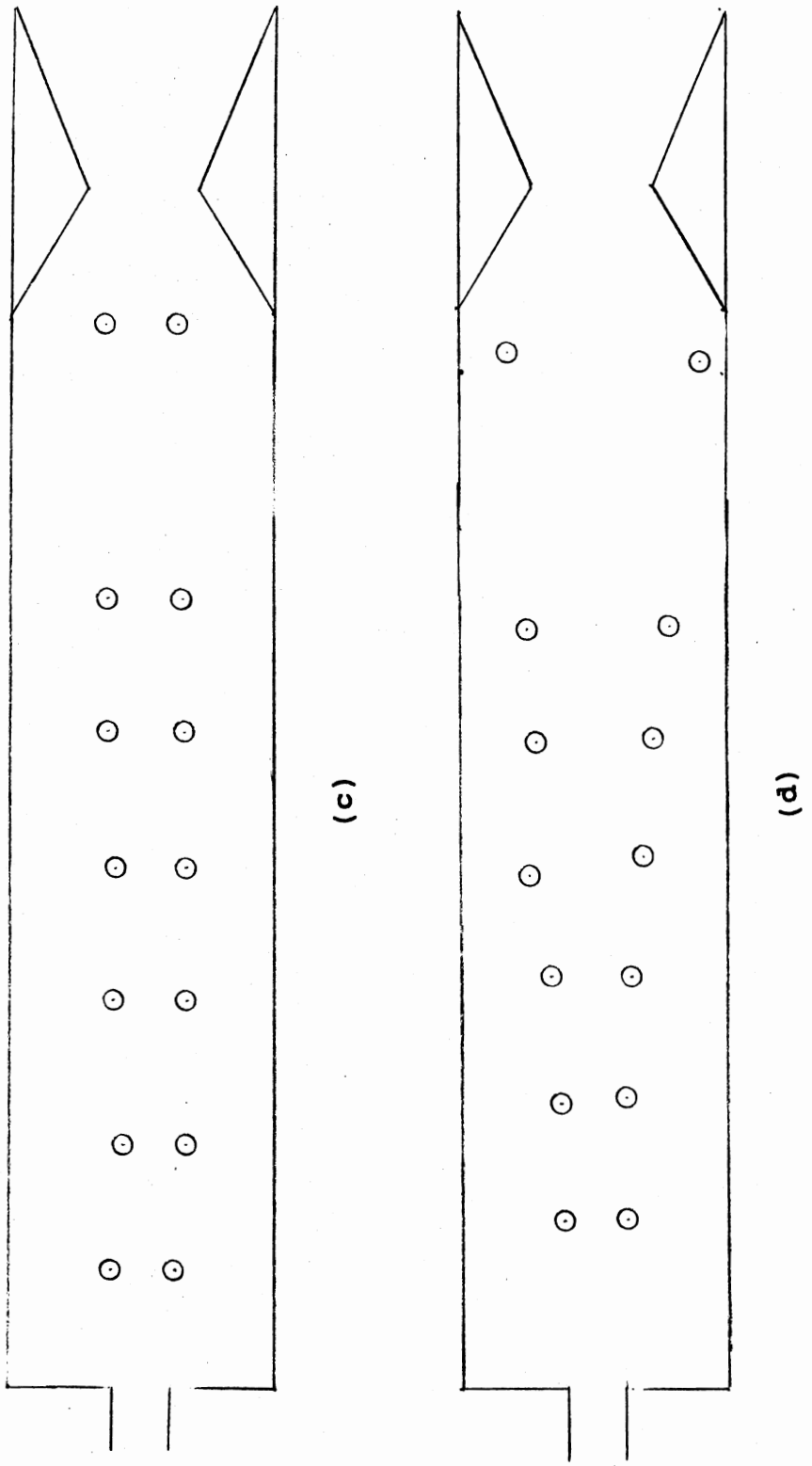

Figure 35. Continued
(c) Case 6 (d) Case 7

APPENDIX C

DATA REDUCTION COMPUTER PROGRAM

```
**** TSO FOREGROUND HARDCOPY ****
DSNAME=U12107A.TEST1.FORT

C     SUBROUTINE MAIN                                                          0000000
C                                                                              0000000
C*************************************************************************** 0000000
C                                                                              0000000
C                                                                              0000000
C     A COMPUTER PROGRAM FOR DATA REDUCTION OF FIVE-HOLE PITOT                 0000000
C     MEASUREMENTS IN TURBULENT, SWIRLING, RECIRCULATING FLOW                  0000000
C     IN COMBUSTOR GEOMETRIES                                                  0000000
C       .                                                                      0000000
C     MODIFIED VERSION FOR INTERACTIVE USE ON CYCLONE FACILITY                 0000000
C     MAY, 1988                                                                0000000
C                                                                              0000000
C     MODIFICATIONS INCLUDE COMBINED RADIAL AND AZIMUTHAL CAPA-                0000000
C     BILITY, REDUCTION OF STATIC PRESSURE DATA, AND CALCULATION               0000000
C     OF MOMENTUM FLUXES AND SWIRL NUMBERS FOR RADIAL PROFILES.                0000000
C                                                                              0000000
C     BASED ON A PROGRAM BY D. L. RHODE (PHD THESIS, OSU, 1981)                0000000
C                                                                              0000000
C                                                                              0000000
C     FIRST MODIFICATION     : G. F. SANDER  (MS THESIS, OSU, 1983)            0000000
C     SECOND MODIFICATION    : L. H. ONG     (MS THESIS, OSU, 1985)            0000000
C     THIRD MODIFICATION     : C. B. MCMURRY (MS THESIS, OSU, 1985)            0000000
C     FORTH MODIFICATION     : W. D. CHAI AND G. EGHNEIM                       0000000
C                                            (MS THESIS, OSU, 1988)            0000000
C                                                                              0000000
C     MECHANICAL AND AEROSPACE ENGINEERING                                     0000000
C     OKLAHOMA STATE UNIVERSITY                                                0000000
C     STILLWATER, OK     74078                                                 0000000
C                                                                              0000000
C*************************************************************************** 0000000
C                                                                              0000000
C---MAJOR FORTRAN VARIABLES IN MAIN PROGRAM (LISTED IN ORDER                   0000000
C           OF FIRST OCCURRENCE IN THE PROGRAM):                               0000000
C                                                                              0000000
C IWRITE - LOGICAL FLAG FOR WRITING INTO OUTPUT DATASET (UNFORMATTED)          0000000
C DIAGNS - FLAG FOR DIAGNOSTIC OUTPUT                                          0000000
C IT     - MAX NO. OF TRAVERSES ALLOWED; DIMENSION VALUE IN SUBROUTINES        0000000
C JT     - MAX NO. OF POINTS ALLOWED PER TRAVERSE; ALSO DIMENSION VALUE        0000000
C HEDM ETC. - ALL VARIABLES STARTING WITH "HED" ARE ALPHANUMERIC ARRAYS        0000000
C             FOR OUTPUT HEADINGS                                              0000000
C NCAL   - NO. OF CALIBRATION DATA POINTS                                      0000000
C CPITCH - CALIBRATION PITCH COEFF. -- (PN-PS)/(PC-PW)                         0000000
C CDELTA - CAL. PITCH ANGLE -- STANDARD RANGE -58 TO +58 DEG.                  0000000
C CVELCF - CAL. VELOCITY COEFF. -- (CAL. DYN. PRESS.)/(PC-PW)                  0000000
C CPSTCF - CAL. STATIC PRESSURE COEFF. -- (PC-PA)/(PC-PW)                      0000000
C HEDID1,HEDID2 - USER HEADINGS TO IDENTIFY THE RUN BEING REDUCED              0000000
C ALPHA  - INLET SIDEWALL EXPANSION ANGLE                                      0000000
C PHI    - SWIRL VANE ANGLE SETTING                                            0000000
C DSINCH - INLET NOZZLE OR SWIRLER DIAMETER, DSMALL, IN INCHES                 0000000
C DLINCH - TEST SECTION DIAMETER, DLARGE, INCHES                               0000000
C AAFR   - AXIAL AIR FLOW RATE,CFM                                             0000000
C TAFR   - TANGENTIAL AIR FLOW RATE,CFM                                        0000000
C KRADTR - INTEGER FLAG FOR TRAVERSE TYPE -- 1 FOR RADIAL, 0 FOR AZIM.         0000000
C NSTATN - NO. OF TRAVERSES TO BE REDUCES                                      0000000
C MAXJPT - MAX NO. OF POINTS IN ANY OF THE TRAVERSES BEING REDUCED             0000000
C XINCHS - AXIAL POSITION OF EACH TRAVERSE, INCHES                             0000000
C NDATA  - NO. OF DATAPOINTS IN EACH TRAVERSE                                  0000000
C RDNPRS - INLET DYNAMIC PRESSURE (UPSTREAM OF SWIRLER), TORR                  0000000
C PREF   - REF. PRESS. USED TO CALC. PDIFF FOR SWIRL NUMBER, TORR              0000000
```

```
C FANSPD - FAN SPEED, RPM                                                    0000000
C TFLOW  - TEMPERATURE OF AIR IN TEST SECTION, DEG. CELSIUS                  0000000
C PATM   - ATMOSPHERIC PRESSURE, TORR                                        0000000
C BZOFF  - BETA ZERO-OFFSET FOR YAW ANGLE READINGS                           0000000
C RINCHS - RADIAL POS. OF DATAPOINT, INCHES (THETA FOR AZIM. TRAVERSES)      0000000
C RBETA  - RAW VALUE OF YAW ANGLE BETA, DEG.                                 0000000
C RPNMPS - MEAS. VALUE OF PNORTH - PSOUTH PRESS. DIFF, TORR                  0000000
C RPCMPW - MEAS. VALUE OF PCENTER - PWEST, TORR                              0000000
C RPCMPA - MEAS. VALUE OF PCENTER - PATMOSPHERE, TORR                        0000000
C RSMALL - INLET NOZZLE OR SWIRLER RADIUS, METERS                            0000000
C RLARGE - TEST SECTION RADIUS, METERS                                       0000000
C X      - AXIAL POSITION OF TRAVERSE, METERS                                0000000
C R      - RADIAL POSITION OF DATAPOINT, METERS                              0000000
C IDID   - FLAG TO USE ENTRY POINT SP IN SPLINE INTERPOLATION ROUTINE        0000000
C PICHCF - REDUCED PITCH COEFF. FOR EACH DATAPOINT                           0000000
C DELTA  - REDUCED PITCH ANGLE FOUND BY INTERPOLATION USING PICHCF           0000000
C VELCF  - REDUCED VELOCITY COEFF. FROM INTERPOLATION USING DELTA            0000000
C PSTCF  - REDUCED STATIC PRESS. COEFF. FROM INTERPOLATION USING DELTA       0000000
C RHO    - DENSITY FOR EACH TRAVERSE, FROM IDEAL-GAS LAW                     0000000
C BETA   - REDUCED VALUE FOR PROBE YAW ANGLE, DEG.                           0000000
C VTOTAL - TOTAL VELOCITY VECTOR MAGNITUDE, M/S                              0000000
C U      - AXIAL COMPONENT OF VELOCITY, M/S                                  0000000
C V      - RADIAL COMP. OF VELOCITY, M/S                                     0000000
C W      - TANGENTIAL (SWIRL) VELOCITY, M/S                                  0000000
C P      - REDUCED VALUE OF STATIC PRESSURE, N/SQ. M (GAGE)                  0000000
C XND    - NONDIMENSIONAL AXIAL POSITION, X/DLARGE                           0000000
C UIN    - INLET REFERENCE VELOCITY (CALC. FROM RDNPRS), M/S                 0000000
C MASFLO - INLET MASS FLOW RATE (ASSUMING UNIFORM AXIAL VELOCITY), KG/S      0000000
C VTSTAR - NONDIM. TOTAL VELOCITY MAGNITUDE, VTOTAL/UIN                      0000000
C USTAR  - NONDIM. AXIAL VELOCITY, U/UIN                                     0000000
C VSTAR  - NONDIM. RADIAL VELOCITY, V/UIN                                    0000000
C WSTAR  - NONDIM. TANGENTIAL VEL., W/UIN                                    0000000
C PSTAR  - NONDIM. STATIC PRESSURE, P/RDNPRS                                 0000000
C RND    - NONDIM. RADIAL POS., R/DLARGE; ALSO THETA FOR AZIM. TRAVERSES     0000000
C DYPS   - "DELTA-Y, POINT-SOUTH" (FOR RADIAL INTEGRATION; FROM STARPIC)     0000000
C DYNP   - "DELTA-Y, NORTH-POINT" (SIM. TO DYPS)                             0000000
C SNS    - "SMALL NORTH-SOUTH" FROM STARPIC; USED AS DELTA-R FOR INTEGR.     0000000
C PDIFF  - PRESS. DIFF. P - PREF USED TO CALCULATE SWIRL NUMBER, N/SQ. M     0000000
C AREA1  - AREA OF DISC ELEMENT AT CENTER OF INTEGRATION REGION              0000000
C FLOW   - SUMMATION FOR MASS FLOW THROUGH RING ELEMENTS                     0000000
C WMOM   - SUMMATION FOR ANGULAR MOMENTUM FLUX                               0000000
C UMOM   - SUMMATION FOR DYNAMIC AXIAL MOM. FLUX (NEGL. PRESS. TERM)        0000000
C UMOMP  - SUMMATION FOR AXIAL MOMENTUM FLUX, INCL. PRESSURE DIFF. TERM      0000000
C AREAJ  - AREA OF EACH RING ELEMENT, SQ. M                                  0000000
C MASS   - INTEGRATED MASS FLOW RATE, KG/S                                   0000000
C UMEAN  - INTEGRATED MEAN AXIAL VELOCITY, M/S                               0000000
C ANGMOM - INTEGRATED AXIAL FLUX OF ANGULAR MOMENTUM, N-M                    0000000
C AXMOM  - INT. AXIAL FLUX OF DYNAMIC AXIAL MOM., N (NEGL. PRESS. TERM)      0000000
C AXMOMP - INT. AXIAL FLUX OF AXIAL MOMENTUM, N (INCL. PRESSURE TERM)        0000000
C SPRIME - SWIRL NUMBER CALC. USING DYNAMIC AXIAL MOMENTUM FLUX              0000000
C S      - SWIRL NUMBER CALC. USING FULL AXIAL MOM. FLUX (INCL. PRESS.)      0000000
C USTAVG - AVERAGE OF USTAR VALUES FOR AZIM. TRAV., OVER ONE BLADE SPACE     0000000
C VSTAVG - AVG. OF VSTAR VALUES                                              0000000
C WSTAVG - AVG. OF WSTAR VALUES                                              0000000
C PDFAVG - AVG. OF PDIFF VALUES                                              0000000
C VISCOS - LAMINAR ABS. VISCOSITY CALCULATED FOR EACH TRAVERSE, KG/M*S       0000000
C REDIN  - INLET REYNOLDS NUMBER, CALC. USING VISCOSITY FOR EACH TRAV.       0000000
C                                                                            0000000
C                                                                            0000000
C*****************************************************************************0000000
CHAPTER  O  O  O  O  O  O  O  O  O  PRELIMINARIES  O  O  O  O  O  O  O  O  O  0000000
C                                                                            0000000
      DIMENSION HEDM(9),HEDUMN(9),HEDNMS(9),HEDCMW(9),HEDCMA(9),             0000000
     #HEDU(9),HEDV(9),HEDW(9),HEDVT(9),HEDUST(9),                            0000000
     #HEDVST(9),HEDWST(9),HEDPST(9),HEDDEL(9),HEDBET(9),                     0000000
     #HEDMMF(9),HEDMIV(9),HEDMIP(9),HEDAM(9),                                0000000
```

```
     #HEDAX(9),HEDAXP(9),HEDSPR(9),HEDS(9),HEDP(9),HEDPDF(9),HEDRED(9),  0000000
     #HEDID1(18),HEDID2(18),HEDUSA(9),HEDVSA(9),HEDWSA(9),HEDPDA(9),     0000000
     #HEDFAN(9),HEDTFL(9),HEDPAT(9),HEDRHO(9),HEDVIS(9),HEDCAL(9)        0000000
C                                                                        0000000
C                                                                        0000000
      COMMON                                                             0000000
     #/CALIB/CPITCH(26),CDELTA(26),CVELCF(26),CPSTCF(26)                 0000000
     #/MEASUR/RBETA(8,24),RPNMPS(8,24),RPCMPW(8,24),RPCMPA(8,24),        0000000
     #     NDATA(8),MAXJPT,RDNPRS(8),                                    0000000
     #     FANSPD(8),TFLOW(8),PATM(8),BZOFF(8)                           0000000
     #/GEOM/X(8),R(24),XND(8),RND(24),DYPS(24),DYNP(24),                 0000000
     #     SNS(24),NSTATN,XINCHS(8),RINCHS(24)                           0000000
     #/CALC/VTOTAL(8,24),U(8,24),V(8,24),W(8,24),P(8,24),                0000000
     #     VTSTAR(8,24),USTAR(8,24),VSTAR(8,24),WSTAR(8,24),             0000000
     #     PICHCF(8,24),VELCF(8,24),DELTA(8,24),BETA(8,24),              0000000
     #     ANGMOM(8),UMEAN(8),UIN(8),RMASS(8),RMASFL(8),                 0000000
     #     PSTAR(8,24),PSTCF(8,24),AXMOM(8),AXMOMP(8),                   0000000
     #     SPRIME(8),S(8),REDIN(8),PREF(8),RHO(8),VISCOS(8),             0000000
     #     USTAVG(8,24),VSTAVG(8,24),WSTAVG(8,24),PSTAVG(8,24)           0000000
     #/OUTPUT/STORE(8)                                                  0000000
C                                                                        0000000
      LOGICAL IWRITE,DIAGNS                                              0000000
C                                                                        0000000
C---SET IWRITE=.TRUE. FOR WRITING SOLN. ON DISK STORAGE;                 0000000
C   SET DIAGNS=.TRUE. TO ACTIVATE DIAGNOSTIC WRITE STATEMENTS            0000000
C                                                                        0000000
      IWRITE=.TRUE.                                                      0000000
      DIAGNS=.TRUE.                                                      0000000
      IT=8                                                               0000000
      JT=24                                                              0000000
C                                                                        0000000
C---READ CHARACTER DATA FOR HEADINGS USED BY SUBROUTINES                 0000000
C   WRITE AND PRINT (ALSO CALIBRATION HEADING)                           0000000
C                                                                        0000000
      READ(7,205) HEDM,HEDUMN,HEDU,HEDV,HEDW,                           0000000
     #     HEDVT,HEDUST,HEDVST,HEDWST,HEDPST,HEDDEL,HEDBET,              0000000
     #     HEDNMS,HEDCMW,HEDCMA,HEDMMF,HEDMIV,HEDMIP,HEDAM,              0000000
     #     HEDAX,HEDAXP,HEDSPR,HEDS,HEDP,HEDPDF,HEDRED,                  0000000
     #     HEDFAN,HEDTFL,HEDPAT,HEDRHO,HEDVIS,                           0000000
     #     HEDUSA,HEDVSA,HEDWSA,HEDPDA,HEDCAL                            0000000
  205 FORMAT(9A4)                                                        0000000
C                                                                        0000000
C---------INITIALIZE VARIABLES TO ZERO                                   0000000
C                                                                        0000000
      CALL INIT                                                          0000000
C                                                                        0000000
C---------READ FIVE-HOLE PITOT CALIBRATION DATA                          0000000
C                                                                        0000000
      NCAL=25                                                            0000000
      DO 10 I=1,NCAL                                                     0000000
        READ(7,210) CPITCH(I),CDELTA(I),CVELCF(I),CPSTCF(I)              0000000
   10 CONTINUE                                                           0000000
  210 FORMAT(4F10.5)                                                     0000000
      IF(DIAGNS) WRITE(8,400) (CPITCH(I),I=1,25)                         0000000
      IF(DIAGNS) WRITE(8,400) (CDELTA(I),I=1,25)                         0000000
      IF(DIAGNS) WRITE(8,400) (CVELCF(I),I=1,25)                         0000000
      IF(DIAGNS) WRITE(8,400) (CPSTCF(I),I=1,25)                         0000000
  400 FORMAT(///,1X,13(F8.4,1X),//,5X,12(F8.4))                          0000000
C                                                                        0000000
C---READ RAW MEASURED DATA TO BE REDUCED                                 0000000
C                                                                        0000000
      READ(7,215) HEDID1,HEDID2                                          0000000
  215 FORMAT(18A4)                                                       0000000
      READ(7,216) ALPHA,PHI,DSINCH,DLINCH,AAFR,TAFR                      0000000
  216 FORMAT(6F10.5)                                                     0000000
      READ(7,217) KRADTR,NSTATN,MAXJPT                                   0000000
```

```
  217 FORMAT(3I10)                                                      0000000
      DO 30 I=1,NSTATN                                                  0000000
        READ(7,230) XINCHS(I),NDATA(I),RDNPRS(I),PREF(I)                0000000
        READ(7,216) FANSPD(I),TFLOW(I),PATM(I),BZOFF(I)                 0000000
        JPTS=NDATA(I)                                                   0000000
        DO 20 J=1,JPTS                                                  0000000
          READ(7,220) RINCHS(J),RBETA(I,J),RPNMPS(I,J),RPCMPW(I,J),     0000000
     #         RPCMPA(I,J)                                              0000000
   20   CONTINUE                                                        0000000
   30   CONTINUE                                                        0000000
C                                                                       0000000
C---------CONVERT X'S AND R'S FROM INCHES TO METERS                     0000000
C                                                                       0000000
      RSMALL=DSINCH*0.0254/2.0                                          0000000
      RLARGE=DLINCH*0.0254/2.0                                          0000000
      DO 35 I=1,NSTATN                                                  0000000
        X(I)=XINCHS(I)*0.0254                                           0000000
        JPTS=NDATA(I)                                                   0000000
        DO 32 J=1,JPTS                                                  0000000
          R(J)=RINCHS(J)*0.0254                                         0000000
   32   CONTINUE                                                        0000000
   35 CONTINUE                                                          0000000
  220 FORMAT(7F10.5)                                                    0000000
  230 FORMAT(1F10.5,1I10,2F10.5)                                        0000000
      IF(DIAGNS) WRITE(8,470) (NDATA(I),I=1,NSTATN)                     0000000
      IF(DIAGNS) WRITE(8,450) (X(I),I=1,NSTATN)                         0000000
      IF(DIAGNS) WRITE(8,500) (R(J),J=1,JPTS)                           0000000
      DO 37 I=1,NSTATN                                                  0000000
        IF(DIAGNS) WRITE(8,500) (RBETA(I,J),J=1,JPTS)                   0000000
        IF(DIAGNS) WRITE(8,500) (RPNMPS(I,J),J=1,JPTS)                  0000000
        IF(DIAGNS) WRITE(8,500) (RPCMPW(I,J),J=1,JPTS)                  0000000
        IF(DIAGNS) WRITE(8,500) (RPCMPA(I,J),J=1,JPTS)                  0000000
   37 CONTINUE                                                          0000000
  450 FORMAT(/,40X,1(F8.4,1X))                                          0000000
  470 FORMAT(///,40X,1(I8,1X))                                          0000000
  500 FORMAT(///,20X,10(F8.4))                                          0000000
C                                                                       0000000
CHAPTER  1  1  1  1  1  DATA REDUCTION  1  1  1  1  1  1                0000000
C                                                                       0000000
C---------CALC PICHCF AND INTERPOLATE FOR DELTA FROM                    0000000
C---------     PITOT CALIBRATION CURVE                                  0000000
C                                                                       0000000
      IDID=0                                                            0000000
      DO 50 I=1,NSTATN                                                  0000000
        JPTS=NDATA(I)                                                   0000000
        DO 40 J=1,JPTS                                                  0000000
          IF((RPCMPW(I,J).EQ.0.0).AND.(RPNMPS(I,J).EQ.0.0)) GO TO 38    0000000
          PICHCF(I,J)=RPNMPS(I,J)/(RPCMPW(I,J)+1.E-6)                   0000000
          IF((PICHCF(I,J).GT.2.544).OR.(PICHCF(I,J).LT.-3.769)) GO TO 380000000
          IF(IDID .EQ. 0) DELTA(I,J)=SPLINE(CPITCH,                     0000000
     #      CDELTA,NCAL,PICHCF(I,J),IDID)                               0000000
          IF(IDID .GT. 0) DELTA(I,J)=SPLINE(CPITCH,CDELTA,              0000000
     #      NCAL,PICHCF(I,J),IDID)                                      0000000
          IDID=1                                                        0000000
          GO TO 40                                                      0000000
   38     CONTINUE                                                      0000000
          DELTA(I,J)=0.0                                                0000000
          WRITE(8,850) I,J                                              0000000
  850     FORMAT(20X,'PICHCF IS OUT OF RANGE OF CALIBRATION AT I=       0000000
     #           ',I3,' AND J=',I3)                                     0000000
   40   CONTINUE                                                        0000000
   50 CONTINUE                                                          0000000
C                                                                       0000000
C---------INTERPOLATE FOR VELCF AND PSTCF FROM PITOT CALIBRATION DATA   0000000
C                                                                       0000000
      IDID=0                                                            0000000
```

```
      DO 80 I=1,NSTATN                                                  0000000
        JPTS=NDATA(I)                                                   0000000
        DO 70 J=1,JPTS                                                  0000000
          IF((RPCMPW(I,J).EQ.0.0).AND.(RPNMPS(I,J).EQ.0.0)) GO TO 65    0000000
          IF((ABS(DELTA(I,J))) .GT. 58.0) GO TO 65                      0000000
          IF(IDID .EQ. 0) VELCF(I,J)=SPLINE(CDELTA,                     0000000
     #      CVELCF,NCAL,DELTA(I,J),IDID)                                0000000
          IF(IDID .GT. 0) VELCF(I,J)=SPLINE(CDELTA,CVELCF,              0000000
     #      NCAL,DELTA(I,J),IDID)                                       0000000
          IF(IDID .EQ. 0) PSTCF(I,J)=SPLINE(CDELTA,                     0000000
     #      CPSTCF,NCAL,DELTA(I,J),IDID)                                0000000
          IF(IDID .GT. 0) PSTCF(I,J)=SPLINE(CDELTA,CPSTCF,              0000000
     #      NCAL,DELTA(I,J),IDID)                                       0000000
          IDID=1                                                        0000000
          GO TO 70                                                      0000000
   65     CONTINUE                                                      0000000
          VELCF(I,J)=0.0                                                0000000
          PSTCF(I,J)=0.0                                                0000000
          WRITE(8,890) I,J                                              0000000
  890     FORMAT(20X,'DELTA IS OUT OF RANGE OF CALIBRATION DATA         0000000
     #           AT I=',I3,' AND J=',I3)                                0000000
   70   CONTINUE                                                        0000000
   80 CONTINUE                                                          0000000
C                                                                       0000000
      DO 85 I=1,NSTATN                                                  0000000
        IF(DIAGNS) WRITE(8,500) (PICHCF(I,J),J=1,JPTS)                  0000000
        IF(DIAGNS) WRITE(8,500) (DELTA(I,J),J=1,JPTS)                   0000000
        IF(DIAGNS) WRITE(8,500) (VELCF(I,J),J=1,JPTS)                   0000000
        IF(DIAGNS) WRITE(8,500) (PSTCF(I,J),J=1,JPTS)                   0000000
   85 CONTINUE                                                          0000000
C                                                                       0000000
C---------CALC MAGNITUDE OF TOTAL MEAN VELOCITY VECTOR,                 0000000
C---------    U, V, & W COMPONENTS, AND STATIC PRESSURE                 0000000
C                                                                       0000000
      PI=3.14159                                                        0000000
      DO 100 I=1,NSTATN                                                 0000000
        RHO(I)=PATM(I)*(133.33)/(286.94*(TFLOW(I)+273.15))              0000000
        JPTS=NDATA(I)                                                   0000000
        DO 90 J=1,JPTS                                                  0000000
          BETA(I,J)=360.+BZOFF(I)-RBETA(I,J)                            0000000
          IF((RPCMPW(I,J).EQ.0.0).AND.(RPNMPS(I,J).EQ.0.0))BETA(I,J)=0.0000000
          VTOTAL(I,J)=SQRT(ABS(2.0/RHO(I)*VELCF(I,J)*RPCMPW(I,J)*133.9))0000000
          U(I,J)=VTOTAL(I,J) * COS(DELTA(I,J)*PI/180.0) *               0000000
     #      COS(BETA(I,J)*PI/180.0)                                     0000000
          V(I,J)=VTOTAL(I,J) * SIN(DELTA(I,J)*PI/180.0)                 0000000
          W(I,J)=VTOTAL(I,J) * COS(DELTA(I,J)*PI/180.0) *               0000000
     #      SIN(BETA(I,J)*PI/180.0)                                     0000000
          P(I,J)=(RPCMPA(I,J)-PSTCF(I,J)*RPCMPW(I,J))*133.33            0000000
   90   CONTINUE                                                        0000000
  100 CONTINUE                                                          0000000
      IF(DIAGNS) WRITE(8,500)(VTOTAL(I,J),J=1,JPTS)                     0000000
      IF(DIAGNS) WRITE(8,500)(U(I,J),J=1,JPTS)                          0000000
      IF(DIAGNS) WRITE(8,500)(V(I,J),J=1,JPTS)                          0000000
      IF(DIAGNS) WRITE(8,500)(W(I,J),J=1,JPTS)                          0000000
      IF(DIAGNS) WRITE(8,500)(P(I,J),J=1,JPTS)                          0000000
C                                                                       0000000
CHAPTER  2  2  2  2  2  2  AUXILIARY CALCULATIONS  2  2  2  2  2         0000000
C                                                                       0000000
C----------NONDIMENSIONALIZE LENGTHS AND VELOCITIES                     0000000
C                                                                       0000000
       DO 150 I=1,NSTATN                                                0000000
        XND(I)=X(I)/(2.0*RLARGE)                                        0000000
        JPTS=NDATA(I)                                                   0000000
        UIN(I)=AAFR*4.7195/(10000.0 * PI * RSMALL**2)                   0000000
        UAV=(AAFR+TAFR)*4.7195/(10000.0 * PI *RLARGE**2)                0000000
        RMASFL(I)=PI*RHO(I)*UIN(I)*RSMALL**2                            0000000
```

```
      IF(DIAGNS) WRITE(8,450) (UIN(II),II=1,NSTATN)                    0000000
      IF(DIAGNS) WRITE(8,450) (RMASFL(II),II=1,NSTATN)                 0000000
        DO 140 J=1,JPTS                                                0000000
          VTSTAR(I,J)=VTOTAL(I,J)/UAV                                  0000000
          USTAR(I,J)=U(I,J)/UAV                                        0000000
          VSTAR(I,J)=V(I,J)/UAV                                        0000000
          WSTAR(I,J)=W(I,J)/UAV                                        0000000
          PSTAR(I,J)=P(I,J)/(RDNPRS(I)*133.33)                         0000000
  140   CONTINUE                                                       0000000
  150 CONTINUE                                                         0000000
      DO 160 J=1,MAXJPT                                                0000000
        RND(J)=R(J)/(2.0*RLARGE)                                       0000000
        IF(KRADTR.EQ.0) RND(J)=RINCHS(J)                               0000000
        IF(KRADTR.EQ.0) R(J)=RINCHS(J)                                 0000000
  160 CONTINUE                                                         0000000
C                                                                      0000000
      IF(KRADTR.EQ.0) GO TO 135                                        0000000
C                                                                      0000000
C---FOR RADIAL PROFILES:  NUMERICAL INTEGRATION TO CALC. MASS          0000000
C   FLOW AND MOMENTUM FLUXES FOR SWIRL NUMBER                          0000000
C                                                                      0000000
C   FOR PROFILES AT AND UPSTREAM OF EXPANSION CORNER, RSMALL           0000000
C   IS USED IN EXPRESSIONS FOR DYNP AND UMEAN; DOWNSTREAM OF           0000000
C   EXPANSION, RLARGE IS USED.                                         0000000
C                                                                      0000000
      DO 130 I=1,NSTATN                                                0000000
        JPTS=NDATA(I)                                                  0000000
        JPTSM1=JPTS-1                                                  0000000
        PREF(I)=P(I,JPTS)                                              0000000
        DYPS(1)=0.0                                                    0000000
        DYNP(JPTS)=2.0*(RSMALL-R(JPTS))                                0000000
C                                                                      0000000
        DO 110 J=1,JPTSM1                                              0000000
          DYNP(J)=R(J+1)-R(J)                                          0000000
          DYPS(J+1)=DYNP(J)                                            0000000
  110   CONTINUE                                                       0000000
        DO 115 J=1,JPTS                                                0000000
          SNS(J)=0.5*(DYNP(J)+DYPS(J))                                 0000000
          PSTAR(I,J)=P(I,J)-PREF(I)                                    0000000
  115   CONTINUE                                                       0000000
C                                                                      0000000
C----INNER 3 (HUB) VALUES OF PSTAR SET TO ZERO FOR SWIRLER             0000000
C    EXIT-PLANE PROFILES:  FOR DOWNSTREAM PROFILES, MAKE THESE         0000000
C    STATEMENTS COMMENTS.                                              0000000
C                                                                      0000000
C         PSTAR(I,1)=0.0                                               0000000
C         PSTAR(I,2)=0.0                                               0000000
C         PSTAR(I,3)=0.0                                               0000000
C                                                                      0000000
        IF(DIAGNS) WRITE(8,500) (DYNP(J),J=1,JPTS)                     0000000
        IF(DIAGNS) WRITE(8,500) (SNS(J),J=1,JPTS)                      0000000
        AREA1=PI*SNS(1)**2                                             0000000
        ARSUM=AREA1                                                    0000000
        FLOW=RHO(I)*U(I,1)*AREA1                                       0000000
        WMOM=W(I,1)*R(2)/4.*FLOW                                       0000000
        UMOM=U(I,1)*FLOW                                               0000000
        UMOMP=(RHO(I)*U(I,1)**2+PSTAR(I,1))*AREA1                      0000000
        IF(DIAGNS) WRITE(8,2030) AREA1,ARSUM,FLOW,WMOM,UMOM,UMOMP      0000000
        DO 120 J=2,JPTS                                                0000000
          AREAJ=2.*PI*R(J)*SNS(J)                                      0000000
          ARSUM=ARSUM+AREAJ                                            0000000
          FLOW=FLOW+RHO(I)*U(I,J)*AREAJ                                0000000
          UMOM=UMOM+RHO(I)*U(I,J)**2*AREAJ                             0000000
          UMOMP=UMOMP+(RHO(I)*U(I,J)**2+PSTAR(I,J))*AREAJ              0000000
          WMOM=WMOM+RHO(I)*U(I,J)*W(I,J)*R(J)*AREAJ                    0000000
          IF(DIAGNS) WRITE(8,2040) AREAJ,ARSUM,FLOW,WMOM,UMOM,UMOMP    0000000
```

```
  120   CONTINUE                                                          0000000
        RMASS(I)=FLOW                                                     0000000
        UMEAN(I)=RMASS(I)/(RHO(I)*PI*RSMALL**2)                           0000000
        ANGMOM(I)=WMOM                                                    0000000
        AXMOM(I)=UMOM                                                     0000000
        AXMOMP(I)=UMOMP                                                   0000000
        IF(DIAGNS) WRITE(8,2050) UMEAN(I),RMASS(I),ANGMOM(I),AXMOM(I),    0000000
     #           AXMOMP(I)                                                0000000
C                                                                         0000000
 2030 FORMAT(//4X,'AREAJ',5X,'ARSUM',5X,'FLOW',6X,'WMOM',6X,              0000000
     #        'UMOM',6X,'UMOMP'//' ',6E10.3)                              0000000
 2040 FORMAT(' ',6E10.3)                                                  0000000
 2050 FORMAT(/14X,'UMEAN',5X,'MASS',6X,'ANGMOM',4X,'AXMOM',               0000000
     #        5X,'AXMOMP'//11X,5E10.3)                                    0000000
C                                                                         0000000
        SPRIME(I)=ANGMOM(I)/(AXMOM(I)*RSMALL)                             0000000
        S(I)=ANGMOM(I)/(AXMOMP(I)*RSMALL)                                 0000000
  130 CONTINUE                                                            0000000
      IF(DIAGNS) WRITE(8,450) (UMEAN(I),I=1,NSTATN)                       0000000
      IF(DIAGNS) WRITE(8,450) (RMASS(I),I=1,NSTATN)                       0000000
      IF(DIAGNS) WRITE(8,450) (ANGMOM(I),I=1,NSTATN)                      0000000
      IF(DIAGNS) WRITE(8,450) (AXMOM(I),I=1,NSTATN)                       0000000
      IF(DIAGNS) WRITE(8,450) (AXMOMP(I),I=1,NSTATN)                      0000000
      IF(DIAGNS) WRITE(8,450) (SPRIME(I),I=1,NSTATN)                      0000000
      IF(DIAGNS) WRITE(8,450) (S(I),I=1,NSTATN)                           0000000
  135 CONTINUE                                                            0000000
C                                                                         0000000
      IF(KRADTR.EQ.1) GO TO 180                                           0000000
C---FOR AZIMUTHAL TRAVERSES:  CALC. PSTAR=(P-PREF) USING SUPPLIED         0000000
C   VALUES OF PREF(I).                                                    0000000
C                                                                         0000000
      DO 178 I=1,NSTATN                                                   0000000
        JPTS=NDATA(I)                                                     0000000
        DO 177 J=1,JPTS                                                   0000000
          PSTAR(I,J)=P(I,J)-PREF(I)*133.33                                0000000
  177   CONTINUE                                                          0000000
  178 CONTINUE                                                            0000000
C                                                                         0000000
C---CALC. AVERAGE VALUES FOR AZIMUTHAL TRAVERSES -- NREP IS NO. OF        0000000
C   POINTS IN REPEATING CYCLE ACROSS ONE BLADE; NAVE IS NO. OF            0000000
C   AVERAGES POSSIBLE CONTAINING NREP CONSECUTIVE POINTS.                 0000000
C                                                                         0000000
      NREP=6                                                              0000000
      DO 180 I=1,NSTATN                                                   0000000
        NAVE=NDATA(I)-NREP+1                                              0000000
        DO 175 K=1,NAVE                                                   0000000
          NAVEND=K+NREP-1                                                 0000000
          USUM=0.                                                         0000000
          VSUM=0.                                                         0000000
          WSUM=0.                                                         0000000
          PSUM=0.                                                         0000000
          DO 174 J=K,NAVEND                                               0000000
            USUM=USUM+USTAR(I,J)                                          0000000
            VSUM=VSUM+VSTAR(I,J)                                          0000000
            WSUM=WSUM+WSTAR(I,J)                                          0000000
            PSUM=PSUM+PSTAR(I,J)                                          0000000
  174     CONTINUE                                                        0000000
          USTAVG(I,K)=USUM/NREP                                           0000000
          VSTAVG(I,K)=VSUM/NREP                                           0000000
          WSTAVG(I,K)=WSUM/NREP                                           0000000
          PSTAVG(I,K)=PSUM/NREP                                           0000000
  175   CONTINUE                                                          0000000
  180 CONTINUE                                                            0000000
C                                                                         0000000
C---CALCULATE VISCOSITY AND INLET REYNOLDS NUMBER (BOTH TRAVERSE TYPES)   0000000
C                                                                         0000000
```

```
C---VISCOSITY FORMULA FROM LAN & ROSKAM, AIRPLANE AERODYNAMICS          0000000
C   & PERFORMANCE, P.42.                                               0000000
C                                                                      0000000
      DO 162 I=1,NSTATN                                                0000000
        DENOM=TFLOW(I)+273.15+110.4                                    0000000
        VISCOS(I)=(1.458E-06)*(TFLOW(I)+273.15)**1.5/DENOM             0000000
        REDIN(I)=UIN(I)*2.*RSMALL*RHO(I)/VISCOS(I)                     0000000
  162 CONTINUE                                                         0000000
C                                                                      0000000
CHAPTER  3  3  3  3  3  OUTPUT  3  3  3  3  3  3  3                    0000000
C                                                                      0000000
      IF(.NOT. IWRITE) GO TO 165                                       0000000
      DO 168 I=1,NSTATN                                                0000000
      WRITE(11,163) XINCHS(I)                                          0000000
      WRITE(11,163) UIN(I)                                             0000000
      WRITE(11,163) PREF(I)                                            0000000
      DO 168 J=1,MAXJPT                                                0000000
      WRITE(11,166) RINCHS(J), USTAR(I,J), VSTAR(I,J), WSTAR(I,J),     0000000
     &              BETA(I,J), DELTA(I,J), PSTAR(I,J)                  0000000
C     WRITE(11,163) RINCHS                                             0000000
C     WRITE(11,163) USTAR                                              0000000
C     WRITE(11,163) VSTAR                                              0000000
C     WRITE(11,163) WSTAR                                              0000000
C     WRITE(11,163) BETA                                               0000000
C     WRITE(11,163) DELTA                                              0000000
C     WRITE(11,163) PSTAR                                              0000000
  163 FORMAT(E10.3)                                                    0000000
  166 FORMAT(7E10.3)                                                   0000000
  168 CONTINUE                                                         0000000
C                                                                      0000000
  165 CONTINUE                                                         0000000
      WRITE(8,311)                                                     0000000
      WRITE(8,312) HEDID1,HEDID2,HEDCAL                                0000000
      WRITE(8,325) ALPHA                                               0000000
      WRITE(8,330) PHI                                                 0000000
      WRITE(8,335) RSMALL                                              0000000
      WRITE(8,340) RLARGE                                              0000000
      CALL WRITE(1,1,NSTATN,1,IT,JT,XINCHS,RINCHS,FANSPD,HEDFAN)       0000000
      CALL WRITE(1,1,NSTATN,1,IT,JT,XINCHS,RINCHS,TFLOW,HEDTFL)        0000000
      CALL WRITE(1,1,NSTATN,1,IT,JT,XINCHS,RINCHS,PATM,HEDPAT)         0000000
      CALL WRITE(1,1,NSTATN,1,IT,JT,XINCHS,RINCHS,RHO,HEDRHO)          0000000
      CALL WRITE(1,1,NSTATN,1,IT,JT,XINCHS,RINCHS,VISCOS,HEDVIS)       0000000
      CALL WRITE(1,1,NSTATN,1,IT,JT,XINCHS,RINCHS,RDNPRS,HEDMIP)       0000000
      CALL WRITE(1,1,NSTATN,1,IT,JT,X,R,UIN,HEDMIV)                    0000000
      CALL WRITE(1,1,NSTATN,1,IT,JT,X,R,RMASFL,HEDMMF)                 0000000
      CALL WRITE(1,1,NSTATN,1,IT,JT,X,R,REDIN,HEDRED)                  0000000
C                                                                      0000000
      IF(KRADTR.EQ.0) GO TO 170                                        0000000
      CALL WRITE(1,1,NSTATN,1,IT,JT,X,R,RMASS,HEDM)                    0000000
      CALL WRITE(1,1,NSTATN,1,IT,JT,X,R,UMEAN,HEDUMN)                  0000000
      CALL WRITE(1,1,NSTATN,1,IT,JT,X,R,ANGMOM,HEDAM)                  0000000
      CALL WRITE(1,1,NSTATN,1,IT,JT,X,R,AXMOMP,HEDAXP)                 0000000
      CALL WRITE(1,1,NSTATN,1,IT,JT,X,R,AXMOM,HEDAX)                   0000000
      CALL WRITE(1,1,NSTATN,1,IT,JT,X,R,S,HEDS)                        0000000
      CALL WRITE(1,1,NSTATN,1,IT,JT,X,R,SPRIME,HEDSPR)                 0000000
C                                                                      0000000
  170 CONTINUE                                                         0000000
      CALL PRINT(1,1,NSTATN,MAXJPT,IT,JT,X,R,U,HEDU)                   0000000
      CALL PRINT(1,1,NSTATN,MAXJPT,IT,JT,X,R,V,HEDV)                   0000000
      CALL PRINT(1,1,NSTATN,MAXJPT,IT,JT,X,R,W,HEDW)                   0000000
      CALL PRINT(1,1,NSTATN,MAXJPT,IT,JT,X,R,P,HEDP)                   0000000
      CALL PRINT(1,1,NSTATN,MAXJPT,IT,JT,X,R,DELTA,HEDDEL)             0000000
      CALL PRINT(1,1,NSTATN,MAXJPT,IT,JT,X,R,BETA,HEDBET)              0000000
      CALL PRINT(1,1,NSTATN,MAXJPT,IT,JT,X,R,VTOTAL,HEDVT)             0000000
      CALL PRINT(1,1,NSTATN,MAXJPT,IT,JT,XND,RND,USTAR,HEDUST)         0000000
      CALL PRINT(1,1,NSTATN,MAXJPT,IT,JT,XND,RND,VSTAR,HEDVST)         0000000
```

```
      CALL PRINT(1,1,NSTATN,MAXJPT,IT,JT,XND,RND,WSTAR,HEDWST)          0000000
      CALL PRINT(1,1,NSTATN,MAXJPT,IT,JT,XND,RND,PSTAR,HEDPST)          0000000
      CALL PRINT(1,1,NSTATN,MAXJPT,IT,JT,XND,RND,VTSTAR,HEDPDF)         0000000
C                                                                       0000000
      IF(KRADTR.EQ.1) GO TO 172                                         0000000
      CALL PRINT(1,1,NSTATN,MAXJPT,IT,JT,XINCHS,RINCHS,USTAVG,HEDUSA)   0000000
      CALL PRINT(1,1,NSTATN,MAXJPT,IT,JT,XINCHS,RINCHS,VSTAVG,HEDVSA)   0000000
      CALL PRINT(1,1,NSTATN,MAXJPT,IT,JT,XINCHS,RINCHS,WSTAVG,HEDWSA)   0000000
      CALL PRINT(1,1,NSTATN,MAXJPT,IT,JT,XINCHS,RINCHS,PSTAVG,HEDPDA)   0000000
  172 CONTINUE                                                          0000000
      CALL PRINT(1,1,NSTATN,MAXJPT,IT,JT,XINCHS,RINCHS,RPNMPS,HEDNMS)   0000000
      CALL PRINT(1,1,NSTATN,MAXJPT,IT,JT,XINCHS,RINCHS,RPCMPW,HEDCMW)   0000000
      CALL PRINT(1,1,NSTATN,MAXJPT,IT,JT,XINCHS,RINCHS,RPCMPA,HEDCMA)   0000000
      STOP                                                              0000000
C                                                                       0000000
C---------FORMAT STATEMENTS                                             0000000
C                                                                       0000000
  311 FORMAT(1H1,T37,'AXISYMMETRIC,ISOTHERMAL, GT COMBUSTOR FLOWFIELD '.0000000
     #'MEASUREMENTS',//,T53,'USING A FIVE-HOLE PITOT PROBE')            0000000
  312 FORMAT(//T10,18A4/T10,18A4//T10,9A4)                              0000000
  325 FORMAT(/T10,'EXPANSION ANGLE(DEG.) =',T50,1PE13.3)                0000000
  330 FORMAT(/T10,'SWIRL VANE ANGLE(DEG.) =',T50,1PE13.3)               0000000
  335 FORMAT (/T10,'INLET RADIUS(M) =',T50,1PE13.3)                     0000000
  340 FORMAT(/T10,'COMBUSTOR RADIUS(M) =',T50,1PE13.3)                  0000000
      END                                                               0000000
C                                                                       0000000
      SUBROUTINE INIT                                                   0000000
C*****************************************************************    0000000
C                                                                       0000000
      COMMON                                                            0000000
     #/MEASUR/RBETA(8,24),RPNMPS(8,24),RPCMPW(8,24),RPCMPA(8,24),       0000000
     #     NDATA(8),MAXJPT,RDNPRS(8),                                   0000000
     #     FANSPD(8),TFLOW(8),PATM(8),BZOFF(8)                          0000000
     #/GEOM/X(8),R(24),XND(8),RND(24),DYPS(24),DYNP(24),                 0000000
     #     SNS(24),NSTATN,XINCHS(8),RINCHS(24)                          0000000
     #/CALC/VTOTAL(8,24),U(8,24),V(8,24),W(8,24),P(8,24),                0000000
     #     VTSTAR(8,24),USTAR(8,24),VSTAR(8,24),WSTAR(8,24),            0000000
     #     PICHCF(8,24),VELCF(8,24),DELTA(8,24),BETA(8,24),             0000000
     #     ANGMOM(8),UMEAN(8),RMASS(8),RMASFL(8),UIN(8),                0000000
     #     PSTAR(8,24),PSTCF(8,24),AXMOM(8),AXMOMP(8),                  0000000
     #     SPRIME(8),S(8),REDIN(8),PREF(8),RHO(8),VISCOS(8),            0000000
     #     USTAVG(8,24),VSTAVG(8,21),WSTAVG(8,24),PSTAVG(8,24)          0000000
C                                                                       0000000
C                                                                       0000000
      DO 20 I=1,NSTATN                                                  0000000
        RMASFL(I)=0.0                                                   0000000
        RMASS(I)=0.0                                                    0000000
        ANGMOM(I)=0.0                                                   0000000
        AXMOM(I)=0.0                                                    0000000
        AXMOMP(I)=0.0                                                   0000000
        SPRIME(I)=0.0                                                   0000000
        S(I)=0.0                                                        0000000
        UMEAN(I)=0.0                                                    0000000
        UIN(I)=0.0                                                      0000000
        DO 10 J=1,MAXJPT                                                0000000
          VTOTAL(I,J)=0.0                                               0000000
          U(I,J)=0.0                                                    0000000
          V(I,J)=0.0                                                    0000000
          W(I,J)=0.0                                                    0000000
          P(I,J)=0.0                                                    0000000
          VTSTAR(I,J)=0.0                                               0000000
          USTAR(I,J)=0.0                                                0000000
          VSTAR(I,J)=0.0                                                0000000
          PSTAR(I,J)=0.0                                                0000000
          RBETA(I,J)=0.0                                                0000000
          BETA(I,J)=0.0                                                 0000000
```

```
            RPNMPS(I,J)=0.0                                                 0000000
            RPCMPW(I,J)=0.0                                                 0000000
            RPCMPA(I,J)=0.0                                                 0000000
            PICHCF(I,J)=0.0                                                 0000000
            VELCF(I,J)=0.0                                                  0000000
            PSTCF(I,J)=0.0                                                  0000000
            DELTA(I,J)=0.0                                                  0000000
            USTAVG(I,J)=0.0                                                 0000000
            VSTAVG(I,J)=0.0                                                 0000000
            WSTAVG(I,J)=0.0                                                 0000000
            PSTAVG(I,J)=0.0                                                 0000000
   10     CONTINUE                                                          0000000
   20   CONTINUE                                                            0000000
        RETURN                                                              0000000
        END                                                                 0000000
C                                                                           0000000
        FUNCTION SPLINE(X, FX, N, X1, IDID)                                 0000000
C*******************************************************************       0000000
                                                                            0000000
C       CUBIC SPLINE CURVE FITTING IN 2 DIMENSIONAL DATA PLANE              0000000
C       INPUT VALUES :                                                      0000000
C       X, FX       DATA ARRAYS, ONE DIMENSIONAL, X IN INCREASING ORDER     0000000
C       N           NUMBER OF DATA POINTS IN X, MAX 26                      0000000
C       X1          POINT OF INTEREST, WHERE F(X1) IS TO BE FOUND           0000000
C                                                                           0000000
C       RETURN VALUE :                                                      0000000
C       SPLINE = F(X1)                                                      0000000
C       THIS ROUTINE ACTIVATES ROUTINE ABUILD, H, AND GAUSS.                0000000
C       FOR INTERPOLATION OF A LARGE NUMBER OF DATA POINTS, FUNCTION        0000000
C       SPLINE MAY BE CALLED ONLY ONCE , AND SUBSEQUENT CALLS MAY USE       0000000
C       ENTRY POINT AT STATEMENT 36.                                        0000000
C*************************************************************************0000000
        DIMENSION X(1), FX(1), A(26,27)                                     0000000
C                                                                           0000000
C---------CONSTRUCT SPLINE MATRIX                                           0000000
C                                                                           0000000
        IF (IDID .GT. 0)GO TO 36                                            0000000
        N1=N+1                                                              0000000
        DO 10  I=1, N                                                       0000000
          DO 10  J=1, N1                                                    0000000
   10       A(I,J)=0.                                                       0000000
        M1=N-1                                                              0000000
        DO 20  I=2, M1                                                      0000000
   20     CALL ABUILD(X, FX, A, N, I)                                       0000000
        A(1,1)=H(X,2)                                                       0000000
        A(1,2)=-H(X,1)-H(X,2)                                               0000000
        A(1,3)=H(X,1)                                                       0000000
        M2=N-2                                                              0000000
        A(N,M2)=H(X,M1)                                                     0000000
        A(N,M1)=-H(X,M2)-H(X,M1)                                            0000000
        A(N,N)=H(X,M2)                                                      0000000
C                                                                           0000000
C---------FIND SECOND DERIVATIVES                                           0000000
C                                                                           0000000
        CALL GAUSS(A, N, N1)                                                0000000
C                                                                           0000000
C---------FIND F(X1)                                                        0000000
C                                                                           0000000
   36   CONTINUE                                                            0000000
        DO 40  I=1, M1                                                      0000000
        I1=I+1                                                              0000000
        IF(X1 .EQ. X(I)) GO TO 50                                           0000000
        IF(X1 .LT. X(I) .AND. X1 .GT. X(I1)) GO TO 41                       0000000
        IF(X1 .GT. X(I) .AND. X1 .LT. X(I1) ) GO TO 41                      0000000
40    CONTINUE                                                              0000000
      IF(X1 .EQ. X(N)) GO TO 60                                             0000000
```

```
      WRITE(8, 42) X1                                                   OOOOOOO
42    FORMAT(' X1=', G14.7, ' OUT OF INTERPOLATION RANGE, RETURNED VALUEOOOOOOO
     *=O')                                                              OOOOOOO
      SPLINE=O.                                                         OOOOOOO
      STOP                                                              OOOOOOO
C                                                                       OOOOOOO
41    CONTINUE                                                          OOOOOOO
      I1=I+1                                                            OOOOOOO
      HI=H(X,I)                                                         OOOOOOO
      HX=X(I1)-X1                                                       OOOOOOO
      HX2=X1-X(I)                                                       OOOOOOO
      FX1=HX**3/HI-HI*HX                                                OOOOOOO
      FX1=FX1*A(I,N1)                                                   OOOOOOO
      STO=HX2**3/HI - HI*HX2                                            OOOOOOO
      FX1=(FX1+STO*A(I1,N1) )/6.                                        OOOOOOO
      SPLINE=(FX(I)*HX+FX(I1)*HX2)/HI+FX1                               OOOOOOO
      RETURN                                                            OOOOOOO
C                                                                       OOOOOOO
50    CONTINUE                                                          OOOOOOO
      SPLINE=FX(I)                                                      OOOOOOO
      RETURN                                                            OOOOOOO
C                                                                       OOOOOOO
60    CONTINUE                                                          OOOOOOO
      SPLINE=FX(N)                                                      OOOOOOO
      RETURN                                                            OOOOOOO
      END                                                               OOOOOOO
C                                                                       OOOOOOO
      FUNCTION H(X,I)                                                   OOOOOOO
C*************************************************************************OOOOOOO
C     CALCULATE DELTA X WHICH IS USUALLY CALLED H.                      OOOOOOO
C*************************************************************************OOOOOOO
      DIMENSION X(1)                                                    OOOOOOO
      I1=I+1                                                            OOOOOOO
      H=X(I1)-X(I)                                                      OOOOOOO
      RETURN                                                            OOOOOOO
      END                                                               OOOOOOO
C                                                                       OOOOOOO
      SUBROUTINE ABUILD(X, F, A, N, I)                                  OOOOOOO
C*************************************************************************OOOOOOO
C     CONSTRUCT  SPLINE MATRIX FOR FINDING 2ND DERIVATIVES.             OOOOOOO
C*************************************************************************OOOOOOO
      DIMENSION X(1), F(1), A(26,27)                                    OOOOOOO
      IM1=I-1                                                           OOOOOOO
      I1=I+1                                                            OOOOOOO
      N1=N+1                                                            OOOOOOO
      STO=H(X,I)                                                        OOOOOOO
      HIM1=H(X,IM1)                                                     OOOOOOO
      A(I,IM1)=HIM1                                                     OOOOOOO
      A(I,I)=2.*(HIM1+STO)                                              OOOOOOO
      A(I,I1)=STO                                                       OOOOOOO
      A(I,N1)=( (F(I1)-F(I))/STO - (F(I)-F(IM1))/HIM1 )*6.              OOOOOOO
      RETURN                                                            OOOOOOO
      END                                                               OOOOOOO
C                                                                       OOOOOOO
      SUBROUTINE GAUSS(A, K, M)                                         OOOOOOO
C*************************************************************************OOOOOOO
C     GAUSS-JORDAN ELIMINATION                                          OOOOOOO
C*************************************************************************OOOOOOO
      DIMENSION A(26,27)                                                OOOOOOO
      M1=M-1                                                            OOOOOOO
      K1=K-1                                                            OOOOOOO
      DO 3  L=1, K1                                                     OOOOOOO
        L1=L+1                                                          OOOOOOO
        DO 3  I=L1, K                                                   OOOOOOO
          CONST=A(I,L)/A(L,L)                                           OOOOOOO
          DO 3  J=L, M                                                  OOOOOOO
```

```
    3       A(I,J)=A(I,J)-CONST*A(L,J)                                      0000000
      DO 6 I=1, K1                                                          0000000
        I1=I+1                                                              0000000
        DO 6  L=I1, M1                                                      0000000
          CONST=A(I,L)/A(L,L)                                               0000000
          DO 6  J=I, M                                                      0000000
6           A(I,J)=A(I,J)-CONST*A(L,J)                                      0000000
      DO 10  I=1, K                                                         0000000
        A(I,M)=A(I,M)/A(I,I)                                                0000000
   10   A(I,I)=1.                                                           0000000
      RETURN                                                                0000000
      END                                                                   0000000
C                                                                           0000000
      SUBROUTINE PRINT(ISTART,JSTART,NI,NJ,IT,JT,X,Y,PHI,HEAD)              0000000
C*************************************************************************0000000
C                                                                           0000000
      DIMENSION PHI(IT,JT),X(IT),Y(JT),HEAD(9)                              0000000
      COMMON /OUTPUT/ STORE(8)                                              0000000
      ISKIP=1                                                               0000000
      JSKIP=1                                                               0000000
      WRITE(8,110)HEAD                                                      0000000
      ISTA=ISTART-10                                                        0000000
  100 CONTINUE                                                              0000000
      ISTA=ISTA+10                                                          0000000
      IEND=ISTA+9                                                           0000000
      IF(NI.LT.IEND)IEND=NI                                                 0000000
      WRITE(8,111)(I,I=ISTA,IEND,ISKIP)                                     0000000
      WRITE(8,114)(X(I),I=ISTA,IEND,ISKIP)                                  0000000
      WRITE(8,112)                                                          0000000
      DO 101 JJ=JSTART,NJ,JSKIP                                             0000000
        J=JSTART+NJ-JJ                                                      0000000
        DO 120 I=ISTA,IEND                                                  0000000
          A=PHI(I,J)                                                        0000000
          IF(ABS(A).LT.1.E-20) A=0.0                                        0000000
  120     STORE(I)=A                                                        0000000
  101   WRITE(8,113)J,Y(J),(STORE(I),I=ISTA,IEND,ISKIP)                     0000000
      IF(IEND.LT.NI)GO TO 100                                               0000000
      RETURN                                                                0000000
  110 FORMAT(1HO,17(2H*-),7X,9A4,7X,17(2H-*))                               0000000
  111 FORMAT(1HO,15H         I =     ,I2,9I11)                              0000000
  112 FORMAT(8HO J     Y)                                                   0000000
  113 FORMAT(I3,OPF8.4,1X,10(1X,E10.3))                                     0000000
  114 FORMAT(13H          X = ,F8.4,9F11.4)                                 0000000
      END                                                                   0000000
C                                                                           0000000
      SUBROUTINE WRITE(ISTART,JSTART,NI,NJ,IT,JT,X,Y,PHI,HEAD)              0000000
C                                                                           0000000
      COMMON /OUTPUT/ STORE(8)                                              0000000
      DIMENSION PHI(IT),X(IT),Y(JT),HEAD(9)                                 0000000
      ISKIP=1                                                               0000000
      JSKIP=1                                                               0000000
      WRITE(8,110)HEAD                                                      0000000
      ISTA=ISTART-12                                                        0000000
  100 CONTINUE                                                              0000000
      ISTA=ISTA+12                                                          0000000
      IEND=ISTA+11                                                          0000000
      IF(NI.LT.IEND)IEND=NI                                                 0000000
      WRITE(8,111)(I,I=ISTA,IEND,ISKIP)                                     0000000
      WRITE(8,114)(X(I),I=ISTA,IEND,ISKIP)                                  0000000
      DO 101 JJ=JSTART,NJ,JSKIP                                             0000000
        J=JSTART+NJ-JJ                                                      0000000
        DO 120 I=ISTA,IEND                                                  0000000
          A=PHI(I)                                                          0000000
          IF(ABS(A).LT.1.E-20) A=0.0                                        0000000
  120     STORE(I)=A                                                        0000000
  101   WRITE(8,113) (STORE(I),I=ISTA,IEND,ISKIP)                           0000000
```

```
      IF(IEND.LT.NI)GO TO 100                                          0000000
      RETURN                                                           0000000
  110 FORMAT(1HO,17(2H*-),7X,9A4,7X,17(2H-*))                          0000000
  111 FORMAT(1HO,15H          I =     ,I2,9I11)                        0000000
  113 FORMAT(/12X,1P10E11.3)                                           0000000
  114 FORMAT(13H          X = ,F8.4,9F11.4)                            0000000
      END                                                              0000000
```

VITA

Ghassan Ali Eghneim

Candidate for the Degree of

Master of Science

Thesis: FIVE-HOLE PITOT PROBE TIME MEAN VELOCITY MEASUREMENTS IN A CYCLONE CHAMBER WITH DOWNSTREAM NOZZLE

Major Field: Mechanical Engineering

Biographical:

Personal Data: The author was born in EL-Bared Tripoli, Lebanon, on January 9, 1965, the son of Mr. and Mrs. Ali Eghneim.

Education: The author graduated from El-Hikhim High School, Tripoli, Lebanon in 1983. He received Bachelor of Science in Mechanical Engineering from Oklahoma State University, Stillwater in May 1987. In July 1988, he completed the requirements for the Master of Science degree at Oklahoma State University, Stillwater, Oklahoma.

Professional Experience: From August, 1987-July, 1988, the author was a graduate teaching and research assistant in the Department of Mechanical Engineering, Oklahoma State University.

Professional Society: The author is a member of, The American Society of Mechanical Engineers, ASME. The American Society of Aeronautics and Astronautics, AIAA. Mechanical Engineering Honorary Society.